

**AN ASSESSMENT OF THE TOXICOLOGICAL IMPACT OF
MEDICALLY RELEVANT NANOMATERIALS IN DISEASED
CONDITIONS**

by

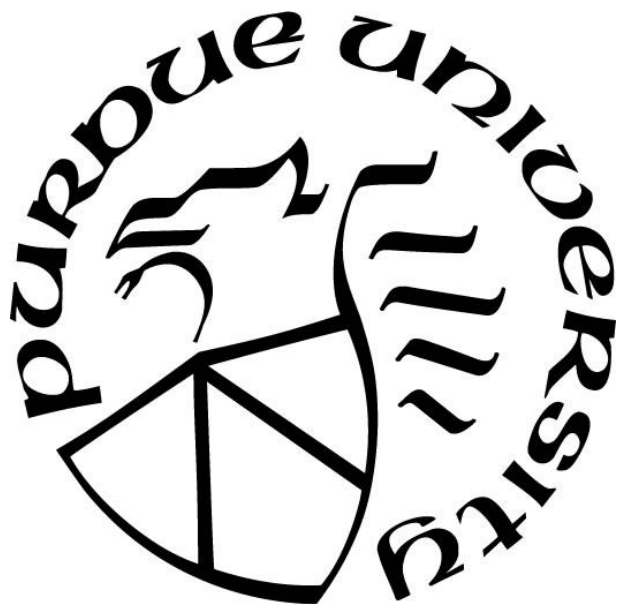
Lisa Kobos

A Dissertation

Submitted to the Faculty of Purdue University

In Partial Fulfillment of the Requirements for the degree of

Doctor of Philosophy



School of Health Sciences

West Lafayette, Indiana

May 2020

THE PURDUE UNIVERSITY GRADUATE SCHOOL
STATEMENT OF COMMITTEE APPROVAL

Dr. Jonathan Shannahan, Chair

Department of Health Sciences

Dr. Wei Zheng

Department of Health Sciences

Dr. Jennifer Freeman

Department of Health Sciences

Dr. Alexander Wei

Department of Chemistry

Approved by:

Dr. Aaron Bowman

To my parents, Duane and Billie. Thanks to you, nothing caught on fire.

Well, nothing that wasn't supposed to.

ACKNOWLEDGMENTS

I would not have reached this point without a robust support network of others who generously offered their time, effort, and resources to contribute to my success. My principal investigator, Dr. Jonathan Shannahan, has been the best advisor I could have possibly hoped for – not only as a brilliant scientist, but as a personal and professional mentor. I never would have guessed based on our first conversation over the phone in a Petco parking lot, but you have grown to be one of the most influential figures in my life thus far. It is by your leadership that I have become the person I am today, and I couldn't be more grateful.

The other members of my graduate committee, Drs. Wei Zheng, Jennifer Freeman, and Alexander Wei, have each proven to be invaluable to my professional and scientific development. Dr. Zheng, thank you for always providing advice on which direction to go next – whether that was how to progress my career or how to pass my oral exam. I feel incredibly lucky that I was able to benefit from your years of experience. I am grateful to Dr. Freeman for your guidance when I first began graduate school. My time in your lab allowed me to build foundational skills that I will doubtlessly utilize for the remainder of my career. Dr. Wei, thank you for providing a fresh perspective and getting me to consider my ideas, as well as research at large, in a new light. I always walked out of your office with more ideas than when I went in.

Dr. Christina Ferreira, thank you for being perhaps the most diligent, hardworking, patient, and kind collaborator I've had the pleasure of working with. Much of the work I've completed during my graduate career would have been impossible without your help.

I also acknowledge the many labmates I have had the pleasure of working alongside and learning from; Dr. Katharine Horzmann for her initial instruction during my rotations, and Dr. Sherleen Fu-Adamson for setting an example, and Rachel Foguth for her endless patience while watching me mangle brain samples. Vincent Coltellino, I thank you for your incredible dedication and enthusiasm – whatever you chose to do in the future, I have no doubt you will succeed. I would also like to acknowledge Mitzi Miramontes, Emily Jung, Riley Kishman, and Alexis Ferngren for keeping the lab running. Saeed Alqahtani, Li Xia, the lab will be yours soon. Keep working hard and try not to break anything (else), and I know you'll do well.

Finally, it was only by the grace of my family that I was able to persist through the times in which I struggled the most. Sarah, thank you for always knowing how to make me laugh and

forcing me to relax when I'd nearly forgotten how. Mom, Dad, there are no words to describe the depth of my gratitude for your unyielding support. Everything that I am and have accomplished is a direct result of you. I hope I've made you proud.

TABLE OF CONTENTS

LIST OF TABLES	10
LIST OF FIGURES	11
LIST OF ABBREVIATIONS.....	16
ABSTRACT	18
CHAPTER 1. INTRODUCTION	20
1.1 Nanoparticles: A Historical Perspective.....	20
1.2 Properties of NPs and Non-medical Applications.....	22
1.3 Biomedical Applications of NPs.....	24
1.4 Disease and NP Exposure.....	27
1.5 The Biocorona.....	30
1.6 Structure of Dissertation	33
1.7 References.....	34
CHAPTER 2. AN INTEGRATIVE PROTEOMIC/LIPIDOMIC ANALYSIS OF THE GOLD NANOPARTICLE BIOCORONA IN HEALTHY AND OBESE CONDITIONS	57
2.1 Abstract.....	57
2.2 Introduction.....	58
2.3 Materials and Methods	60
2.3.1 AuNP characterization.....	60
2.3.2 Human serum characterization.....	60
2.3.3 Formation of the AuNP BC	60
2.3.4 Assessment of the protein components of the AuNP BC	61
2.3.5 Analysis of proteomics data.....	62
2.3.6 Sample preparation for lipid screening of the AuNP BC	62
2.3.7 Lipid screening data acquisition.....	63
2.3.8 Cell culture and toxicity assessment.....	64
2.3.9 Statistics and biomolecular data analysis.....	64
2.4 Results	65
2.4.1 Serum and AuNP characterization	65

2.4.2 Protein components of the BC—identification and relative quantification between AuNPs	66
2.4.3 Comparison of healthy and obese BCs—protein identities	70
2.4.4 Comparison of healthy and obese BCs—relative quantification	71
2.4.5 Lipid components of the AuNP BCs—identification and relative quantification between AuNPs.....	73
2.4.6 Comparison of healthy and obese BCs—lipid identities.....	77
2.4.7 Obese and healthy comparisons—relative lipid quantification	78
2.4.8 BC-induced variations in macrophage viability and inflammatory response	81
2.5 Discussion.....	84
2.6 Conclusions.....	89
2.7 References.....	90
CHAPTER 3. ALTERED FORMATION OF THE IRON OXIDE NANOPARTICLE-BIOCORONA DUE TO INDIVIDUAL VARIABILITY AND EXERCISE	100
3.1 Abstract.....	100
3.2 Introduction.....	100
3.3 Materials and Methods	102
3.3.1 Blood collection	102
3.3.2. Plasma sample characterization	104
3.3.3 Fe ₃ O ₄ NP characterization	104
3.3.4 Formation of the Fe ₃ O ₄ NP-BC.....	104
3.3.5 Assessment of the protein components of the Fe ₃ O ₄ NP-BC	105
3.3.6 Proteomic data analysis - identified proteins.....	105
3.3.7 Proteomic data analysis - relative abundance	106
3.3.8 Cells and cell culture	106
3.3.9 Viability, uptake, and inflammation.....	106
3.4 Results	107
3.4.1 Characterization of experimental materials	107
3.4.1.1 Human blood characterization	107
3.4.1.2. Nanoparticle characterization	108
3.4.2 Inter-individual variability within the biocorona	110

3.4.2.1 Evaluation of the effect of individual variability on the pre-exercise BC – protein identities	110
3.4.2.2 Evaluation of the effect of individual variability on the pre-exercise BC – protein quantification.....	111
3.4.3. Intra-individual variability within the biocorona	115
3.4.3.1. Evaluation of the effect of exercise on variations in the BC – protein identities .	115
3.4.3.2 Evaluation of the effect of exercise on variations in the BC – protein quantification	116
3.4.4 Assessment of immune cells response to NP exposure	117
3.4.4.1. Cellular viability, NP association, and inflammatory response	117
3.5 Discussion	121
3.5.1 NP properties modified following addition of BCs.....	121
3.5.2 Interindividual variations in the NP-BC	122
3.5.3 Intraindividual differences in the NP-BC related to exercise	123
3.5.4 Immune cell response to NP-BCs	125
3.6 Study Limitations and Conclusions.....	125
3.7 References.....	126
CHAPTER 4. COMPARISON OF SILVER NANOPARTICLE BIODISTRIBUTION AND RESPONSE BETWEEN HEALTHY AND METABOLIC SYNDROME MOUSE MODELS	
4.1 Abstract.....	132
4.2 Introduction.....	132
4.3 Materials and Methods	135
4.3.1 AgNP Characterization.	135
4.3.2 Induction of MetS and AgNP Exposure.	135
4.3.4 Gene Expression Assessment.....	137
4.3.5 Metal Quantification.....	137
4.3.6 Statistical Analysis.	137
4.4 Results	137
4.4.1 Characterization of Mouse Model and AgNPs.	137
4.4.2 AgNP Biodistribution.	138
4.4.3 Gene Expression.....	141

4.5 Discussion	144
4.6 References.....	158
CHAPTER 5. CONCLUSION	172
5.1 Overall Conclusions and the Future of NP Therapeutics in Medicine.....	172
5.2 References.....	179
VITA	185
PUBLICATIONS.....	190

LIST OF TABLES

Table 2.1. Pooled human serum from healthy and obese male and female individuals was characterized for traditional lipid end points used in health clinics through commercially available kits to measure triglycerides, total cholesterol, HDL, and LDL/VLDL. All analyses are reported as mean \pm SEM (n = 5/group). Statistical significance was determined by t-test, $p < 0.05$. *Denotes statistical significant difference between healthy and obese serum ($p < 0.05$).....65

Table 2.2. AuNP Characterization Prior to and Following the Addition of a BC. Data represent mean \pm standard deviation, n=3-5/group. AuNPs were diluted in and incubated for 8 h at 4 °C in 10% pooled human serum. AuNPs were characterized with and without BCs via assessment of ζ -potential, hydrodynamic size, and polydispersion index. * denotes statistical significance when compared to an AuNP with no BC. # denotes statistical significance when compared to an AuNP with healthy BC. Statistical significance was determined by one-way ANOVA using Tukey's multiple comparisons test $p < 0.05$66

Table 3.1. After subjects' blood was drawn, aliquots were analyzed by Mid America Laboratories. A. Blood parameters prior to completion of 7-day exercise regimen. B. Blood parameters following completion of 7-day exercise regimen. * and bold indicate subjects selected for further analysis due to large (2, 5, 7) or small (1, 6, 8) change in triglycerides pre- to post-exercise.... 103

Table 4.1. AgNP Characterization. Data represent mean \pm SEM, n=4/group. AgNPs were characterized via assessment of ζ -potential, hydrodynamic size, and polydispersion index. 138

Table 4.2. Characterization of Healthy and MetS Mice. Serum from healthy and MetS mice was characterized for traditional lipid endpoints via commercially available kits to measure total bound and unbound cholesterol, HDL, LDL/VLDL, insulin, and glycated hemoglobin (HBA1c). # denotes statistical significance as compared to the corresponding healthy group. Comparisons were performed by two-way ANOVA with Tukey post hoc analysis; $p < 0.05$). All analyses are reported as mean \pm SEM, n= 7-8/group. 138

Table 4.3. Summary of Changes in Gene Expression Following Exposure to AgNPs. Statistically significant increases and decreases in expression as compared to unexposed groups are denoted by "up" and "down" arrows, respectively. Lack of any statistically significant change is indicated by a dash. 140

LIST OF FIGURES

Figure 2.1. Comparison of BC composition of all four particles in healthy or obese serum. Proteins identified from each AuNP BC were compared to proteins in all other AuNP BCs under the same condition, either (A) healthy or (B) obese. Venn diagrams were used to illustrate all comparisons. A comprehensive list of all proteins found in each BC may be found in Supplementary Table S2.1. List of specific proteins used to generate Venn diagram (A, B) may be found in Supplementary Tables S2.3 and S2.4, respectively. AuNPs, gold nanoparticles; BC, biocorona.....67

Figure 2.2. Relative abundance comparison of selected proteins found in the BCs of all four AuNPs in the healthy condition. Proteins identified as present with the BCs of all four AuNPs in the healthy condition were compared in their abundance. Peak intensities were log₁₀ transformed to convert the raw values to a more readily understandable format. Comparisons were performed by one-way ANOVA with Tukey post hoc analysis ($p < 0.05$). *Denotes statistical significance compared to the corresponding 20 nm AuNP with the same coating, #denotes statistical significance compared to the corresponding citrate-coated AuNP with the same size.....69

Figure 2.3. Relative abundance comparison of selected proteins found in the BCs of all four AuNPs in the obese condition. Proteins identified as present with the BCs of all four AuNPs in the obese condition were compared in their abundance. Peak intensities were log₁₀ transformed to convert the raw values to a more readily understandable format. Comparisons were performed by one-way ANOVA with Tukey post hoc analysis ($p < 0.05$). *Denotes statistical significance compared to the corresponding 20 nm AuNP with the same coating, #denotes statistical significance compared to the corresponding citrate-coated AuNP with the same size.70

Figure 2.4. Comparison of BC composition between healthy and obese conditions for all four AuNPs. Proteins identified as present in each AuNP BC formed from healthy serum were compared to proteins within the same AuNP BC formed from obese serum. Venn diagrams were used to illustrate all comparisons. A comprehensive list of all proteins found in each BC is found in Supplementary Table S2.1. A list of specific proteins used to generate the Venn diagrams in the figure is found in Supplementary Table S2.5.71

Figure 2.5. Fold changes of proteins between the healthy and obese BCs. Quantities of shared proteins between each AuNP BC are depicted as fold changes. Negative values indicate that the protein was more abundant in healthy conditions, while positive values indicate that the protein was more abundant in obese conditions. Individual graphs depict the 10 most altered proteins in terms of abundance between healthy and obese conditions. Supplementary Table S2.1 includes a comprehensive list of all protein fold changes between healthy and obese conditions for each AuNP tested.72

Figure 2.6. Comparison of BC composition of all four particles in healthy or obese serum. Lipids identified from each AuNP BC were compared to lipids in all other AuNP BCs under the same condition, either (A) healthy or (B) obese. Venn diagrams were used to illustrate all comparisons. A comprehensive list of all lipids found in each BC is found in Supplementary Table S2.2. List of specific lipids used to generate Venn diagram (A, B) is found in Supplementary Tables S2.6 and S2.7, respectively.74

Figure 2.7. Relative abundance comparison of selected lipids found in the BCs of all four AuNPs in the healthy condition. Lipids identified as present with the BCs of all four AuNPs in the healthy condition were compared in their abundance. Comparisons were performed by one-way ANOVA with Tukey post hoc analysis ($p < 0.05$). *Denotes statistical significance compared to the corresponding 20 nm AuNP with the same coating, #denotes statistical significance compared to the corresponding citrate-coated AuNP with the same size. FA, fatty acids; PCo, phosphatidylcholine alkyl ether lipids; TAG, triglycerides.76

Figure 2.8. Relative abundance comparison of selected lipids found in the BCs of all four AuNPs in the obese condition. Lipids identified as present with the BCs of all four AuNPs in the obese condition were compared in their abundance. Comparisons were performed by one-way ANOVA with Tukey post hoc analysis ($p < 0.05$). *Denotes statistical significance compared to the corresponding 20 nm AuNP with the same coating, #denotes statistical significance compared to the corresponding citrate-coated AuNP with the same size. PC, phosphatidylcholine lipids.77

Figure 2.9. Comparison of BC composition between healthy and obese conditions for all four AuNPs. Lipids identified as present in each AuNP BC formed from healthy serum were compared to lipids within the same AuNP BC formed from obese serum. Venn diagrams were used to illustrate all comparisons. A comprehensive list of all lipids found in each BC is found in Supplementary Table S2.2. A list of specific lipids used to generate the Venn diagrams in the figure is found in Supplementary Table S2.8.78

Figure 2.10. Fold changes of lipids between the healthy and obese BCs. Quantities of shared lipids between each AuNP BCs are depicted as fold changes. Negative values indicate that the lipid was more abundant in healthy conditions, while positive values indicate that the lipid was more abundant in obese conditions. Individual graphs depict the 10 most altered lipids in terms of abundance between healthy and obese conditions. Supplementary Table S2.2 includes a comprehensive list of all lipid fold changes between healthy and obese conditions for each AuNP tested. PC indicates phosphatidylcholine lipids, and PCo indicates phosphatidylcholine alkyl ether lipids. Certain lipid names were shortened for brevity, which are listed in full here. 20:0 Cholesteryl ester... ester indicates 20:0 Cholesteryl ester, 18:0 Sitosteryl ester. Cholesteryl 11-hydroperoxy-eicosatetraenoate... indicates Cholesteryl 11-hydroperoxy-eicosatetraenoate, 22:2 Cholesteryl ester, 20:1 Stigmasteryl ester, 20:2 Sitosteryl ester. Lanosteryl palmitoleate... indicates lanosteryl palmitoleate, 18:2 Campesteryl ester. 18:3 Cholesteryl ester... indicates 18:3 Cholesteryl ester, 16:2 Stigmasteryl ester, 16:3 Sitosteryl ester. 18:2 Cholesteryl ester... ester indicates 18:2 Cholesteryl ester, zymosteryl oleate, 16:1 Stigmasteryl ester, 16:2 Sitosteryl ester.80

Figure 2.11. Changes in gene expression following exposure to AuNPs with or without a healthy or obese BC. Expression of mRNA was assessed relative to serum-free media control cells (untreated) (dotted line). Cells were grown to 90% confluency in a 96-well plate before exposure to 50 $\mu\text{g}/\text{mL}$ AuNPs with no BC, a healthy BC, or an obese BC for 24 hours. Gene expression of TNF- α , CCL2, CXCL2, and GAPDH (control) was assessed through PCR to evaluate the inflammatory response induced by AuNP exposure. *Denotes statistical significance compared to the expression of the unexposed control, #denotes statistical significance compared to the AuNP with no BC, and †denotes statistical significance compared to the AuNP with a healthy BC. Comparisons were performed by one-way ANOVA with Tukey post hoc analysis ($p < 0.05$). GAPDH, glyceraldehyde 3-phosphate dehydrogenase; TNF- α , tumor necrosis factor- α82

Figure 3.1. NP Characterization Prior to and Following the Addition of a BC. NPs were diluted in and incubated for 8 h at 4 °C in 10% subject plasma. NPs were characterized with and without BCs via assessment of A) hydrodynamic size and B) ζ-potential. * denotes statistical significance from Fe₃O₄ NPs without a BC, # denotes statistical significance between pre-exercise NP-BC and post-exercise NP-BC (n = 6/group; two-way ANOVA with Tukey post hoc analysis; p < 0.05). 109

Figure 3.2. Comparison of Pre-Exercise Fe₃O₄ NP-BC Composition: Number of Proteins shared with Subject 1. Proteins identified from each subject's BC were compared to proteins identified from subject 1's BC. Subject 1 was selected as a baseline due to it being the subject with lowest pre-exercise cholesterol levels. Venn diagrams were created to illustrate each comparison. Supplemental Table S3.1 contains a comprehensive list comparing identified proteins between all the pre-exercise subjects. List of specific proteins used to generate Venn diagrams in Fig. 3.2 are in Supplemental Table S3.2B. 111

Figure 3.3. Fold Change of Selected Proteins Compared to Sample 1. Quantities of shared proteins between each subject and subject 1 are depicted as fold changes. Negative values indicate that the subject was more abundant in subject 1, while positive values indicate that the subject was less abundant in subject 1. Individual graphs depict the 10 most significantly altered proteins in terms of abundance between subjects and subject 1 (n = 3/group; one-way ANOVA with Tukey post hoc analysis; p < 0.05). Supplemental Table S3.3 includes a comprehensive list of all protein fold changes compared to subject 1. 112

Figure 3.4. Relative Abundances of Specific Proteins across All Individual Pre-Exercise Subjects. Relative quantities of proteins shared between all 10 pre-exercise subjects were plotted to make global comparisons between all samples. * = statistical significance p < 0.05 compared to subject 1 by one-way ANOVA with Tukey post hoc analysis (n = 3/group). Supplemental Table S3.3 includes a comprehensive list of the calculated abundances for all proteins forming NP-BC in all subjects. 113

Figure 3.5. Comparison of Pre-Exercise to Post-Exercise Biocorona Composition within the Same Subject: Number of Proteins Shared Between Pre- and Post-Exercise Subjects. Proteins identified from each pre-exercise BC were compared to proteins identified from its corresponding post-exercise BC. Subjects were selected due their low (Subjects 1, 6, 8) or high (Subjects 2, 5, 7) changes in triglyceride levels pre- to post- exercise. Venn diagrams were created to illustrate each comparison. Supplemental Table S3.5A contains a comprehensive list comparing all identified proteins in pre- and post-exercise subjects. List of specific proteins used to generate Venn diagrams in Fig. 3.5 specifically are found in Supplemental Table S3.5B. 116

Figure 3.6. Fold Change of Specific Proteins in the Pre- and Post-Exercise Fe₃O₄ NP-BC. Quantities of shared proteins between each pre-exercise and post-exercise BC are depicted as fold changes. Supplemental Table S3.6 contains a comprehensive list of all protein quantity comparisons. Individual graphs depict the 10 most significantly different proteins in terms of fold change between pre- and post-exercise subjects (n = 3/group; one-way ANOVA with Tukey post hoc analysis; p < 0.05). Negative values indicate that the subject was more abundant prior to exercise, while positive values indicate that the subject was more abundant after exercise..... 117

Figure 3.7. Macrophage response following exposure to Individual Fe₃O₄ NP-BCs. Differentiated human macrophages were exposed to Fe₃O₄ NPs with a distinct BC at a concentration of 25 μg/ml for 24 h. Blue bars indicate Fe₃O₄ NPs with a BC formed following incubation in plasma collected

from individuals prior to the exercise regimen. Red bars indicate Fe₃O₄ NPs with a BC formed following incubation in plasma collected from individuals following completion of the exercise regimen. A, E. Cytotoxicity after a 24 h exposure to Fe₃O₄ NPs with BCs. Dotted line indicates controls with a cell viability of 100%. B, F. Macrophage association of Fe₃O₄ NPs with BCs after a 24 h exposure. C, G. TNF- α mRNA expression relative to serum-free media control cells following 24 h exposure to 25 μ g/ml Fe₃O₄ NPs with BCs. D, H. Protein levels of TNF- α in supernatant following 24 h exposure to 25 μ g/ml Fe₃O₄ NPs with BCs. A–D Utilized pre-exercise BCs, while E–H utilized pre and post-exercise BCs. * denotes statistical significance compared to controls (n = 6/group; one-way ANOVA with Tukey post hoc analysis; p < 0.05). # denotes statistical significance between Fe₃O₄ NPs with pre- and post-exercise BCs (n = 6/group; two-way ANOVA with Tukey post hoc analysis; p < 0.05)..... 119

Figure 4.1. Average Abundance of AgNPs in Each Organ of Healthy and MetS Mice Treated with AgNPs. The Ag content of each organ of mice treated with AgNPs was assessed via atomic absorption spectroscopy. 142

Figure 4.2. Average Concentration of AgNPs in Selected Organs of Treated and Control Healthy and MetS Mice. The Ag content of each organ was assessed via atomic absorption spectroscopy. The metal content in μ g was divided by the weight of the organ in g in order to assess data in terms of Ag concentration. * denotes statistical significance as compared to the corresponding untreated control group, and # denotes statistical significance as compared to the corresponding healthy group. Comparisons were performed by two-way ANOVA with Tukey post hoc analysis; p < 0.05). 146

Figure 4.3. Changes in Gene Expression in the Liver Following Exposure to AgNPs in Healthy or MetS Mice. Gene expression of TNF- α , CCL2, CXCL1, CXCL2, HO-1, and TGF- β and GAPDH (control) was assessed through PCR to evaluate the inflammatory, pro-fibrotic, and oxidative stress responses induced by AgNP exposure. * denotes statistical significance as compared to the corresponding untreated control group, and # denotes statistical significance as compared to the corresponding healthy group. Comparisons were performed by two-way ANOVA with Tukey post hoc analysis; p < 0.05). 148

Figure 4.4. Changes in Gene Expression in the Spleen Following Exposure to AgNPs in Healthy or MetS Mice. Gene expression of TNF- α , CCL2, CXCL1, CXCL2, HO-1, and TGF- β and GAPDH (control) was assessed through PCR to evaluate the inflammatory, pro-fibrotic, and oxidative stress responses induced by AgNP exposure. * denotes statistical significance as compared to the corresponding untreated control group, and # denotes statistical significance as compared to the corresponding healthy group. Comparisons were performed by two-way ANOVA with Tukey post hoc analysis; p < 0.05)..... 150

Figure 4.5. Changes in Gene Expression in the Kidney Following Exposure to AgNPs in Healthy or MetS Mice. Gene expression of TNF- α , CCL2, CXCL1, CXCL2, HO-1, and TGF- β and GAPDH (control) was assessed through PCR to evaluate the inflammatory, pro-fibrotic, and oxidative stress responses induced by AgNP exposure. * denotes statistical significance as compared to the corresponding untreated control group, and # denotes statistical significance as compared to the corresponding healthy group. Comparisons were performed by two-way ANOVA with Tukey post hoc analysis; p < 0.05)..... 152

Figure 4.6. Changes in Gene Expression in the Heart Following Exposure to AgNPs in Healthy or MetS Mice. Gene expression of TNF- α , CCL2, CXCL1, CXCL2, HO-1, and TGF- β and GAPDH (control) was assessed through PCR to evaluate the inflammatory, pro-fibrotic, and oxidative stress responses induced by AgNP exposure. * denotes statistical significance as compared to the corresponding untreated control group, and # denotes statistical significance as compared to the corresponding healthy group. Comparisons were performed by two-way ANOVA with Tukey post hoc analysis; $p < 0.05$). 153

Figure 4.7. Changes in Gene Expression in the Lung Following Exposure to AgNPs in Healthy or MetS Mice. Gene expression of TNF- α , CCL2, CXCL1, CXCL2, HO-1, and TGF- β and GAPDH (control) was assessed through PCR to evaluate the inflammatory, pro-fibrotic, and oxidative stress responses induced by AgNP exposure. * denotes statistical significance as compared to the corresponding untreated control group, and # denotes statistical significance as compared to the corresponding healthy group. Comparisons were performed by two-way ANOVA with Tukey post hoc analysis; $p < 0.05$). 155

Figure 4.8. Changes in Gene Expression in the Brain Following Exposure to AgNPs in Healthy or MetS Mice. Gene expression of TNF- α , CCL2, CXCL1, CXCL2, HO-1, and TGF- β and GAPDH (control) was assessed through PCR to evaluate the inflammatory, pro-fibrotic, and oxidative stress responses induced by AgNP exposure. * denotes statistical significance as compared to the corresponding untreated control group, and # denotes statistical significance as compared to the corresponding healthy group. Comparisons were performed by two-way ANOVA with Tukey post hoc analysis; $p < 0.05$). 156

LIST OF ABBREVIATIONS

AAS	Atomic Absorption Spectrometry
ACTB	Beta Actin
AgNP	Silver Nanoparticle
AuNP	Gold Nanoparticle
BC	Biocorona
BMI	Body Mass Index
CCL2	Monocyte Chemoattractant Protein-1
CDC	Centers for Disease Control and Prevention
CETP	Cholesteryl Ester Transfer Protein
CXCL1	Chemokine (C-X-C motif) Ligand 1
CXCL2	Chemokine (C-X-C motif) Ligand 2
DDI	Distilled De-Ionized
ELISA	Enzyme-Linked Immunosorbent Assay
Fe ₃ O ₄	Iron Oxide
Fe ₃ O ₄ NP	Iron Oxide Nanoparticle
FBS	Fetal Bovine Serum
GAPDH	Glyceraldehyde 3-Phosphate Dehydrogenase
HDL	High-Density Lipoprotein
HNO ₃	Nitric Acid
HO-1	Hemoxygenase-1
IL-4	Interleukin-4
IL-6	Interleukin-6
IL-13	Interleukin-13
ISDD	<i>In Vitro</i> Sedimentation, Diffusion and Dosimetry
LDL	Low-Density Lipoprotein
LFQ	Label-Free Quantification
LPS	Lipopolysaccharide
MCP-1	Monocyte Chemoattractant Protein-1

MetS	Metabolic Syndrome
MIP2	Macrophage Inflammatory Protein-2
MRI	Magnetic Resonance Imaging
MRM	Multiple Reaction Monitoring
mRNA	Messenger Ribonucleic Acid
MTT	Thiazolyl Blue Tetrazolium Bromide
NP	Nanoparticle
PBS	Phosphate Buffered Saline
PCR	Polymerase Chain Reaction
PDI	Polydispersion Index
PVP	Poly-N-vinylpyrrolidone
ROS	Reactive Oxygen Species
SEM	Standard Error of the Mean
SFM	Serum Free Media
SR-B1	Scavenger Receptor Class B Type 1
TEM	Transmission Electron Microscopy
TGF- β	Transforming Growth Factor β
TNF- α	Tumor Necrosis Factor- α
VLDL	Very Low-Density Lipoprotein

ABSTRACT

The use of nanoparticles in biomedical applications has greatly increased in recent years due to their unique properties, which allow them to supplement or even surpass the effectiveness of traditional treatments. Multiple types of nanoparticles are currently utilized or proposed for use in medicine, including gold, silver, and iron oxide. Each of these substances confer a unique set of benefits; gold has anti-inflammatory properties, silver is antibacterial, and iron oxide, in addition to being relatively inert, is useful in treating those with anemia. Unfortunately, many of the properties which make nanoparticles potentially useful for medical applications frequently contribute to their toxicity. While studies have been performed which examine the toxicity of nanoparticle therapeutics, virtually all have taken place in healthy conditions. This is not representative of the conditions in which these nanoparticles will be used, as treatments are, by definition, given to individuals who are somehow unhealthy. Additionally, a large and growing proportion of the population in the United States and worldwide suffer from a chronic disease, with some of the most common being obesity, high cholesterol, and metabolic syndrome. It is therefore important to consider these individuals in the development and testing of nanoparticle therapeutics. Specifically, these diseases alter the content of the circulation beyond the differences which exist solely due to individual variability. This may in turn may alter the biocorona, the term given to the coating of biomolecules which forms on the nanoparticle surface following exposure to a physiological environment. We hypothesized that individual variability and disease, specifically the common diseases obesity, high cholesterol, and metabolic syndrome, would alter the content of the biocorona, and that this would translate to differential nanoparticle toxicity. It was determined that both disease and individual variability caused distinct alterations in the biomolecular content of the biocorona. Further, these alterations were found to elicit distinct inflammatory responses when comparing between individuals or healthy to diseased conditions. These results have implications for the use of nanoparticles in biomedicine, as the variability observed within the biocorona in disease and between individuals may have a significant impact on the efficacy of the treatment, as well as any toxicological effects. It is therefore in the interest of public health to modify the process of developing, testing, and utilizing nanoparticle therapeutics such that the biocorona may work in conjunction with or regardless of differences in the biological milieu which exist as a result of individual variability or disease. By this, researchers

may maximize the safety and efficacy of nanoparticles in medicine and protect vulnerable subpopulations who may be predisposed to the development or worsening of a disease.

CHAPTER 1. INTRODUCTION

1.1 Nanoparticles: A Historical Perspective

While nanoparticles (NPs) are increasingly utilized in a wide variety of applications, their toxicity in living systems is poorly characterized. Additionally, it is not widely understood what NPs are or why they are included in many of the practices in which they are utilized. While the definition of a NP is somewhat variable, it is generally defined as an object with at least one dimension in the nanoscale, between 1-100 nm (Auffan et al., 2009). NPs are manufactured in a large variety of configurations and their properties can vary greatly. NPs are made in a variety of shapes, sizes, coatings, and core materials. Due to their unique properties, which will be the subject of further discussion later in this chapter, NPs have the capacity to greatly advance many of the products and systems which we use daily. Carbon nanotubes have been used to improve the strength and durability of dozens of products, ranging from tennis rackets to airplane parts (Esawi & Farag, 2007; Gohardani, Chapartegui, & Elizetxea, 2014; Volder, Tawfick, Baughman, & Hart, 2013). Zinc oxide and titanium dioxide are used to make more effective sunscreens, and iron NPs have been used to clean and purify groundwater of various contaminants, including organic solvents, pesticides, and other compounds (Wiench, Landsiedel, Schulte, Inman, & Riviere, 2011; W. Zhang & Elliott, 2006; Zhao et al., 2016). Of particular interest is the use of NPs in biomedical applications, as this provides perhaps the most direct contact of NPs with the human body. Gold, silver, and iron oxide all have current and proposed uses in the field of medicine, many of which, by their nature, introduce NPs directly to the circulation (B. Y. S. Kim, Rutka, & Chan, 2010; Lee & Jun, 2019). However, despite NPs being used in all these and many more applications, their effects in living systems are largely unknown. Most of the research which has been conducted has taken place in healthy models; however, the limited research which has taken place in models of disease supports that individuals with a pre-existing disease may have increased susceptibility to adverse health outcomes as a result of NP exposure (Raghavendra, Fritz, Fu, Brown, & Shannahan, 2017; Shannahan et al., 2016). Given the high and increasing prevalence of pre-existing disease in the United States and worldwide, investigation into variable NP toxicity between healthy and diseased individuals is an area of critical importance. Thus, given the increasing utilization of NPs in a variety of medical applications and everyday products, in combination with the concurrently

increasing prevalence of pre-existing disease, it was our goal to provide a deeper understanding of the toxicity of medically relevant NPs in common diseases. The overall hypothesis and specific aims of this dissertation are outlined at the end of the chapter.

While nanotechnology and the use of NPs by humans is thought of as a relatively recent phenomenon, NPs are formed from the combustion that occurs as a result of wildfires and volcanic activity and have existed for at least hundreds of millions of years (Bisiaux et al., 2011; Rietmeijer & Mackinnon, 1997; Tepe & Bau, 2014). NPs are produced by fire, but also through a number of other natural processes such as precipitation, oxidation, and reduction (Griffin et al., 2018). As a result, NPs are present throughout nature, found in sulfur springs, icebergs, and ore deposits (Faulstich et al., 2017; Guo & Barnard, 2013; Hough, Noble, & Reich, 2011). While NPs have only been identified and recognized for their unique properties relatively recently, humanity has been unknowingly utilizing NPs for hundreds of years, primarily for aesthetic purposes. One of the earliest uses of NPs took place in Rome in the 4th century, where gold and silver NPs were used to form what is today known as the Lycurgus cup (Freestone, Meeks, Sax, & Higgitt, 2007). The Lycurgus cup is made from an ancient form of dichroic glass that utilizes NPs to reflect certain wavelengths of light while allowing others to pass through at specific angles, meaning that the cup will appear as different colors depending on the angle of the light source (Scott, 1995). NPs have been used in many other artistic endeavors across centuries, as well. In the 9th century, Mesopotamians used silver and copper NPs in to add metallic luster decorations to glazed pottery (Sciau, Mirguet, Roucau, Chabanne, & Schvoerer, 2009). The ancient Egyptians used lead sulfide NPs in hair dye, and Neolithic Russians utilized natural asbestos nanofibers to reinforce their ceramics (Kulkova, Gusentzova, Nesterov, Sorokin, & Sapelko, 2012; Walter et al., 2000).

It is only within the past few decades that science has begun to be able to intentionally create, recognize, and identify NPs. Michael Faraday is widely considered to be the first individual to have purposely synthesized NPs in a scientific context. Using gold salt and a solution of phosphorous and carbon disulfide, Faraday was able to cause a color change from yellow to bright red, indicating the presence of gold nanoparticles (AuNPs), though Faraday was unaware of this at the time (Faraday, 1857; Thompson, 2007). While other scientists unknowingly utilized NPs in their work or proposed their existence, it wasn't until the 1980s that NPs began to be recognized

and identified in a meaningful way. Both quantum dots and fullerenes were first identified in the 1980s (Ekimov, Efros, & Onushchenko, 1985; Kroto, Allaf, & Balm, 1985; Sen, Yadav, & Shukla, 2015). The 1980s also saw the invention of atomic microscopy, allowing for the first time the visualization and intentional manipulation of materials on the nano-scale (Parot et al., 2007). It was in the 1990s that the number of patents for nanotechnology began to increase, and carbon nanotubes, arguably one of the most important nanomaterials to this day, were discovered (H. Chen, Roco, Li, & Lin, 2008; Iijima, 1991, 2002). Around this time, quantum dots were intentionally synthesized for the first time (Brichkin & Razumov, 2016). By the year 2000, the incredible potential of nanotechnology was beginning to be realized, and President Bill Clinton launched the National Nanotechnology Initiative to promote and advance the study of nanotechnology within the United States (Roco, 2011). Between 2001 and 2004, over 60 countries followed suit and created their own government-sponsored nanotechnology research programs (Clunan, Rodine-Hardy, Hsuch, Kosal, & McManus, 2014). This support has led to both an increased rate of scientific discovery and increased public awareness, resulting in greater understanding by the public and scientific community of the existence, properties, and potential applications of NPs.

1.2 Properties of NPs and Non-medical Applications

While early attempts to characterize and synthesize NPs gave scientists some idea of the special properties of nanomaterials, today we have a much better understanding of what makes nanomaterials distinct from similar materials on the macro-scale. Due to their small size, NPs have a very large surface area, making them ideal for applications including energy harvesting, photodegradation, and thermal conductivity (I. Khan, Saeed, & Khan, 2019). The greater amount of surface area available allows for a larger number of reactions to take place more quickly, making NPs an efficient material. Further, NPs have unique optical properties. Specifically, NPs are highly modifiable, resulting in tunable extinction, plasmonic resonance, and emission wavelength (Coronado, Encina, & Stefani, 2011). Many of these properties are due to the quantum confinement effect, in which the size of the particle may be changed in order to tune the distance between the positive and negative charges, and thus control the excitation and emission wavelengths (Kumbhakar, Ray, & Stepanov, 2014; Wageh, Su, & Xu-rong, 2003). NPs have many proposed and current uses which take advantage of their modifiability and unique quantum

properties, including uses in photodetectors, solar cells, television screens and medical imaging applications (Bourzac, 2013; Livache et al., 2019; Matea, Mocan, Pop, Puia, & Iancu, 2017; Nozik, 2002). NPs may also possess a number of magnetic, thermal, and physical properties which are distinct from the behavior of the material on a macro scale. For instance, sufficiently small NPs composed of magnetic material may exhibit superparamagnetism, in which the direction of magnetization may randomly flip under the influence of temperature (D. K. Kim, Zhang, Voit, Rao, & Muhammed, 2001; Woods, Kirtley, Sun, & Koch, 2001). Metal NPs have been shown to have high thermal conductivity, with NP-fluid mixtures having much greater conductivity than the base fluid by itself (Wang & Xu, 1999). This has the potential to enhance the efficiency of devices which utilize heat transfer fluids, such as refrigerators, air conditioners, and heat pumps (Abbas, Walvekar, Hajibeigy, & Farhood, 2013; Fadhilah, Marhamah, & Izzat, 2014; Li, Yang, Yu, & Zhao, 2015). Material properties may also be altered at a fundamental level, as demonstrated by copper. While bulk copper is fairly malleable and easy to shape, copper NPs are considered a super-hard material (Suresh, Annapurna, Bhikshamaiah, & Singh, 2016). This is because the movement of bulk copper is due to the displacement of copper clusters approximately 50 nm in size; at sizes smaller than 50 nm, copper loses its malleability (Glatzmaier, Pradhan, Kang, Curtis, & Blake, 2010). While science is far from a complete understanding of the unique properties of NPs, it is known that these unique characteristics may be utilized to the advantage of science. The high modifiability of NPs may be utilized to enhance certain properties and refine a product or process to create the most desirable result possible.

Our current understanding of special properties unique to NPs has allowed for their use in a wide variety of applications. Silver is the most commonly utilized nanomaterial in commercial applications, largely due to its antimicrobial properties. While silver NPs (AgNPs) are toxic to both bacteria and fungi, these toxicities are due to two distinct mechanisms. AgNPs act against bacteria primarily through the dissolution of silver ions, which cause damage to cellular components such as membranes, DNA, and enzymes, resulting in cytotoxicity. The antimycotic activity of AgNPs is a result of their adherence to spores, inhibiting fungal growth (Siemer et al., 2018). These properties make AgNPs particularly useful, and as a result they may be found in food packaging, cosmetics, electronics, textiles, and more (Echegoyen & Nerín, 2013; Tran, Nguyen, & Le, 2013; Xi-feng Zhang, Liu, Shen, & Gurunathan, 2016). As previously mentioned, zinc oxide

and titanium dioxide NPs are included in many modern sunscreens, mainly due to their ability to deflect and scatter UV rays, protecting the skin from sun exposure (Smijs & Pavel, 2011). Additionally, nano-sized particles are less opaque than their macro-sized counterparts, avoiding the opaque, chalky appearance that is associated with many traditional sunscreen products, and are therefore desirable for aesthetic reasons, as well (Smijs & Pavel, 2011). NPs are also used as a colorant in inks, paints, and dyes (Cao et al., 2017; Gotoh et al., 2007; Ishibashi, 2008; Z. Zhang, Lv, Chen, & An, 2019). Due to their unique optical properties, NPs may be tuned to appear as a specific color, and are less prone to fading than traditional pigments (B. Tang, Sun, Kaur, Yu, & Wang, 2014; B. Tang et al., 2015). NPs are used in a plethora of other applications, as well, including agriculture, home appliances, air filters, and others (Mavani & Shah, 2013; Meyer, Ann, & Gonzalez, 2011; Siddiqui, Firoz, & Impact, 2015). While the many applications of NPs and the reasons for their inclusion in products could be a thesis unto itself, the focus of this dissertation is NPs in biomedical applications.

1.3 Biomedical Applications of NPs

The first individual to propose the use of nanotechnology in medicine was Richard Feynman, who mentioned in 1959 the potential benefits of being able to “swallow a surgeon” (Feynman, 1959). The first application of nanotechnology in biomedical research occurred only a short while later, when NPs were investigated as a potential vehicle for sustained release of antigen in order to eliminate the need for multiple vaccine injections (G Birrenbach & Speiser, 1976; Gerd Birrenbach, 1973). While the antibody generation stimulated by the NP vaccines was promising, the technology was not developed further, likely due to the significant material cost and the high toxicity of some of the agents involved. It was in the mid to late 1970s that NPs were investigated for drug delivery, and in 80s when their potential was first demonstrated in a living animal through localization of NPs to a Yoshida tail tumor (Kramer, 1974; J. Widder, Marino, & Morris, 1983; K. J. Widder, Senyei, & Scarpelli, 1978). Shortly later, K. Eric Drexler published several books describing the theory of “molecular engineering,” or the construction of nanomachines from individual atoms that could then proceed to themselves manipulate individual atoms and molecules, producing new products, or even more of themselves (Drexler, Peterson, & Pergamit, 1991; Drexler K, 1986). While Drexler arguably originated the term “nanomedicine,” it became popularized by Robert Freitas in his book *Nanomedicine* (Freitas, 1999). In the past 20 years, the

field of nanomedicine has expanded rapidly, and NPs have been investigated for a great many biomedical applications, including drug delivery, imaging, biosensors and more (Tibbals, 2011). Currently, a variety of NPs are approved for use in oral, topical, local, and intravenous administration for multitude of applications, and many other NP therapeutics are currently in clinical trials (Anselmo & Mitragotri, 2016). To focus the scope of the research performed for the purpose of this dissertation, three NPs which have current and/or proposed uses in biomedicine were studied.

Superparamagnetic iron oxide NPs (Fe_3O_4 NPs) have been proposed for many applications in biomedicine, including as target-specific carriers for drug delivery/gene therapy, magnetic resonance imaging (MRI) contrast agents, and diagnostic magnetic sensing probes (Babes, Jacques, Jeune, & Jallet, 1999; Ghazanfari, Kashefi, Shams, & Jaafari, 2016; Neuberger, Scho, Hofmann, & Rechenberg, 2005; P. Á. Tartaj, Morales, & Gonza, 2005; P. Tartaj, Morales, Veintemillas-verdaguer, & Gonz, 2003). Currently, Fe_3O_4 NPs are used a treatment for anemia in the form of Feraheme, an injectable bolus dose which increases blood iron levels (Bullivant, Zhao, Willenberg, & Kozissnik, 2013; Macdougall, 2013). Fe_3O_4 NP are considered to have high potential for use in biomedicine due to their stability, biocompatibility, modifiability, and reduced oxidation sensitivity (Ghazanfari et al., 2016; J. S. Kim et al., 2006; Majewski & Thierry, 2007). As Fe_3O_4 and other NPs are further developed and increasingly utilized in biomedical applications, the risk of human exposure increases (Inturi et al., 2015; Ryan & Brayden, 2014; W. Dobrucki, Pan, & M. Smith, 2015). While widely considered as biocompatible, various toxicity studies have shown adverse effects of Fe_3O_4 NP exposure. Multiple *in vitro* studies utilizing a variety of cell types have demonstrated toxicity, with fibroblasts experiencing losses in viability, cytoskeletal dysfunction, and disruption of the cellular membrane (Berry, Wells, Charles, & Curtis, 2003; Gupta, Berry, Gupta, & Curtis, 2003; Gupta & Curtis, 2004; Gupta & Wells, 2004). Macrophages also experience a severe decrease in cellular viability, likely due the production of reactive oxygen species via the Fenton reaction (Naqvi et al., 2010; Pawelczyk et al., 2008; Voinov, Paga, Morrison, Smirnova, & Smirnov, 2011). Other relevant cell types have had similarly adverse reactions to Fe_3O_4 NP exposure, experiencing altered mitochondrial function and DNA lesions (Au et al., 2007; Karlsson, Cronholm, Gustafsson, & Moller, 2008). Adverse effects have also been observed *in vivo*, inducing inflammation, alterations in enzyme activity, and tissue damage in the liver, kidney,

and lungs when injected (Hanini et al., 2011; Radu et al., 2015). Injection into the circulatory system may potentially result in both cardiovascular toxicity and systemic toxicity due to the translocation of Fe₃O₄ NPs throughout the body. In order to utilize Fe₃O₄ NPs in biomedicine safely and effectively, it is necessary to understand the degree and mechanism by which they elicit toxicological effects.

AuNPs have many current and proposed uses in biomedicine, as they are considered to have possess anti-inflammatory properties and elicit few if any toxicological effects (M. A. Khan & Khan, 2018; Shukla et al., 2005). While still considered an emerging technology, AuNPs are currently clinically utilized in modern biomedicine as imaging agents and to increase the specificity of chemotherapies (Haume et al., 2016; Thakor, Jokerst, Zavaleta, Massoud, & Gambhir, 2011). In the future, AuNPs may have far more uses in medicine than they do currently. AuNPs are proposed for use in photodynamic cancer therapy, drug delivery, and vaccines (Y. Cheng, Samia, Meyers, & Panagopoulos, 2008; Pati, Shevtsov, & Sonawane, 2018; Stuchinskaya, Moreno, Cook, Edwards, & Russell, 2011). Of particular interest is the utilization of AuNPs in brachytherapy, a type of radiation treatment in which radioactive material is placed inside the body near or inside of the cancerous area (S. Cho, Jeong, & Kim, 2010; Sinha et al., 2016; Yook et al., 2016). AuNPs have been shown to have advantages over traditional brachytherapy materials in that they may produce fewer artifacts in medical imaging, are easily tunable, and may be more easily administered (Laprise-pelletier, Lagueux, Côté, Lagrange, & Fortin, 2017; Laprise-pelletier, Simão, & Fortin, 2018). However, despite the potential of AuNPs to improve treatment efficacy, there is still a degree of trepidation regarding the use of AuNPs in medicine. This concern may be well-founded, as previous studies have found toxic effects in both *in vitro* and *in vivo* studies. Specifically, AuNPs have been observed to induce cytotoxic effects in human cells such as oxidative stress, cell death, and decreased proliferation, adhesion, and motility, particularly at smaller sizes (Pan et al., 2009, 2007; Pernodet et al., 2006; Tsoli, Kuhn, & Brandau, 2005). In *in vivo* rodent studies, AuNPs have been observed to induce inflammation and apoptosis within the liver, as well as alterations in the immune function of the spleen (E. C. Cho, Xie, Wurm, & Xia, 2009; W. Cho et al., 2009; Xiao-dong Zhang et al., 2011). Further research is needed in order to resolve these contradictory results regarding the toxicity of AuNPs, particularly if their use in biomedical applications is to continue and expand.

As previously mentioned, AgNPs are one of the most popular nanomaterials utilized due to their antimicrobial activity. Because of this, AgNPs are used in burn creams, wound dressings, venous catheters, surgical implants, and other applications which result in direct introduction of the nanomaterials to the circulatory system (Chaloupka, Malam, & Seifalian, 2010; L. Ge et al., 2014; Song & Kim, 2009). While AgNPs are frequently used in biomedical applications, the understanding of their toxicological effects in humans is still incomplete. Exposure to AgNPs causes cytotoxic effects, including loss of viability and the production of ROS, in human cells such as macrophages and stem cells (Haase et al., 2011; Hackenberg et al., 2011). Direct studies of AgNPs used in medicinal dressings have shown that keratinocytes and fibroblasts experience a loss of viability following exposure, possibly indicating that AgNPs may slow wound healing (Lam, Chan, Ho, & In, 2004; Paddle-Ledinek, Nasa, & Cleland, 2006; Poon & Burd, 2004). Research of the effects of AgNPs exposure *in vivo* has primarily focused on the liver, as it is the primarily site of deposition for inhaled or subcutaneously injected AgNPs; however, they are also found in the brain, lungs, and kidneys (Takenaka et al., 2001; J. Tang et al., 2009). Similar to many *in vitro* studies, animal models have produced results that indicate potential hazards of utilization, with AgNP exposure inducing inflammation and apoptosis within the liver and brain (R. Chen et al., 2016; Rahman et al., 2009; Ramadi et al., 2016). The kinetics of AgNP elimination are an additional cause for concern, as injected and ingested AgNPs are retained within the brain for months (Dziendzikowska et al., 2012; Zande et al., 2012). AgNP exposure has also been shown to elicit a robust inflammatory response in macrophages, fibroblasts, and endothelial cells, as well as in the liver tissue of animal models (R. Chen et al., 2016; M. V. D. Z. Park et al., 2011; Ramadi et al., 2016; Trickler et al., 2010). Despite the extent of the current research on AgNP toxicity and NP toxicity at large, there is still a great deal which is unknown regarding susceptibility to exposure.

1.4 Disease and NP Exposure

While NPs utilized in biomedical applications will, by definition, be used in unhealthy individuals, their toxicity and efficacy in disease models is very poorly characterized. This is problematic, as a large proportion of the United States and worldwide population suffers from a form of chronic disease. Specifically, approximately 60% of adults in the United States and 30% of adults worldwide have at least one chronic health condition (CDC, 2019; Hajat & Stein, 2018). While chronic diseases have traditionally been associated with highly industrialized, wealthy countries,

they have recently begun to emerge as a leading cause of death in developing countries, as well (Nugent, 2008). Cardiovascular disease, cancer, and diabetes are considered to be the most common of the end-stage diseases, contributing to approximately 45% of deaths worldwide (Beaglehole, Ebrahim, Reddy, & Leeder, 2007). However, there are other, more common mid-stage conditions which may be considered diseases in their own right, but are also risk factors for the development of end-stage diseases such as diabetes and cardiovascular disease. Obesity, metabolic syndrome (MetS), and high cholesterol are among the most common of these mid-stage diseases, affecting approximately 40%, 20%, and 12% of adults in the United States, respectively (Aguilar, Bhuket, Torres, Liu, & Wong, 2015; Beltrán-Sánchez, Harhay, Harhay, & McElligott, 2013; Carroll, Fryar, & Kit, 2015; Flegal, Kruszon-moran, Carroll, Fryar, & Ogden, 2019). These diseases are also frequently comorbid with one another, with obesity and high cholesterol constituting two core factors for the identification of MetS, along with elevated triglyceride levels, fasting glycemia, and high blood pressure (Despres & Lemieux, 2006). In addition to being common, the prevalence of these each of these diseases is increasing with time both within and outside of the United States (CDC, 2012; Desroches & Lamarche, 2007; Devito, French, & Goldacre, 2018; Filozof, Gonzalez, Sere day, Mazza, & Braguinsky, 2001; Ford, Giles, & Mokdad, 2004). The increasing prevalence of MetS, and with it obesity and high cholesterol, presents an additional problem regarding environmental exposures.

While MetS presents a specific set of symptoms which afflicted individuals must contend with, it also predisposes such individuals to the development of various conditions such as kidney disease, gallstone disease, and cataracts (Kurella, Lo, & Chertow, 2005; Méndez-sánchez et al., 2005; Reddy, Giridharan, & Reddy, 2012). Additionally, MetS may increase the chance of experiencing adverse reactions following exposures to various environmental toxicants and pathogens. For instance, research has demonstrated that individuals with MetS are more susceptible to autonomic dysfunction as a result of low-level lead exposure, making diseased individuals more prone to cardiac events and heart failure (S. K. Park et al., 2006). Additionally, it has been shown to cause individuals to be more susceptible to adverse health outcomes as a consequence of exposure to carbon monoxide, with greater negative effects on cardiac autonomic function taking place for those with MetS (Min, Paek, Cho, & Min, 2009). This phenomenon extends to non-chemical exposures, as well. Individuals with MetS have been shown to be more vulnerable to the effects

of *Aggregatibacter actinomycetemcomitans*, a common periodontal infection. It was determined that not only was MetS associated with higher antibody levels against *A. actinomycetemcomitans*, but a more severe degree of periodontal disease as identified by a higher number of missing teeth (Hyvarinen, Salminen, Salomaa, & Pussinen, 2015). MetS has also been shown to exacerbate the adverse reaction to nano-sized exposures; specifically, individuals with MetS see greater inflammation, autonomic dysfunction, and cardiovascular depression than healthy individuals following exposure to nano-sized particulate matter (J. Chen & Schwartz, 2008; Devlin et al., 2014; S. K. Park et al., 2010; Wagner et al., 2014). While the mechanisms responsible for this increased susceptibility in disease are not fully understood, it is thought that the higher level of baseline inflammation that frequently exists in individuals with MetS may predispose them to adverse acute and chronic health outcomes (Esser, Legrand-poels, Piette, Scheen, & Paquot, 2014; Haffner, 2006; Isomaa et al., 2001; Paoletti, Bolego, Poli, & Cignarella, 2006). As shown by the above described research, the mechanisms which are responsible for the exacerbation of responses in MetS are not exclusive to one specific substance. Therefore, it is likely that these mechanisms will influence how individuals respond to NP exposure in biomedical settings.

Unfortunately, there is a lack of information regarding how the increased susceptibility of individuals with MetS impacts their reactions to NP exposure. However, the limited research which has taken place has demonstrated that MetS and its components exacerbate adverse reactions to NP exposure. Most of the research which has examined the effects of disease on NP toxicity has been performed using *in vitro* models. One such study examined the influence of a hyperlipidemic physiological environment, and found that under such conditions, NPs exposure caused enhanced activation of endothelial cells and increased expression of inflammatory cytokines such as interleukin 6 and monocyte chemoattractant protein 1 when compared to the same NP under healthy conditions (Shannahan et al., 2016). Similar studies that have examined the effect of high HDL cholesterol specifically have supported this finding and found that compared to healthy conditions, high HDL cholesterol conditions cause enhanced NP uptake and pro-inflammatory gene expression (Persaud et al., 2019; Shannahan et al., 2015). While multiple epidemiological and *in vivo* studies have been performed examining the effects of nano-sized particulate matter on humans and animal models with MetS, such as those detailed above, investigations of the toxicity of engineered NPs in disease utilizing *in vivo* models have been less

frequent. However, the findings have supported the conclusions of previous *in vitro* studies in that MetS exacerbates the response to NP exposure. Specifically, it was determined that oral exposure to carbon black NPs caused a deterioration in the vascular function of both healthy and MetS mice, and that the MetS mice had worse vascular function than the healthy mice following carbon black NP exposure (Folkmann, Vesterdal, Sheykhzade, Loft, & Møller, 2012). While the research which has taken place thus far has provided valuable insights, there remains much which is unknown regarding the effect of disease on NP toxicity. Many of the *in vitro* studies which have examined the impact of disease on NP toxicity have utilized rat or bovine serum in order to model human physiological conditions. While this is useful to a point, utilization of human-derived experimental materials would allow for more accurate extrapolation to real-world scenarios and thus more relevant conclusions. There is also a dearth of *in vivo* studies examining the impact of MetS and other diseases on NP toxicity in a whole organism. Finally, the mechanism by which diseases such as MetS predispose individuals to exacerbated inflammatory responses and subsequent cardiac dysfunction following NP exposure is poorly understood; however, it is likely that repeated NP exposure may contribute to diseases which have significant inflammatory and cardiovascular components, such as coronary artery disease.

1.5 The Biocorona

Despite the potential of NP therapeutics to improve medicine, their use is still limited, and many therapeutics which show promise in experiments go on to fail clinical trials (Schutz, Juillerat-Jeanneret, Mueller, Lynch, & Riediker, 2013). This is largely due to a lack of translatability that has been observed in studies of NP toxicity, both in healthy and diseased models. Findings *in vitro* have not translated to *in vivo* experiments, and results which have seen robust support in the laboratory have proven to be untrue in clinical applications. These issues in translatability are due to the inability to properly model complex human systems, resulting in unforeseen differences in kinetics, delivery, accumulation, toxicity, and efficacy once NP therapeutics enter clinical trials (Bisht & Maitra, 2009; Schutz et al., 2013). The difficulties in translating findings on NP efficacy and toxicity from the lab to the clinic is due at least in part to the biocorona (BC). The BC is a biomolecular coating which forms on the surface of the NP upon exposure to a physiological environment. The identities and quantities of biomolecules within the BC are influenced by many factors, including time, the composition of the surrounding biological milieu, and properties of the

NP such as size, coating, charge, surface curvature, and hydrophobicity (Kobos, Adamson, Evans, Gavin, & Shannahan, 2018; Sahneh, Scoglio, & Riviere, 2013; Shannahan et al., 2016; Walkey & Chan, 2012). The first publications regarding the protein adsorption to the NP surface were released in 2005, and the term “corona” was coined by the scientific community as a way to describe this coating soon after in 2007 (Cedervall et al., 2007; Goppert & Muller, 2005; Labarre et al., 2005). While traditionally the NP has been considered to consist primarily of proteins, recent research has demonstrated that the BC is in fact a complex network proteins, lipids, and other biomolecules (Hellstrand et al., 2009; Landry et al., 2015; Müller et al., 2018; Raesch et al., 2015). It has been shown that the presence of a BC impacts the use on NPs in biomedicine. Specifically, the BC has been shown to alter the relaxivity of superparamagnetic Fe₃O₄ NPs, which subsequently caused changes in their function as MRI contrast agents (Amiri et al., 2013). Additionally, transferrin-coated NPs lose their targeting abilities when coated with a BC (Salvati et al., 2013). The BC is thought to be the reason for many of the difficulties that have occurred in translating NP therapeutics to clinical use, as the biomolecular coating covers the surface area of the NP, preventing any cells which interact with it from “seeing” the particle underneath.

But it is not only functionality in biomedical applications that is impacted by the BC. NP toxicity is also greatly altered both by its presence and composition. Generally speaking, the BC attenuates NP toxicity. This has been demonstrated in numerous studies utilizing multiple cell types; for instance, a plasma BC has been shown to enhance the viability and decrease the expression of genes associated with stress and damage in endothelial cells (Chandran et al., 2017; Tenzer et al., 2013). Similar results have been observed in A549 epithelial cells, with the toxicity of graphene oxide nanosheets, silica NPs, and poly-3-hydroxybutyrate-co-3-hydroxyhexanoate NPs mitigated by the presence of a BC (Hu et al., 2011; Lesniak et al., 2012; Panas et al., 2013; Peng et al., 2013). However, it is not always the case the BC lessens NP toxicity; depending on composition of the NP and the BC, toxicity may be unaffected or even heightened when compared to a bare NP. Studies utilizing AuNPs, which are relatively inert in biological environments, have shown no changes in the viability of exposed epithelial cells due to the presence of a BC (X. Cheng et al., 2015; Connor, Mwamuka, Gole, Murphy, & Wyatt, 2005). The inflammatory response of endothelial cells following exposure to Fe₃O₄ NPs and multi-walled carbon nanotubes was greater with a BC than with a bare particle (Shannahan et al., 2016; Vidanapathirana et al., 2012). These

studies indicate that while the BC is frequently protective and acts as a barrier to toxic effects, this is not the case for all NPs. In addition to the core NP's influence on such interactions, specific components of the BC have been found to influence the cellular response, both in terms of attenuating and enhancing toxicity. Fibrinogen and albumin within the BC enhance endothelial cell viability following NP exposure (C. Ge et al., 2011; Lu, Sui, Tian, & Peng, 2018). However, other proteins within the BC have decidedly less positive effects. A BC consisting primarily of immunoglobulin has been determined to cause a significant increase in the release of myeloperoxidase by neutrophils, indicating immune activation (Lu et al., 2018). Low density lipoprotein within the BC also enhances NP toxicity in the form of eliciting an exaggerated inflammatory response (Shannahan et al., 2015). It is clear that the composition of the BC has a significant impact on the reaction to NP exposure, with some proteins enhancing toxicity and others attenuating it. The influence of the BC adds an additional factor that must be considered when testing NPs in the laboratory and utilizing NP therapeutics in clinical settings.

Though the BC is frequently considered as an obstacle to the use of NPs in medicine, it may in fact be utilized as a method to more effectively model the biomolecular interactions which take place during clinical use. Despite this potential, there has been limited study of the BC under variable conditions. Theoretically, any disease or condition which alters the protein chemistry of the serum has the capacity to alter the content of a BC which enters circulation. This has been proven in studies of the effect of hyperlipidemic physiological conditions on BC composition. Not only do diseased BCs vary in the number and quantity of proteins they contain, NPs with hyperlipidemic BCs elicit a differential biological response (Raghavendra et al., 2017; Shannahan et al., 2016). Specifically, endothelial cells which are exposed to a NP with a hyperlipidemic BC have a greater inflammatory response than those exposed to a NP with a healthy BC (Shannahan et al., 2016). While it is clear that hyperlipidemia impacts BC composition and NP toxicity, the effects of other diseases and conditions are unknown. Few researchers have examined how the BC is altered due to factors such as disease or individual variability, despite the potential effect that these variables may have on NP efficacy and toxicity. It is the goal of the research described in this dissertation to identify and detail variations which exist BC as a result of common diseases and to describe how these variations impact toxicity in both *in vitro* and *in vivo* models. By this,

NP therapeutics may be further developed and utilized in a manner that maximizes both their efficacy and safety.

1.6 Structure of Dissertation

The central hypothesis is that the presence of disease and individual variability will alter composition of the biocorona and the toxicity of NPs. Specially, we hypothesize that obesity, high cholesterol, and MetS will cause differences in the quantities and varieties of biomolecules adsorbed to the NP surface, which will result in exacerbated adverse reactions to medically relevant NPs. Both *ex vivo*, *in vitro*, and *in vivo* models will be used to examine this hypothesis and evaluate the inflammatory response that occurs in response to exposure to medically relevant NPs. The overall impact of this research will assist in the continued development and utilization of NPs in biomedical applications.

Specific Aim 1 (Chapter 2): To test the hypothesis that obesity impacts the BC composition of AuNPs, and that this variation affects particle toxicity. While obesity is exceedingly common in the United States and worldwide, its impact on the NP-BC and AuNP toxicity is unknown. The aim utilized pooled serum collected from healthy and obese individuals in order to form BCs on a variety of AuNPs and assess differences in BC composition as a result of obesity. Mass spectrometry was used to identify and quantify differences in the biomolecular content of the BC, and PCR was used to examine the inflammatory response of macrophages following exposure to AuNPs with a healthy BC or obese BC.

Specific Aim 2 (Chapter 3): This study examines the impact of individual variability and exercise on the BC of Fe₃O₄ NPs, and how NP toxicity is altered by these factors. Fe₃O₄ NPs are commonly utilized in biomedical applications, but it is unknown if differences in the biological milieu that occur as a result of individual variability and lifestyle changes such as exercise may impact the content of the BC, and if this may affect NP efficacy and toxicity. This aim utilized plasma from individual human subjects prior to and following a 7-day exercise regimen. Mass spectrometry was used to identify and quantify differences in the biomolecular content of the BC, and PCR was used to examine the inflammatory response of macrophages following exposure to Fe₃O₄ NPs with pre- and post-exercise BCs from select subjects.

Specific Aim 3 (Chapter 4): This study examines whether the NP-induced toxicological effects which were previously observed *in vitro* effects translate to an *in vivo* model. Given the frequency of use of AgNPs in biomedicine, and the prevalence of MetS in the United States, it is necessary to understand the influence of this disease on the toxicity of AgNP exposure. Healthy and MetS C57BL6 mice were injected with AgNPs and their response examined in the form of inflammation and biodistribution. Atomic absorption spectrometry was used to determine the metal content of each organ following injection, and PCR was used to examine the expression of inflammatory genes in organs which were found to accumulate AgNPs.

By the completion of these studies, gaps that currently exist within the scientific knowledge will be filled. Specifically, the described experiments will discover how common diseases and individual variability impact BC composition, and further, how this variation affects the immune and inflammatory responses. This information may aid in the future development and utilization of NPs in biomedical applications through the identification of vulnerable subpopulations who may at risk for adverse or exacerbated reactions following NP exposure, and thus contribute to the goal of protecting public health.

1.7 References

- Abbas, M., Walvekar, R. G., Hajibeigy, M. T., & Farhood, S. (2013). Efficient Air-Condition Unit By Using Nano-Refrigerant. *Eureca*, *1*, 87–88.
- Aguilar, M., Bhuket, T., Torres, S., Liu, B., & Wong, R. J. (2015). Prevalence of the Metabolic Syndrome in the United States, 2003-2012. *Jama*, *313*(19), 1973–1974.
- Amiri, H., Bordonali, L., Lascialfari, A., Wan, S., Monopoli, M. P., Lynch, I., ... Mahmoudi, M. (2013). Protein corona affects the relaxivity and MRI contrast efficiency of magnetic nanoparticles. *Nanoscale*, *5*(18), 8656–8665. <https://doi.org/10.1039/c3nr00345k>
- Anselmo, A. C., & Mitragotri, S. (2016). Nanoparticles in the clinic. *Bioengineering & Translational Medicine*, *1*, 10–29. <https://doi.org/10.1002/btm2.10003>

- Au, C., Mutkus, L., Dobson, A., Riffle, J., Lalli, J., & Aschner, M. (2007). Effects of Nanoparticles on the Adhesion and Cell Viability on Astrocytes. *Biological Trace Element Research*, 120, 248–256. <https://doi.org/10.1007/s12011-007-0067-z>
- Auffan, M., Rose, J., Bottero, J., Lowry, G. V, Jolivet, J., & Wiesner, M. R. (2009). Towards a definition of inorganic nanoparticles from an environmental, health and safety perspective. *Nature Nanotechnology*, 4(10), 634. <https://doi.org/10.1038/nnano.2009.242>
- Babes, L., Jacques, J., Jeune, L., & Jallet, P. (1999). Synthesis of Iron Oxide Nanoparticles Used as MRI Contrast Agents : A Parametric Study. *Journal of Colloid and Interface Science*, 212, 474–482.
- Beaglehole, R., Ebrahim, S., Reddy, S., & Leeder, S. (2007). Prevention of chronic diseases : a call to action. *The Lancet*, 370, 2152–2157. [https://doi.org/10.1016/S0140-6736\(07\)61700-0](https://doi.org/10.1016/S0140-6736(07)61700-0)
- Beltrán-Sánchez, H., Harhay, M. O., Harhay, M. M., & McElligott, S. (2013). Prevalence and trends of Metabolic Syndrome in the adult US population, 1999–2010. *Journal of the American College of Cardiology*, 62(8), 697–703. <https://doi.org/10.1016/j.jacc.2013.05.064>.Prevalence
- Berry, C. C., Wells, S., Charles, S., & Curtis, A. S. G. (2003). Dextran and albumin derivatised iron oxide nanoparticles : influence on fibroblasts in vitro. *Biomaterials*, 24, 4551–4557. [https://doi.org/10.1016/S0142-9612\(03\)00237-0](https://doi.org/10.1016/S0142-9612(03)00237-0)
- Birrenbach, G., & Speiser, P. P. (1976). Polymerized Micelles and Their Use as Adjuvants in Immunology. *Journal of Pharmaceutical Sciences*, 65(12), 1763–1766. <https://doi.org/10.1002/jps.2600651217>
- Birrenbach, Gerd. (1973). Ueber Mizellpolymerisate, mögliche Einschlussverbindungen(Nanokapseln) und deren Eignung als Adjuvantien. *Doctoral Dissertation, ETH Zurich*.
- Bisht, S., & Maitra, A. (2009). Dextran-doxorubicin/chitosan nanoparticles for solid tumor therapy, 415–425. <https://doi.org/10.1002/wnan.043>

- Bisiaux, M. M., Edwards, R., Heyvaert, A. C., Thomas, J. M., Fitzgerald, B., Susfalk, R. B., ... Thaw, M. (2011). Stormwater and Fire as Sources of Black Carbon Nanoparticles to Lake Tahoe. *Environmental Science and Technology*, 45(6), 2065–2071.
<https://doi.org/10.1021/es103819v>
- Bourzac, K. (2013). Quantum dots go on display. *Nature*, 493, 283.
- Brichkin, S. B., & Razumov, V. F. (2016). Colloidal quantum dots : synthesis , properties and applications. *Russian Chemical Reviews*, 85(12), 1297–1312.
<https://doi.org/10.1070/RCR4656>
- Bullivant, J. P., Zhao, S., Willenberg, B. J., & Kozissnik, B. (2013). Materials Characterization of Feraheme / Ferumoxytol and Preliminary Evaluation of Its Potential for Magnetic Fluid Hyperthermia. *International Journal of Molecular Sciences*, 14, 17501–17510.
<https://doi.org/10.3390/ijms140917501>
- Cao, L., Bai, X., Lin, Z., Zhang, P., Deng, S., Du, X., & Li, W. (2017). The Preparation of Ag Nanoparticle and Ink Used for Inkjet Printing of Paper Based Conductive Patterns. *Materials*, 10(1004), 1–9. <https://doi.org/10.3390/ma10091004>
- Carroll, M. D., Fryar, C. D., & Kit, B. K. (2015). Total and High-density Lipoprotein Cholesterol in Adults : United States , 2011 – 2014. *NCHS Data Brief*, 226(December).
- CDC. (2012). Prevalence of Cholesterol Screening and High Blood Cholesterol Among Adults — United States, 2005, 2007, and 2009. *Centers for Disease Control and Prevention Morbidity and Mortality Weekly Report*, 61(35), 697–702.
- CDC. (2019). *Chronic diseases in america*.
- Cedervall, T., Lynch, I., Foy, M., Berggård, T., Donnelly, S. C., Cagney, G., ... Dawson, K. A. (2007). Detailed Identification of Plasma Proteins Adsorbed on Copolymer. *Angewandte Chemie International Edition*, 46, 5754–5756. <https://doi.org/10.1002/anie.200700465>

- Chaloupka, K., Malam, Y., & Seifalian, A. M. (2010). Nanosilver as a new generation of nanoparticle in biomedical applications. *Trends in Biotechnology*, 28(11), 580–588. <https://doi.org/10.1016/j.tibtech.2010.07.006>
- Chandran, P., Riviere, J. E., Monteiro-riviere, N. A., Chandran, P., Riviere, J. E., & Monteiro-riviere, N. A. (2017). Surface chemistry of gold nanoparticles determines the biocorona composition impacting cellular uptake, toxicity and gene expression profiles in human endothelial cells. *Nanotoxicology*, 5390. <https://doi.org/10.1080/17435390.2017.1314036>
- Chen, H., Roco, M. C., Li, X., & Lin, Y. (2008). Trends in nanotechnology patents. *Nature Nanotechnology*, 3(March), 123–125.
- Chen, J., & Schwartz, J. (2008). Metabolic Syndrome and Inflammatory Responses to Long-Term Particulate Air Pollutants. *Environmental Health Perspectives*, 116(5), 612–617. <https://doi.org/10.1289/ehp.10565>
- Chen, R., Zhao, L., Bai, R., Liu, Y., Han, L., Xu, Z., ... Chen, C. (2016). Silver nanoparticles induced oxidative and endoplasmic reticulum stresses in mouse tissues: implications for the development of acute toxicity after intravenous administration. *Toxicology Research*, 1, 602–608. <https://doi.org/10.1039/c5tx00464k>
- Cheng, X., Tian, X., Wu, A., Li, J., Tian, J., Chong, Y., ... Ge, C. (2015). Protein Corona Influences Cellular Uptake of Gold Nanoparticles by Phagocytic and Nonphagocytic Cells in a Size-Dependent Manner. <https://doi.org/10.1021/acsami.5b04290>
- Cheng, Y., Samia, A. C., Meyers, J. D., & Panagopoulos, I. (2008). Highly Efficient Drug Delivery with Gold Nanoparticle Vectors for in Vivo Photodynamic Therapy of Cancer. *Journal of the American Chemical Society*, 10643–10647. <https://doi.org/10.1021/ja801631c>
- Cho, E. C., Xie, J., Wurm, P. A., & Xia, Y. (2009). Understanding the Role of Surface Charges in Cellular Adsorption versus Internalization by Selectively Removing Gold Nanoparticles on the Cell Surface with a I₂ / KI Etchant 2009. *Nano Letters*, 9(3), 1080–1084.

- Cho, S., Jeong, J. H., & Kim, C. H. (2010). Monte Carlo Simulation Study on Dose Enhancement by Gold Nanoparticles in Brachytherapy. *Journal of the Korean Physical Society*, 56(6), 1754~1758. <https://doi.org/10.3938/jkps.56.1754>
- Cho, W., Cho, M., Jeong, J., Choi, M., Cho, H., Seok, B., ... Jeong, J. (2009). Acute toxicity and pharmacokinetics of 13 nm-sized PEG-coated gold nanoparticles. *Toxicology and Applied Pharmacology*, 236(1), 16–24. <https://doi.org/10.1016/j.taap.2008.12.023>
- Clunan, A. L., Rodine-Hardy, K., Hsuch, R., Kosal, M. E., & McManus, I. (2014). Nanotechnology in a Globalized World Strategic Assessments of an Emerging Technology. *Project on Advanced Systems and Concepts for Countering Weapons of Mass Destruction*, 1, 1–100.
- Connor, E. E., Mwamuka, J., Gole, A., Murphy, C. J., & Wyatt, M. D. (2005). Gold nanoparticles are taken up by human cells but do not cause acute cytotoxicity. *Small*, 1(3), 325–327. <https://doi.org/10.1002/sml.200400093>
- Coronado, E. A., Encina, E. R., & Stefani, F. D. (2011). Nanoscale Optical properties of metallic nanoparticles : manipulating light , heat and forces at the nanoscale. *Nanoscale*, 3, 4042–4059. <https://doi.org/10.1039/c1nr10788g>
- Despres, J.-P., & Lemieux, I. (2006). Abdominal obesity and metabolic syndrome. *Nature*, 444, 881–887.
- Desroches, S., & Lamarche, B. (2007). The evolving definitions and increasing prevalence of the metabolic syndrome. *Applied Physiology, Nutrition, and Metabolism*, 32(1), 23–32. <https://doi.org/10.1139/H06-095>
- Devito, N. J., French, L., & Goldacre, B. (2018). Trends in Obesity and Severe Obesity Prevalence in US Youth and Adults by Sex and Age , 2007-2008 to 2015-2016. *Jama*, 319(16), 1723–1725.

- Devlin, R. B., Smith, C. B., Schmitt, M. T., Rappold, A. G., Hinderliter, A., & Graff, D. (2014). Controlled Exposure of Humans with Metabolic Syndrome to Concentrated Ultrafine Ambient Particulate Matter Causes Cardiovascular Effects. *Toxicological Sciences*, *140*(1), 61–72. <https://doi.org/10.1093/toxsci/kfu063>
- Drexler, K. E., Peterson, C., & Pergamit, G. (1991). *Unbounding the future*.
- Drexler K, E. (1986). *Engines of Creation. The Coming Era of Nanotechnology*.
- Dziendzikowska, K., Gromadzka-ostrowska, J., Lankoff, A., Oczkowski, M., Krawczy, A., Chwastowska, J., ... Du, M. (2012). Time-dependent biodistribution and excretion of silver nanoparticles in male Wistar rats. *Journal of Applied Toxicology*, *32*(11), 920–928. <https://doi.org/10.1002/jat.2758>
- Echegoyen, Y., & Nerín, C. (2013). Nanoparticle release from nano-silver antimicrobial food containers. *Food and Chemical Toxicology*, *62*, 16–22. <https://doi.org/10.1016/j.fct.2013.08.014>
- Ekimov, A. I., Efros, A. L., & Onushchenko, A. A. (1985). Quantum Size Effect in Semiconductor Microcrystals. *Solid State Communications*, *56*(11), 921–924. [https://doi.org/10.1016/S0038-1098\(85\)80025-9](https://doi.org/10.1016/S0038-1098(85)80025-9)
- Esawi, A. M. K., & Farag, M. M. (2007). Materials & Design Carbon nanotube reinforced composites : Potential and current challenges. *Materials & Design*, *28*, 2394–2401. <https://doi.org/10.1016/j.matdes.2006.09.022>
- Esser, N., Legrand-poels, S., Piette, J., Scheen, J., & Paquot, N. (2014). Inflammation as a link between obesity , metabolic syndrome and type 2 diabetes. *Diabetes Research and Clinical Practice*, *105*, 141–150. <https://doi.org/10.1016/j.diabres.2014.04.006>
- Fadhilah, S. A., Marhamah, R. S., & Izzat, A. H. M. (2014). Copper Oxide Nanoparticles for Advanced Refrigerant Thermophysical Properties : Mathematical Modeling. *Journal of Nanoparticles*, *1*, 2–7.

- Faraday, M. (1857). Experimental relations of gold (and other metals) to light.—The bakerian lecture. *Philosophical Transactions of the Royal Society of London*, 147, 145–191.
<https://doi.org/10.1080/14786445708642424>
- Faulstich, L., Grif, S., Jawad, M., Irfan, M., Ali, W., Alhamound, S., ... Jacob, C. (2017). International Biodeterioration & Biodegradation Nature ' s Hat-trick : Can we use sulfur springs as ecological source for materials with agricultural and medical applications ? *International Biodeterioration & Biodegradation*, 119, 678–686.
<https://doi.org/10.1016/j.ibiod.2016.08.020>
- Feynman, R. P. (1959). There's Plenty of Room at the Bottom: An Invitation to Enter a New Field of Physics. *Engineering and Science*, XXIII(5), 22–36.
- Filozof, C., Gonzalez, C., Sereday, M., Mazza, C., & Braguinsky, J. (2001). Obesity prevalence and trends in Latin-American. *Obesity Reviews*, 2, 99–106.
- Flegal, K. M., Kruszon-moran, D., Carroll, M. D., Fryar, C. D., & Ogden, C. L. (2019). Trends in Obesity Among Adults in the United States, 2005 to 2014. *Jama*, 20782(21), 2284–2291.
<https://doi.org/10.1001/jama.2016.6458>
- Folkmann, J. K., Vesterdal, L. K., Sheykhzade, M., Loft, S., & Møller, P. (2012). Endothelial Dysfunction in Normal and Prediabetic Rats With Metabolic Syndrome Exposed by Oral Gavage to Carbon Black Nanoparticles. *Toxicological Sciences*, 129(1), 98–107.
<https://doi.org/10.1093/toxsci/kfs180>
- Ford, E. S., Giles, W. H., & Mokdad, A. H. (2004). Increasing Prevalence of the Metabolic Syndrome Among U.S Adults. *Diabetes Care*, 27(10), 2444–2449.
- Freestone, I., Meeks, N., Sax, M., & Higgitt, C. (2007). The Lycurgus Cup - A Roman Nanotechnology. *Gold Bulletin*, 40(4), 270–277.
- Freitas, R. A. (1999). *Nanomedicine, volume I: basic capabilities*.
- Ge, C., Du, J., Zhao, L., Wang, L., Liu, Y., Li, D., ... Zhou, R. (2011). Binding of blood proteins to carbon nanotubes reduces cytotoxicity. <https://doi.org/10.1073/pnas.1105270108>

- Ge, L., Li, Q., Wang, M., Ouyang, J., Li, X., & Xing, M. M. (2014). Nanosilver particles in medical applications : synthesis , performance , and toxicity. *International Journal of Nanomedicine*, *9*, 2399–2407.
- Ghazanfari, M. R., Kashefi, M., Shams, S. F., & Jaafari, M. R. (2016). Perspective of Fe₃O₄ Nanoparticles Role in Biomedical Applications. *Biochemistry Research International*, *1*.
- Glatzmaier, G. C., Pradhan, S., Kang, J., Curtis, C., & Blake, D. (2010). Encapsulated Nanoparticle Synthesis and Characterization for Improved Storage Fluids. *National Renewable Energy Lab*, *1*, 1–7.
- Gohardani, O., Chapartegui, M., & Elizetxea, C. (2014). Progress in Aerospace Sciences Potential and prospective implementation of carbon nanotubes on next generation aircraft and space vehicles : A review of current and expected applications in aerospace sciences. *Progress in Aerospace Sciences*, *70*, 42–68. <https://doi.org/10.1016/j.paerosci.2014.05.002>
- Goppert, T. M., & Muller, R. H. (2005). Protein adsorption patterns on poloxamer- and poloxamine-stabilized solid lipid nanoparticles (SLN). *European Journal of Pharmaceutics and Biopharmaceutics*, *60*, 361–372. <https://doi.org/10.1016/j.ejpb.2005.02.006>
- Gotoh, A., Uchida, H., Ishizaki, M., Satoh, T., Kaga, S., Okamoto, S., ... Kurihara, M. (2007). Simple synthesis of three primary colour nanoparticle inks of Prussian blue and its analogues. *Nanotechnology*, *18*, 1–6. <https://doi.org/10.1088/0957-4484/18/34/345609>
- Griffin, S., Masood, M. I., Nasim, M. J., Sarfraz, M., Ebokaiwe, A. P., Schäfer, K., ... Jacob, C. (2018). Natural Nanoparticles : A Particular Matter Inspired by Nature. *Antioxidants*, *7*(1). <https://doi.org/10.3390/antiox7010003>
- Guo, H., & Barnard, A. S. (2013). Naturally occurring iron oxide nanoparticles: morphology, surface chemistry and environmental stability. *Journal of Materials Chemistry A*, *1*(1), 27–42. <https://doi.org/10.1039/c2ta00523a>

- Gupta, A. K., Berry, C., Gupta, M., & Curtis, A. (2003). Receptor-Mediated Targeting of Magnetic Nanoparticles Using Insulin as a Surface Ligand to Prevent Endocytosis. *IEEE Transactions on Nanobioscience*, 2(4), 255–261.
- Gupta, A. K., & Curtis, A. S. G. (2004). Lactoferrin and ceruloplasmin derivatized superparamagnetic iron oxide nanoparticles for targeting cell surface receptors. *Biomaterials*, 25, 3029–3040. <https://doi.org/10.1016/j.biomaterials.2003.09.095>
- Gupta, A. K., & Wells, S. (2004). Surface-Modified Superparamagnetic Nanoparticles for Drug Delivery : Preparation , Characterization , and Cytotoxicity Studies. *IEEE Transactions on Nanobioscience*, 3(1), 66–73.
- Haase, A., Tentschert, J., Jungnickel, H., Graf, P., Manton, A., Draude, F., ... Luch, A. (2011). Toxicity of silver nanoparticles in human macrophages: uptake , intracellular distribution and cellular responses. *Journal of Physics: Conference Series*, 304(1). <https://doi.org/10.1088/1742-6596/304/1/012030>
- Hackenberg, S., Scherzed, A., Kessler, M., Hummel, S., Technau, A., Froelich, K., ... Kleinsasser, N. (2011). Silver nanoparticles : Evaluation of DNA damage , toxicity and functional impairment in human mesenchymal stem cells. *Toxicology Letters*, 201(1), 27–33. <https://doi.org/10.1016/j.toxlet.2010.12.001>
- Haffner, S. M. (2006). The Metabolic Syndrome: Inflammation , Diabetes Mellitus, and Cardiovascular Disease. *The American Journal of Cardiology*, 97, 2–11. <https://doi.org/10.1016/j.amjcard.2005.11.010>
- Hajat, C., & Stein, E. (2018). The global burden of multiple chronic conditions : A narrative review. *Preventive Medicine Reports*, 12, 284–293. <https://doi.org/10.1016/j.pmedr.2018.10.008>
- Hanini, A., Schmitt, A., Kacem, K., Chau, F., Ammar, S., & Gavard, J. (2011). Evaluation of iron oxide nanoparticle biocompatibility. *International Journal of Nanomedicine*, 6, 787–794. <https://doi.org/10.2147/IJN.S17574>

- Haume, K., Rosa, S., Grellet, S., Śmiałek, M. A., Butterworth, K. T., Solov, A. V., ... Mason, N. J. (2016). Gold nanoparticles for cancer radiotherapy : a review. *Cancer Nanotechnology*. <https://doi.org/10.1186/s12645-016-0021-x>
- Hellstrand, E., Lynch, I., Andersson, A., Drakenberg, T., Dahlbäck, B., Dawson, K. A., ... Cedervall, T. (2009). Complete high-density lipoproteins in nanoparticle corona. *FEBS Journal*, 276(12), 3372–3381. <https://doi.org/10.1111/j.1742-4658.2009.07062.x>
- Hough, R. M., Noble, R. R. P., & Reich, M. (2011). Natural gold nanoparticles. *Ore Geology Reviews*, 42(1), 55–61. <https://doi.org/10.1016/j.oregeorev.2011.07.003>
- Hu, W., Peng, C., Lv, M., Li, X., Zhang, Y., Chen, N., ... Huang, Q. (2011). Protein Corona-Mediated Mitigation of Cytotoxicity of Graphene Oxide, (5), 3693–3700. <https://doi.org/10.1021/nn200021j>
- Hyvarinen, K., Salminen, A., Salomaa, V., & Pussinen, P. J. (2015). Systemic exposure to a common periodontal pathogen and missing teeth are associated with metabolic syndrome. *Acta Diabetol*, 52, 179–182. <https://doi.org/10.1007/s00592-014-0586-y>
- Iijima, S. (1991). Helical microtubules of graphitic carbon. *Nature*, 354(November), 56–58.
- Iijima, S. (2002). Carbon nanotubes : past , present , and future. *Physica B*, 323, 1–5.
- Inturi, S., Wang, G., Chen, F., Banda, N. K., Holers, V. M., Wu, L., ... Simberg, D. (2015). Modulatory Role of Surface Coating of Superparamagnetic Iron Oxide Nanoworms in Complement Opsonization and Leukocyte Uptake. *ACS Nano*, 9(11), 10758–10768. <https://doi.org/10.1021/acs.nano.5b05061>
- Ishibashi, H. (2008). Application of Gold Nanoparticles to Paint Colorants. *Journal of the Vacuum Society of Japan*, 51(11), 737–742.
- Isomaa, B., Almgren, P., Tuomi, T., Forsen, B., Lahti, K., Nissen, M., ... Groop, L. (2001). Cardiovascular Morbidity and Mortality Associated With the Metabolic Syndrome. *Diabetes Care*, 24(4), 683–689.

- Karlsson, H. L., Cronholm, P., Gustafsson, J., & Moller, L. (2008). Copper Oxide Nanoparticles Are Highly Toxic : A Comparison between Metal Oxide Nanoparticles and Carbon Nanotubes. *Chemical Research in Toxicology*, *21*, 1726–1732.
- Khan, I., Saeed, K., & Khan, I. (2019). Nanoparticles : Properties , applications and toxicities. *Arabian Journal of Chemistry*, *12*(7), 908–931. <https://doi.org/10.1016/j.arabjc.2017.05.011>
- Khan, M. A., & Khan, M. J. (2018). Nano-gold displayed anti-inflammatory property via NF-kB pathways by suppressing COX-2 activity. *Artificial Cells, Nanomedicine, and Biotechnology*, *46*(S1), S1149–S1158. <https://doi.org/10.1080/21691401.2018.1446968>
- Kim, B. Y. S., Rutka, J. T., & Chan, W. C. W. (2010). Nanomedicine. *New England Journal of Medicine*, *363*(25), 2434–2443.
- Kim, D. K., Zhang, Y., Voit, W., Rao, K. V., & Muhammed, M. (2001). Synthesis and characterization of surfactant-coated superparamagnetic monodispersed iron oxide nanoparticles. *Journal of Magnetism and Magnetic Materials*, *225*, 30–36.
- Kim, J. S., Yoon, T., Yu, K. N., Kim, B. G., Park, S. J., Kim, H. W., ... Cho, M. H. (2006). Toxicity and Tissue Distribution of Magnetic Nanoparticles in Mice. *Toxicological Sciences*, *89*(1), 338–347. <https://doi.org/10.1093/toxsci/kfj027>
- Kobos, L. M., Adamson, S. X. F., Evans, S., Gavin, T. P., & Shannahan, J. H. (2018). Altered formation of the iron oxide nanoparticle-biocorona due to individual variability and exercise. *Environmental Toxicology and Pharmacology*, *62*(July), 215–226. <https://doi.org/10.1016/j.etap.2018.07.014>
- Kramer, P. A. (1974). Albumin Microspheres as Vehicles for Achieving Specificity in Drug Delivery Keyphrases. *Journal of Pharmaceutical Sciences*, *63*(10), 1646–1647.
- Kroto, H. W., Allaf, A. W., & Balm, S. P. (1985). C60: Buockminsterfullerine. *Nature*, *318*(6042), 162–163. <https://doi.org/10.1021/cr00006a005>

- Kulkova, M., Gusentzova, T., Nesterov, E., Sorokin, P., & Sapelko, T. (2012). Chronology of Neolithic-Early Metal Age Sites at the Okhta River Mouth (Saint Petersburg, Russia). *Radiocarbon*, *54*(3), 1049–1063.
- Kumbhakar, P., Ray, S. S., & Stepanov, A. L. (2014). Optical Properties of Nanoparticles and Nanocomposites. *Journal of Nanomaterials*, *1*, 2–4.
- Kurella, M., Lo, J. C., & Chertow, G. M. (2005). Metabolic Syndrome and the Risk for Chronic Kidney Disease among Nondiabetic Adults. *Journal of the American Society of Nephrology*, *16*, 2134–2140. <https://doi.org/10.1681/ASN.2005010106>
- Labarre, D., Vauthier, C., Chauvierre, C., Petri, B., Muller, R., & Chehimi, M. M. (2005). Interactions of blood proteins with poly (isobutylcyanoacrylate) nanoparticles decorated with a polysaccharidic brush. *Biomaterials*, *26*, 5075–5084. <https://doi.org/10.1016/j.biomaterials.2005.01.019>
- Lam, P. K., Chan, E. S. Y., Ho, W. S., & In, C. T. L. (2004). In vitro cytotoxicity testing of a nanocrystalline silver dressing (Acticoat) on cultured keratinocytes. *British Journal of Biomedical Science*, *61*(3), 125–127. <https://doi.org/10.1080/09674845.2004.11732656>
- Landry, M. P., Vukovic, L., Kruss, S., Bisker, G., Landry, A. M., Islam, S., ... Strano, M. S. (2015). Comparative Dynamics and Sequence Dependence of DNA and RNA Binding to Single Walled Carbon Nanotubes. *The Journal of Physical Chemistry C*, *119*, 10048–10058. <https://doi.org/10.1021/jp511448e>
- Laprise-pelletier, M., Lagueux, J., Côté, M., Lagrange, T., & Fortin, M.-A. (2017). Low-Dose Prostate Cancer Brachytherapy with Radioactive Palladium – Gold Nanoparticles. *Advanced Healthcare Materials*, *6*. <https://doi.org/10.1002/adhm.201601120>
- Laprise-pelletier, M., Simão, T., & Fortin, M. (2018). Gold Nanoparticles in Radiotherapy and Recent Progress in Nanobrachytherapy. *Advanced Healthcare Materials*, *7*. <https://doi.org/10.1002/adhm.201701460>
- Lee, S. H., & Jun, B. (2019). Silver Nanoparticles : Synthesis and Application for Nanomedicine. *International Journal of Molecular Sciences*, *20*(4). <https://doi.org/10.3390/ijms20040865>

- Lesniak, A., Fenaroli, F., Monopoli, M. P., Åberg, C., Dawson, K. A., & Salvati, A. (2012). Effects of the presence or absence of a protein corona on silica nanoparticle uptake and impact on cells. *ACS Nano*, *6*(7), 5845–5857. <https://doi.org/10.1021/nn300223w>
- Li, H., Yang, W., Yu, Z., & Zhao, L. (2015). The performance of a heat pump using nanofluid (R22 + TiO₂) as the working fluid – an experimental study. *Energy Procedia*, *75*, 1838–1843. <https://doi.org/10.1016/j.egypro.2015.07.158>
- Livache, C., Martinez, B., Goubet, N., Gréboval, C., Qu, J., Chu, A., ... Lhuillier, E. (2019). A colloidal quantum dot infrared photodetector and its use for intraband detection. *Nature Communications*, *10*, 1–10. <https://doi.org/10.1038/s41467-019-10170-8>
- Lu, N., Sui, Y., Tian, R., & Peng, Y. Y. (2018). Adsorption of Plasma Proteins on Single-Walled Carbon Nanotubes Reduced Cytotoxicity and Modulated Neutrophil Activation. *Chemical Research in Toxicology*, *31*(10), 1061–1068. research-article. <https://doi.org/10.1021/acs.chemrestox.8b00141>
- Macdougall, I. C. (2013). *Pocket Reference to Renal Anemia Second edition*.
- Majewski, P., & Thierry, B. (2007). Functionalized Magnetite Nanoparticles — Synthesis , Properties , and Bio- Applications. *Critical Reviews in Solid State and Materials Sciences*, *32*, 203–215. <https://doi.org/10.1080/10408430701776680>
- Matea, C. T., Mocan, T., Pop, T., Puia, C., & Iancu, C. (2017). Quantum dots in imaging , drug delivery and sensor applications. *International Journal of Nanomedicine*, *12*, 5421–5431.
- Mavani, K., & Shah, M. (2013). Synthesis of Silver Nanoparticles by using Sodium Borohydride as a Reducing Agent. *International Journal of Engineering Research & Technology (IJERT)*, *2*(3), 1–5. <https://doi.org/10.13140/2.1.3116.8648>
- Méndez-sánchez, N., Chavez-tapia, N. C., Motola-kuba, D., Sanchez-lara, K., Ponciano-, G., Baptista, H., ... Chavez-tapia, N. C. (2005). Metabolic syndrome as a risk factor for gallstone disease. *World Journal of Gastroenterology*, *11*(11), 1653–1657.

- Meyer, D. E., Ann, M., & Gonzalez, M. A. (2011). An examination of silver nanoparticles in socks using screening-level life cycle assessment. *Journal of Nanoparticle Research*, *13*, 147–156. <https://doi.org/10.1007/s11051-010-0013-4>
- Min, J., Paek, D., Cho, S., & Min, K. (2009). Exposure to environmental carbon monoxide may have a greater negative effect on cardiac autonomic function in people with metabolic syndrome. *Science of the Total Environment*, *407*(17), 4807–4811. <https://doi.org/10.1016/j.scitotenv.2009.05.028>
- Müller, J., Prozeller, D., Ghazaryan, A., Kokkinopoulou, M., Mailänder, V., Morsbach, S., & Landfester, K. (2018). Beyond the protein corona – lipids matter for biological response of nanocarriers. *Acta Biomaterialia*, *71*, 420–431. <https://doi.org/10.1016/j.actbio.2018.02.036>
- Naqvi, S., Samim, M., Abdin, M., Ahmed, F. J., Maitra, A., Prashant, C., & Dinda, A. K. (2010). Concentration-dependent toxicity of iron oxide nanoparticles mediated by increased oxidative stress. *International Journal of Nanomedicine*, *5*, 983–989. <https://doi.org/10.2147/IJN.S13244>
- Neuberger, T., Scho, B., Hofmann, M., & Rechenberg, B. Von. (2005). Superparamagnetic nanoparticles for biomedical applications : Possibilities and limitations of a new drug delivery system. *Journal of Magnetism and Magnetic Materials*, *293*, 483–496. <https://doi.org/10.1016/j.jmmm.2005.01.064>
- Nozik, A. J. (2002). Quantum dot solar cells. *Physica E*, *14*, 115–120.
- Nugent, R. (2008). Chronic Diseases in Developing Countries: Health and Economic Burdens. *New York Academy of Sciences*, *1136*(2008), 70–79. <https://doi.org/10.1196/annals.1425.027>
- Paddle-Ledinek, J. E., Nasa, Z., & Cleland, H. J. (2006). Effect of Different Wound Dressings on Cell Viability and Proliferation. *Plastic and Reconstructive Surgery*, *117*(7S), 110S-118S. <https://doi.org/10.1097/01.prs.0000225439.39352.ce>

- Pan, Y., Leifert, A., Ruau, D., Neuss, S., Bornemann, J., Schmid, G., ... Jahnen-Dechent, W. (2009). Gold Nanoparticles of Diameter 1.4 nm Trigger Necrosis by Oxidative Stress and Mitochondrial Damage. *Small*, 18(5), 2067–2076. <https://doi.org/10.1002/sml.200900466>
- Pan, Y., Neuss, S., Leifert, A., Fischler, M., Wen, F., Simon, U., ... Jahnen-Dechent, W. (2007). Size-dependent cytotoxicity of gold nanoparticles. *Small*, 3(11), 1941–1949. <https://doi.org/10.1002/sml.200700378>
- Panas, A., Marquardt, C., Nalcaci, O., Bockhorn, H., Baumann, W., Paur, H. R., ... Weiss, C. (2013). Screening of different metal oxide nanoparticles reveals selective toxicity and inflammatory potential of silica nanoparticles in lung epithelial cells and macrophages. *Nanotoxicology*, 7(3), 259–273. <https://doi.org/10.3109/17435390.2011.652206>
- Paoletti, R., Bolego, C., Poli, A., & Cignarella, A. (2006). Metabolic syndrome, inflammation and atherosclerosis. *Vascular Health and Risk Management*, 2(2), 145–152.
- Park, M. V. D. Z., Neigh, A. M., Vermeulen, J. P., De, L. J. J., Verharen, H. W., Briedé, J. J., ... Jong, W. H. De. (2011). The effect of particle size on the cytotoxicity, inflammation, developmental toxicity and genotoxicity of silver nanoparticles. *Biomaterials*, 32(36), 9810–9817. <https://doi.org/10.1016/j.biomaterials.2011.08.085>
- Park, S. K., Auchincloss, A. H., Neill, M. S. O., Prineas, R., Correa, J. C., Keeler, J., ... Roux, A. V. D. (2010). Particulate Air Pollution , Metabolic Syndrome , and Heart Rate Variability : The Multi-Ethnic Study of Atherosclerosis (MESA). *Environmental Health Perspectives*, 118(10), 1406–1411. <https://doi.org/10.1289/ehp.0901778>
- Park, S. K., Schwartz, J., Weisskopf, M., Sparrow, D., Vokonas, P. S., Wright, R. O., ... Hu, H. (2006). Low-Level Lead Exposure , Metabolic Syndrome , and Heart Rate Variability : The VA Normative Aging Study. *Environmental Health Perspectives*, 114(11), 1718–1724. <https://doi.org/10.1289/ehp.8992>
- Parot, P., Dufre, Y. F., Hinterdorfer, P., Grimellec, C. Le, Navajas, D., Pellequer, J.-L., & Scheuring, S. (2007). Past , present and future of atomic force microscopy in life sciences and medicine. *Journal of Molecular Recognition*, 20, 418–431. <https://doi.org/10.1002/jmr>

- Pati, R., Shevtsov, M., & Sonawane, A. (2018). Nanoparticle Vaccines Against Infectious Diseases. *Frontiers in Immunology*, 9(October). <https://doi.org/10.3389/fimmu.2018.02224>
- Pawelczyk, E., Arbab, A. S., Chaudhry, A., Balakumaran, A., Robey, P. G., & Frank, J. A. (2008). In Vitro Model of Bromodeoxyuridine or Iron Oxide Nanoparticle Uptake by Activated Macrophages from Labeled Stem Cells: Implications for Cellular Therapy. *Stem Cells*, 26, 1366–1375. <https://doi.org/10.1634/stem-cells.2007-0707>
- Peng, Q., Zhang, S., Yang, Q., Zhang, T., Wei, X. Q., Jiang, L., ... Lin, Y. F. (2013). Preformed albumin corona, a protective coating for nanoparticles based drug delivery system. *Biomaterials*, 34(33), 8521–8530. <https://doi.org/10.1016/j.biomaterials.2013.07.102>
- Pernodet, N., Fang, X., Sun, Y., Bakhtina, A., Ramakrishnan, A., Sokolov, J., ... Rafailovich, M. (2006). Adverse Effects of Citrate / Gold Nanoparticles on Human Dermal Fibroblasts. *Small*, 2(6), 766–773. <https://doi.org/10.1002/sml.200500492>
- Persaud, I., Shannahan, J. H., Raghavendra, A. J., Alsaleh, N. B., Podila, R., & Brown, J. M. (2019). Biocorona formation contributes to silver nanoparticle induced endoplasmic reticulum stress. *Ecotoxicology and Environmental Safety*, 170(April 2018), 77–86. <https://doi.org/10.1016/J.ECOENV.2018.11.107>
- Poon, V. K. M., & Burd, A. (2004). In vitro cytotoxicity of silver : implication for clinical wound care. *Burns*, 30(2), 140–147. <https://doi.org/10.1016/j.burns.2003.09.030>
- Radu, M., Din, I. M., Hermenean, A., Cinteza, L. O., Rurlacu, R., Ardelean, A., & Dinischiotu, A. (2015). Exposure to Iron Oxide Nanoparticles Coated with Phospholipid-Based Polymeric Micelles Induces Biochemical and Histopathological Pulmonary Changes in Mice. *International Journal of Molecular Sciences*, 16, 29417–29435. <https://doi.org/10.3390/ijms161226173>
- Raesch, S. S., Tenzer, S., Storck, W., Rurainski, A., Selzer, D., Ruge, C. A., ... Lehr, C. M. (2015). Proteomic and Lipidomic Analysis of Nanoparticle Corona upon Contact with Lung Surfactant Reveals Differences in Protein, but Not Lipid Composition. *ACS Nano*, 9(12), 11872–11885. <https://doi.org/10.1021/acsnano.5b04215>

- Raghavendra, A. J., Fritz, K., Fu, S., Brown, J. M., & Shannahan, J. H. (2017). Variations in biocorona formation related to defects in the structure of single walled carbon nanotubes and the hyperlipidemic disease state. *Scientific Reports*, (April), 1–11.
<https://doi.org/10.1038/s41598-017-08896-w>
- Rahman, M. F., Wang, J., Patterson, T. A., Saini, U. T., Robinson, B. L., Newport, G. D., ... Ali, S. F. (2009). Expression of genes related to oxidative stress in the mouse brain after exposure to silver-25 nanoparticles. *Toxicology Letters*, 187(1), 15–21.
<https://doi.org/10.1016/j.toxlet.2009.01.020>
- Ramadi, K. B., Mohamed, Y. A., Al-sbiei, A., Almarzooqi, S., Bashir, G., Dhanhani, A. Al, ... Al-ramadi, B. K. (2016). Acute systemic exposure to silver-based nanoparticles induces hepatotoxicity and NLRP3- dependent inflammation. *Nanotoxicology*, 10(8), 1061–1074.
<https://doi.org/10.3109/17435390.2016.1163743>
- Reddy, P. Y., Giridharan, N. V., & Reddy, G. B. (2012). Activation of sorbitol pathway in metabolic syndrome and increased susceptibility to cataract in Wistar-Obese rats. *Molecular Vision*, 18, 495–503.
- Rietmeijer, F. J. M., & Mackinnon, I. D. R. (1997). Bismuth oxide nanoparticles in the stratosphere Bi from which we derive the particle number densities ($p\ m^{-3}$) for " average. *Journal of Geophysical Research*, 102(96), 6621–6627.
- Roco, M. C. (2011). The long view of nanotechnology development : the National Nanotechnology Initiative at 10 years. *Journal of Nanoparticle Research*, 13, 427–445.
<https://doi.org/10.1007/s11051-010-0192-z>
- Ryan, M., & Brayden, D. J. (2014). ScienceDirect Progress in the delivery of nanoparticle constructs : towards clinical translation. *Current Opinion in Pharmacology*, 18, 120–128.
<https://doi.org/10.1016/j.coph.2014.09.019>
- Sahneh, F. D., Scoglio, C., & Riviere, J. (2013). Dynamics of Nanoparticle-Protein Corona Complex Formation: Analytical Results from Population Balance Equations. *PloS One*, 8(5), 1–10. <https://doi.org/10.1371/journal.pone.0064690>

- Salvati, A., Pitek, A. S., Monopoli, M. P., Prapainop, K., Bombelli, F. B., Hristov, D. R., ... Dawson, K. A. (2013). Transferrin-functionalized nanoparticles lose their targeting capabilities when a biomolecule corona adsorbs on the surface. *Nature Nanotechnology*, 8(2), 137–143. <https://doi.org/10.1038/nnano.2012.237>
- Schutz, C. A., Juillerat-Jeanneret, L., Mueller, H., Lynch, I., & Riediker, M. (2013). Therapeutic nanoparticles in clinics and under clinical evaluation, 449–467.
- Sciau, P., Mirguet, C., Roucau, C., Chabanne, D., & Schvoerer, M. (2009). Double Nanoparticle Layer in a 12 th Century Lustreware Decoration : Accident or Technological Mastery ? *Journal of Nano Research*, 8, 133–139. <https://doi.org/10.4028/www.scientific.net/JNanoR.8.133>
- Scott, G. D. (1995). A Study of the Lycurgus Cup. *Journal of Glass Studies*, 37, 51–64.
- Sen, D. K., Yadav, A. K., & Shukla, A. (2015). An incredible diagnostic tool Quantum Dots : A review. *Asian Journal of Biomaterial Research*, 1(2), 46–50.
- Shannahan, J. H., Fritz, K. S., Raghavendra, A. J., Podila, R., Persaud, I., & Brown, J. M. (2016). Disease-induced disparities in formation of the nanoparticle-biocorona and the toxicological consequences. *Toxicological Sciences*, 152(2), 406–416. <https://doi.org/10.1093/toxsci/kfw097>
- Shannahan, J. H., Podila, R., Aldossari, A. A., Emerson, H., Powell, B. A., Ke, P. C., ... Brown, J. M. (2015). Formation of a protein corona on silver nanoparticles mediates cellular toxicity via scavenger receptors. *Toxicological Sciences : An Official Journal of the Society of Toxicology*, 143(1), 136–146. <https://doi.org/10.1093/toxsci/kfu217>
- Shukla, R., Bansal, V., Chaudhary, M., Basu, A., Bhonde, R. R., & Sastry, M. (2005). Biocompatibility of Gold Nanoparticles and Their Endocytotic Fate Inside the Cellular Compartment : A Microscopic Overview. *Langmuir*, (25), 10644–10654. <https://doi.org/10.1021/la0513712>

- Siddiqui, M. H., Firoz, M. H. A., & Impact, T. (2015). *Nanotechnology and Plant Sciences*.
- Siemer, S., Westmeier, D., Vallet, C., Becker, S., Voskuhl, J., Ding, G., ... Knauer, S. K. (2018). Resistance to Nano-Based Antifungals Is Mediated by Biomolecule Coronas. *ACS Applied Materials & Interfaces*, *11*, 104–114. research-article.
<https://doi.org/10.1021/acsami.8b12175>
- Sinha, N., Cifter, G., Sajo, E., Kumar, R., Sridhar, S., Nguyen, P., ... Ngwa, W. (2016). Brachytherapy Application with in situ Dose-painting Administered via Gold-nanoparticle Eluters. *International Journal of Radiation Oncology • Biology • Physics*, *91*(2), 385–392.
<https://doi.org/10.1016/j.ijrobp.2014.10.001.Brachytherapy>
- Smijs, T. G., & Pavel, S. (2011). Titanium dioxide and zinc oxide nanoparticles in sunscreens : focus on their safety and effectiveness. *Nanotechnology, Science and Applications*, *4*, 95–112.
- Song, J. Y., & Kim, B. S. (2009). Rapid biological synthesis of silver nanoparticles using plant leaf extracts. *Bioprocess and Biosystems Engineering*, *32*(1), 79–84.
<https://doi.org/10.1007/s00449-008-0224-6>
- Stuchinskaya, T., Moreno, M., Cook, M. J., Edwards, D. R., & Russell, D. A. (2011). Targeted photodynamic therapy of breast cancer cells using antibody–phthalocyanine–gold nanoparticle conjugates. *Photochemical & Photobiological Sciences*.
<https://doi.org/10.1039/c1pp05014a>
- Suresh, Y., Annapurna, S., Bhikshamaiah, G., & Singh, A. K. (2016). Rapid and eco-friendly synthesis of copper nanoparticles. *AIP Conference Proceedings*, *1591*, 372–374.
<https://doi.org/10.1063/1.4872606>
- Takenaka, S., Karg, E., Roth, C., Schulz, H., Ziesenis, A., Heinzmann, U., ... Heyder, J. (2001). Pulmonary and Systemic Distribution of Inhaled Ultrafine Silver Particles in Rats. *Environmental Health Perspectives*, *109*(suppl 4), 547–551.

- Tang, B., Sun, L., Kaur, J., Yu, Y., & Wang, X. (2014). Dyes and Pigments In-situ synthesis of gold nanoparticles for multifunctionalization of silk fabrics. *Dyes and Pigments*, *103*, 183–190. <https://doi.org/10.1016/j.dyepig.2013.12.008>
- Tang, B., Sun, L., Li, J., Kaur, J., Zhu, H., Qin, S., ... Wang, X. (2015). Dyes and Pigments Functionalization of bamboo pulp fabrics with noble metal nanoparticles. *Dyes and Pigments*, *113*, 289–298. <https://doi.org/10.1016/j.dyepig.2014.08.015>
- Tang, J., Xiong, L., Wang, S., Wang, J., Liu, L., Li, J., ... Xi, T. (2009). Distribution , Translocation and Accumulation of Silver Nanoparticles in Rats. *Journal of Nanoscience and Nanotechnology*, *9*(8), 4924–4932. <https://doi.org/10.1166/jnn.2009.1269>
- Tartaj, P. Ã., Morales, M. P. Ã., & Gonza, T. (2005). Advances in magnetic nanoparticles for biotechnology applications. *Journal of Magnetism and Magnetic Materials*, *291*, 28–34. <https://doi.org/10.1016/j.jmmm.2004.11.155>
- Tartaj, P., Morales, P., Veintemillas-verdaguer, S., & Gonz, T. (2003). The preparation of magnetic nanoparticles for applications in biomedicine. *Journal of Physics D: Applied Physics*, *36*, R182–R197.
- Tenzer, S., Musyanovych, A., Fetz, V., Docter, D., Hecht, R., Schlenk, F., ... Schild, H. (2013). Rapid formation of plasma protein corona critically affects nanoparticle pathophysiology, *8*(September). <https://doi.org/10.1038/nnano.2013.181>
- Tepe, N., & Bau, M. (2014). Science of the Total Environment Importance of nanoparticles and colloids from volcanic ash for riverine transport of trace elements to the ocean : Evidence from glacial-fed rivers after the 2010 eruption of Eyjafjallajökull Volcano , Iceland. *Science of the Total Environment*, *The*, *488–489*, 243–251. <https://doi.org/10.1016/j.scitotenv.2014.04.083>
- Thakor, A. S., Jokerst, J., Zavaleta, C., Massoud, T. F., & Gambhir, S. S. (2011). Gold Nanoparticles : A Revival in Precious Metal Administration to Patients. *Nano Letters*, *11*, 4029–4036. <https://doi.org/10.1021/nl202559p>

- Thompson, D. (2007). Michael Faraday's Recognition of Ruby Gold: the Birth of Modern Nanotechnology. *Gold Bulletin*, 40(4), 267–269.
- Tibbals, H. F. (2011). *Medical Nanotechnology and Nanomedicine*.
- Tran, Q. H., Nguyen, V. Q., & Le, A. (2013). Silver nanoparticles: synthesis, properties, toxicology, applications and perspectives. *Advances in Natural Sciences: Nanoscience and Nanotechnology*, 4(3).
- Trickler, W. J., Lantz, S. M., Murdock, R. C., Schrand, A. M., Robinson, B. L., Newport, G. D., ... Ali, S. F. (2010). Silver Nanoparticle Induced Blood-Brain Barrier Inflammation and Increased Permeability in Primary Rat Brain Microvessel Endothelial Cells. *Toxicological Sciences*, 118(1), 160–170. <https://doi.org/10.1093/toxsci/kfq244>
- Tsoli, M., Kuhn, H., & Brandau, W. (2005). Gold cluster toxicity Cellular Uptake and Toxicity of Au 55 Clusters**. *Small*, 1(8–9), 841–844. <https://doi.org/10.1002/sml.200500104>
- Vidanapathirana, A. K., Lai, X., Hilderbrand, S. C., Pitzer, J. E., Podila, R., Sumner, S. J., ... Brown, J. M. (2012). Multi-walled carbon nanotube directed gene and protein expression in cultured human aortic endothelial cells is influenced by suspension medium. *Toxicology*, 302(2–3), 114–122. <https://doi.org/10.1016/j.tox.2012.09.008>
- Voinov, M. A., Paga, J. O. S., Morrison, E., Smirnova, T. I., & Smirnov, A. I. (2011). Surface-Mediated Production of Hydroxyl Radicals as a Mechanism of Iron Oxide Nanoparticle Biototoxicity. *Journal of the American Chemical Society*, 133, 35–41.
- Volder, M. F. L. De, Tawfick, S. H., Baughman, R. H., & Hart, A. J. (2013). Carbon Nanotubes : Present and Future Commercial Applications. *Science*, 339(6119), 535–539.
- W. Dobrucki, L., Pan, D., & M. Smith, A. (2015). Multiscale Imaging of Nanoparticle Drug Delivery. *Current Drug Targets*, 16(6), 560–570.
- Wageh, S., Su, Z., & Xu-rong, X. (2003). Growth and optical properties of colloidal ZnS nanoparticles. *Journal of Crystal Growth*, 255, 332–337. [https://doi.org/10.1016/S0022-0248\(03\)01258-2](https://doi.org/10.1016/S0022-0248(03)01258-2)

- Wagner, J. G., Allen, K., Yang, H., Nan, B., Morishita, M., & Mukherjee, B. (2014). Cardiovascular Depression in Rats Exposed to Inhaled Particulate Matter and Ozone : Effects of Diet-Induced Metabolic Syndrome. *Environmental Health Perspectives*, *122*(1), 27–33.
- Walkey, C. D., & Chan, W. C. W. (2012). Understanding and controlling the interaction of nanomaterials with proteins in a physiological environment. *Chemical Society Reviews*, *41*(7), 2780–2799. <https://doi.org/10.1039/c1cs15233e>
- Walter, P., Halle, P., Zaluzec, N. J., Deeb, C., Castaing, J., & Veysie, P. (2000). Early Use of PbS Nanotechnology for an Ancient Hair Dyeing Formula. *Nano Letters*, *6*(10), 2215–2219. <https://doi.org/10.1021/nl061493u>
- Wang, X., & Xu, X. (1999). Thermal Conductivity of Nanoparticle – Fluid Mixture. *Journal of Thermophysics and Heat Transfer*, *13*(4), 474–480.
- Widder, J., Marino, A., & Morris, M. (1983). Selective Targeting of Magnetic Albumin Microspheres to the Yoshida Sarcoma : Ultra structural Evaluation of Microsphere Disposition *. *European Journal of Cancer and Clinical Oncology*, *19*(1), 141–147.
- Widder, K. J., Senyei, A. E., & Scarpelli, D. G. (1978). Magnetic microspheres: a model system for site specific drug delivery in vivo. *Proceedings of the Society for Experimental Biology and Medicine*, *158*(2), 141–146.
- Wiench, K., Landsiedel, R., Schulte, S., Inman, A. O., & Riviere, J. E. (2011). Safety Evaluation of Sunscreen Formulations Containing Titanium Dioxide and Zinc Oxide Nanoparticles in UVB Sunburned Skin : An In Vitro and In Vivo Study. *Toxicological Sciences*, *123*(1), 264–280. <https://doi.org/10.1093/toxsci/kfr148>
- Woods, S. I., Kirtley, J. R., Sun, S., & Koch, R. H. (2001). Direct Investigation of Superparamagnetism in Co Nanoparticle Films. *Physical Review Letters*, *87*(13), 1–4. <https://doi.org/10.1103/PhysRevLett.87.137205>

- Yook, S., Cai, Z., Lu, Y., Winnik, M. A., Pignol, J., & Reilly, R. M. (2016). Gold Nanoseed Brachytherapy with Application for Neoadjuvant Treatment of Locally Advanced Breast Cancer. *The Journal of Nuclear Medicine*, *57*(6), 936–943.
<https://doi.org/10.2967/jnumed.115.168906>
- Zande, M. Van Der, Vandebriel, R. J., Doren, E. Van, Kramer, E., Rivera, Z. H., Serrano-rojero, C. S., ... Bouwmeester, H. (2012). Distribution , Elimination , and Toxicity of Silver Nanoparticles and Silver Ions in Rats after 28-Day Oral Exposure. *ACS Nano*, *6*(8), 7427–7442. <https://doi.org/10.1021/nn302649p>
- Zhang, W., & Elliott, D. W. (2006). Applications of Iron Nanoparticles for Groundwater Remediation. *Remediation Journal: The Journal of Environmental Cleanup Costs, Technologies & Techniques*, *16*(2), 7–21. <https://doi.org/10.1002/rem.20078>
- Zhang, Xi-feng, Liu, Z., Shen, W., & Gurunathan, S. (2016). Silver Nanoparticles : Synthesis , Characterization , Properties , Applications , and Therapeutic Approaches. *International Journal of Molecular Sciences*, *17*(9), 1534. <https://doi.org/10.3390/ijms17091534>
- Zhang, Xiao-dong, Wu, D., Shen, X., Liu, P.-X., Yang, N., Zhao, B., ... Fan, F. (2011). Size-dependent in vivo toxicity of PEG-coated gold nanoparticles. *International Journal of Nanomedicine*, *6*, 2071–2081.
- Zhang, Z., Lv, X., Chen, Q., & An, J. (2019). Complex coloration and antibacterial functionalization of silk fabrics based on noble metal nanoparticles. *Journal of Engineered Fibers and Fabrics*, *14*, 1–8. <https://doi.org/10.1177/1558925019866948>
- Zhao, X., Liu, W., Cai, Z., Han, B., Qian, T., & Zhao, D. (2016). An overview of preparation and applications of stabilized zero-valent iron nanoparticles for soil and groundwater remediation. *Water Research*, *100*, 245–266. <https://doi.org/10.1016/j.watres.2016.05.019>

CHAPTER 2. AN INTEGRATIVE PROTEOMIC/LIPIDOMIC ANALYSIS OF THE GOLD NANOPARTICLE BIOCORONA IN HEALTHY AND OBESE CONDITIONS

A version of this chapter has been previously published in *Applied In Vitro Toxicology*.

Kobos, L. M., Alqatani, S., Ferreira, C. R., Aryal, U. K., Hedrick, V., Sobreira, T. J., & Shannahan, J. H. (2019). An Integrative Proteomic/Lipidomic Analysis of the Gold Nanoparticle Biocorona in Healthy and Obese Conditions. *Applied In Vitro Toxicology*, 5(3), 150-166. <https://doi.org/10.1089/aivt.2019.0005>

2.1 Abstract

When nanoparticles (NPs) enter a physiological environment, a coating of biomolecules or biocorona (BC) forms on the surface. Formation of the NP-BC is dependent on NP properties, the physiological environment, and time. The BC influences NP properties and biological interactions such as cellular internalization, immune responses, biodistribution, and others, leading to pharmacological and toxicological consequences. To date, examination of the NP-BC has focused primarily on protein components and healthy conditions. Therefore, we evaluated the protein and lipid content of BCs that formed on physicochemically distinct gold nanoparticles (AuNPs) under healthy and obese conditions. A comprehensive understanding of the NP-BC is necessary for the translation of *in vitro* toxicity assessments to clinical applications. AuNPs with two coatings (poly-N-vinylpyrrolidone [PVP] or citrate) and diameters (20 or 100 nm) were incubated in pooled human serum, and an integrated proteomic/lipidomic approach was used to evaluate BC composition. Macrophages were utilized to evaluate differential immune responses due to variations in the AuNP-BC. AuNPs form distinct BCs based on physicochemical properties and the surrounding environment, with the obese BC containing more proteins and fewer lipids than the healthy BC. Differential macrophage inflammatory responses were observed based on AuNP properties and BC composition. Overall, these findings demonstrate that AuNP size and coating, as well as physiological environment, influence the protein and lipid composition of the BC, which impacts cellular responses following exposure. These findings demonstrate that incorporation of BCs representing distinct physiological conditions may enhance the translatability of nanosafety *in vitro* studies.

2.2 Introduction

Nanoparticles are increasingly utilized in a variety of processes and technologies, impacting manufacturing procedures, medicine, electronics, and consumer products. Gold nanoparticles (AuNPs) are considered a promising candidate for a number of biomedical applications due to their biocompatibility and anti-inflammatory properties (Khan & Khan, 2018; Shukla et al., 2005). Currently, gold salts and AuNPs are used in the treatment of arthritis and as an agent for some cancer treatments (Dykman & Khlebtsov, 2011; Haume et al., 2016). Proposed uses of AuNPs have a broad scope, ranging from photodynamic cancer therapy and targeted drug delivery to their inclusion in vaccines (Cheng, Samia, Meyers, & Panagopoulos, 2008; Pati, Shevtsov, & Sonawane, 2018; Stuchinskaya, Moreno, Cook, Edwards, & Russell, 2011). The small size of nano-gold enhances therapeutic efficacy compared to conventional methods. Specifically related to size, AuNPs have increased surface area, allowing for the association of larger amounts of drug while also more effectively penetrating biological barriers. To translate AuNPs to a clinical setting, it is necessary to understand initial interactions between AuNPs and biomolecules that dictate subsequent biological responses. When NPs enter a physiological environment, they form a coating of biomolecules known as a biocorona (BC). The BC imparts a new surface to the NP, altering NP physicochemical properties, influencing interactions with cells, biodistribution, clearance, functionality and toxicity (Adamson, Lin, Chen, Kobos, & Shannahan, 2018; Maiorano et al., 2010; Monopoli, Åberg, Salvati, & Dawson, 2012; Shannahan, Podila, & Brown, 2015; Walczyk, Bombelli, Monopoli, Lynch, & Dawson, 2010). The clinical application of AuNP-based theragnostic approaches requires a comprehensive assessment of the NP-biomolecular interactions forming the BC and their influence on cellular responses.

The formation of the NP-BC is governed by NP physicochemical properties, the biological environment, and time (Eudald, Tobias, Albert, Gertie Janneke, & Victor, 2010; Frost, Langhammer, & Cedervall, 2017; Neagu, Piperigkou, Karamanou, & Engin, 2017; Shannahan et al., 2016). The majority of BC research has focused on NP properties (material, charge, size, surface coating, etc.) influencing surface interactions with proteins (Jedlovszky-hajdu, Bombelli, Monopoli, Tomba, & Dawson, 2012; Lundqvist et al., 2008; Neagu et al., 2017; Walkey, Olsen, Guo, Emili, & Chan, 2012). However, fewer studies have examined the impact of the biological environment on BC formation. It is known that many factors, such as gender, diet, underlying

disease states, and others can influence the biomolecular profile within the circulation (Jenkins et al., 1993; Murphy, 2014; Tran, Weltman, Glass, & Mood, 1983). Previous research has demonstrated that the changes in circulating biomolecules that occur in hyperlipidemia result in altered iron oxide NP-BC composition, cellular interactions, and toxicological consequences (Kobos, Adamson, Evans, Gavin, & Shannahan, 2018). To date, many common disease states that likely influence BC formation have not been adequately examined. Chronic underlying disease conditions are increasingly pervasive within our population. Further, individuals suffering from these conditions are known to often be susceptible to exposures and are more likely to receive medical treatments (Dong et al., 2013; Dubowsky, Suh, Schwartz, Coull, & Gold, 2006). Obesity is increasingly prevalent (approximately 40% of adults in the United States) and predisposes individuals to serious diseases including heart disease, stroke, apnea, diabetes, cancer and others (“Adult Obesity Prevalence Maps,” 2019; Berghöfer et al., 2008; Flegal, Kruszon-moran, Carroll, Fryar, & Ogden, 2019). Obesity is associated with modifications in metabolism and circulating factors including proteins and lipids (Eisinger, Liebisch, Schmitz, & Aslanidis, 2014; Fjeldborg et al., 2013; Park, Yul, & Yu, 2005; Suzuki et al., 2003). Currently, little is known about NP-lipid interactions and how this may impact BC formation. Our previous assessment demonstrated that hyperlipidemia alters the protein content of the BC that forms on single walled carbon nanotubes (Raghavendra, Fritz, Fu, Brown, & Shannahan, 2017). To safely and effectively utilize AuNPs for theragnostic applications, it is necessary to understand how widespread diseases such as obesity may impact biological responses.

While NP therapeutics have generated significant interest in recent years, there has been difficulty in translating *in vitro* laboratory findings to clinical application. The BC represents a major challenge for the development and use of NPs in medicine, particularly those designed to act as “stealth” therapeutics meant to avoid immune system detection (Ke, Lin, Parak, Davis, & Caruso, 2017). The translation of cell-based toxicity assessments may be assisted by the incorporation of the BC into study designs. Through the inclusion of the BC, *in vitro* studies may more accurately depict the *in vivo* environment and appropriately model NP-cellular interactions and responses. Further, high throughput cell-based screening methods could allow for the evaluation of a number of physiological environments to identify potential susceptible populations to exposure.

In this study, variations in AuNP-BC composition due to differences in physicochemical properties and a common disease condition, obesity, were examined through the utilization of pooled human serum. Additionally, a macrophage cell line was used to assess the toxicological implications of these altered BCs. A comprehensive examination of the biomolecules (proteins and lipids) composing the AuNP-BC in prevalent subpopulations will allow for a more complete understanding regarding initial interactions that occur when AuNPs are introduced into biological environments. Ultimately, these results will assist in the utilization of *in vitro* studies to more effectively evaluate AuNPs prior to *in vivo* studies and clinical usage.

2.3 Materials and Methods

2.3.1 AuNP characterization

Four AuNPs that differed based on size (diameter 20 or 100 nm) and suspension material (poly-N-vinylpyrrolidone [PVP] or citrate) were purchased (Nanocomposix, San Diego, CA). AuNPs were characterized to verify manufacturer's specifications. The hydrodynamic size, polydispersion index, and ζ -potential (ZetaSizer Nano, Malvern) were assessed in deionized water with AuNPs at a concentration of 25 $\mu\text{g}/\text{mL}$ ($n = 3/\text{AuNP}$). The number of AuNPs per mL was determined by NP tracking software (NanoSight, Malvern, Westborough, MA) ($n = 3/\text{AuNP}$).

2.3.2 Human serum characterization

Pooled human sera from healthy or obese individuals (males and females) were purchased from Lee Biosolutions (Maryland Heights, MO). Sera were characterized for traditional lipid end points used in health clinics through commercially available kits to measure triglycerides (Cayman Chemical, Ann Arbor, MI), as well as total cholesterol, high-density lipoprotein (HDL), and low-density lipoprotein/very low-density lipoprotein (LDL/VLDL) (Bioassay Systems, Hayward, CA) ($n = 5$).

2.3.3 Formation of the AuNP BC

BCs were formed on AuNPs as described in our recent publications (Adamson et al., 2018; Kobos et al., 2018). Briefly, AuNPs were incubated for 8 hours at 4°C in 10% serum while being constantly mixed. Specifically, 250 μL of AuNPs (1 mg/mL), 650 μL of deionized water, and

100 μ L of healthy or obese pooled human serum (Lee Biosolutions) were combined in a 1.5 mL tube. Following incubation, AuNPs were pelleted by centrifugation at 15,000 g for 10 minutes and washed with phosphate-buffered saline (PBS). A total of three washes with PBS were performed to remove any free biomolecules not associated with the AuNPs. Four replicates of each AuNP-BC were produced for subsequent proteomic analysis. Furthermore, four were produced and combined for lipid screening and library construction. Identification of lipid components of the BC and relative quantification of lipids were performed using three additional replicates.

2.3.4 Assessment of the protein components of the AuNP BC

Protein components of the BC were prepared and analyzed in a manner similar to our previous publications (Kobos et al., 2018). Briefly, proteins were digested using porcine trypsin (0.2 ng/ μ L) before being concentrated to dryness, resuspended in 0.1% trifluoroacetic acid in water, and purified using UltraMicroSpin columns (The Nest Group, Southborough, MA). Purified peptide samples following concentration were resuspended in 0.1% formic acid in HPLC-grade water for mass spectrometry analysis.

All MS data were acquired using the Dionex UltiMate 3000 RSLC Nano LC System attached to the Q Exactive™ HF Hybrid Quadrupole-Orbitrap Mass Spectrometer (Thermo Scientific, Waltham, MA) with a loading pump at a flow rate of 5 mL/min and settings similar to those which are described in our previous publications (Kobos et al., 2018).

Briefly, 1 μ g of peptide solution was loaded into the trap column and washed for 5 minutes using 2% acetonitrile in purified water followed by separation of peptides using a 120-minute method. Peptides were eluted at a flow rate of 300 nL/min with a linear gradient of 5% to 30% buffer B in 80 minutes and reaching 45% B in 91 minutes, then 100% of B in 93 minutes. B was held for 7 minutes at 100% before reverting back to 5% B in 100 minutes. After each 120-minute sample run, columns were washed 2 \times with a linear gradient of 5% to 100% of B to keep them clean and reduce sample carry over before running the next sample.

2.3.5 Analysis of proteomics data

The files from the mass spectrometer were processed using the MaxQuant computational proteomics platform version 1.6.2.10 (Cox & Mann, 2008). The peak list generated was searched against the *Homo sapiens* sequences from UNIPROT retrieved on September 19, 2018 and a common contaminant database. The following settings were used for MaxQuant: default Orbitrap parameters, minimum peptide length of seven amino acids, data were analyzed with the iBAQ method and “Match between runs” interval set to 1 minute, protein FDR was set to 1%, enzyme trypsin allowing for two missed cleavage and three modifications per peptide, fixed modifications were Carbamidomethyl (C), and variable modifications were set to Acetyl (Protein N-term) and Oxidation (M).

An in-house script was used to perform the following steps on the MaxQuant results: removed all the common contaminant proteins and generated Venn Diagrams of proteins shared between conditions and particles. The statistical analyses were performed in the R environment (www.cran.r-project.org). A *t*-test was performed on the iBAQ intensities, and only proteins with *p*-value <0.05 were used in all analyses. Supplementary Table S2.1 contains protein data, including identification and average abundance.

2.3.6 Sample preparation for lipid screening of the AuNP BC

Following formation of the BC, lipids were extracted from the particle surface using the Bligh–Dyer lipid extraction method (Bligh & Dyer, 1959). Briefly, AuNPs were centrifuged at 20,000 *g* for 20 minutes before removal of supernatant followed by the addition of PBS, methanol, and chloroform. Mixtures were then vortexed briefly before the introduction of purified water and additional chloroform, after which they were centrifuged at 16,000 *g* for 10 minutes. This caused the mixture to separate into the aqueous alcoholic (top) phase and the organic chloroform (bottom) phase. The bottom phase was isolated and concentrated to dryness. Before analysis, samples were resuspended in a 3:6.65:0.35 mixture of methanol, acetonitrile, and ammonium acetate.

2.3.7 Lipid screening data acquisition

Samples were diluted 3.5× in a 3:6.65:0.35 mixture of methanol, acetonitrile, and ammonium acetate. A volume of 8 μL of diluted sample was used for flow injection at a triple quadrupole mass spectrometer (6410 Agilent) equipped with a capillary pump (Agilent 1100 series) and an autosampler (G1377A Agilent). Pump flow rate was set at 20 μL/min, and the machine was pumped with 0.1% formic acid in acetonitrile between sample injections. Capillary voltage on the instrument was 3.5–5 kV, and the gas flow was 5.1 L/min at 300°C.

The multiple reaction monitoring (MRM) profiling approach was used. The MRM profiling is based on chemical functional group screening and flow injection and consists of a “discovery” phase to first identify all lipids and classes present before a “screening” phase, which is used to further determine the presence and relative quantity of lipids found in distinct samples (Casey et al., 2018; Cordeiro et al., 2017; de Lima et al., 2018; Dhillon, Ferreira, Jose, Sobreira, & Mattes, 2017; Dipali, Ferreira, Zhou, Pritchard, & Duncan, 2019; Ferreira et al., 2016; Franco, Ferreira, Sobreira, Sundberg, & Hogenesch, 2018; Yannell, Ferreira, Tichy, & Cooks, 2018). The triple quadrupole mass spectrometer was set to monitor lists of MRMs related to different lipid classes: ceramides, phosphatidylcholines and sphingomyelins, phosphatidylethanolamines, phosphatidylglycerols, phosphatidylinositols, phosphatidylserines, cholesteryl esters, triacylglycerols (triglycerides), and the metabolite class of acyl-carnitines. Free fatty acids were monitored only by the parent mass. The parent masses of the MRMs screened were based on the lipid maps, and the product ions were related to class-related fragments (e.g., m/z 184 for Phosphatidylcholine/Sphingomyelin [PC/SM] lipids).

Due to the large number of lipid isomers, the many MRMs corresponded to multiple individual lipids, meaning that the number of lipids reported as present in this publication is the lowest theoretical value for the possible number of lipids present. Egg yolk lipid extract was used as a quality control sample to monitor instrument performance. Pure methanol (8 μL) was used to flush the system between the injections of different samples. Supplementary Table S2.2 contains all lipid data, including identities and average abundance.

2.3.8 Cell culture and toxicity assessment

Macrophages were selected to evaluate BC alterations in NP-cellular interactions due to their presence at sites of NP deposition, as well as their role in recognizing and removing foreign materials. RAW 264.7 macrophages were grown at 37°C and 5% CO₂ in a Galaxy 170 S incubator (New Brunswick Scientific, Edison, NJ) using DMEM media with 10% fetal bovine essence and 1% penicillin/streptomycin. Cells were plated in a 96-well plate and allowed to grow to 90% confluency before exposure to AuNPs with or without a healthy or obese BC at 12.5 or 50 µg/mL in serum-free media for 3 or 24 hours.

Cellular viability was assessed using the MTT assay ($n = 4/\text{group}$). BC-induced variations in the inflammatory response were measured following a 24-hour exposure to 50 µg/mL of AuNP through assessment of gene expression of tumor necrosis factor- α (*TNF- α*), macrophage inflammatory protein-2 (*MIP-2*), monocyte chemoattractant protein (*MCP-1*), and glyceraldehyde 3-phosphate dehydrogenase (*GAPDH*) (control) using real-time reverse transcriptase PCR ($n = 6/\text{group}$). Untreated macrophages in serum-free media were utilized as controls for the MTT assay and assessment of gene expression.

2.3.9 Statistics and biomolecular data analysis

Only proteins found in three of four replicates were counted as present and used in subsequent analyses. Lipids were required to be 30% above the blank in all three replicates to be counted as present and used in subsequent analyses. Identified biomolecules from each AuNP BC were compared, and Venn diagrams were generated using the online tool Venny 2.1.0 (<http://bioinfogp.cnb.csic.es/tools/venny>) to determine commonalities and differences in the identities of biomolecules within the BC of each AuNP. Biomolecule abundance differences between healthy and obese were determined as significant by a student's *t*-test; $p < 0.05$. Comparisons of biomolecule abundance between AuNPs were determined by one-way ANOVA with Tukey *post hoc* analysis; $p < 0.05$. Comparisons of macrophage inflammatory responses were also performed by one-way ANOVA with Tukey *post hoc* analysis; $p < 0.05$.

2.4 Results

2.4.1 Serum and AuNP characterization

Obese serum was found to have elevated triglycerides, HDL, LDL/VLDL, and total cholesterol compared to healthy serum (Table 2.1). The hydrodynamic size, ζ -potential, and polydispersion index of all four AuNPs were characterized with no BC and following addition of either a healthy BC or obese BC (Table 2.2). Addition of all BCs increased the hydrodynamic size of the AuNPs, with obese BCs causing a larger increase than healthy BCs (Table 2.2). The 20 nm PVP AuNP, while following the same pattern, had a smaller hydrodynamic size than the 20 nm citrate coated AuNPs in both healthy and obese serum. Limited polydispersion was observed for all AuNPs with and without a BC (Table 2.2). ζ -potential of all AuNPs was decreased following addition of either the healthy or obese BC (Table 2.2).

Table 2.1. Pooled human serum from healthy and obese male and female individuals was characterized for traditional lipid end points used in health clinics through commercially available kits to measure triglycerides, total cholesterol, HDL, and LDL/VLDL. All analyses are reported as mean \pm SEM (n = 5/group). Statistical significance was determined by t-test, $p < 0.05$. *Denotes statistical significant difference between healthy and obese serum ($p < 0.05$).

	Triglycerides (mg/dL)	HDL (mg/dL)	LDL (mg/dL)	Total Cholesterol (mg/dL)
Healthy Serum	38.8 \pm 0.5	26.0 \pm 0.6	145.4 \pm 3.2	183.1 \pm 1.9
Obese Serum	191.6 \pm 3.0*	56.5 \pm 0.8*	225.2 \pm 1.6*	231.5 \pm 0.7*

Table 2.2. AuNP Characterization Prior to and Following the Addition of a BC. Data represent mean \pm standard deviation, n=3-5/group. AuNPs were diluted in and incubated for 8 h at 4 °C in 10% pooled human serum. AuNPs were characterized with and without BCs via assessment of ζ -potential, hydrodynamic size, and polydispersion index. * denotes statistical significance when compared to an AuNP with no BC. # denotes statistical significance when compared to an AuNP with healthy BC. Statistical significance was determined by one-way ANOVA using Tukey's multiple comparisons test p<0.05.

	BC	Citrate 20	Citrate 100	PVP 20	PVP 100
Particle Concentration (NPs/ $\mu\text{g} \times 10^8$)	None	6.9 \pm 1.6	3.2 \pm 0.3	2.8 \pm 0.6	2.0 \pm 0.5
Hydrodynamic Size (nm)	None	23.4 \pm 0.5	103.9 \pm 2.0	43.9 \pm 7.9	134.5 \pm 3.2
	Healthy	870.9 \pm 165.0*	915.9 \pm 157.3*	134.4 \pm 2.3*	955.8 \pm 190.9*
	Obese	1303.3 \pm 95.0*#	1435 \pm 104.8*#	328.1 \pm 53.6*#	1420 \pm 22.3*#
Polydispersion Index	None	0.16 \pm 0.02	0.09 \pm 0.01	0.17 \pm 0.05	0.11 \pm 0.08
	Healthy	0.29 \pm 0.06*	0.27 \pm 0.07	0.07 \pm 0.01*	0.39 \pm 0.12*
	Obese	0.34 \pm 0.02*	0.14 \pm 0.13	0.19 \pm 0.03#	0.10 \pm 0.05#
ζ Potential (mV)	None	-35.5 \pm 2.6	-43.0 \pm 3.7	-30.3 \pm 2.9	-28.3 \pm 3.8
	Healthy	-15.1 \pm 2.7*	-7.3 \pm 2.2*	-16.5 \pm 3.3*	-8.6 \pm 1.2*
	Obese	-13.5 \pm 1.7*	-8.2 \pm 2.1*	-14.2 \pm 2.1*	-5.7 \pm 1.8*

2.4.2 Protein components of the BC—identification and relative quantification between AuNPs

Following incubation in healthy serum, a total of 225, 215, 226, and 146 proteins were found in the BCs of the 20 nm PVP-, 100 nm PVP-, 20 nm citrate-, and 100 nm citrate-coated AuNPs, respectively (Fig. 2.1A and Supplementary Table S2.3). In the healthy serum environment, a total of 128 proteins (49.6% of all proteins identified) were shared between all four AuNPs, including apolipoproteins A-1, A-2, A-4, B, C-1, C-2, D, E, as well as gelsolin, complement factor H, coagulation factor XII, plasminogen, prothrombin, fibronectin 1, vitronectin, clusterin, and others. The BCs on 20 nm PVP-, 100 nm PVP-, 20 nm citrate-, and 100 nm citrate-coated AuNPs contained 4, 9, 10, and 5 unique proteins, respectively (Fig. 2.1A and Supplementary Table S2.3).

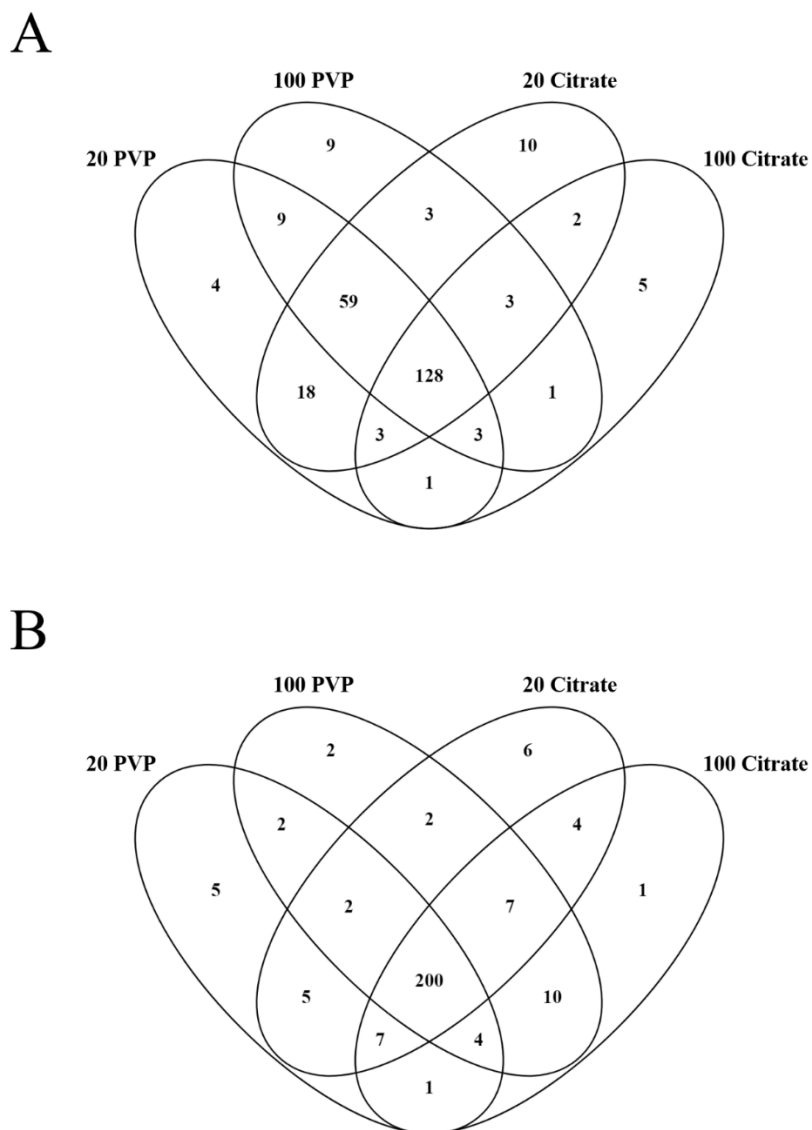


Figure 2.1. Comparison of BC composition of all four particles in healthy or obese serum. Proteins identified from each AuNP BC were compared to proteins in all other AuNP BCs under the same condition, either (A) healthy or (B) obese. Venn diagrams were used to illustrate all comparisons. A comprehensive list of all proteins found in each BC may be found in Supplementary Table S2.1. List of specific proteins used to generate Venn diagram (A, B) may be found in Supplementary Tables S2.3 and S2.4, respectively. AuNPs, gold nanoparticles; BC, biocorona.

A total of 18 proteins were exclusive to the 20 nm AuNPs incubated in healthy serum. Among these 18 were complement factor 9, soluble scavenger receptor, and multimerin-1. There were nine proteins found only in the PVP-coated AuNPs, including insulin-like growth factor 2, ficolin-2, and histone H2A. Only 2 proteins, metalloredutase STEAP3 and epididymis luminal protein 213,

were exclusive to the two 20 citrate-coated AuNPs. Cholesterol ester transfer protein was found in the BCs of the two 100 nm AuNPs and not the 20 nm AuNP BCs.

In obese serum, 20 nm PVP-, 100 nm PVP-, 20 nm citrate-, and 100 nm citrate-coated AuNPs adsorbed 226, 229, 233, and 234 proteins, respectively. AuNPs incubated in obese serum formed BCs that shared 200 proteins, or 77.5% of all proteins identified, including apolipoproteins A-I, A-II, A-IV, C-I, C-III, E, and LI, complement components 1, C6, and H, von Willebrand factor, transthyretin, clusterin, gelsolin, and others (Fig. 2.1B and Supplementary Table S2.4). All AuNPs were determined to associate unique proteins, with the 20 nm PVP-, 100 nm PVP-, 20 nm citrate-, and 100 nm citrate-coated AuNP BCs containing 5, 2, 6, and 1 exclusive proteins, respectively.

The 20 nm AuNPs contain 5 exclusive proteins, which include retinoic acid receptor responder protein 2 and immunoglobulin heavy variables 1–18 and 3–38, while the 100 nm AuNPs have 10, including β -2-microglobulin and soluble scavenger receptor. The PVP-coated AuNPs exclusively share 2 proteins, ficolin-2 and cDNA FLJ95778 (similar to SERPINA10), while the citrate-coated AuNPs have 4, including serpin peptidase inhibitor and cDNA FLJ56989 (similar to MARCO).

Although the majority of proteins identified were shared between AuNPs, differences in quantity were determined due to variations in AuNP size and surface coating (Fig. 2.2). For example, in healthy serum, apolipoprotein A-1 and complement H both bind 20 nm AuNPs in greater abundance than their 100 nm counterparts (Fig. 2.2). Transthyretin and prothrombin associated citrate-coated AuNPs in a size dependent manner (20 nm >100 nm) while equivalently binding PVP-coated AuNPs. The PVP-coated 100 nm AuNPs adsorbed more apolipoprotein A-1, complement H, transthyretin, and prothrombin than the citrate-coated 100 nm AuNPs. There was also more complement H protein on the PVP-coated 20 nm AuNP than the citrate-coated 20 nm AuNP. The opposite was true for transthyretin and lipoprotein-A, both of which were more abundant on the citrate-coated 20 nm AuNPs than the PVP-coated 20 nm AuNPs. All AuNPs were determined to associate similar amounts of serum amyloid A.

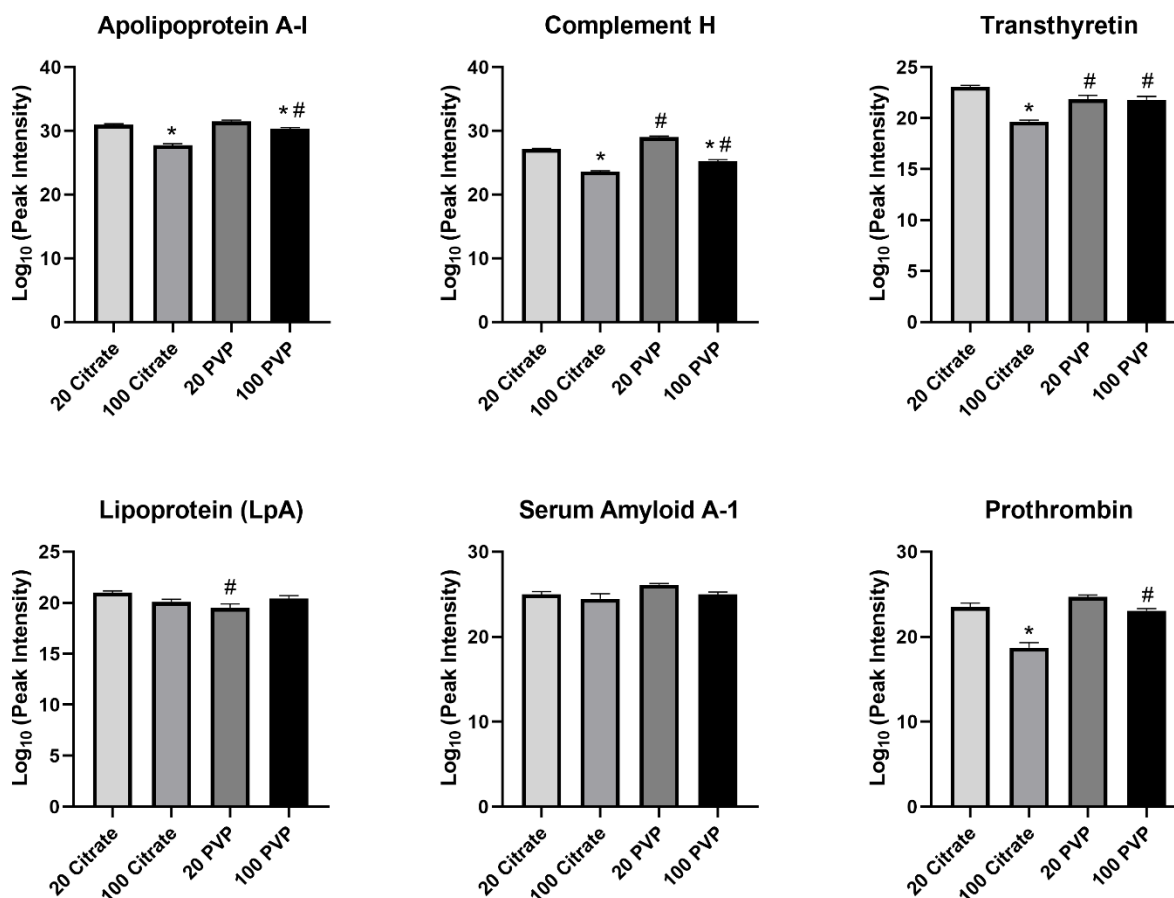


Figure 2.2. Relative abundance comparison of selected proteins found in the BCs of all four AuNPs in the healthy condition. Proteins identified as present with the BCs of all four AuNPs in the healthy condition were compared in their abundance. Peak intensities were log₁₀ transformed to convert the raw values to a more readily understandable format. Comparisons were performed by one-way ANOVA with Tukey post hoc analysis ($p < 0.05$). *Denotes statistical significance compared to the corresponding 20 nm AuNP with the same coating, #denotes statistical significance compared to the corresponding citrate-coated AuNP with the same size.

Abundance differences were also observed when AuNPs were incubated in obese serum to form BCs. Apolipoprotein A-1, transthyretin, and lipoprotein-A are more abundant in the 100 nm PVP-coated AuNPs than the 20 nm PVP-coated AuNPs (Fig. 2.3). The 100 nm citrate-coated AuNP BC contains more von Willebrand factor than the 20 nm citrate-coated AuNP BC. Complement H protein associated more with 20 nm PVP-coated AuNPs than the 100 nm PVP-coated AuNPs. Coating also influenced protein adsorption, as apolipoprotein A-1 and cadherin are more abundant in both sizes of PVP-coated AuNP than their citrate-coated counterparts. Von Willebrand factor is more abundant in the PVP-coated 20 nm AuNP BC than the citrate-coated 20 nm AuNP BC.

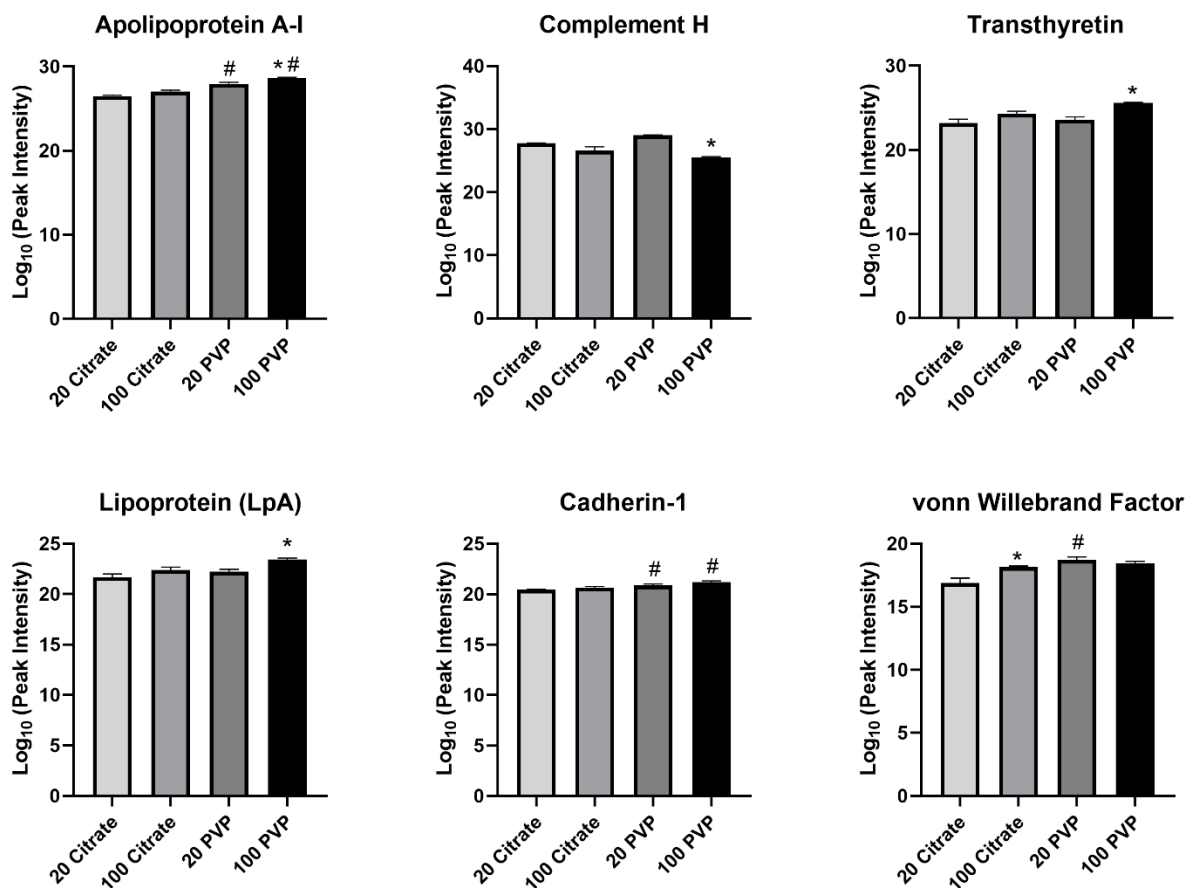


Figure 2.3. Relative abundance comparison of selected proteins found in the BCs of all four AuNPs in the obese condition. Proteins identified as present with the BCs of all four AuNPs in the obese condition were compared in their abundance. Peak intensities were log₁₀ transformed to convert the raw values to a more readily understandable format. Comparisons were performed by one-way ANOVA with Tukey post hoc analysis ($p < 0.05$). *Denotes statistical significance compared to the corresponding 20 nm AuNP with the same coating, #denotes statistical significance compared to the corresponding citrate-coated AuNP with the same size.

2.4.3 Comparison of healthy and obese BCs—protein identities

AuNPs incubated in obese serum generally adsorbed a larger number of proteins than those incubated in healthy serum (Fig. 2.4 and Supplementary Table S2.5). The PVP-coated 20 nm AuNPs were the exception, adsorbing an approximately equal number of total proteins between conditions, although it should be noted that proteomic profiles were distinct between conditions, with 35 and 36 proteins exclusive to the healthy and obese conditions, respectively (Fig. 2.4 and Supplementary Table S2.5). The pattern of more proteins being present in the obese BCs was more prominent in 100 nm AuNPs than 20 nm AuNPs (Fig. 2.4). For 100 nm AuNPs, a smaller

number of these proteins were shared between the healthy and obese conditions, demonstrating adsorption of distinct proteins due to serum environment.

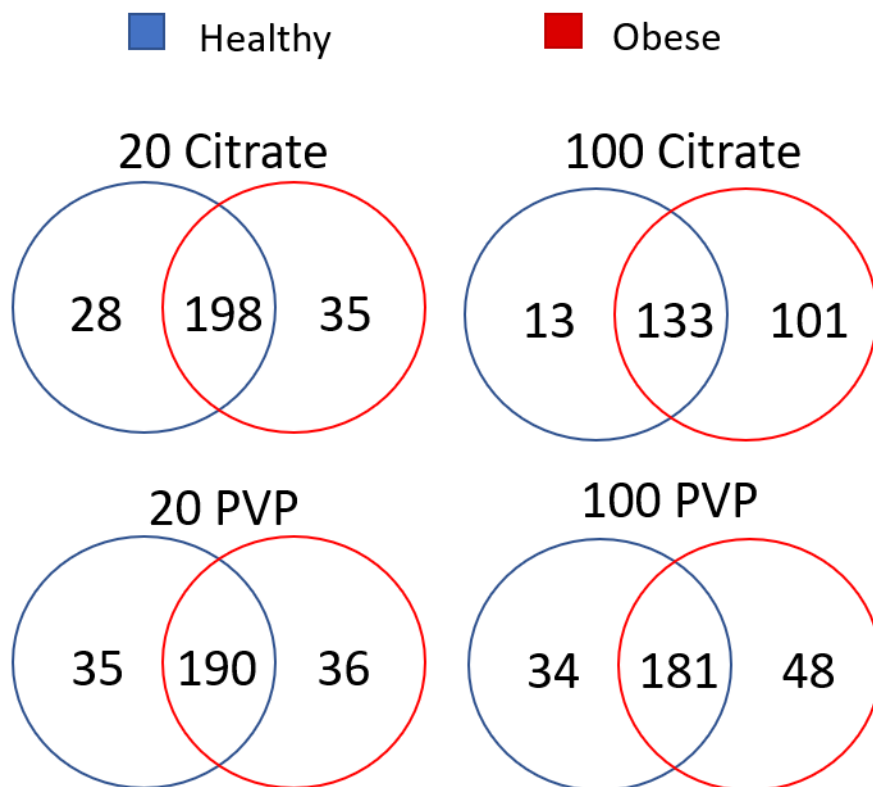


Figure 2.4. Comparison of BC composition between healthy and obese conditions for all four AuNPs. Proteins identified as present in each AuNP BC formed from healthy serum were compared to proteins within the same AuNP BC formed from obese serum. Venn diagrams were used to illustrate all comparisons. A comprehensive list of all proteins found in each BC is found in Supplementary Table S2.1. A list of specific proteins used to generate the Venn diagrams in the figure is found in Supplementary Table S2.5.

2.4.4 Comparison of healthy and obese BCs—relative quantification

Of the 10 proteins that demonstrated the largest differences between healthy and obese conditions, most were found to be more abundant in the obese condition compared to the healthy (Fig. 2.5 and Supplementary Table S2.1). Several proteins were found to be repeated between the 10 most altered proteins for all AuNPs, including von Willebrand factor, which was found as more abundant in the obese BCs for all four AuNPs. Furthermore, fibrinogen alpha chain and testicular tissue protein Li 70 were found as more abundant in the obese BC for all AuNPs except citrate 100 nm. Commonalities were observed based on AuNP properties as well; lectin galactoside-

binding soluble 3 binding protein isoform 1 was found as more abundant in the healthy BC for PVP-coated AuNPs, and platelet factor 4 was found as more abundant in the obese BC for citrate-coated AuNPs.

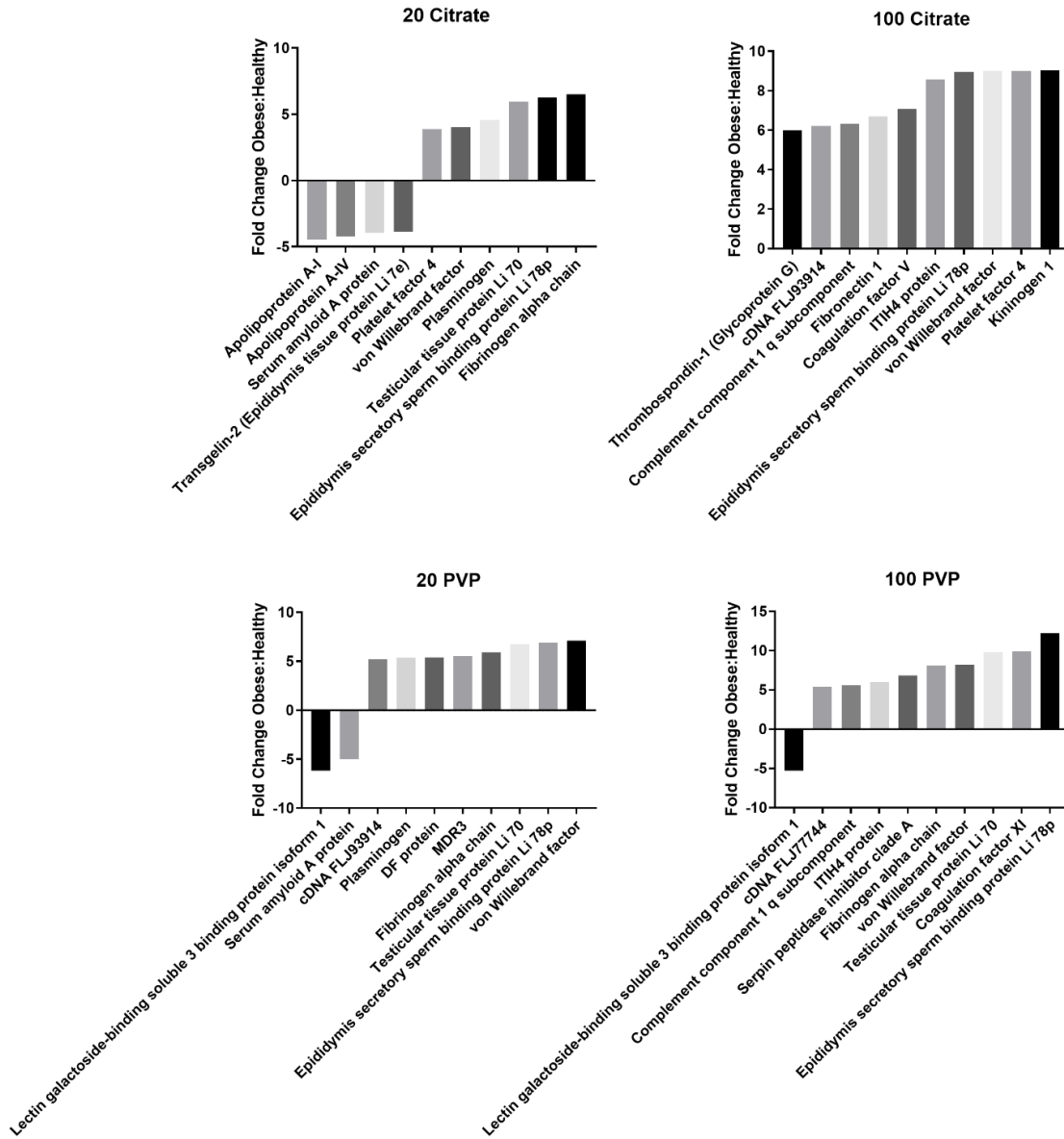


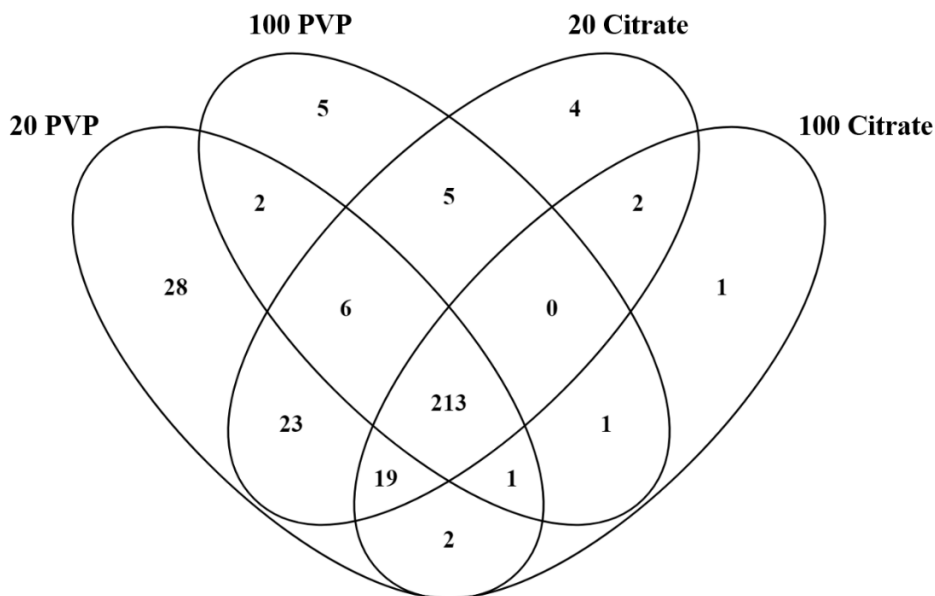
Figure 2.5. Fold changes of proteins between the healthy and obese BCs. Quantities of shared proteins between each AuNP BC are depicted as fold changes. Negative values indicate that the protein was more abundant in healthy conditions, while positive values indicate that the protein was more abundant in obese conditions. Individual graphs depict the 10 most altered proteins in terms of abundance between healthy and obese conditions. Supplementary Table S2.1 includes a comprehensive list of all protein fold changes between healthy and obese conditions for each AuNP tested.

Furthermore, protein binding was influenced by AuNP size, with Complement Component 1q subcomponent and ITIH4 protein more abundant in the obese BC of 100 nm AuNPs. Both serum amyloid AI protein and plasminogen experienced large fold changes between conditions, with serum amyloid AI being more abundant in the healthy BC and plasminogen being more abundant in the obese BC. Each AuNP had at least two proteins that experienced substantial fold changes between healthy and obese conditions that were unique to that particle, underlying that each particle forms a unique BC despite commonalities between AuNPs.

2.4.5 Lipid components of the AuNP BCs—identification and relative quantification between AuNPs

A total of 294, 233, 272, and 239 MRMs related to lipids (hereafter referred to as lipids for simplification) were found in the healthy BCs of the 20 nm PVP-, 100 nm PVP-, 20 nm citrate-, and 100 nm citrate-coated AuNPs, respectively (Fig. 2.6A and Supplementary Table S2.6). A total of 213 lipids, or ~68% of the lipids identified, were shared between all four AuNPs following incubation in healthy serum. These 213 included such lipids as cholest-5-en-3 β -yl hexadecanoate, 16:1 cholesteryl ester, phosphatidylcholine (38:8), sphingomyelin (d18:2/22:1), and others. The 20 nm PVP-coated AuNP BC was the most unique, with 28 distinct lipids, while 100 nm PVP-, 20 nm citrate-, and 100 nm citrate-coated AuNPs contained 5, 4, and 1 unique lipids, respectively (Fig. 2.6A and Supplementary Table S2.6). A total of 23 lipids were found only in the 20 nm AuNP BCs, including 20:0 campesterol ester, 22:3 stigmasteryl ester, and ceramide (d18:1/22:0), while 1 lipid [phosphatidylcholine plasmalogen (42:6); phosphatidylcholine (41:7)] was only in the 100 nm AuNP BCs.

A



B

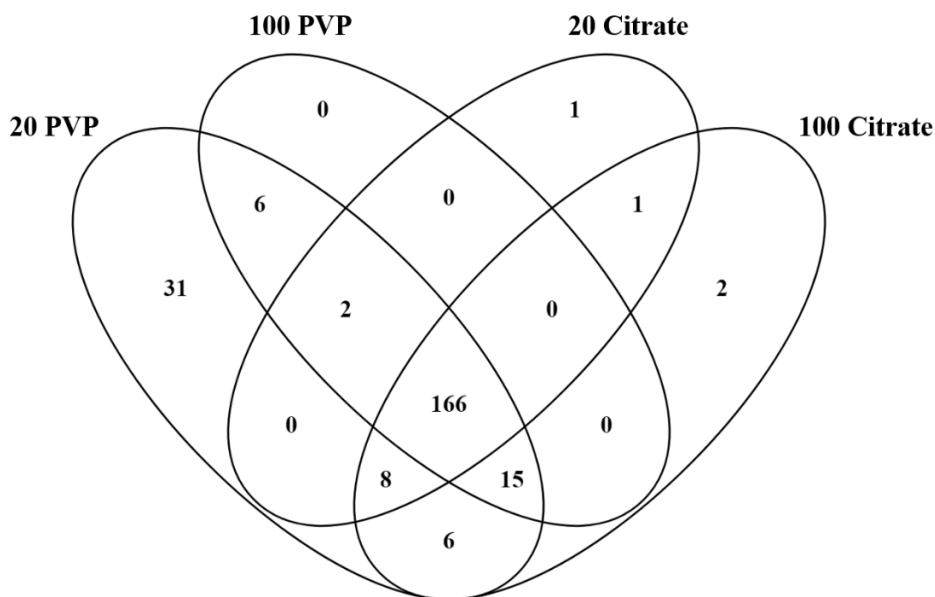


Figure 2.6. Comparison of BC composition of all four particles in healthy or obese serum. Lipids identified from each AuNP BC were compared to lipids in all other AuNP BCs under the same condition, either (A) healthy or (B) obese. Venn diagrams were used to illustrate all comparisons. A comprehensive list of all lipids found in each BC is found in Supplementary Table S2.2. List of specific lipids used to generate Venn diagram (A, B) is found in Supplementary Tables S2.6 and S2.7, respectively.

The PVP and citrate coated AuNP BCs each had two lipids which were exclusive to that coating, including 2-Hydroxy-lauroylcarnitine, 3-hydroxydodecanoylcarnitine for citrate-coated AuNPs, and triglyceride (54:4) fatty acid 18:2 for PVP-coated AuNPs. Size seems to have an influence on the total number of unique lipids adsorbed to the AuNP surface, as both 20 nm AuNPs adsorbed more unique proteins than the 100 nm AuNP of the same coating when incubated in healthy serum.

Within obese serum, the BCs of the 20 nm PVP-, 100 nm PVP-, 20 nm citrate-, and 100 nm citrate-coated AuNPs contained 234, 189, 178, and 198 lipids, respectively, with 166 lipids shared between all four AuNPs. This 166 included lipids such as triglyceride (50:2) fatty acid 16:0, (5Z,8Z)-tetradecadienoylcarnitine, and N-(dodecanoyl)-sphing-4-enine-1-phosphocholine. The 20 nm PVP-, 100 nm PVP-, 20 nm citrate-, and 100 nm citrate-coated AuNPs contain 31, 0, 1, and 2 unique lipids, respectively (Fig. 2.6B and Supplementary Table S2.7). No lipids were unique to the 20 or 100 nm AuNPs. Six lipids, including triglyceride (48:1) fatty acid 16:0, were only in the PVP-coated AuNP BCs, and the citrate-coated AuNP BCs share only a single unknown lipid found during acyl-carnitine class screenings.

All AuNPs were found to adsorb a number of lipids in common; however, differences in abundance of these shared lipids were determined. In the healthy condition, many lipids were more abundant in the BC of the 20 nm PVP-coated AuNP than the 100 nm PVP-coated AuNP, including 17:1 campesterol ester, 16:1 cholesteryl ester, triglyceride (52:2) fatty acid 16:0, phosphatidylcholine alkyl ether (34:3), and 20:5 cholesteryl ester (Fig. 2.7). Conversely, 16:0 cholesteryl ester was more abundant in the 100 nm PVP-coated AuNP BC than the 20 nm PVP-coated AuNP BC.

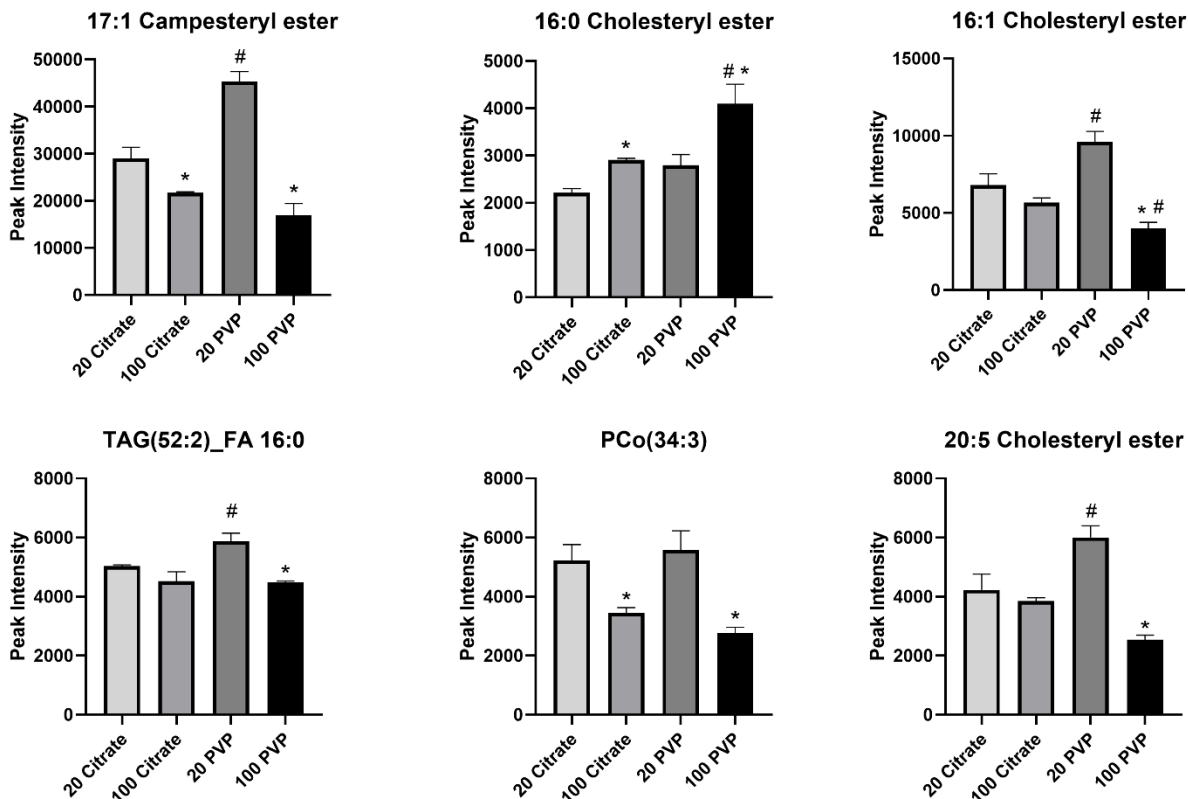


Figure 2.7. Relative abundance comparison of selected lipids found in the BCs of all four AuNPs in the healthy condition. Lipids identified as present with the BCs of all four AuNPs in the healthy condition were compared in their abundance. Comparisons were performed by one-way ANOVA with Tukey post hoc analysis ($p < 0.05$). *Denotes statistical significance compared to the corresponding 20 nm AuNP with the same coating, #denotes statistical significance compared to the corresponding citrate-coated AuNP with the same size. FA, fatty acids; PCo, phosphatidylcholine alkyl ether lipids; TAG, triglycerides.

Within the citrate-coated AuNP BCs, 17:1 campesteryl ester and phosphatidylcholine alkyl ether (34:3) were more abundant in the 20 nm AuNP BCs, and 16:0 cholesteryl ester was more abundant in the 100 nm AuNP BC. Coating also dictates the adsorption of lipids, as the PVP-coated 20 nm AuNP BCs tended to contain more 17:1 campesteryl ester, 16:1 cholesteryl ester, triglyceride (52:2) fatty acid 16:0, and 20:5 cholesteryl ester than the citrate-coated 20 nm AuNP BCs. The 16:0 cholesteryl ester was more abundant in the PVP-coated 100 nm AuNP than the citrate-coated 100 nm AuNP, while the opposite pattern was found for 16:1 cholesteryl ester.

Differences in lipid adsorption were also observed in the obese BCs, although to a lesser extent. The 20 nm PVP-coated AuNP adsorbed more 17:1 campesteryl ester, triglyceride (52:2) fatty acid

16:0, triglyceride (52:4) fatty acid 16:0, and phosphatidylcholine (36:8) than the 100 nm PVP-coated AuNP (Fig. 2.8). Furthermore, the 20 nm PVP-coated AuNP adsorbed more of each of these lipids than the citrate-coated 20 nm AuNP. No differences between AuNPs were found in the abundances of 16:0 cholesteryl ester or 16:1 cholesteryl ester.

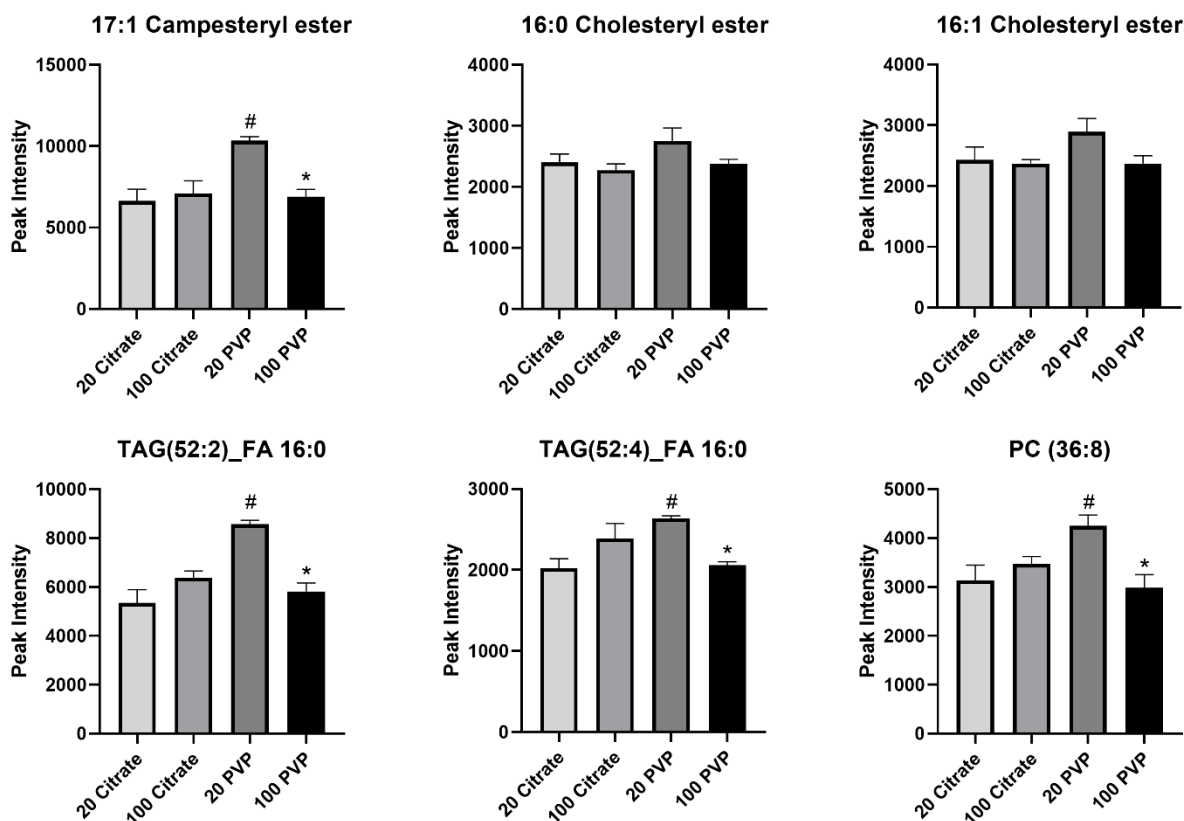


Figure 2.8. Relative abundance comparison of selected lipids found in the BCs of all four AuNPs in the obese condition. Lipids identified as present with the BCs of all four AuNPs in the obese condition were compared in their abundance. Comparisons were performed by one-way ANOVA with Tukey post hoc analysis ($p < 0.05$). *Denotes statistical significance compared to the corresponding 20 nm AuNP with the same coating, #denotes statistical significance compared to the corresponding citrate-coated AuNP with the same size. PC, phosphatidylcholine lipids.

2.4.6 Comparison of healthy and obese BCs—lipid identities

The identities of lipids found to associate with each AuNP in either healthy or obese serum were compared (Fig. 2.9). AuNPs incubated in obese serum adsorbed a smaller number of lipids than the corresponding AuNP incubated in healthy serum. This pattern was more prominent in 20 nm AuNPs than 100 nm AuNPs (Fig. 2.9 and Supplementary Table S2.8). For 20 nm AuNPs, a larger

number of lipids were unique to the healthy condition, indicating the formation of a BC distinct from the BC formed in obese conditions. 100 nm AuNP BCs were more similar between conditions, with similar numbers of lipids shared between conditions and smaller numbers of lipids unique to the healthy BC.

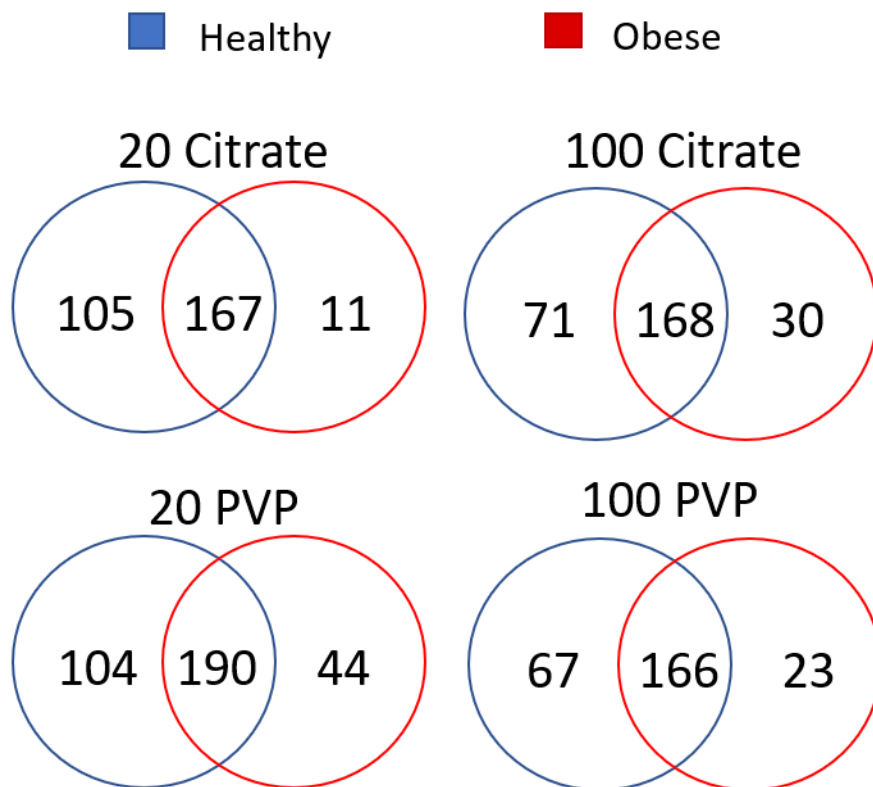


Figure 2.9. Comparison of BC composition between healthy and obese conditions for all four AuNPs. Lipids identified as present in each AuNP BC formed from healthy serum were compared to lipids within the same AuNP BC formed from obese serum. Venn diagrams were used to illustrate all comparisons. A comprehensive list of all lipids found in each BC is found in Supplementary Table S2.2. A list of specific lipids used to generate the Venn diagrams in the figure is found in Supplementary Table S2.8.

2.4.7 Obese and healthy comparisons—relative lipid quantification

Of the 10 lipids which had the largest fold changes between the healthy and obese BCs, all were more abundant in the healthy BC (Fig. 2.10 and Supplementary Table S2.2). These lipids were almost exclusively cholesteryl esters and were highly conserved between AuNPs. Six lipids were shared between all four AuNPs, including 19:0 campesteryl ester; 20:0 cholesteryl ester, 18:0

sitosteryl ester; cholesteryl 11-hydroperoxy-eicosatetraenoate, 22:2 cholesteryl ester, 20:1 stigmasteryl ester, 20:2 sitosteryl ester; 18:1 campesteryl ester; lanosteryl palmitoleate, 18:2 campesteryl ester; and 18:3 cholesteryl ester, 16:2 stigmasteryl ester, 16:3 sitosteryl ester. Three more lipids, specifically 20:3 campesteryl Ester and two unknown lipids detected during the cholesteryl ester class screenings, also had large fold changes between healthy and obese, but only for three AuNP types; the PVP-coated 100 nm AuNP was the exception.

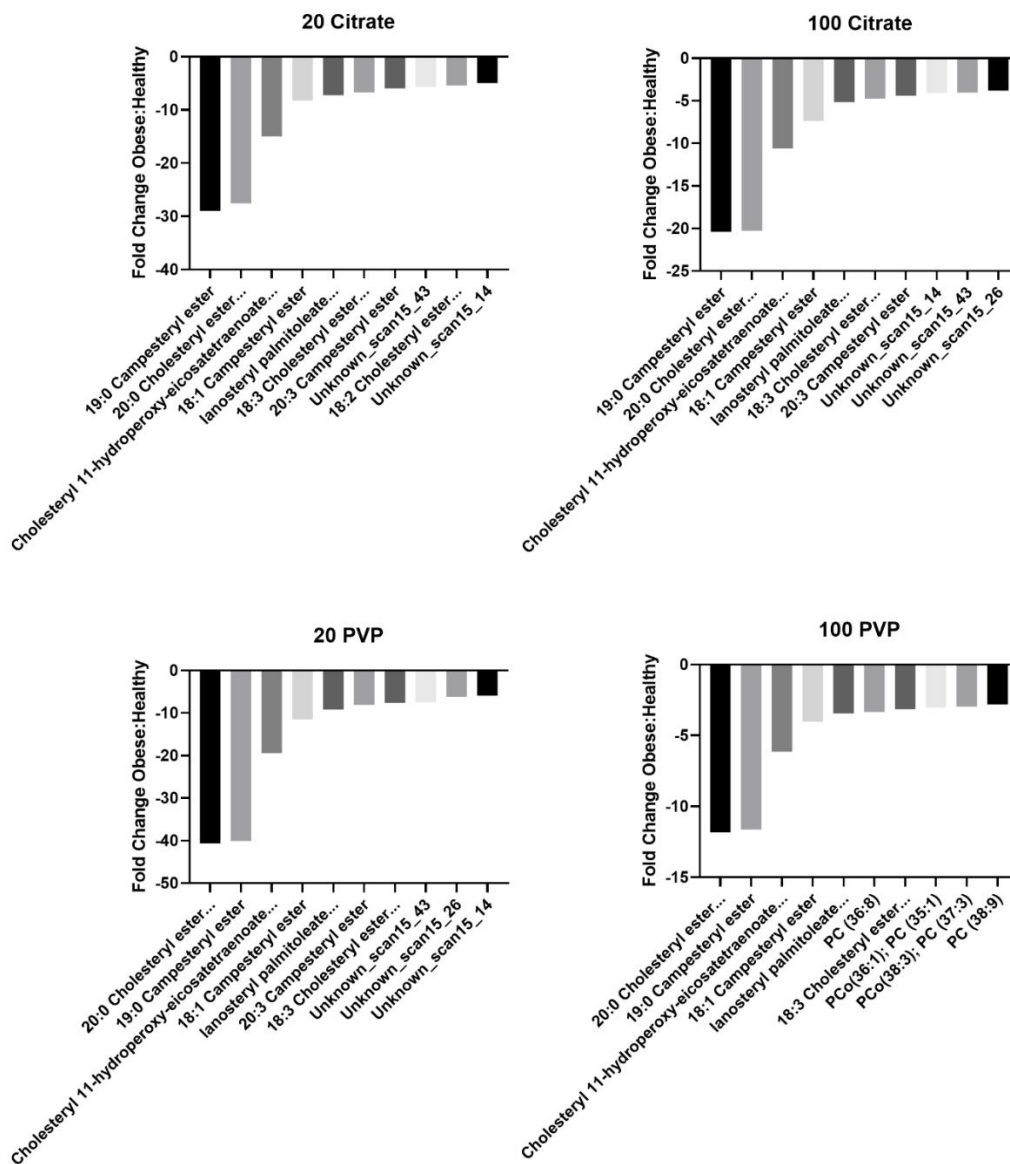


Figure 2.10. Fold changes of lipids between the healthy and obese BCs. Quantities of shared lipids between each AuNP BCs are depicted as fold changes. Negative values indicate that the lipid was more abundant in healthy conditions, while positive values indicate that the lipid was more abundant in obese conditions. Individual graphs depict the 10 most altered lipids in terms of abundance between healthy and obese conditions. Supplementary Table S2.2 includes a comprehensive list of all lipid fold changes between healthy and obese conditions for each AuNP tested. PC indicates phosphatidylcholine lipids, and PCo indicates phosphatidylcholine alkyl ether lipids. Certain lipid names were shortened for brevity, which are listed in full here. 20:0 Cholesteryl ester... ester indicates 20:0 Cholesteryl ester, 18:0 Sitosteryl ester. Cholesteryl 11-hydroperoxy-eicosatetraenoate... indicates Cholesteryl 11-hydroperoxy-eicosatetraenoate, 22:2 Cholesteryl ester, 20:1 Stigmasteryl ester, 20:2 Sitosteryl ester. Lanosteryl palmitoleate... indicates lanosteryl palmitoleate, 18:2 Campesteryl ester. 18:3 Cholesteryl ester... indicates 18:3 Cholesteryl ester, 16:2 Stigmasteryl ester, 16:3 Sitosteryl ester. 18:2 Cholesteryl ester... ester indicates 18:2 Cholesteryl ester, zymosteryl oleate, 16:1 Stigmasteryl ester, 16:2 Sitosteryl ester.

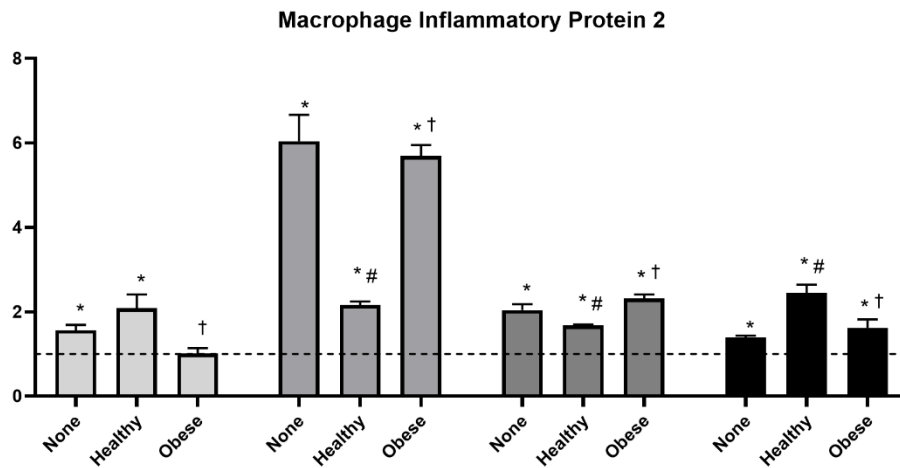
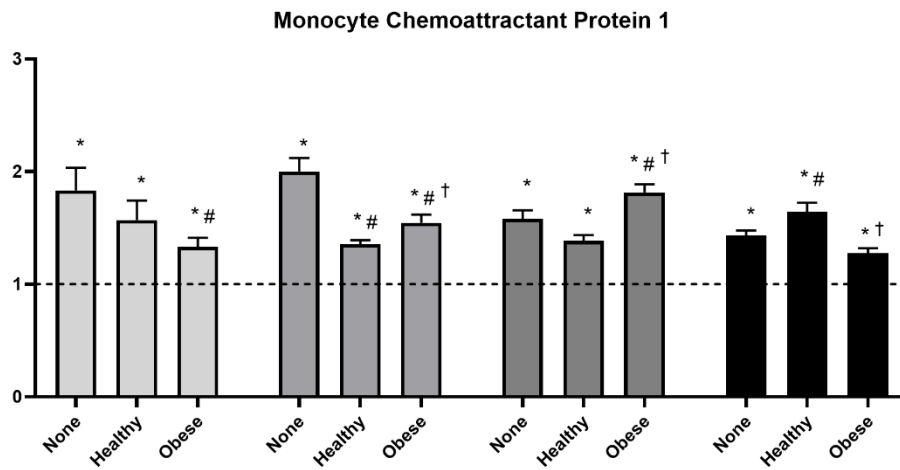
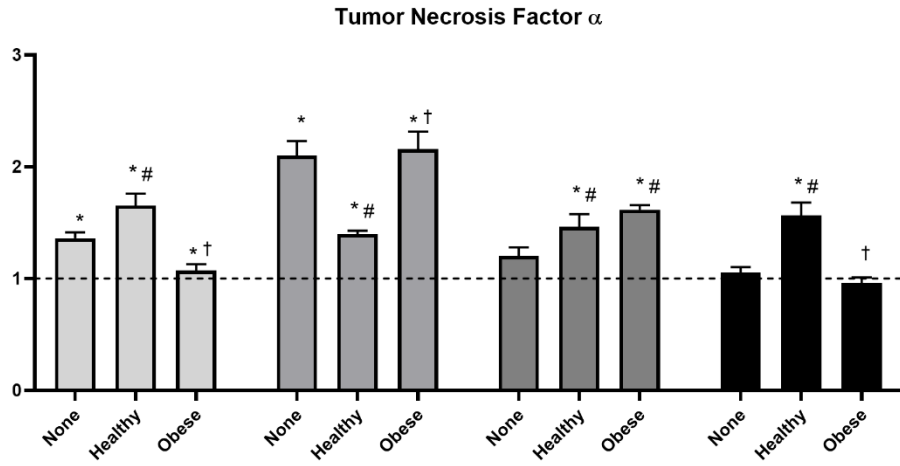
Only the citrate-coated 20 nm and PVP-coated 100 nm AuNP BCs contained lipids, which were exclusive to one AuNP BC. The 18:2 cholesteryl ester, zymosteryl oleate, 16:1 stigmasteryl ester, 16:2 sitosteryl ester was exclusive to the citrate-coated 20 nm AuNP BC, and phosphatidylcholine (36:8), phosphatidylcholine alkyl ether (36:1); phosphatidylcholine (35:1), phosphatidylcholine alkyl ether (38:3); phosphatidylcholine (37:3); and phosphatidylcholine (38:9) were exclusive to the PVP-coated 100 nm AuNP BC.

2.4.8 BC-induced variations in macrophage viability and inflammatory response

At concentrations (12.5 or 50 $\mu\text{g/mL}$) and time points (3 or 24 hours), no alterations in cell viability were determined due to AuNP exposures with or without BCs (Supplementary Fig. S2.1). The citrate-coated 20 nm AuNP without a BC increased expression of *TNF- α* , *MCP-1*, and *MIP-2* (Fig. 2.11). The addition of a healthy BC induced similar upregulation of *MCP-1* or *MIP-2* while increasing expression of *TNF- α* compared to the 20 nm citrate-coated AuNP without a BC. The obese BC reduced expression of *TNF- α* and *MIP-2* compared to the healthy BC. The addition of the obese BC on 20 nm citrate-coated AuNPs induced *MCP-1* expression similar to when a healthy BC was present. All three inflammatory markers were increased by exposure to citrate-coated 100 nm AuNP without a BC. The healthy BC significantly and uniformly reduced expression compared to AuNPs without a BC. The addition of an obese BC caused increased expression of *TNF- α* and *MIP-2* compared to the healthy BC.

Figure 2.11. Changes in gene expression following exposure to AuNPs with or without a healthy or obese BC. Expression of mRNA was assessed relative to serum-free media control cells (untreated) (dotted line). Cells were grown to 90% confluency in a 96-well plate before exposure to 50 $\mu\text{g}/\text{mL}$ AuNPs with no BC, a healthy BC, or an obese BC for 24 hours. Gene expression of TNF- α , CCL2, CXCL2, and GAPDH (control) was assessed through PCR to evaluate the inflammatory response induced by AuNP exposure. *Denotes statistical significance compared to the expression of the unexposed control, #denotes statistical significance compared to the AuNP with no BC, and †denotes statistical significance compared to the AuNP with a healthy BC. Comparisons were performed by one-way ANOVA with Tukey post hoc analysis ($p < 0.05$). GAPDH, glyceraldehyde 3-phosphate dehydrogenase; TNF- α , tumor necrosis factor- α .

20 Citrate AuNP
 100 Citrate AuNP
 20 PVP AuNP
 100 PVP AuNP



Macrophages exposed to PVP-coated 20 nm AuNP without a BC demonstrated increased expression of *MCP-1* and *MIP-2*, although *TNF- α* was not changed compared to control. The healthy BC caused an increase in *TNF- α* expression, a decrease in *MIP-2* expression, and had no effect on the expression of *MCP-1*. Compared to the healthy BC, the obese BC caused increases in *MCP-1* and *MIP-2* expression, but had no effect on *TNF- α* . The PVP-coated 100 nm AuNP without a BC caused an increase in the expression of *MCP-1* and *MIP-2*, but not *TNF- α* . The healthy BC caused expression of all three inflammatory markers to increase compared to the AuNP without a BC. The obese BC reduced the expression of all three inflammatory gene markers to levels comparable to the AuNP without a BC.

2.5 Discussion

The application of *in vitro* assessments to evaluate the safety of biomedical NPs and exposures to NPs in general is dependent on understanding the formation of the BC and its impact on cellular interactions and toxicity. Currently, scientific knowledge is lacking regarding how NP physicochemical properties and underlying diseases, such as obesity, impact NP-BC formation. Further, most investigations of the NP-BC have focused primarily on the protein content. Our findings demonstrate variability in the protein and lipid content of the BC due to AuNP physicochemical properties and obesity. This variability in the BC impacted AuNP properties and cellular responses, which may influence their functionality and use.

NPs are highly modifiable and can be engineered with specific physicochemical properties (size, composition, charge, and surface coating) enabling their usage in a variety of technologies. These properties may be altered by the addition of a BC, impacting NP functionality (Amiri et al., 2013; Salvati et al., 2013). NPs in medicine may be particularly vulnerable to BC-induced alterations in functionality, as the environment in which they are used is not only rich in biomolecules, but highly variable between individuals, as well. Introduction of AuNPs into obese serum resulted in increased hydrodynamic size compared to those in a healthy serum environment. This increase in size is likely due to agglomeration of AuNPs, as demonstrated in previous studies (Sharma et al., 2014). Enhanced agglomeration that may occur in obesity could alter therapeutic functionality of AuNPs by reducing NP surface area and altering size-dependent biodistribution. The 20 nm PVP-coated AuNPs demonstrated smaller changes in size and polydispersion following addition of the

BCs. These findings suggest that 20 nm PVP-coated AuNPs more effectively resisted agglomeration in biological environments compared to larger AuNPs and those coated with citrate. The increased agglomeration seen for citrate coated AuNPs may be due to the dynamic relationship that is formed between citrate and the AuNP upon introduction of proteins. Specifically, proteins displace the citrate from the NP surface, and citrate then associates and dissociates from the NP surface in a concentration-dependent manner (Ding et al., 2013). The 20 nm PVP-coated AuNPs are more capable of maintaining their nano-properties in biological environments, potentially assisting in their utilization in biomedicine.

Previous investigations of the NP-BC have focused almost exclusively on protein components (Chandran et al., 2017; Lundqvist et al., 2011; Wen et al., 2013). Our current study attempted to more comprehensively examine the BC by utilizing both proteomic and lipidomic approaches. Use of this combination of methods identified a similar number of proteins and lipids associating with the surface of all AuNPs. This suggests that previous research utilizing only a proteomic approach may not be able to fully establish relationships between NP-BC formation and cellular responses. Incorporation of both approaches provides a fuller understanding of the complexity of the NP-BC and may assist in the understanding of its biological interactions and responses. The use of physicochemically-distinct AuNPs allowed for comparisons of 2 modifiable NP properties (size and coating) that influence BC formation. Adsorption of proteins and lipids was determined to be influenced by both AuNP size and surface coating. When incubated in healthy serum, 20 nm AuNPs adsorbed more unique proteins and lipids compared to 100 nm AuNPs of the same coating. This indicates that the surface curvature and increased surface area of the 20 nm AuNPs may allow for a more diverse set of biomolecules to associate with the AuNP surface. Unique proteins and lipids were also determined to associate with AuNPs based upon citrate or PVP coating. Specifically, 20 nm PVP AuNPs were determined to bind the greatest number of unique lipids and a higher abundance of many shared lipids compared to other AuNPs. The addition of the lipid-rich BC likely facilitates their increased resistance to agglomeration, as studies have demonstrated that increased surface lipid content enhances NP suspension stability (Ke, 2007; Wu et al., 2006). Although all AuNPs demonstrated differential association of proteins and lipids, size appears to be the primary contributor to differences in BC formation. This is similar to a previous work investigating the association of proteins with the surfaces of spherical silver NPs of similar size

and coatings following incubation in fetal bovine serum (Shannahan et al., 2013). Together these findings suggest that the association of proteins and also lipids can somewhat be controlled via modifications in NP size and coating. This could allow for the selective removal of biomolecules from the circulation or the ability to utilize the natural BC to assist in NP functionality via alterations in NP targeting and clearance.

To date, the majority of investigations of NP safety have been performed in scenarios utilizing healthy animal and cell culture models. However, a growing portion of the global population exists with some form of underlying disease. Common examples include obesity, hyperlipidemia, metabolic syndrome, diabetes, and cardiovascular disease. Individuals with these diseases are often increasingly sensitive to exposures, demonstrating exacerbated responses, and are more likely to receive medical treatments than healthy individuals (Dong et al., 2013; Dubowsky et al., 2006). Obesity underlies a number of other chronic conditions and is known to modify circulating biomolecules, including proteins and lipids (Eisinger et al., 2014; Fjeldborg et al., 2013; Park et al., 2005; Suzuki et al., 2003). Our current study demonstrated that protein and lipid components of the AuNP-BC were modified in obese serum environments compared to healthy. Interestingly, the BCs that formed on AuNPs in the obese environment were less dependent on NP physicochemical properties compared to BC created in the healthy environment. This was demonstrated by an increased percentage of proteins shared by all AuNPs and a less unique lipid profile for each AuNP in obese serum. Additionally, the abundance of lipids such as 17:1 campesterol ester were more variable in healthy conditions than obese. Together, these findings suggest that alterations in BC formation resulting from NP physicochemical properties may be less of a concern in an obese environment, as they associate more similar biomolecules.

AuNPs in an obese biological environment associate distinct BCs compared to those forming in a healthy environment. Previously, we have demonstrated differences in protein components of the iron oxide NP-BC due to incubation in hyperlipidemic rat serum compared to healthy. This evaluation demonstrated that the hyperlipidemic conditions increased the number of distinct proteins forming the BC. Similar results were observed in our current study, which demonstrated that obesity increased the number of proteins associating with the AuNP surface. Additionally, the abundance of many proteins was determined to be increased within the BC due to obesity. Many of these differences are likely related to disease-related alterations in protein abundance within the

serum. Specifically, von Willebrand factor, fibrinogen alpha chain, serum amyloid AI and inter-alpha-trypsin inhibitor heavy chain-4 are known to be increased in the circulation of individuals suffering from obesity (Blann et al., 1993; Doumatey et al., 2016; Wiewiora, Piecuch, Sedek, & Mazur, 2017; Zhao, He, & Shi, 2010). Not all changes in protein abundance can be directly explained by disease-related differences in circulating abundance. For instance, complement component 1q was increased on 100 nm citrate- and PVP-coated AuNPs in obese conditions compared to healthy. Complement component 1q is known to remain stable despite body weight and maintains similar levels in obese and anorexic women (Pomeroy et al., 1997). Recently, it has been shown that lung cancer patients have a greater amount of complement component 1q in their serum BCs than healthy individuals, and that this difference may be exploited to produce NP therapeutics with prolonged circulation (Ren et al., 2019). This indicates that 100 nm AuNPs may remain in circulation for longer periods of time in obese individuals, and perhaps those with other diseases, due to their BCs containing greater amounts of complement component 1q. Further, these data identify complement component 1q as an important element within the diseased BC that should be considered, and potentially utilized, when designing or testing NPs for clinical and therapeutic use. Additionally, the obese BC demonstrated increased amounts of lectin galactoside-binding soluble 3 binding protein isoform 1 on 20 and 100 nm PVP-coated AuNPs and platelet factor 4 on 20 and 100 nm citrate-coated AuNPs compared to the healthy BC. The association of these proteins with the AuNP may be due to disease-related reductions in the abundance of other biomolecules increasing the ability of these proteins to interact with the surface of AuNPs. Many proteins related to blood clotting and coagulation (platelet factor 4, coagulation factor V, kininogen-1, coagulation factor XI, von Willebrand factor, and others) were more abundant in obese BCs compared to healthy. Obesity is known to cause abnormalities in blood coagulation, and factors involved in the coagulation cascade accumulate at interfaces between biological surfaces and implanted medical devices (Pergola & Pannacciulli, 2002; Xu, Bauer, Siedlecki, & State, 2014). These findings suggest that obesity alters biomolecular content of serum, which may impact protein-NP interactions forming the BC. These interactions may specifically predispose individuals suffering from obesity to dysregulation of coagulation.

Dysregulation of lipids is involved in the progression and development of obesity (Despres, 1991; Singh, Niemczyk, Saini, Awasthi, & Zimniak, 2008; Susumu et al., 2011). Overall, AuNPs

incubated in healthy serum was determined to associate more diverse lipids than those in obese serum. Further, shared lipids of the AuNP-BCs were found to be more abundant in the healthy BC compared to the obese BC. These disease-related variations in lipid accumulation may be due to differences in the association of proteins. Specifically, more distinct proteins were found to absorb to the surface of AuNPs in obese conditions and they may reduce available surface area for lipid accumulation. The BCs that formed on AuNPs in a healthy environment were found to be rich in cholesteryl esters, whereas the obese BCs had more triglycerides. The increased amount of cholesteryl esters in the healthy BC was unexpected. Obesity induced by a high-fat diet has been shown to have little to no effect of the serum concentrations of major cholesteryl ester species (Eisinger et al., 2014). Therefore, the increase in cholesteryl ester abundance within the healthy BC is not driven purely by short-term dietary-induced obesity. Rather, the increase in cholesteryl esters in the healthy BC may be due to some of the longer-term health effects that occur in obese humans over time. Specifically, obese individuals are known to have higher circulating levels of cholesteryl ester transfer protein (CETP), which transfers cholesteryl esters from high-density lipoprotein to low- and very-low density lipoproteins (Arai et al., 1994; Asayama, Hayashibe, Dobashi, Uchida, & Nakane, 2002). Individuals who suffer from cardiovascular disease do not convert cholesterol to cholesteryl ester as efficiently as healthy individuals (Gerl et al., 2018). Further, the accumulation of cholesteryl esters within macrophages has been shown to lead to the formation of atherosclerotic plaques, contributing to heart disease (Ghosh, Zhao, Bie, & Song, 2011; Kunnert & Krug, 1971). Therefore, these factors in combination could lead to a sequestration of cholesteryl esters within atherosclerotic plaques, resulting in a lower circulating concentration in obese individuals. As a direct result of this sequestration, fewer cholesteryl esters are available to bind the AuNP surface in obese serum, resulting in a greater abundance in both healthy serum and within the AuNP BC formed from healthy serum. The increased amount of triglycerides within the obese BC was expected and likely is abundance-driven, as triglycerides are a dietary lipid class and have been shown, both in our own samples and previous research, to be elevated in obesity (Hollister, Overall, & Snow, 1967; Nieman et al., 1999).

The disease-related variations in BC formation on AuNPs were determined to impact macrophage responses in cell culture. As expected, none of the AuNPs evaluated caused any significant decreases in macrophage viability. This is consistent with previous research demonstrating the

absence of direct cytotoxic effects due to AuNP exposure (Anwar, Janát-Amsbury, Ray, Peterson, & Ghandehari, 2012; Shukla et al., 2005). AuNP physicochemical properties and disease-related differences in the BC induced differential gene expression of macrophage inflammatory cytokines. Effects of the healthy and obese BC in terms of inflammatory gene expression were not found to be consistent between AuNPs. This is likely due to the uniqueness of each BC as a result of physicochemical properties of the AuNP. The complexity of the BC implies that it is unlikely a single protein or lipid governs cellular responses. A previous evaluation was performed investigating the contribution of bovine serum albumin in the cellular response to the NP-BC (Shannahan et al., 2015). This study compared silver NPs with either a full BC formed following incubation in fetal bovine serum or a BC consisting of only bovine serum albumin. It was determined that although albumin was the primary protein present within the BC, its presence did not correlate to cellular effects induced by the full BC. In our current study, healthy and obese BCs demonstrated differential induction of inflammatory gene expression following exposure to AuNPs with different BCs. This variability highlights how disease environments can modify NP surfaces, resulting in altered immune cell responses. Previous research has demonstrated that the addition of a hyperlipidemic BC on iron oxide NPs enhances endothelial cell expression of inflammatory genes and cell adhesion markers (Shannahan et al., 2016). Together, these findings demonstrate that the comparative assessment of NP toxicity utilizing *in vitro* studies performed in serum-free environments where the BC is not able to form may not generate relevant cellular responses. Additionally, each NP's ability to instigate immune responses following association of the BC is not similar due to variations in the formation of the BC that may occur due to NP properties and biomolecule content of the biological environment.

2.6 Conclusions

While we believe that both the design and conclusions of this study are robust, it is not without limitations. While the use of pooled mixed-gender serum is ideal for making broad, generalizable conclusions, it does not allow for the assessment of individual variability. The pooling of subject serum was random and did not control for factors such as age or preexisting disease. While pooling the serum likely reduced the influence of many extraneous factors, it is unlikely that they were eliminated entirely. Our previous study demonstrated unique variations in the protein content of the BC that forms on iron oxide NPs between individuals based on sex, blood parameters, and

exercise (Kobos et al., 2018). Future studies will evaluate specific individual variations in the lipid content of the NP-BC.

In conclusion, our findings demonstrate that physicochemically distinct AuNPs form unique BCs that differ based upon protein and lipid content. Furthermore, underlying disease states, such as obesity, may impact the association of biomolecules with the NPs surface. The addition of these BCs may differentially influence cellular interactions and responses. The incorporation of the BC into *in vitro* toxicity assessment models may enhance the translatability of results to clinical applications and outcomes of nano-enable therapeutics. The use of the BC also can be an efficient and effective tool for the screening of subpopulation susceptibility in cell culture. A more comprehensive understanding of the initial interactions between the biological environment and the NP surface will allow for the development and expanded usage of NPs in biomedical applications.

2.7 References

- Adamson, S. X. F., Lin, Z., Chen, R., Kobos, L., & Shannahan, J. (2018). Experimental challenges regarding the *in vitro* investigation of the nanoparticle-biocorona in disease states. *Toxicology in Vitro*, *51*(January), 40–49. <https://doi.org/10.1016/j.tiv.2018.05.003>
- Adult Obesity Prevalence Maps. (2019). Retrieved July 8, 2019, from <https://www.cdc.gov/obesity/data/prevalence-maps.html>
- Amiri, H., Bordonali, L., Lascialfari, A., Wan, S., Monopoli, M. P., Lynch, I., ... Mahmoudi, M. (2013). Protein corona affects the relaxivity and MRI contrast efficiency of magnetic nanoparticles. *Nanoscale*, *5*(18), 8656–8665. <https://doi.org/10.1039/c3nr00345k>
- Anwar, A., Janát-Amsbury, M. ., Ray, A., Peterson, C. M., & Ghandehari, H. (2012). Geometry and Surface Characteristics of Gold Nanoparticles Influence their Biodistribution and Uptake by Macrophages. *European Journal of Pharmaceutics and Biopharmaceutics*, *77*(3), 417–423. <https://doi.org/10.1016/j.ejpb.2010.11.010>.Geometry

- Arai, T., Fujioka, S., Nozaki, S., Keno, Y., Yamane, M., & Shinohara, E. (1994). Increased Plasma Cholesteryl Ester Transfer Protein in Obese Subjects. *Arteriosclerosis and Thrombosis: A Journal of Vascular Biology*, *14*(7), 1129–1136.
- Asayama, K., Hayashibe, H., Dobashi, K., Uchida, N., & Nakane, T. (2002). Increased Serum Cholesteryl Ester Transfer Protein in Obese Children. *Obesity Research*, *10*(6), 439–446.
- Berghöfer, A., Pischon, T., Reinhold, T., Apovian, C. M., Sharma, A. M., & Willich, S. N. (2008). Obesity prevalence from a European perspective : a systematic review. *BMC Public Health*, *10*, 1–10. <https://doi.org/10.1186/1471-2458-8-200>
- Blann, A., Bushell, D., Davies, A., Farager, E., Miller, J., & McCollum, C. (1993). von Willebrand factor, the endothelium and obesity. *International Journal of Obesity and Related Metabolic Disorders: Journal of the International Association for the Study of Obesity*, *17*(12), 723–725.
- Bligh, E. G., & Dyer, W. J. (1959). A Rapid Method of Total Lipid Extracation and Purification. *Canadian Journal of Biochemistry and Physiology*, *37*.
- Casey, T., Harlow, K., Ferreira, C. R., Sobreira, T. J. P., Schinckel, A., Stewart, K., ... Casey, T. (2018). The potential of identifying replacement gilts by screening for lipid biomarkers in reproductive tract swabs taken at weaning. *Journal of Applied Animal Research*, *2119*. <https://doi.org/10.1080/09712119.2017.1384733>
- Chandran, P., Riviere, J. E., Monteiro-riviere, N. A., Chandran, P., Riviere, J. E., & Monteiro-riviere, N. A. (2017). Surface chemistry of gold nanoparticles determines the biocorona composition impacting cellular uptake , toxicity and gene expression profiles in human endothelial cells. *Nanotoxicology*, *5390*. <https://doi.org/10.1080/17435390.2017.1314036>
- Cheng, Y., Samia, A. C., Meyers, J. D., & Panagopoulos, I. (2008). Highly Efficient Drug Delivery with Gold Nanoparticle Vectors for in Vivo Photodynamic Therapy of Cancer. *Journal of the American Chemical Society*, *10643–10647*. <https://doi.org/10.1021/ja801631c>

- Cordeiro, F. B., Ferreira, C. R., Sobreira, T. J. P., Yannell, K. E., Jarmusch, A. K., Cooks, R. G., & Turco, E. G. Lo. (2017). Multiple reaction monitoring (MRM) - profiling for biomarker discovery applied to human polycystic ovarian syndrome. *Rapid Communications in Mass Spectrometry*, (May), 1462–1470. <https://doi.org/10.1002/rcm.7927>
- Cox, J., & Mann, M. (2008). MaxQuant enables high peptide identification rates, individualized p.p.b.-range mass accuracies and proteome-wide protein quantification. *Nature Biotechnology*, 26(12), 1367–1372. <https://doi.org/10.1038/nbt.1511>
- de Lima, C. B., Ferreira, C. R., Milazzotta, M. P., Sobreira, T. J. P., Vireque, A. A., & Cooks, G. R. (2018). Comprehensive lipid profiling of early stage oocytes and embryos by MRM profiling. *Journal of Mass Spectrometry*. <https://doi.org/10.1002/jms.4301>
- Despres, J.-P. (1991). Obesity and lipid metabolism: relevance of body fat distribution. *Current Opinion in Lipidology*, 5–15.
- Dhillon, J., Ferreira, C. R., Jose, T., Sobreira, P., & Mattes, R. D. (2017). Multiple Reaction Monitoring Profiling to Assess Compliance with an Almond Consumption Intervention. *Current Developments in Nutrition*, (2), 1–8.
- Ding, F., Radic, S., Chen, R., Chen, P., Geitner, N. K., Brown, J. M., & Ke, P. C. (2013). Direct observation of a single nanoparticle-ubiquitin corona formation. *Nanoscale*, 5(19), 9162–9169. <https://doi.org/10.1039/c3nr02147e>.Direct
- Dipali, S. S., Ferreira, C. R., Zhou, L. T., Pritchard, M. T., & Duncan, F. E. (2019). Histologic analysis and lipid profiling reveal reproductive age-associated changes in peri-ovarian adipose tissue. *Reproductive Biology and Endocrinology*, 6, 1–13.
- Dong, G. H., Qian, Z., Liu, M., Wang, D., Ren, W., Fu, Q., ... Trevathan, E. (2013). Obesity enhanced respiratory health effects of ambient air pollution in Chinese children : the Seven Northeastern Cities study. *International Journal of Obesity*, (July 2012), 94–100. <https://doi.org/10.1038/ijo.2012.125>

- Doumatey, A. P., Zhou, J., Zhou, M., Prieto, D., Rotimi, C. N., & Adeyemo, A. (2016). Proinflammatory and Lipid Biomarkers Mediate Metabolically Healthy Obesity : A Proteomics Study. *Obesity*, 24(6), 1257–1265. <https://doi.org/10.1002/oby.21482>
- Dubowsky, S. D., Suh, H., Schwartz, J., Coull, B. A., & Gold, D. R. (2006). Diabetes , Obesity , and Hypertension May Enhance Associations between Air Pollution and Markers of Systemic Inflammation. *Environmental Health Perspectives*, 992(7), 992–998. <https://doi.org/10.1289/ehp.8469>
- Dykman, L. A., & Khlebtsov, N. G. (2011). Gold Nanoparticles in Biology and Medicine : Recent Advances and Prospects. *Acta Naturae (Англоязычная Версия)*, 3(9), 34–55.
- Eisinger, K., Liebisch, G., Schmitz, G., & Aslanidis, C. (2014). Lipidomic Analysis of Serum from High Fat Diet Induced Obese Mice. *International Journal of Molecular Sciences*, 2991–3002. <https://doi.org/10.3390/ijms15022991>
- Eudald, C., Tobias, P., Albert, D., Gertie Janneke, O., & Victor, P. (2010). Time evolution of the nanoparticle protein corona. *ACS Nano*, 4(7), 3623–3632. <https://doi.org/10.1021/nn901372t>
- Ferreira, C. R., Yannell, K. E., Mollenhauer, B., Espy, R. D., Cordeiro, F. B., Ouyang, Z., & Cooks, R. G. (2016). Chemical profiling of cerebrospinal fluid by multiple reaction monitoring mass spectrometry. *Analyst*, 5252–5255. <https://doi.org/10.1039/c6an01618a>
- Fjeldborg, K., Christiansen, T., Bennetzen, M., Mooler, H. J., Pedersen, S., & Richelsen, B. (2013). The Macrophage-Specific Serum Marker , Soluble CD163 , Is Increased in Obesity and Reduced After Dietary-Induced. *Obesity*. <https://doi.org/10.1002/oby.20376>
- Flegal, K. M., Kruszon-moran, D., Carroll, M. D., Fryar, C. D., & Ogden, C. L. (2019). Trends in Obesity Among Adults in the United States, 2005 to 2014. *Jama*, 20782(21), 2284–2291. <https://doi.org/10.1001/jama.2016.6458>
- Franco, J., Ferreira, C., Sobreira, T. J. P., Sundberg, J. P., & Hogenesch, H. (2018). Profiling of epidermal lipids in a mouse model of dermatitis : Identification of potential biomarkers. *PloS One*, 1–21.

- Frost, R., Langhammer, C., & Cedervall, T. (2017). Real-time in situ analysis of biocorona formation and evolution on silica nanoparticles in defined and complex biological environments. *Nanoscale*, 3620–3628. <https://doi.org/10.1039/c6nr06399c>
- Gerl, M. J., Vaz, W. L. C., Domingues, N., Klose, C., Surm, M. A., Sampaio, J. L., ... Vieira, O. V. (2018). Cholesterol is Inefficiently Converted to Cholesteryl Esters in the Blood of Cardiovascular Disease Patients. *Scientific Reports*, (April), 1–11. <https://doi.org/10.1038/s41598-018-33116-4>
- Ghosh, S., Zhao, B., Bie, J., & Song, J. (2011). Macrophage Cholesteryl Ester Mobilization and Atherosclerosis. *Vascular Pharmacology*, 52, 1–10. <https://doi.org/10.1016/j.vph.2009.10.002.Macrophage>
- Haume, K., Rosa, S., Grellet, S., Śmiałek, M. A., Butterworth, K. T., Solov, A. V., ... Mason, N. J. (2016). Gold nanoparticles for cancer radiotherapy : a review. *Cancer Nanotechnology*. <https://doi.org/10.1186/s12645-016-0021-x>
- Hollister, L. E., Overall, J. E., & Snow, H. L. (1967). Relationship of Obesity to Serum Triglyceride, Cholesterol, and Uric Acid, and to Plasma-Glucose Levels. *The American Journal of Clinical Nutrition*, 20(7), 777–782.
- Jedlovszky-hajdu, A., Bombelli, F. B., Monopoli, M. P., Tomba, E., & Dawson, K. A. (2012). Surface Coatings Shape the Protein Corona of SPIONs with Relevance to Their Application in Vivo. *Langmuir*. <https://doi.org/10.1021/la302446h>
- Jenkins, D. J., Wolever, T. M., Venketeshwer Rao, A., Hegele, R. A., Mitchell, S. J., Ransom, T. P., ... Wursch, P. (1993). Effect on Blood Lipid of Very High Intakes of Fiber In Diets Low in Saturated Fat and Cholesterol. *The New England Journal of Medicine*, 329(1), 21–26.
- Ke, P. C. (2007). Fiddling the string of carbon nanotubes with amphiphiles. *Physical Chemistry Chemical Physics*, 439–447. <https://doi.org/10.1039/b611142d>
- Ke, P. C., Lin, S., Parak, W. J., Davis, T. P., & Caruso, F. (2017). A Decade of the Protein Corona. *ACS Nano*, (Figure 1), 5–8. <https://doi.org/10.1021/acsnano.7b08008>

- Khan, M. A., & Khan, M. J. (2018). Nano-gold displayed anti-inflammatory property via NF-kB pathways by suppressing COX-2 activity. *Artificial Cells, Nanomedicine, and Biotechnology*, 46(S1), S1149–S1158. <https://doi.org/10.1080/21691401.2018.1446968>
- Kobos, L. M., Adamson, S. X. F., Evans, S., Gavin, T. P., & Shannahan, J. H. (2018). Altered formation of the iron oxide nanoparticle-biocorona due to individual variability and exercise. *Environmental Toxicology and Pharmacology*, 62(July), 215–226. <https://doi.org/10.1016/j.etap.2018.07.014>
- Kunnert, B., & Krug, H. (1971). The Composition of Cholesterol Esters in Fatty Streaks and Atherosclerotic Plaques of the Human Aorta. *Atherosclerosis*, 13(1), 93–101.
- Lundqvist, M., Stigler, J., Cedervall, T., Berggard, T., Flanagan, M. B., Lynch, I., ... Dawson, K. (2011). The Evolution of the Protein Corona around Nanoparticles : A Test Study. *ACS Nano*, 5(9), 7503–7509. <https://doi.org/10.1021/nn202458g>
- Lundqvist, M., Stigler, J., Elia, G., Lynch, I., Cedervall, T., & Dawson, K. A. (2008). Nanoparticle size and surface properties determine the protein corona with possible implications for biological impacts. *Proceedings of the National Academy of Sciences*, 105(38), 14265–14270.
- Maiorano, G., Sabella, S., Sorce, B., Brunetti, V., Malvindi, M. A., Cingolani, R., & Pompa, P. P. (2010). Effects of Cell Culture Media on the Protein - Nanoparticle Complexes and Influence on the Cellular Response. *ACS Nano*, 4(12), 7481–7491.
- Monopoli, M. P., Åberg, C., Salvati, A., & Dawson, K. A. (2012). Biomolecular coronas provide the biological identity of nanosized materials. *Nature Nanotechnology*, 7(12), 779–786. <https://doi.org/10.1038/nnano.2012.207>
- Murphy, W. G. (2014). The sex difference in haemoglobin levels in adults - Mechanisms, causes, and consequences. *Blood Reviews*, 28(2), 41–47. <https://doi.org/10.1016/j.blre.2013.12.003>
- Neagu, M., Piperigkou, Z., Karamanou, K., & Engin, A. B. (2017). Protein bio - corona : critical issue in immune nanotoxicology. *Archives of Toxicology*, 91(3), 1031–1048. <https://doi.org/10.1007/s00204-016-1797-5>

- Nieman, D., Henson, D., Nehlsen-Cannarella, S., Ekkens, M., Utter, A. C., Butterworth, D. E., & Fagoaga, O. R. (1999). Influence of Obesity on Immune Function. *Journal of the American Dietetic Association*, 99(3), 294–299.
- Park, H. S., Yul, J., & Yu, R. (2005). Relationship of obesity and visceral adiposity with serum concentrations of CRP , TNF- a and IL-6. *Diabetes Research and Clinical Practice*, 69, 29–35. <https://doi.org/10.1016/j.diabres.2004.11.007>
- Pati, R., Shevtsov, M., & Sonawane, A. (2018). Nanoparticle Vaccines Against Infectious Diseases. *Frontiers in Immunology*, 9(October). <https://doi.org/10.3389/fimmu.2018.02224>
- Pergola, G. O., & Pannacciulli, N. (2002). Coagulation and fibrinolysis abnormalities in obesity. *Journal of Endocrinological Investigation*, 899–904.
- Pomeroy, C., Mitchell, J., Eckert, E., Raymond, N., Crosby, R., & Dalmasso, A. P. (1997). Effect of body weight and caloric restriction on serum complement proteins , including Factor D / adipsin : studies in anorexia nervosa and obesity. *Clinical & Experimental Immunology*, 507–515.
- Raghavendra, A. J., Fritz, K., Fu, S., Brown, J. M., & Shannahan, J. H. (2017). Variations in biocorona formation related to defects in the structure of single walled carbon nanotubes and the hyperlipidemic disease state. *Scientific Reports*, (April), 1–11. <https://doi.org/10.1038/s41598-017-08896-w>
- Ren, J., Cai, R., Wang, J., Daniyal, M., Baimanov, D., Liu, Y., ... Chen, C. (2019). Precision Nanomedicine Development Based on Specific Opsonization of Human Cancer Patient- Personalized Protein Coronas. *Nano Letters*, 19, 4692–4701. rapid-communication. <https://doi.org/10.1021/acs.nanolett.9b01774>
- Salvati, A., Pitek, A. S., Monopoli, M. P., Prapainop, K., Bombelli, F. B., Hristov, D. R., ... Dawson, K. A. (2013). Transferrin-functionalized nanoparticles lose their targeting capabilities when a biomolecule corona adsorbs on the surface. *Nature Nanotechnology*, 8(2), 137–143. <https://doi.org/10.1038/nnano.2012.237>

- Shannahan, J. H., Fritz, K. S., Raghavendra, A. J., Podila, R., Persaud, I., & Brown, J. M. (2016). Disease-induced disparities in formation of the nanoparticle-biocorona and the toxicological consequences. *Toxicological Sciences*, *152*(2), 406–416.
<https://doi.org/10.1093/toxsci/kfw097>
- Shannahan, J. H., Lai, X., Ke, P. C., Podila, R., Brown, J. M., & Witzmann, F. A. (2013). Silver Nanoparticle Protein Corona Composition in Cell Culture Media. *PloS One*, *8*(9).
<https://doi.org/10.1371/journal.pone.0074001>
- Shannahan, J. H., Podila, R., & Brown, J. M. (2015). A hyperspectral and toxicological analysis of protein corona impact on silver nanoparticle properties, intracellular modifications, and macrophage activation. *International Journal of Nanomedicine*, *10*, 6509–6520.
<https://doi.org/10.2147/IJN.S92570>
- Sharma, G., Kodali, V., Gaffrey, M., Wang, W., Minard, K. R., Karin, N. J., ... Thrall, B. D. (2014). Iron oxide nanoparticle agglomeration influences dose rates and modulates oxidative stress-mediated dose – response profiles in vitro modulates oxidative stress-mediated dose – response profiles in vitro. *Nanotoxicology*, *5390*.
<https://doi.org/10.3109/17435390.2013.822115>
- Shukla, R., Bansal, V., Chaudhary, M., Basu, A., Bhonde, R. R., & Sastry, M. (2005). Biocompatibility of Gold Nanoparticles and Their Endocytotic Fate Inside the Cellular Compartment : A Microscopic Overview. *Langmuir*, *(25)*, 10644–10654.
<https://doi.org/10.1021/la0513712>
- Singh, S. P., Niemczyk, M., Saini, D., Awasthi, Y. C., & Zimniak, L. (2008). Role of the Electrophilic Lipid Peroxidation Product 4-Hydroxynonenal in the Development and Maintenance of Obesity in Mice †. *Biochemistry*, 3900–3911.
- Stuchinskaya, T., Moreno, M., Cook, M. J., Edwards, D. R., & Russell, D. A. (2011). Targeted photodynamic therapy of breast cancer cells using antibody–phthalocyanine–gold nanoparticle conjugates. *Photochemical & Photobiological Sciences*.
<https://doi.org/10.1039/c1pp05014a>

- Susumu, M., Ikawa, M., Okabe, M., Tanaka, Y., Yamashita, T., Takemoto, H., & Okazaki, T. (2011). Dynamic Modification of Sphingomyelin in Lipid Microdomains Controls Development of Obesity, Fatty Liver, and Type 2 Diabetes * □. *Journal of Biological Chemistry*, 286(32), 28544–28555. <https://doi.org/10.1074/jbc.M111.255646>
- Suzuki, K., Ito, Y., Ochiai, J., Kusuhara, Y., Hashimoto, S., Tokudome, S., ... Maruta, M. (2003). Relationship between Obesity and Serum Markers of Oxidative Stress and Inflammation in Japanese. *Asian Pacific Journal of Cancer Prevention*, 4, 259–266.
- Tran, Z. V., Weltman, A., Glass, G. V., & Mood, D. P. (1983). The effects of exercise on blood lipids and lipoproteins: a meta-analysis of studies. *Medicine & Science in Sports & Exercise*, 15(5), 393–402. Retrieved from <http://europepmc.org/abstract/MED/6645868>
- Walczyk, D., Bombelli, F. B., Monopoli, M. P., Lynch, I., & Dawson, K. A. (2010). What the Cell “ Sees ” in Bionanoscience. *Journal of the American Chemical Society*, (19), 5761–5768.
- Walkey, C. D., Olsen, J. B., Guo, H., Emili, A., & Chan, W. C. W. (2012). Nanoparticle Size and Surface Chemistry Determine Serum Protein Adsorption and Macrophage Uptake. *Journal of the American Chemical Society*. <https://doi.org/10.1021/ja2084338>
- Wen, Y., Geitner, N. K., Chen, R., Ding, F., Chen, P., Andorfer, R. E., ... Ke, P. C. (2013). Binding of cytoskeletal proteins with silver nanoparticles. *Rsc Advances*, (Cd), 22002–22007. <https://doi.org/10.1039/c3ra43281e>
- Wiewiora, M., Piecuch, J., Sedek, L., & Mazur, B. (2017). The Effects of Obesity on CD47 Expression in Erythrocytes. *Cytometry Part B: Clinical Cytometry*, 491(December 2014), 485–491. <https://doi.org/10.1002/cyto.b.21232>
- Wu, Y., Hudson, J. S., Lu, Q., Moore, J. M., Mount, A. S., Rao, A. M., ... Ke, P. C. (2006). Coating Single-Walled Carbon Nanotubes with Phospholipids. *The Journal of Physical Chemistry B*, 2475–2478. <https://doi.org/10.1021/jp057252c>

- Xu, L., Bauer, J., Siedlecki, C. A., & State, T. P. (2014). Proteins, Platelets, and Blood Coagulation at Biomaterial Interfaces. *Colloids and Surfaces B: Biointerfaces*, (717), 49–68. <https://doi.org/10.1016/j.colsurfb.2014.09.040>.Proteins
- Yannell, K. E., Ferreira, C. R., Tichy, S. E., & Cooks, R. G. (2018). Multiple reaction monitoring (MRM)-profiling with biomarker identification by LC-QTOF to characterize coronary artery disease. *Analyst*, 5014–5022. <https://doi.org/10.1039/c8an01017j>
- Zhao, Y., He, X., & Shi, X. (2010). Association between serum amyloid A and obesity : a meta-analysis and systematic review. *Inflammation Research*, 323–334. <https://doi.org/10.1007/s00011-010-0163-y>

CHAPTER 3. ALTERED FORMATION OF THE IRON OXIDE NANOPARTICLE-BIOCORONA DUE TO INDIVIDUAL VARIABILITY AND EXERCISE

A version of this chapter has been previously published in *Environmental Toxicology and Pharmacology*.

Kobos, L. M., Adamson, S. X. F., Evans, S., Gavin, T. P., & Shannahan, J. H. (2018). Altered formation of the iron oxide nanoparticle-biocorona due to individual variability and exercise. *Environmental Toxicology and Pharmacology*, 62(July), 215–226.
<https://doi.org/10.1016/j.etap.2018.07.014>

3.1 Abstract

Nanoparticles (NPs), introduced into a biological environment, accumulate a coating of biomolecules or biocorona (BC). Although the BC has toxicological and pharmacological consequences, the effects of inter-individual variability and exercise on NP-BC formation are unknown. We hypothesized that NPs incubated in plasma form distinct BCs between individuals, and exercise causes additional intra-individual alterations. 20 nm iron oxide (Fe_3O_4) NPs were incubated in pre- or post-exercise plasma ex vivo, and proteomics was utilized to evaluate BC components. Analysis demonstrated distinct BC formation between individuals, while exercise was found to enhance NP-BC complexity. Abundance differences of NP-BC proteins were determined between individuals and resulting from exercise. Differential human macrophage response was identified due to NP-BC variability. These findings demonstrate that individuals form unique BCs and that exercise influences NP-biomolecule interactions. An understanding of NP-biomolecule interactions is necessary for elucidation of mechanisms responsible for variations in human responses to NP exposures and/or nano-based therapies.

3.2 Introduction

Nanoparticles (NPs) have the capacity to revolutionize a multitude of technologies across a number of fields, including electronics, consumer products, textiles, biomedicine, and others. Iron oxide (Fe_3O_4) NPs specifically have the ability to be utilized in the field of biomedicine as MRI

contrast agents, treatments for anemia, magnetic sensing probes, and drug delivery agents (Babes et al., 1999; Ghazanfari et al., 2016; Jain et al., 2005; Neuberger et al., 2005). When NPs enter biological environments, such as the circulatory system, a coating of biomolecules forms as proteins, lipids, and other compounds adsorb to the NP surface. This coating or biocorona (BC) imparts a new interactive interface thus altering NP physicochemical properties (hydrodynamic size, ζ -potential, and dissolution), resulting in modified NP functionality as well as cellular and biological responses (Clift et al., 2010; Maiorano et al., 2010; Monopoli et al., 2012; Shannahan et al., 2015b; Walczyk et al., 2010). BC-induced variations in cellular interactions will likely impact the use of NPs for biomedical applications by modifying biodistribution, clearance, immune response, and toxicity (Kreuter, 2013; Mornet et al., 2004; Tenzer et al., 2013). Specifically, addition of the BC to superparamagnetic Fe_3O_4 NPs decreases their effectiveness as MRI contrast agents and drug delivery vehicles (Amiri et al., 2013; Gupta and Gupta, 2005). In order to fully utilize NP-based therapeutics, it is necessary to first understand these initial NP-biomolecule interactions and their biological implications.

The formation of the NP-BC is governed by NP physicochemical properties, time, and the biological environment. To date, the majority of investigations have examined specific NP properties (composition, charge, size, surface coating, defects, etc.) and their role in NP-BC formation (Jedlovszky-Hajdu et al., 2012; Lundqvist et al., 2008; Monopoli et al., 2011; Raghavendra et al., 2017; Walkey and Chan, 2012). Few studies, however, have evaluated the impact of variations in the biological environment (Raghavendra et al., 2017; Shannahan, 2017). Due to their many biomedical applications, NPs will be utilized in highly variable biological environments, which may impact their functionality. Specifically, individual variations in the biomolecular composition within the circulation are of concern for Fe_3O_4 NPs. Numerous conditions and factors can contribute to variability in circulating macromolecules, including underlying disease state, gender, diet, and others (Gordon et al., 1977; Jenkins et al., 1993; Murphy, 2014; Tran et al., 1983). Exercise, which is one of the focuses of our current study, is known to alter circulating biomolecules differently based on the type, duration, and intensity of the exercise (Balfoussia et al., 2014; Dreyer et al., 2006; Kraus et al., 2002; Tran et al., 1983). Ultimately, the variability of biological environments present within our population, as well as

activity-induced alterations in circulating biomolecules, could modify BC formation and result in differential biological interactions.

In our current study, we examined differences in the formation of the Fe₃O₄ NP-BC due to inter-individual variations as well as exercise-induced intra-individual variability by utilizing human plasma samples. Further, a human macrophage cell line was utilized to assess the toxicological consequences (cellular association, cytotoxicity, and inflammatory activation) of distinct Fe₃O₄ NP-BCs. In order to perform this investigation, 10 human subjects who did not exercise regularly were recruited and blood samples were collected prior to and following a 7-day exercise regimen. Overall, this descriptive study was designed to demonstrate potential differences between individuals' NP-BCs, as well as the influence of exercise. By elucidating possible variability in the formation of the NP-BC and consequential alterations in immune cell interactions, individual susceptibility to NP-induced health effects may be identified and mitigated.

3.3 Materials and Methods

3.3.1 Blood collection

Fasting plasma samples were isolated from blood extracted from human subjects (six male, four female) between the ages of 21–32 y who, according to a self-survey, did not smoke or exercise regularly (Table 3.1). Subjects were exercised once a day at 70% of maximum for 45 min on a stationary exercise bicycle for 7 consecutive days. On days 2, 4, and 6, subjects also performed 3 sets (8–12 repetitions at 80% of maximum) of leg press resistance exercise. Subjects were instructed to not modify any additional aspects of their lifestyle, including diet, for the duration of the study. Fasting blood was again collected from each subject on day 8 at least 12–14 hours after the final exercise session. After each collection, blood was treated with heparin to prevent clotting. The Biomedical Institutional Review Board at Purdue University approved the study protocol, recruitment materials, and consent forms. All study participants gave informed consent and received monetary compensation for their participation.

Table 3.1. After subjects' blood was drawn, aliquots were analyzed by Mid America Laboratories. A. Blood parameters prior to completion of 7-day exercise regimen. B. Blood parameters following completion of 7-day exercise regimen. * and bold indicate subjects selected for further analysis due to large (2, 5, 7) or small (1, 6, 8) change in triglycerides pre- to post-exercise.

A. Pre-Exercise Blood Results

Subject #	Sex	Age	BMI	Glucose (mg/dl)	Insulin (uIU/ml)	Triglyceride (mg/dl)	HDL (mg/dl)	LDL (mg/dl)	Total Cholesterol (mg/dl)
1	M	27	24.5	86	5	65	40	90	143
2	M	21	30.8	99	12	128	38	90	154
3	M	21	23.3	96	11	88	37	101	156
4	F	29	24.1	90	8	63	56	100	169
5	F	27	33.7	82	52	176	42	101	178
6	F	30	21.8	92	9	90	52	118	188
7	M	24	22.0	81	9	143	59	105	193
8	M	32	25.9	96	8	111	34	161	217
9	F	21	23.3	75	12	131	54	152	232
10	M	32	34.1	89	27	194	33	196	268

B. Post-Exercise Blood Results

Subject #	Sex	Age	BMI	Glucose (mg/dl)	Insulin (uIU/ml)	Triglyceride (mg/dl)	HDL (mg/dl)	LDL (mg/dl)	Total Cholesterol (mg/dl)
1*	M	27	24.5	93	5	54	44	86	141
2*	M	21	30.8	92	5	65	48	118	179
3	M	21	23.3	96	11	62	36	80	128
4	F	29	24.1	94	7	46	61	96	166
5*	F	27	33.4	92	12	77	45	109	162
6*	F	30	21.8	87	11	80	49	84	149
7*	M	24	22.0	84	7	76	51	88	154
8*	M	32	26	96	7	104	36	151	208
9	F	21	23.5	84	10	107	58	135	214
10	M	32	33	87	25	152	29	210	269

3.3.2. Plasma sample characterization

An aliquot of each blood sample was analyzed by Mid America Laboratories to determine glucose, insulin, triglycerides, high-density lipoprotein (HDL), low-density lipoprotein (LDL), and total cholesterol levels. Subjects were ordered 1–10 based on total cholesterol content, with 1 having the lowest total pre-exercise cholesterol and 10 having the highest. Each subject retained the same number pre- to post-exercise. Plasma was isolated from another aliquot of blood by centrifugation at 1300 rcf for 15 min at 4 °C and stored at -80 °C. Plasma samples from the 10 subjects collected prior to exercise were used to determine inter-individual differences in NP-BC formation. Plasma samples collected from 6 subjects post-exercise were used to evaluate exercise-induced differences in BC formation. This was accomplished by comparing the NP-BC produced following incubation in post-exercise plasma to that produced from pre-exercise plasma from the same human subject. These 6 post-exercise plasma samples were selected based on alterations in triglyceride levels following exercise. Specifically, 3 subjects demonstrated minor alterations in triglyceride levels following exercise, whereas 3 other subjects exhibited greater alterations in triglycerides levels (Table 3.1).

3.3.3 Fe₃O₄ NP characterization

Spherical Fe₃O₄ NPs with a diameter of 20 nm and suspended in poly-*N*-vinylpyrrolidone (PVP) at a concentration of 20 mg/ml were purchased from Nanocomposix (San Diego, California) and characterized to verify manufacturer specifications. The hydrodynamic size and ζ-potential (ZetaSizer Nano, Malvern) were assessed in DI water with Fe₃O₄ NPs at a concentration of 25 µg/ml (n = 6). The number of particles per µg of NP was determined by nanoparticle tracking software (Nanosight, Malvern) (n = 3). Shape and size were characterized via transmission electron microscopy (FEI Tecnai G2 20) (Supplemental Figure S3.1).

3.3.4 Formation of the Fe₃O₄ NP-BC

BCs were formed on Fe₃O₄ NPs as described in our recent publications (Shannahan et al., 2016, 2013b; Shannahan et al., 2015b). Briefly, Fe₃O₄ NPs were incubated *ex vivo* in 10% plasma for 8 h at 4 °C while being constantly mixed. Specifically, 125 µl of Fe₃O₄ NPs (1 mg/ml), 325 µl of deionized water, and 50 µl of plasma were combined in a 1.5 ml tube. Following incubation,

Fe₃O₄ NPs were pelleted via centrifugation at 20,817 rcf for 10 min and washed with PBS. A total of 3 washes with PBS were performed to remove free proteins not associated with the Fe₃O₄ NPs. Following addition of the BC, NPs were reassessed for alterations in hydrodynamic size and ζ-potential (n = 6/plasma sample).

3.3.5 Assessment of the protein components of the Fe₃O₄ NP-BC

Protein components of the Fe₃O₄ NP-BC were evaluated utilizing a label-free proteomics approach to determine the effects of individual variation and the influence of exercise on the formation of the NP-BC. Three replicates of each Fe₃O₄ NP-BC were produced for proteomic analysis (n = 3/plasma sample). The proteomics approach used was similar to our previous studies investigating the NP-BC (Shannahan et al., 2013a, b). Further details regarding the proteomics approach including peptide isolation, mass spectrometry, and data analysis can be found in Supplemental Methods File 3.1. Following isolation, peptides were analyzed by reverse-phase HPLC-ESI-MS/MS using a Dionex UltiMate 3000 RSLC Nano System (Thermo Scientific, Waltham, MA) which was directly connected to a Q-Exactive™ HF Hybrid Quadrupole-Orbitrap MS (Thermo Scientific) and a Nanospray Flex™ Ion Source (Thermo Scientific). The files from the mass spectrometer were processed using the MaxQuant computational proteomics platform version 1.6.0.1 (Cox and Mann, 2008). The peak list generated was searched against the *Homo sapiens* sequences from UNIPROT retrieved on 02/22/2017 and a common contaminants database. Statistical analyses were performed in the R environment (www.cran.r-project.org). A *t*-test was performed on the LFQ intensities and only proteins with p-value <0.05 were used in all analyses.

3.3.6 Proteomic data analysis - identified proteins

Identified proteins from each subject were compared and Venn diagrams were produced to determine commonalities and differences in the identities of proteins that associated with Fe₃O₄ NPs forming the BC.

3.3.7 Proteomic data analysis - relative abundance

To compare differences in abundance between individual subjects' samples, label-free quantification (LFQ) intensity values were utilized to quantify fold change differences between proteins found to associate in common with Fe₃O₄ NPs following incubation in individual plasma samples. t-tests were utilized to determine if fold changes were statistically significant, $p < 0.05$. A similar assessment was performed to evaluate differences in protein abundance between Fe₃O₄ NPs incubated in pre-exercise samples and post-exercise samples. To examine how the quantities of specific proteins on Fe₃O₄ NPs were modified following incubation in individual plasma samples, the LFQ intensity was compared. Graphs and analyses were performed using GraphPad Prism 7 software (GraphPad Software Inc., La Jolla, CA, USA). LFQ intensities from replicates were averaged and used to produce a standard error of the means ($n = 3/\text{group}$). Protein LFQs from all subjects' samples were then statistically compared to subject 1 using a one-way ANOVA with a Dunnett's multiple comparisons test. Statistical significance was determined by $p < 0.05$. A Pearson's correlation analysis was performed to determine relationships between the mean abundance of specific proteins within the NP-BC and measured subject parameters, significance was determined by $p < 0.05$.

3.3.8 Cells and cell culture

Human monocytes (U937, ATCC, Manassas, VA) were maintained and grown at 37 °C in a Galaxy 170 S incubator (New Brunswick Scientific, Edison, NJ) using RPMI1640 media (VWR Life Science, Radnor, PA) supplemented with 10% fetal bovine essence and 1% penicillin/streptomycin. Monocytes were then differentiated into macrophages using 100 ng/ml of phorbol 12-myristate 13-acetate for 72 h. Following differentiation, macrophages were exposed to Fe₃O₄ NPs with BCs and evaluated for BC-induced alterations in macrophage viability, uptake, and inflammatory response.

3.3.9 Viability, uptake, and inflammation

Cells were differentiated in 96 well plates in 100 μl cell media to a confluency of 90%. After removal of the cell media, suspensions of Fe₃O₄ NP-BCs at 25 $\mu\text{g}/\text{ml}$ in serum free media were added to the wells. The concentration utilized for this cell response assessment was selected based

on previous *in vitro* experimentation of Fe₃O₄ NPs and other NPs as well as a pilot study investigating concentration-dependent cytotoxicity in human macrophages (Shannahan et al., 2015a; Xia et al., 2013) (Supplemental Figure S3.2). The cells were exposed to the NP-BC suspensions for a total of 24 h before being assessed for cell viability via the MTT assay. To analyze NP-cellular association, cells were washed with PBS and collected for BCA assay (Thermo Scientific), followed by digestion in nitric acid. The cellular-associated Fe content was then quantified using atomic absorption spectroscopy (AAS) (Agilent Technologies, Santa Clara, CA). The amount of iron in each sample was normalized to the protein content. The ability of distinct BCs to activate macrophages was evaluated by measuring *TNF- α* cellular mRNA expression and supernatant protein levels. Additional details regarding the evaluation of inflammatory endpoints can be found in Supplemental Methods File 3.2. Quantitative real-time RT-PCR was performed for *TNF- α* and beta actin (*ACTB*) (control). Relative mRNA fold changes were calculated considering serum-free media exposed cells as control and normalized to the housekeeping gene *ACTB*. Supernatants were also collected at 24 h following exposure and examined by a human-specific *TNF- α* enzyme-linked immunosorbent assay kit via manufacturer's instructions (R&D Systems, Inc., Minneapolis, MN, USA). Statistical analysis was performed using Prism software. All data (cytotoxicity, uptake, and inflammation) are presented as mean \pm standard error of the mean (n = 6/group). Significant differences between exposures were determined by one-way ANOVA with a Tukey's posthoc test (p < 0.05).

3.4 Results

3.4.1 Characterization of experimental materials

3.4.1.1 Human blood characterization

Blood samples were collected from 10 human subjects who, according to a self-survey, did not smoke or exercise regularly. Subjects were then exercised once a day for 7 consecutive days. Subjects were requested to not change their daily routines outside of the assigned exercise. At the conclusion of the 7 days, subjects' blood was drawn a second time. The pre- and post-exercise blood samples from each subject were then characterized on a number of parameters, including triglycerides, LDL, HDL, and total cholesterol. Body mass index was calculated for each subject based on height and weight (Table 3.1). Subjects demonstrated variation in total

cholesterol, with pre-exercise levels ranging from 143 mg/dl to 268 mg/dl in subjects 1 and 10, respectively (Table 3.1A). All individuals demonstrated decreased triglyceride levels following exercise, with changes up to 99 mg/dl observed (Subject 5, Table 3.1B). Specifically, exercise was determined to only result in statistically significant reductions in triglyceride levels between pre-exercise (118.9 \pm 14) and post-exercise (82.3 \pm 9.9) groups ($p = 0.0467$) (data not shown). Six subjects were selected for analysis of exercise-related modifications in the NP-BC based on changes in triglyceride levels that occurred after completion of the exercise plan (Table 3.1B, bolded). Subjects selected were those with the highest changes in triglycerides (2, 5, 7) and the lowest (1, 6, 8) (Table 3.1).

3.4.1.2. Nanoparticle characterization

Fe₃O₄ NPs were found to have $2.6 \pm 0.3 \times 10^9$ NPs/ μ g (Mean \pm SEM) as determined by NanoSight (Malvern, Westborough, MA)). Transmission electron microscopy verified the manufacturer's stated initial particle size and spherical morphology (Supplemental Figure S3.1). Nanoparticles were characterized by assessment of hydrodynamic size and ζ -potential both with and without a BC present. Addition of all BCs increased NP hydrodynamic size and decreased ζ -potential (Fig. 3.1). Incubation in individual plasma samples and addition of BCs to the Fe₃O₄ NP surface resulted in non-uniform alterations in hydrodynamic size (Fig. 3.1A). NPs incubated in plasma from subjects 1, 6, and 7 demonstrated increases in Fe₃O₄ NP hydrodynamic size post-exercise (red bars) as compared to pre-exercise (blue bars) (Fig. 3.1A). Polydispersion index of NPs without a BC was 0.108 \pm 0.002 (mean \pm SEM), while addition of BCs resulted in an average polydispersion index of 0.269 \pm 0.028 (mean \pm SEM), supporting limited polydispersion of Fe₃O₄ NPs (data not shown). NP ζ - potential was decreased uniformly between subjects, and no exercise-related changes were observed (Fig. 3.1B).

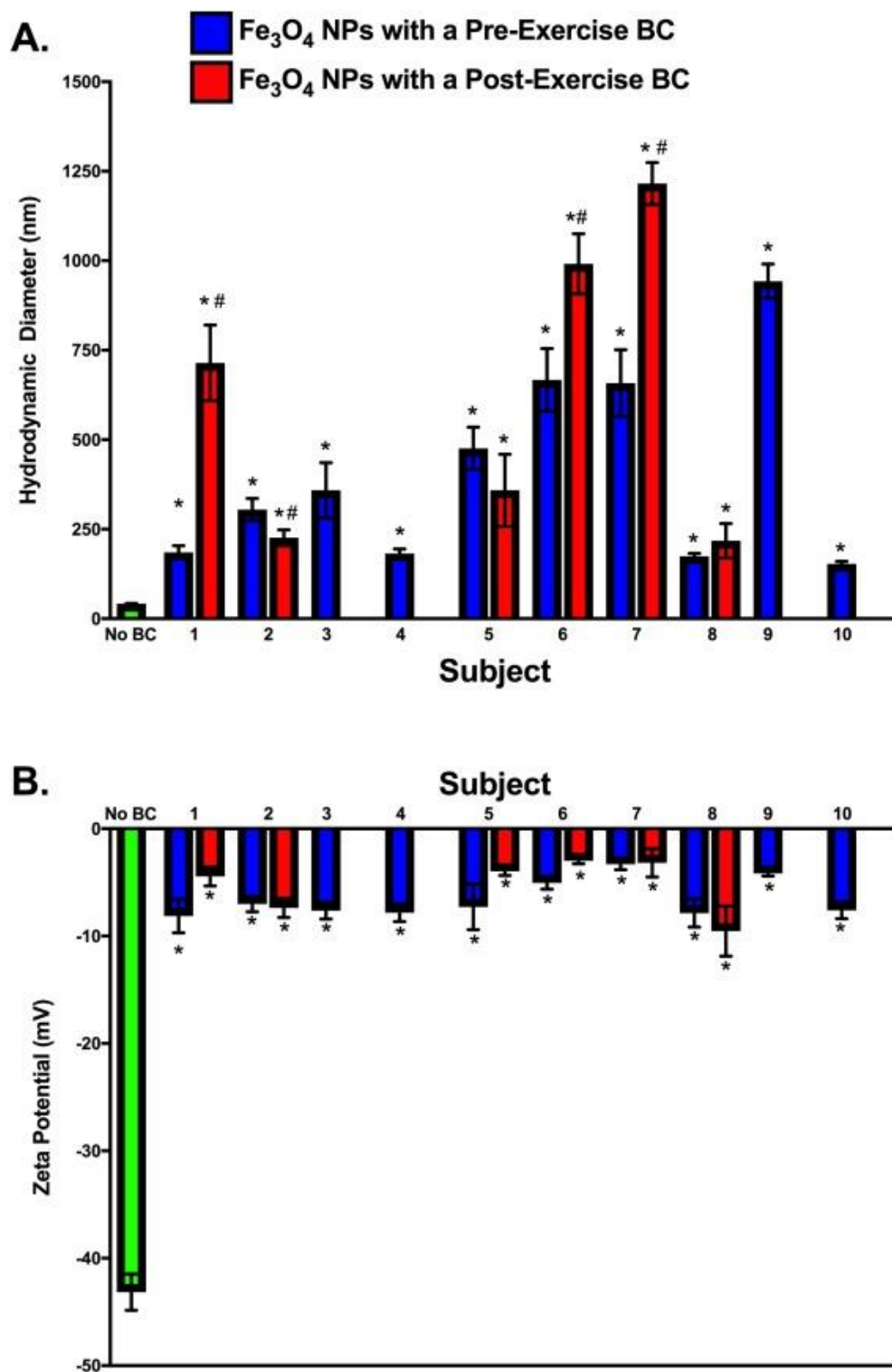


Figure 3.1. NP Characterization Prior to and Following the Addition of a BC. NPs were diluted in and incubated for 8 h at 4 °C in 10% subject plasma. NPs were characterized with and without BCs via assessment of A) hydrodynamic size and B) ζ -potential. * denotes statistical significance from Fe_3O_4 NPs without a BC, # denotes statistical significance between pre-exercise NP-BC and post-exercise NP-BC (n = 6/group; two-way ANOVA with Tukey post hoc analysis; p < 0.05).

3.4.2 Inter-individual variability within the biocorona

3.4.2.1 Evaluation of the effect of individual variability on the pre-exercise BC – protein identities

A label-free mass spectrometry approach was used to identify proteins present in the BC of Fe₃O₄ NP following *ex vivo* incubation in plasma from subjects pre- and post-exercise. (Supplemental Table S3.1). Identified proteins were compared between the pre-exercise plasma of all subjects. A total of 99 proteins were found in common between all 10 subjects pre-exercise, including hemopexin; thrombospondin-1; coagulation factors V, IX, and XI; immunoglobulin κ variables 1–5, 1–8, 1–17, 2–30, 3–15, 3–20, 4-1, and 3D-11; and apolipoproteins A, A1, A2, A4, B, C1, C2, C3, E, and H (Supplemental Table S3.2A). Subject 3's pre-exercise BC was the most unique, containing 32 proteins specific to that subject (Supplemental Table S3.2A). To demonstrate inter-individual differences in the formation of the NP-BC, the protein composition of each pre-exercise BC was compared to the protein composition of subject 1's pre-exercise BC (Fig. 3.2, Supplemental Table S3.2B). Although many proteins were found to bind in common to Fe₃O₄ NPs, unique proteins were determined to associate for each subject. The BC of subject 3 was determined to be the most unique compared to subject 1, with 41 distinct proteins. Subject 5 was the most similar, demonstrating the presence of only 7 unique proteins compared to subject 1 (Fig. 3.2). Although the utilized plasma samples were from both males and females, only one protein, immunoglobulin lambda variable 4–69, was found exclusively in male subjects (Supplemental Table S3.2A).

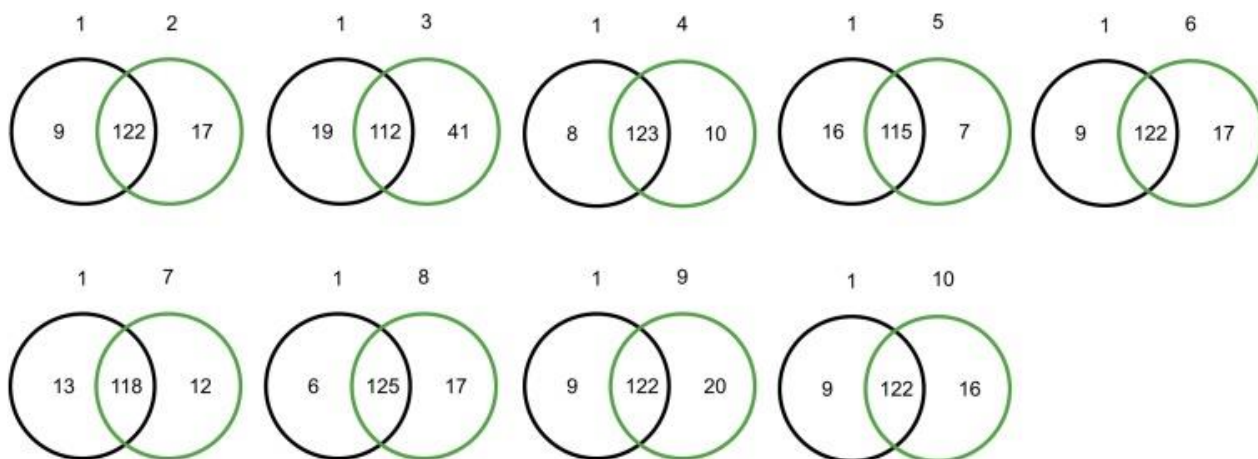


Figure 3.2. Comparison of Pre-Exercise Fe₃O₄ NP-BC Composition: Number of Proteins shared with Subject 1. Proteins identified from each subject's BC were compared to proteins identified from subject 1's BC. Subject 1 was selected as a baseline due to it being the subject with lowest pre-exercise cholesterol levels. Venn diagrams were created to illustrate each comparison. Supplemental Table S3.1 contains a comprehensive list comparing identified proteins between all the pre-exercise subjects. List of specific proteins used to generate Venn diagrams in Fig. 3.2 are in Supplemental Table S3.2B.

3.4.2.2 Evaluation of the effect of individual variability on the pre-exercise BC – protein quantification

Although most proteins were shared between individual BCs, there were quantifiable differences (Supplemental Table S3.3). Fig. 3.3 shows the top ten most significantly altered proteins as compared to subject 1 for all other subjects (2–10) ($p < 0.05$). Several proteins were commonly found in this list of top ten most significantly different proteins, such as complement C4-B and cytoplasmic actin 1. However, it should be noted that the directionality of these proteins was not always uniform between subjects. Complement C4-B had a positive fold change (indicating that the protein was less abundant in the BC of subject 1) in subjects 5, 7, and 9, but a negative fold change (indicating that the protein was more abundant in the BC of subject 1) in subjects 2, 6, and 8. Cytoplasmic actin 1 had a positive fold change in all subjects, meaning it was less abundant on Fe₃O₄ NPs incubated in plasma from subject 1 compared to plasma from all other subjects. In four subjects, cytoplasmic actin 1 had the greatest positive fold change of significance among all proteins, indicating that it was less abundant in the BC of subject 1 compared to other subjects.

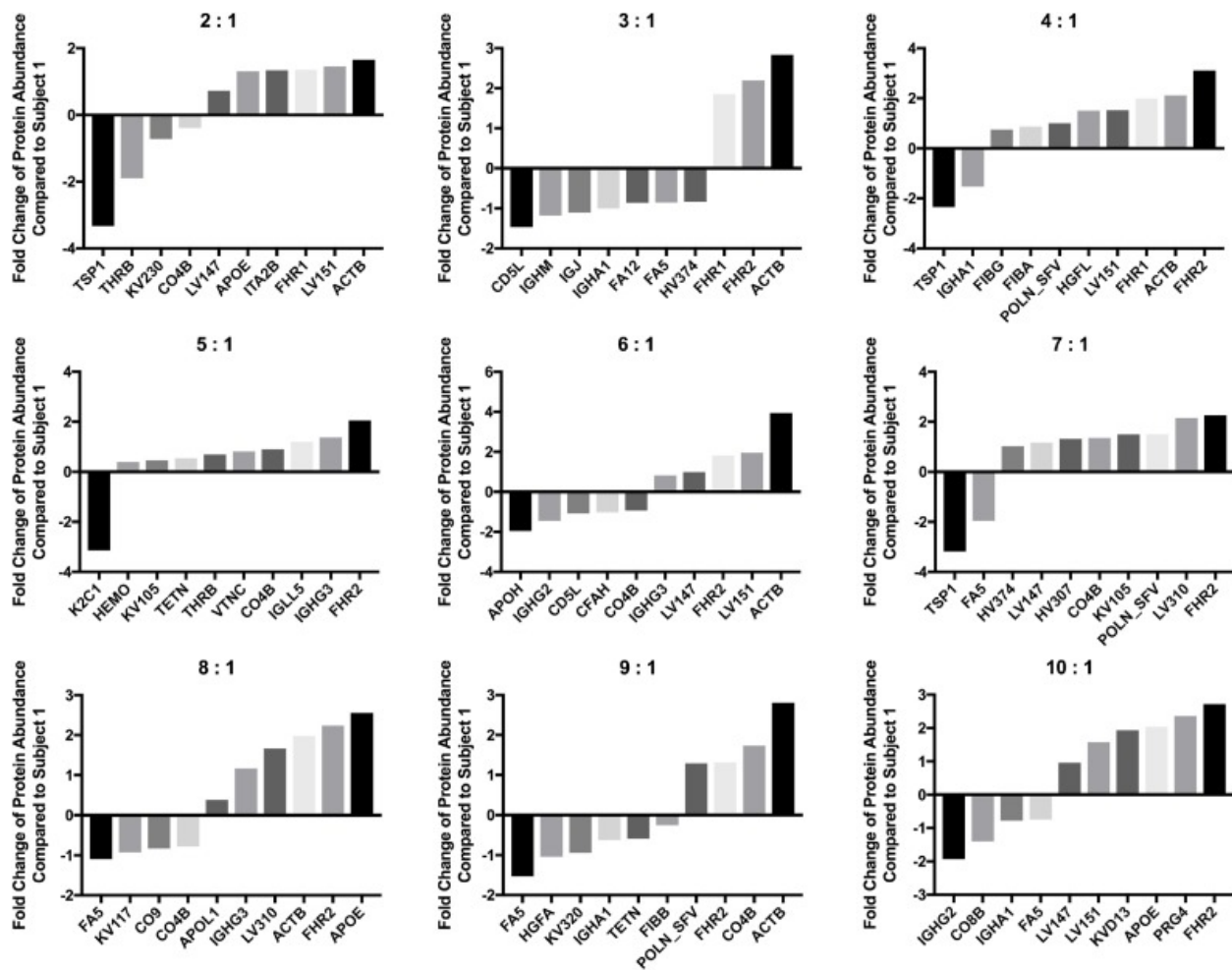


Figure 3.3. Fold Change of Selected Proteins Compared to Sample 1. Quantities of shared proteins between each subject and subject 1 are depicted as fold changes. Negative values indicate that the subject was more abundant in subject 1, while positive values indicate that the subject was less abundant in subject 1. Individual graphs depict the 10 most significantly altered proteins in terms of abundance between subjects and subject 1 ($n = 3/\text{group}$; one-way ANOVA with Tukey post hoc analysis; $p < 0.05$). Supplemental Table S3.3 includes a comprehensive list of all protein fold changes compared to subject 1.

Assessing the ten most changed proteins allows for a global perspective, however; by examining quantities of individual proteins (Fig. 3.4, Supplemental Table S3.3), specific information may be gained regarding the effect of individual variability. Protein levels vary across subjects, demonstrating the impact of individual variability on the NP-BC composition (Fig. 3.4). For several of these proteins, changes in relative quantity are observed between subject 1 and others. A statistically significantly higher relative level of APOC1 was observed in 3 subjects, APOE in 7 subjects, and CO4B in 3 subjects compared to subject 1. All nine comparisons showed a lower

relative quantity of FINC as compared to subject 1, with all comparisons being statistically significant, with the exception of subject 6. No statistically significant changes were observed across subjects in the levels of APOC2, PLMN, or TTHY. APOA1 was statistically elevated in only one individual; subject 2. TSP1 had both statistically significant increases and decreases as compared to subject 1, with six of the nine comparisons showing levels far lower than those in subject 1, and two of the subjects showing levels far higher than those in subject 1.

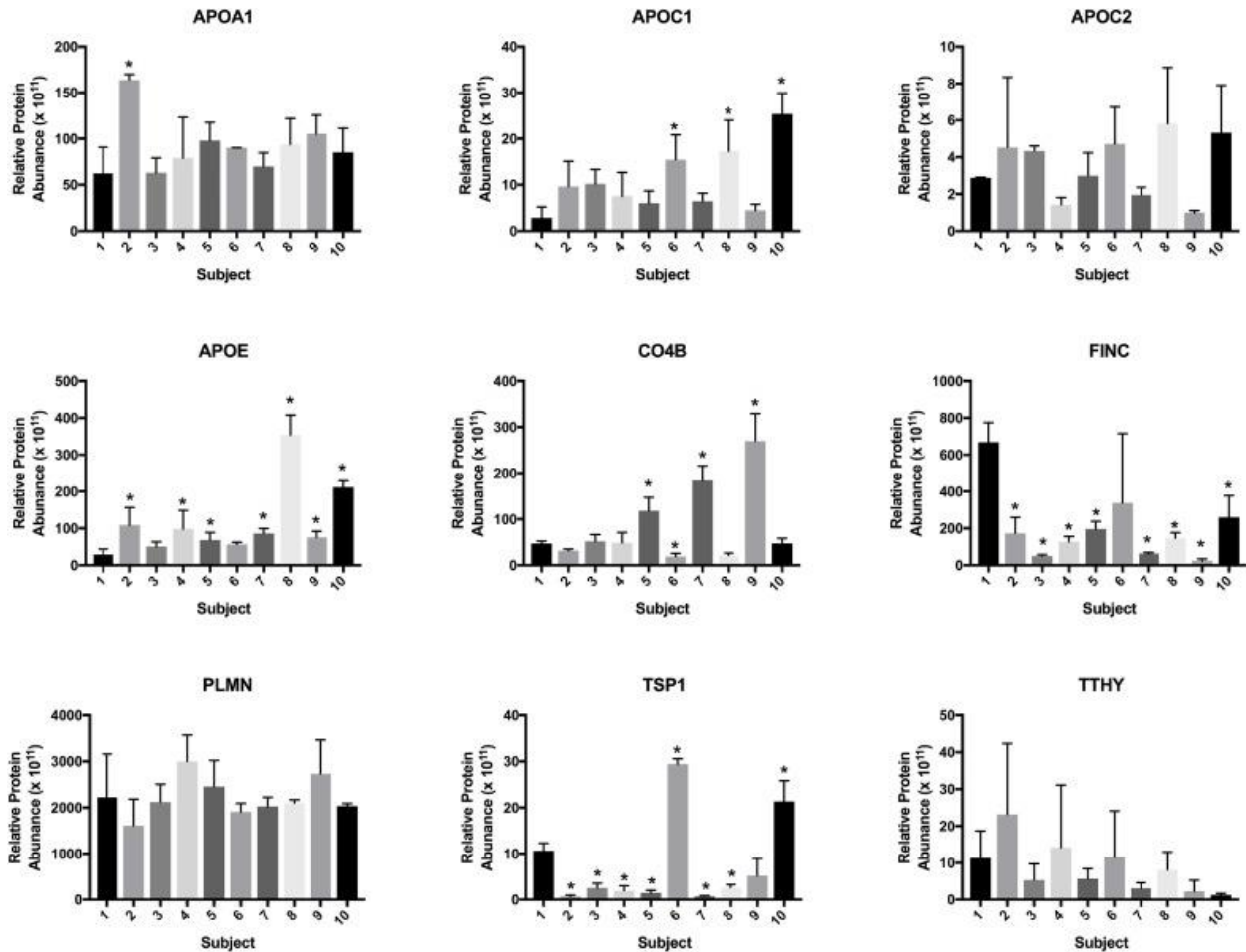


Figure 3.4. Relative Abundances of Specific Proteins across All Individual Pre-Exercise Subjects. Relative quantities of proteins shared between all 10 pre-exercise subjects were plotted to make global comparisons between all samples. * = statistical significance $p < 0.05$ compared to subject 1 by one-way ANOVA with Dunnett's post hoc analysis ($n = 3/\text{group}$). Supplemental Table S3.3 includes a comprehensive list of the calculated abundances for all proteins forming NP-BC in all subjects.

Relationships between the abundance of distinct proteins in the NP-BC (Supplemental Table S3.3) and subject characteristics (Total Cholesterol, LDL, HDL, Triglycerides, Glucose, Insulin, and BMI) (Table 3.1) were evaluated to determine correlations between typically measured medical parameters and nanoparticle-protein interactions (Supplemental Table S3.4). Certain proteins tended to increase in abundance within the NP-BC as total cholesterol increased, including apolipoprotein C1 ($R^2 = 0.42$, $p = 0.04$) and proteoglycan 4 ($R^2 = 0.44$, $p = 0.04$), whereas proteins such as transthyretin ($R^2 = 0.4$, $p = 0.049$) and immunoglobulin κ constant ($R^2 = 0.6$, $p = 0.01$) were decreased. Hepatocyte growth factor-like protein ($R^2 = 0.61$, $p = 0.001$), immunoglobulin κ variable 4-1 ($R^2 = 0.51$, $p = 0.02$), and insulin-like growth factor-binding protein 4 ($R^2 = 0.41$, $p = 0.04$), appear to increase directly with HDL, while apolipoprotein C3 ($R^2 = 0.41$, $p = 0.04$), and insulin-like growth factors 2 ($R^2 = 0.72$, $p = 0.002$) and 3 ($R^2 = 0.57$, $p = 0.01$) appear to decrease within the BC as HDL increases. The BC associated proteins apolipoprotein C1 ($R^2 = 0.55$, $p = 0.01$), proteoglycan 4 ($R^2 = 0.43$, $p = 0.04$), and platelet basic protein ($R^2 = 0.42$, $p = 0.04$) increased in abundance on the NP surface as LDL levels increased, whereas immunoglobulin κ constant ($R^2 = 0.50$, $p = 0.02$), and immunoglobulin κ variable 4-1 ($R^2 = 0.45$, $p = 0.03$) decreased. As plasma triglyceride levels increased, proteoglycan 4 ($R^2 = 0.48$, $p = 0.03$) and immunoglobulin heavy constant γ 3 ($R^2 = 0.43$, $p = 0.04$) increased within the NP-BC. Conversely, kinnogen-1 ($R^2 = 0.44$, $p = 0.04$) abundance decreased as triglyceride levels increased. As plasma glucose levels increased, so did insulin-like growth factor-2 ($R^2 = 0.64$, $p = 0.01$), apolipoprotein C2 ($R^2 = 0.59$, $p = 0.01$), and transferrin ($R^2 = 0.48$, $p = 0.03$), while prothrombin ($R^2 = 0.50$, $p = 0.02$), insulin-like growth factor-binding protein complex acid labile subunit ($R^2 = 0.56$, $p = 0.01$), and immunoglobulin heavy constant γ 1 ($R^2 = 0.49$, $p = 0.02$) decreased. Complement C3 ($R^2 = 0.81$, $p = 0.0004$), prothrombin ($R^2 = 0.43$, $p = 0.04$), and properdin ($R^2 = 0.4$, $p = 0.048$) increased within the BC with increased individual levels of insulin. Proteoglycan 4 ($R^2 = 0.56$, $p = 0.01$), and vitronectin ($R^2 = 0.44$, $p = 0.04$) within the BC tended to increase as BMI increased. To evaluate sex-related differences in NP-BC formation in terms of protein abundance, mean relative abundances of individual proteins were compared between male and female subjects (Supplemental Table S3.4). Male subjects were determined to have significantly more immunoglobulin κ variable 3–15, complement C1q subcomponent subunit A and B compared to female subjects (Supplemental Table S3.4). BCs formed following incubation in female plasma samples were determined to have significantly greater amounts

of inter- α -trypsin inhibitor heavy chain H4, coagulation factor XII, and plasminogen (Supplemental Table S3.4).

3.4.3. Intra-individual variability within the biocorona

3.4.3.1. Evaluation of the effect of exercise on variations in the BC – protein identities

Six subjects were selected for pre- to post- exercise comparisons based on changes in triglyceride levels (Table 3.1). Subjects 1, 6, and 8 were selected because they demonstrated the smallest changes in triglyceride levels pre- to post-exercise, while subjects 2, 5, and 7 were selected because they exhibited the largest triglyceride changes (Table 3.1, Bolded). A label-free mass spectrometry approach was used to identify proteins present in all subjects' post-exercise BCs. (Supplemental Table S3.1). Protein components of the post-exercise Fe₃O₄ NP BCs were initially compared to pre-exercise BCs based on the presence of identified proteins (Supplemental Table S3.5A). A total of 104 proteins were found in be in common between all subjects pre- and post-exercise (Supplemental Table S3.5A). Protein IDs were also compared within individual subjects and differences were observed due to exercise (Fig. 3.5, Supplemental Table S3.5B). In general, the post-exercise BC contained a larger number of unique proteins than the pre-exercise BC, with the exception of subject 8. Subject 2 had the largest number of unique post-exercise proteins, with 22 proteins present in the post-exercise BC that were not present in the pre-exercise BC. Subject 8 had the smallest number, at 10. In general, the post-exercise BCs from individuals with larger changes in triglyceride levels (subjects 2, 5, 7) contained increased numbers of unique proteins (as compared to the corresponding pre-exercise BC) than the post-exercise BCs of those with smaller changes in triglycerides (subjects 1, 6, 8) (Fig. 3.5, Supplemental Table S3.5B). Certain proteins were only present in pre-exercise NP-BCs (matrix gla protein, inter- α -trypsin inhibitor heavy chain H1) or only present in post-exercise NP-BCs (lipopolysaccharide binding protein, immunoglobulin heavy variable 2–5, immunoglobulin heavy variable 3–33).

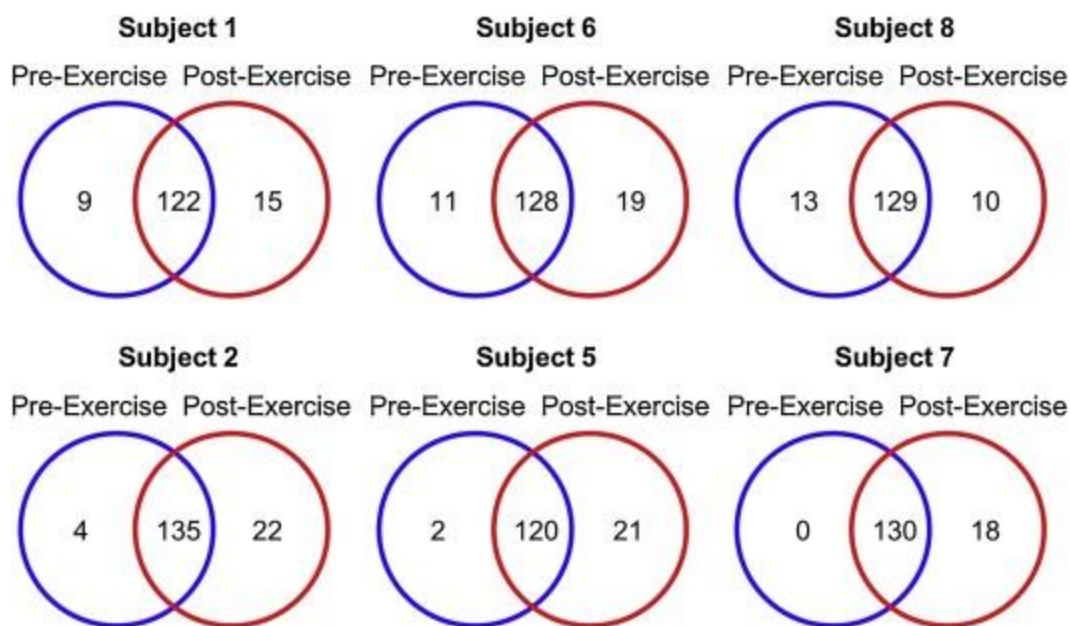


Figure 3.5. Comparison of Pre-Exercise to Post-Exercise Biocorona Composition within the Same Subject: Number of Proteins Shared Between Pre- and Post-Exercise Subjects. Proteins identified from each pre-exercise BC were compared to proteins identified from its corresponding post-exercise BC. Subjects were selected due their low (Subjects 1, 6, 8) or high (Subjects 2, 5, 7) changes in triglyceride levels pre- to post- exercise. Venn diagrams were created to illustrate each comparison. Supplemental Table S3.5A contains a comprehensive list comparing all identified proteins in pre- and post-exercise subjects. List of specific proteins used to generate Venn diagrams in Fig. 3.5 specifically are found in Supplemental Table S3.5B.

3.4.3.2 Evaluation of the effect of exercise on variations in the BC – protein quantification

Despite the many commonalities in protein identities in subjects' BCs pre- to post-exercise, quantities of these shared proteins differed due to exercise. Fig. 3.6 shows the top ten most significantly altered proteins as compared to the corresponding pre-exercise BC ($p < 0.05$) (Supplemental Table S3.6). Few commonalities existed between these top ten most significantly altered proteins. Exercise was determined to increase the quantity of most of these shared proteins. In some subjects, increases were observed post-exercise in both non-structural polyprotein and immunoglobulin κ variable 1–16. In subjects 5 and 7, the post-exercise increase in immunoglobulin κ variable 1–16 was the largest positive fold change among all shared proteins. Non-structural polyprotein experienced the largest positive fold change of significance following exercise among all proteins in subjects 2 and 6. Five of the six subjects experienced a fold change

above 4 for insulin-like growth factor-binding protein 2 following exercise (Supplemental Table S3.6). Apolipoprotein C3 and gelsolin were decreased in all subjects' BCs following exercise (Supplemental Table S3.6).

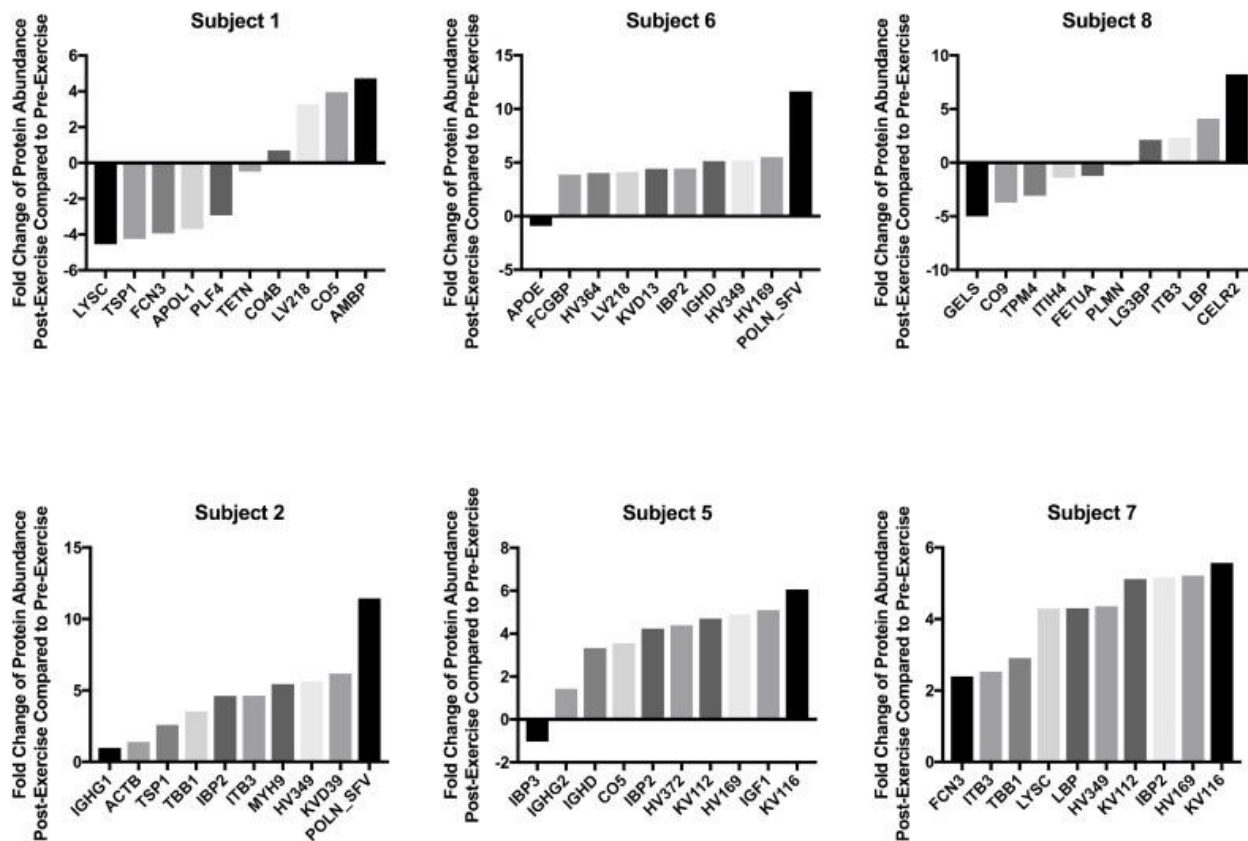


Figure 3.6. Fold Change of Specific Proteins in the Pre- and Post-Exercise Fe₃O₄ NP-BC. Quantities of shared proteins between each pre-exercise and post-exercise BC are depicted as fold changes. Supplemental Table S3.6 contains a comprehensive list of all protein quantity comparisons. Individual graphs depict the 10 most significantly different proteins in terms of fold change between pre- and post-exercise subjects (n = 3/group; one-way ANOVA with Tukey post hoc analysis; p < 0.05). Negative values indicate that the subject was more abundant prior to exercise, while positive values indicate that the subject was more abundant after exercise.

3.4.4 Assessment of immune cells response to NP exposure

3.4.4.1. Cellular viability, NP association, and inflammatory response

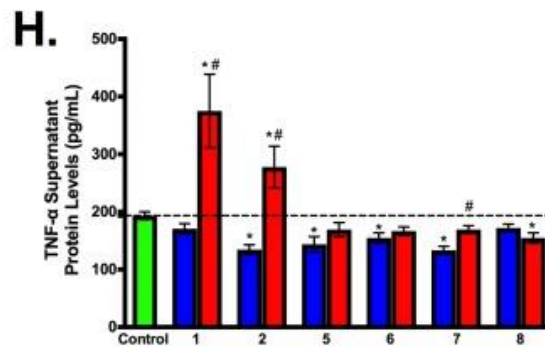
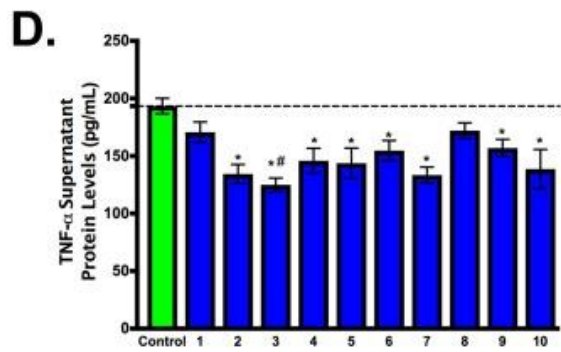
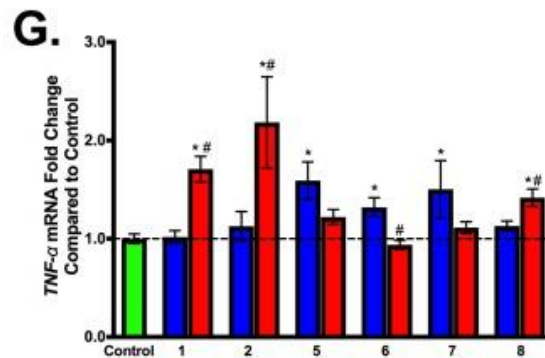
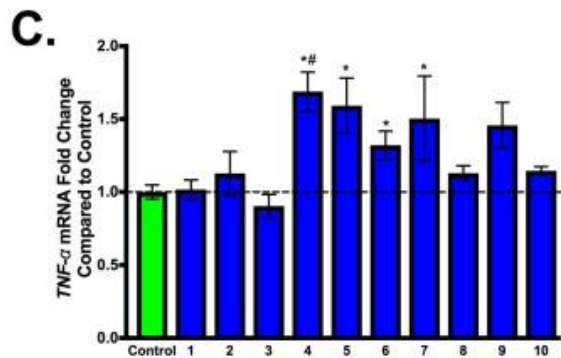
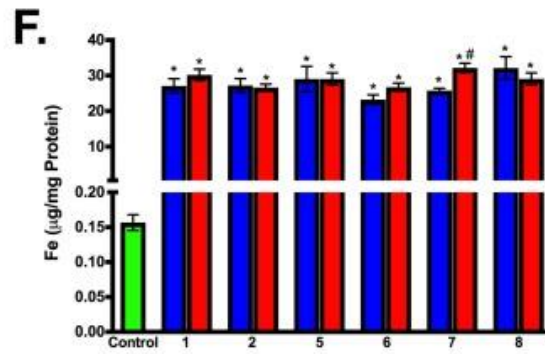
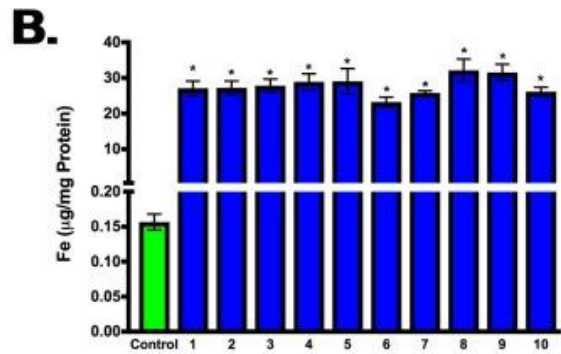
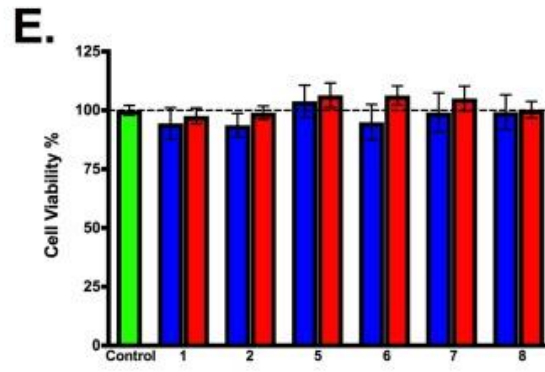
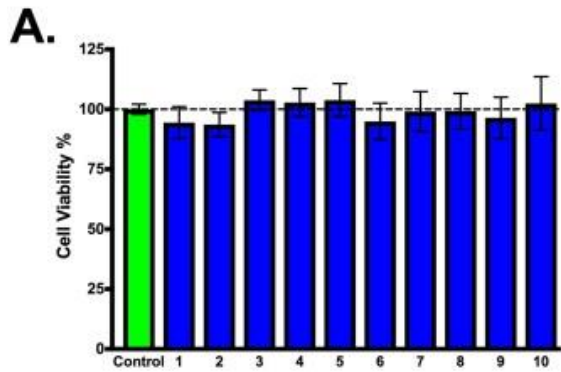
A concentration of 25 µg/ml was selected based on preliminary dose-response experiments in which human macrophages were exposed to Fe₃O₄ NPs, both with and without a BC formed from a representative human serum sample, at concentrations of 6.25, 12.5, 25, and 50 µg/mL for 24 h

(Supplemental Figure S3.2). None of the exposures at these concentrations demonstrated overt toxicity following a 24 h exposure (Supplemental Figure S3.2). Exposure to Fe₃O₄ NPs with a pre-exercise BC caused no significant differences in cell viability compared to the control (Fig. 3.7A). While macrophages associated NPs with the BC, no statistically significant differences were observed between NPs coated with any of the pre-exercise BCs (Fig. 3.7B). Inflammation was assessed by analysis of alterations in mRNA expression of *TNF- α* and macrophage release of *TNF- α* into the supernatant (Fig. 3.7C and D). *TNF- α* mRNA expression was significantly increased due to exposure to NPs with BCs formed from pre-exercise plasma from subjects 4, 5, 6, and 7 compared to controls (Fig. 3.7C). A decrease in protein levels of *TNF- α* was observed in the supernatant of all samples exposed to subjects' pre-exercise BCs. This decrease was statistically significant compared to the control for eight of the ten subjects, with the exceptions being subjects 1 and 8 (Fig. 3.7D).

Figure 3.7. Macrophage response following exposure to Individual Fe₃O₄ NP-BCs. Differentiated human macrophages were exposed to Fe₃O₄ NPs with a distinct BC at a concentration of 25 µg/ml for 24 h. Blue bars indicate Fe₃O₄ NPs with a BC formed following incubation in plasma collected from individuals prior to the exercise regimen. Red bars indicate Fe₃O₄ NPs with a BC formed following incubation in plasma collected from individuals following completion of the exercise regimen. A, E. Cytotoxicity after a 24 h exposure to Fe₃O₄ NPs with BCs. Dotted line indicates controls with a cell viability of 100%. B, F. Macrophage association of Fe₃O₄ NPs with BCs after a 24 h exposure. C, G. TNF-α mRNA expression relative to serum-free media control cells following 24 h exposure to 25 µg/ml Fe₃O₄ NPs with BCs. D, H. Protein levels of TNF-α in supernatant following 24 h exposure to 25 µg/ml Fe₃O₄ NPs with BCs. A–D Utilized pre-exercise BCs, while E–H utilized pre and post-exercise BCs. * denotes statistical significance compared to controls (n = 6/group; one-way ANOVA with Tukey post hoc analysis; p < 0.05). # denotes statistical significance between Fe₃O₄ NPs with pre- and post-exercise BCs (n = 6/group; two-way ANOVA with Tukey post hoc analysis; p < 0.05)

■ Fe₃O₄ NPs with a Pre-Exercise BC

■ Fe₃O₄ NPs with a Post-Exercise BC



Post-exercise BCs were also evaluated and compared to their corresponding pre-exercise BCs to determine differences in immune cell response. As with the pre-exercise BCs, no change in cell viability was observed after 24 h exposure (Fig. 3.7E). In general, cellular association of Fe₃O₄ NPs was similar between post-exercise and pre-exercise BCs (Fig. 3.7F). Subject 7 was the only exception to this; the cellular association of the NP with the post-exercise BC was significantly higher than the association of the pre-exercise BC. (Fig. 3.7F). *TNF-α* mRNA was increased post-exercise (as compared to pre-exercise) for three of the six subject BC exposures tested (1, 2, and 8) and decreased in the other three (5, 6, and 7), though this difference was only statistically significant for subjects 1, 2, 6 and 8 (Fig. 3.7G). Upon examination of supernatant *TNF-α* protein levels following exposure to NPs with pre-exercise or post-exercise BCs, post-exercise subject 8 had significantly lower levels of *TNF-α* (Fig. 3.7H). In exposures to post-exercise BCs of subjects 1, 2, and 7, supernatant levels of *TNF-α* were significantly higher than the subjects' corresponding pre-exercise BCs, and for subjects 1 and 2, the level of post-exercise *TNF-α* was significantly higher than that of the control.

3.5 Discussion

In order to efficiently and safely utilize NPs in biomedicine, it is essential to understand the formation of the BC and its impact on subsequent NP-cellular interactions. Presently, our knowledge is lacking regarding the influences of individual variability and exercise in relation to the composition of the BC, as well as the possible subsequent toxicological consequences. Our findings demonstrate variability between individuals, as well as variability due to exercise, in NP-BC protein composition. These compositional alterations in the BC were determined to impact NP hydrodynamic size and resulted in differential macrophage interactions and inflammatory response. Ultimately, this variability in NP-BC composition may contribute to inconsistencies in response to exposures and therapeutics observed within the general population.

3.5.1 NP properties modified following addition of BCs

NPs can be designed with an array of diverse physicochemical properties (size, surface coating, charge, composition, etc.) allowing for their utilization in a variety of technologies and applications. Addition of the BC can impact NP properties, therefore disrupting their intended

function (Amiri et al., 2013; Salvati et al., 2013). Our current study demonstrated that NP hydrodynamic size increased as cholesterol levels of the pre-exercise subjects increased, suggesting enhanced agglomeration of NPs. These changes in agglomeration and the observed variability are likely due to compositional differences in the BC. Evaluation of protein compositional differences did not demonstrate clear proteins associated with altered agglomeration between individuals. Past research has demonstrated that NPs in a hyperlipidemic environment associate large amounts of cholesterol, which may initiate alterations in NP agglomeration (Shannahan et al., 2016). Our findings demonstrate that NP properties such as agglomeration may be distinctively modified between individuals, resulting in differential functionality in their use as MRI contrast agents.

3.5.2 Interindividual variations in the NP-BC

NPs were determined to form unique BCs following incubation in each of the 10 pre-exercise plasma samples. While many proteins were shared between NP-BCs, 8 of the 10 pre-exercise BCs contained at least one unique protein that was not found in the other BCs, underling the impact of inter-individual variability. Proteins that were shared between individuals differed in the quantity in which they were present within the NP-BCs. Proteins frequently appearing in the list of those most quantifiably changed as compared to subject 1 included thrombospondin1, cytoplasmic 1 actin, complement factor H-related protein 2, and complement C4. The BCs of female subjects had higher levels of plasminogen and coagulation factor XII than those of male subjects, possibly due to elevated levels in the blood caused by the menstrual cycle and/or the use of birth control (Casslen and Ohlsson, 1981; Gordon et al., 1980; Lackner and Javid, 1973). In summary, correlation analysis demonstrated that association of specific proteins with the NP surface could only be partial explained by the measured subject parameters. This suggests that interactions are complex and likely dependent on multiple physiological factors.

The ability of NPs to differentially associate proteins due to variations in the physiological environment has potential use in fields of both pharmacology and toxicology. Specifically, if NPs are able to reduce levels of specific proteins via preferential adsorption, this association could assist in the targeted removal of proteins from the circulation, contributing to disease treatments. Further, the association of specific proteins could assist in the targeting of nano-based theragnostic

approaches. Previous research has shown that apolipoprotein-rich BCs enhance interactions between NPs and LDL receptors, as well as increasing transport across the blood-brain barrier (Kreuter, 2004, 2013). From a toxicological perspective, differential binding of proteins in disease environments could interfere with normal biological processes or enhance inflammatory responses, resulting in adverse outcomes. Ultimately, our current data supports that NPs introduced intravenously will not form consistent BCs between individuals. This variation may result in differential effectiveness of nano-based therapeutics between individuals, as well as disruption of biological systems by association of specific circulating biomolecules.

3.5.3 Intraindividual differences in the NP-BC related to exercise

An exercise model was utilized to evaluate the potential for intra-individual differences in the formation of the NP-BC. Specifically, a mixed exercise model including both endurance and resistance components was used, as it represents the ideal exercise paradigm according to guidelines set by the federal United States Health Department (United States Department of Health and Human Services, 2009). Exercise resulted in unique BC formation on Fe₃O₄ NPs following *ex vivo* incubation in collected subject plasma pre- and post-exercise. The post-exercise BC tended to be more diverse than the pre-exercise BC in terms of the number of unique proteins that were present. Interestingly, triglycerides were decreased following exercise for all subjects (Table 3.1). High intensity exercise has been shown to elevate triglycerides (Kraus et al., 2002) therefore this effect was most likely due to the resistance exercise component. These exercise-induced changes in triglyceride levels were found to influence BC formation, as subjects that demonstrated greater changes in triglyceride levels were found to have greater protein diversity within the BC.

Specific proteins were found to exclusively associate with NPs based on pre- or post-exercise conditions. Inter-alpha-trypsin inhibitor heavy chain H1 and matrix Gla protein were found only in the pre-exercise BCs, while immunoglobulin heavy variable 2–5, immunoglobulin heavy variable 3–33, immunoglobulin heavy variable 1–69, and lipopolysaccharide-binding protein were found only in the post-exercise BCs. Lipopolysaccharide-binding protein, which was only seen post-exercise, has been shown to be associated with stress, inflammation, and obesity. Because the recruited subjects within our study typically did not exercise, they likely responded to the stress of exercise with an acute phase response, leading to induction of lipopolysaccharide-binding protein

(Branescu et al., 2012; Stehle et al., 2012). Conversely, matrix Gla protein was only found in pre-exercise BCs. Matrix Gla protein has been shown to be increased in individuals with hyperlipidemia compared to controls (Kulich et al., 2003). Further, matrix Gla protein correlates with cholesterol, triglyceride, and low-density lipoprotein levels in the circulation (Kulich et al., 2003). Decreased abundance of matrix Gla protein on the NP surface suggests exercise-induced reductions within the circulation. It is likely that exercise resulted in reductions of certain circulating biomolecules, thus allowing lower abundance proteins an opportunity to associate with the NP surface. Further, certain proteins were likely increased within the NP-BC due to their increased availability resulting from exercise-induced synthesis. Other proteins, while not unique to the pre- or post-exercise conditions, were found to exhibit quantifiable differences following exercise, further demonstrating the dynamic nature of nano-based pharmaceutical interactions within a physiological environment. A decrease in the abundance of gelsolin on the NP surface following exercise was observed post-exercise. Gelsolin has been shown to be increased following acute eccentric exercise-induced muscle damage (Tekus et al., 2017). It is likely that muscle damage occurred early in our exercise regimen as a result of the resistance exercise component, causing an increase in gelsolin, and that the observed decrease in NP association of gelsolin was a result of the ongoing recovery process occurring at the time point we collected the plasma sample. The amount of insulin-like growth factor-binding protein 2 within the NP-BC was increased following exercise. Endurance exercise, such as the cycling performed in our study, is known to increase the circulating levels of insulin-like growth factor binding proteins in humans, which may have increased NP interactions (Suikkari et al., 1989).

Overall, these quantifiable changes suggest that exercise induces alterations in circulating biomolecule content, thereby altering BC formation. Due to the subjects' sedentary lifestyles, it is likely that exercise induced a general stress response and that the observed changes in the NP-BC are not all exercise-specific. However, our study indicates that minor or major lifestyle variations which impact the composition of the biological environment, such as exercise, diet, disease states, or stress, could also affect the composition of the BC, thereby resulting in altered NP efficacy and/or toxicity.

3.5.4 Immune cell response to NP-BCs

As expected, exposure to all Fe₃O₄ NPs with a BC was not found to induce cytotoxicity in human macrophages at the concentrations and time points assessed in this study. Macrophages were selected due to their distribution at sites of NP deposition, role in the induction of the immune response, and ability to phagocytize foreign materials such as NPs (Arnida et al., 2011; Walkey et al., 2012; Zhang et al., 2002). TNF- α mRNA and protein levels in cells exposed to Fe₃O₄ NPs with BCs varied both between individuals and following exercise. NPs incubated in post-exercise serum were found to be more likely to increase the inflammatory response than decrease it. Alterations observed in NP properties following addition of the BC appeared to have no impact on the cellular response, suggesting that the changes in immune cell response were due to the presence of specific biomolecules on the NP surface. Together, these findings demonstrate that alterations in NP-biomolecule interactions may result in differential immune cell activation dependent upon an individual's characteristics.

3.6 Study Limitations and Conclusions

A few limitations should be considered in regards to this study. First, although study participants were encouraged to maintain their normal lifestyles, it is unknown if individuals modified their diet or other aspects, which may have further altered circulating biomolecules. Additionally, only protein components of the BC were evaluated, however, it is likely that lipids and other biomolecules absorbed to the NP surface were also altered. Finally, our evaluation was performed on ten recruited individuals. For more patterns to be evident in regards to NP-biomolecule interactions, this study would have to be expanded to include a larger sample size.

In conclusion, these data substantiate that NP-biomolecule interactions are variable between individuals and can vary due to changes in an individual's activity. Further, this variability in the formation of the NP-BC was determined to modify NP toxicity, which may correspond to the differential toxicity which is often observed with pharmaceuticals in the general population. This study provides foundational knowledge and rationale to proceed with mechanistic examinations of the BC and its biological implications for nano-based precision therapeutics. Future investigation should incorporate other factors which may alter the BC, such as disease states, diet, longer-term exercise, drug/alcohol use, stress, etc. Ultimately, a thorough understanding of initial

interactions between NPs and biomolecules will allow for safer utilization of NP-enabled theragnostics in the complex biological environments that exist within our population.

3.7 References

2009. 2008 Physical Activity Guidelines for Americans. *J Cardiovasc Nurs* 24, 2-3.

Amiri, H., Bordonali, L., Lascialfari, A., Wan, S., Monopoli, M.P., Lynch, I., Laurent, S., Mahmoudi, M. (2013). Protein corona affects the relaxivity and MRI contrast efficiency of magnetic nanoparticles. *Nanoscale* 5, 8656-8665.

Arnida, Janat-Amsbury, M.M., Ray, A., Peterson, C.M., Ghandehari, H. (2011). Geometry and surface characteristics of gold nanoparticles influence their biodistribution and uptake by macrophages. *Eur J Pharm Biopharm* 77, 417-423.

Babes, L., Denizot, B., Tanguy, G., Le Jeune, J.J., Jallet, P. (1999). Synthesis of iron oxide nanoparticles used as MRI contrast agents: A parametric study. *J Colloid Interf Sci* 212, 474-482.

Balfoussia, E., Skenderi, K., Tsironi, M., Anagnostopoulos, A.K., Parthimos, N., Vougas, K., Papassotiriou, I., Tsangaris, G.T., Chrousos, G.P. (2014). A proteomic study of plasma protein changes under extreme physical stress. *J Proteomics* 98, 1-14.

Branescu, C., Serban, D., Savlovschi, C., Dascalu, A.M., Kraft, A. (2012). Lipopolysaccharide binding protein (L.B.P.)--an inflammatory marker of prognosis in the acute appendicitis. *J Med Life* 5, 342-347.

Casslen, B., Ohlsson, K. (1981). Cyclic Variation of Plasminogen Activation in Human Uterine Fluid and the Influence of an Intrauterine-Device. *Acta Obstet Gyn Scan* 60, 97-101.

Clift, M.J.D., Bhattacharjee, S., Brown, D.M., Stone, V. (2010). The effects of serum on the toxicity of manufactured nanoparticles. *Toxicol Lett* 198, 358-365.

- Dreyer, H.C., Fujita, S., Cadenas, J.G., Chinkes, D.L., Volpi, E., Rasmussen, B.B. (2006). Resistance exercise increases AMPK activity and reduces 4E-BP1 phosphorylation and protein synthesis in human skeletal muscle. *The Journal of physiology* 576, 613-624.
- Ghazanfari, M.R., Kashefi, M., Shams, S.F., Jaafari, M.R. (2016). Perspective of Fe₃O₄ Nanoparticles Role in Biomedical Applications. *Biochem Res Int*.
- Gordon, E.M., Ratnoff, O.D., Saito, H., Donaldson, V.H., Pensky, J., Jones, P.K. (1980). Rapid Fibrinolysis, Augmented Hageman-Factor (Factor-Xii) Titers, and Decreased C1-Esterase Inhibitor Titers in Women Taking Oral-Contraceptives. *J Lab Clin Med* 96, 762-769.
- Gordon, T., Castelli, W.P., Hjortland, M.C., Kannel, W.B., Dawber, T.R. (1977). Diabetes, blood lipids, and the role of obesity in coronary heart disease risk for women: the Framingham Study. *Annals of internal medicine* 87, 393-397.
- Gupta, A.K., Gupta, M. (2005). Synthesis and surface engineering of iron oxide nanoparticles for biomedical applications. *Biomaterials* 26, 3995-4021.
- Jain, T.K., Morales, M.A., Sahoo, S.K., Leslie-Pelecky, D.L., Labhasetwar, V. (2005). Iron oxide nanoparticles for sustained delivery of anticancer agents. *Mol Pharmaceut* 2, 194-205.
- Jedlovsky-Hajdu, A., Bombelli, F.B., Monopoli, M.P., Tombacz, E., Dawson, K.A. (2012). Surface Coatings Shape the Protein Corona of SPIONs with Relevance to Their Application in Vivo. *Langmuir* 28, 14983-14991.
- Jenkins, D.J.A., Wolever, T.M.S., Rao, A.V., Hegele, R.A., Mitchell, S.J., Ransom, T.P.P., Boctor, D.L., Spadafora, P.J., Jenkins, A.L., Mehling, C., Relle, L.K., Connelly, P.W., Story, J.A., Furumoto, E.J., Corey, P., Wursch, P. (1993). Effect on Blood-Lipids of Very High Intakes of Fiber in Diets Low in Saturated Fat and Cholesterol. *New Engl J Med* 329, 21-26.

- Kraus, W.E., Houmard, J.A., Duscha, B.D., Knetzger, K.J., Wharton, M.B., McCartney, J.S., Bales, C.W., Henes, S., Samsa, G.P., Otvos, J.D., Kulkarni, K.R., Slentz, C.A. (2002). Effects of the amount and intensity of exercise on plasma lipoproteins. *New Engl J Med* 347, 1483-1492.
- Kreuter, J. (2004). Influence of the surface properties on nanoparticle-mediated transport of drugs to the brain. *J Nanosci Nanotechnol* 4, 484-488.
- Kreuter, J. (2013). Mechanism of polymeric nanoparticle-based drug transport across the blood-brain barrier (BBB). *J Microencapsul* 30, 49-54.
- Kulich, W., Machreich, K., Hawa, G., Eichinger, B., Klein, G. (2003). [Calcification marker matrix G1a protein in patients with hyperlipidemia]. *Wien Med Wochenschr* 153, 360-364.
- Lackner, H., Javid, J.P. (1973). The clinical significance of the plasminogen level. *Am J Clin Pathol* 60, 175-181.
- Lundqvist, M., Stigler, J., Elia, G., Lynch, I., Cedervall, T., Dawson, K.A. (2008). Nanoparticle size and surface properties determine the protein corona with possible implications for biological impacts. *P Natl Acad Sci USA* 105, 14265-14270.
- Maiorano, G., Sabella, S., Sorce, B., Brunetti, V., Malvindi, M.A., Cingolani, R., Pompa, P.P. (2010). Effects of Cell Culture Media on the Dynamic Formation of Protein-Nanoparticle Complexes and Influence on the Cellular Response. *Acs Nano* 4, 7481-7491.
- Monopoli, M.P., Aberg, C., Salvati, A., Dawson, K.A. (2012). Biomolecular coronas provide the biological identity of nanosized materials. *Nat Nanotechnol* 7, 779-786.
- Monopoli, M.P., Walczyk, D., Campbell, A., Elia, G., Lynch, I., Bombelli, F.B., Dawson, K.A. (2011). Physical-Chemical Aspects of Protein Corona: Relevance to in Vitro and in Vivo Biological Impacts of Nanoparticles. *J Am Chem Soc* 133, 2525-2534.
- Mornet, S., Vasseur, S., Grasset, F., Duguet, E. (2004). Magnetic nanoparticle design for medical diagnosis and therapy. *J Mater Chem* 14, 2161-2175.

- Murphy, W.G. (2014). The sex difference in haemoglobin levels in adults - Mechanisms, causes, and consequences. *Blood Rev* 28, 41-47.
- Neuberger, T., Schopf, B., Hofmann, H., Hofmann, M., von Rechenberg, B. (2005). Superparamagnetic nanoparticles for biomedical applications: Possibilities and limitations of a new drug delivery system. *J Magn Magn Mater* 293, 483-496.
- Raghavendra, A.J., Fritz, K., Fu, S., Brown, J.M., Podila, R., Shannahan, J.H. (2017). Variations in biocorona formation related to defects in the structure of single walled carbon nanotubes and the hyperlipidemic disease state. *Sci Rep-Uk* 7.
- Salvati, A., Pitek, A.S., Monopoli, M.P., Prapainop, K., Bombelli, F.B., Hristov, D.R., Kelly, P.M., Aberg, C., Mahon, E., Dawson, K.A. (2013). Transferrin-functionalized nanoparticles lose their targeting capabilities when a biomolecule corona adsorbs on the surface. *Nat Nanotechnol* 8, 137-143.
- Shannahan, J. (2017). The biocorona: a challenge for the biomedical application of nanoparticles. *Nanotechnol Rev* 6, 345-353.
- Shannahan, J.H., Brown, J.M., Chen, R., Ke, P.C., Lai, X.Y., Mitra, S., Witzmann, F.A. (2013a). Comparison of Nanotube-Protein Corona Composition in Cell Culture Media. *Small* 9, 2171-2181.
- Shannahan, J.H., Fritz, K.S., Raghavendra, A.J., Podila, R., Persaud, I., Brown, J.M. (2016). Disease-Induced Disparities in Formation of the Nanoparticle-Biocorona and the Toxicological Consequences. *Toxicol Sci* 152, 406-416.
- Shannahan, J.H., Lai, X.Y., Ke, P.C., Podila, R., Brown, J.M., Witzmann, F.A. (2013b). Silver Nanoparticle Protein Corona Composition in Cell Culture Media. *Plos One* 8.
- Shannahan, J.H., Podila, R., Aldossari, A.A., Emerson, H., Powell, B.A., Ke, P.C., Rao, A.M., Brown, J.M. (2015a). Formation of a Protein Corona on Silver Nanoparticles Mediates Cellular Toxicity via Scavenger Receptors. *Toxicol Sci* 143, 136-146.

- Shannahan, J.H., Podila, R., Brown, J.M. (2015b.) A hyperspectral and toxicological analysis of protein corona impact on silver nanoparticle properties, intracellular modifications, and macrophage activation. *Int J Nanomed* 10, 6509-6521.
- Stehle, J.R., Leng, X.Y., Kitzman, D.W., Nicklas, B.J., Kritchevsky, S.B., High, K.P. (2012). Lipopolysaccharide-Binding Protein, a Surrogate Marker of Microbial Translocation, Is Associated With Physical Function in Healthy Older Adults. *J Gerontol a-Biol* 67, 1212-1218.
- Suikkari, A.M., Sane, T., Seppala, M., Ykijarvinen, H., Karonen, S.L., Koivisto, V.A. (1989). Prolonged Exercise Increases Serum Insulin-Like Growth Factor-Binding Protein Concentrations. *J Clin Endocr Metab* 68, 141-144.
- Tekus, E., Vaczi, M., Horvath-Szalai, Z., Ludany, A., Koszegi, T., Wilhelm, M. (2017). Plasma Actin, Gelsolin and Orosomucoid Levels after Eccentric Exercise. *J Hum Kinet* 56, 99-108.
- Tenzer, S., Docter, D., Kuharev, J., Musyanovych, A., Fetz, V., Hecht, R., Schlenk, F., Fischer, D., Kiouptsi, K., Reinhardt, C., Landfester, K., Schild, H., Maskos, M., Knauer, S.K., Stauber, R.H. (2013). Rapid formation of plasma protein corona critically affects nanoparticle pathophysiology. *Nat Nanotechnol* 8, 772-U1000.
- Tran, Z.V., Weltman, A., Glass, G.V., Mood, D.P. (1983). The Effects of Exercise on Blood-Lipids and Lipoproteins - a Meta-Analysis of Studies. *Med Sci Sport Exer* 15, 393-402.
- Walczyk, D., Bombelli, F.B., Monopoli, M.P., Lynch, I., Dawson, K.A. (2010). What the Cell "Sees" in Bionanoscience. *J Am Chem Soc* 132, 5761-5768.
- Walkey, C.D., Chan, W.C.W. (2012). Understanding and controlling the interaction of nanomaterials with proteins in a physiological environment. *Chem Soc Rev* 41, 2780-2799.
- Walkey, C.D., Olsen, J.B., Guo, H.B., Emili, A., Chan, W.C.W. (2012). Nanoparticle Size and Surface Chemistry Determine Serum Protein Adsorption and Macrophage Uptake. *J Am Chem Soc* 134, 2139-2147.

Xia, T., Hamilton, R.F., Bonner, J.C., Crandall, E.D., Elder, A., Fazlollahi, F., Girtsman, T.A., Kim, K., Mitra, S., Ntim, S.A., Orr, G., Tagmount, M., Taylor, A.J., Telesca, D., Tolic, A., Vulpe, C.D., Walker, A.J., Wang, X., Witzmann, F.A., Wu, N.Q., Xie, Y.M., Zink, J.I., Nel, A., Holian, A. (2013). Interlaboratory Evaluation of in Vitro Cytotoxicity and Inflammatory Responses to Engineered Nanomaterials: The NIEHS Nano GO Consortium. *Environ Health Persp* 121, 683-690.

Zhang, Y., Kohler, N., Zhang, M.Q. (2002). Surface modification of superparamagnetic magnetite nanoparticles and their intracellular uptake. *Biomaterials* 23, 1553-1561.

CHAPTER 4. COMPARISON OF SILVER NANOPARTICLE-INDUCED INFLAMMATORY RESPONSES BETWEEN HEALTHY AND METABOLIC SYNDROME MOUSE MODELS

A version of this chapter is pending publication in the *Journal of Toxicology and Environmental Health, Part A: Current Issues*.

4.1 Abstract

Silver nanoparticles (AgNPs) are utilized in surgical implants and medical textiles, thus providing access to the circulation. While research has been conducted primarily in healthy models, AgNP-induced toxicity evaluations in disease conditions are critical, as many individuals have preexisting conditions. Specifically, over 20% of United States adults suffer from metabolic syndrome (MetS). It was hypothesized that MetS may increase susceptibility to AgNP-mediated toxicity due to induction of differential inflammation and altered biodistribution. Mice were injected with 2 mg/kg AgNPs, and organs assessed for inflammatory gene expression (TNF- α , CXCL1, CXCL2, CCL2, TGF- β , HO-1, IL-4, IL13), and Ag content. AgNPs were determined to induce differential inflammation in healthy and MetS mice. While AgNP exposure increased TNF- α , CXCL1, TGF- β , HO-1, and IL-4 expression within healthy mouse spleens, MetS-treated animals demonstrated decreased CXCL1, IL-4, and IL-13 expression. Healthy and MetS mice livers exhibited similar inflammatory responses to one another. AgNPs localized primarily to the liver and spleen, although Ag was present in all examined organs. In organs of minor AgNP deposition, such as kidney, gene expression was variable. Induction of inflammatory genes did not correspond with biodistribution, suggesting disease-related variations in AgNP-mediated adverse responses. These findings indicate that disease may influence inflammation and biodistribution, impacting AgNP clinical applications.

4.2 Introduction

In recent years, the use of nanoparticles has expanded to include a multitude of applications, including manufacturing, consumer products, electronics, and medicine. Silver nanoparticles (AgNPs) are one of the most popular nanomaterials due to their antimicrobial activity, leading to

their incorporation into cosmetics, electronics, textiles, and food packaging (Echegoyen and Nerín 2013; Kaweeteerawat et al. 2017; Tran, Nguyen, and Le 2013; Zhang et al. 2016a). AgNPs are also utilized in a variety of biomedical applications that result in their direct introduction into the circulatory system, including burn creams, wound dressings, venous catheters, and surgical implants (Chaloupka, Malam, and Seifalian 2010; Ge et al. 2014; Song and Kim 2009). Previously, Benn and Cavanagh (2010) demonstrated that medical textiles with AgNP coatings are particularly prone to leaching and releasing AgNPs to the surrounding environment. However, direct introduction may not be strictly necessary due to their small size, as inhaled or ingested AgNPs may translocate to the circulation (Johanson and Carlander 2016). In addition, AgNPs were proposed to be utilized as a vaccine adjuvant and as a component of cancer treatment, which might result in their direct injection into the circulation (Chugh et al. 2018; Sanchez-Guzman et al. 2019; Taha, Djouider, and Banoqitah 2019). Despite their widespread potential applications in medicine, the toxicity of AgNPs to humans remains a subject of scientific investigation (Alaraby et al. 2016; Kermanizadeh et al. 2016). Investigators reported that exposure to AgNPs produced oxidative stress, cytotoxicity, and genotoxicity in human cell lines (macrophages, lung adenocarcinoma, and mesenchymal stem cells), potentially indicating that AgNP exposure may result in impaired immune responses and slower healing (Haase et al. 2011; Hackenberg et al. 2011; Rosario et al. 2018). Other studies have more directly examined the use of AgNPs in medicine, focusing on the effects of AgNPs within commercially available dressings, and found these to be hazardous to keratinocytes and fibroblasts, inducing cytotoxicity (Lam et al. 2004; Paddle-Ledinek, Nasa, and Cleland 2006; Poon and Burd 2004). While AgNPs are utilized increasingly in biomedicine, it is not known if the benefits of their use outweigh potential toxicity concerns. Mammalian models have provided further evidence of unintended adverse effects resulting from AgNP exposure. When inhaled or injected subcutaneously, AgNPs subsequently biodistribute throughout the body, depositing primarily in the liver but also reaching the brain, lungs, kidneys, and other organs (Takenaka et al. 2001; Tang et al. 2009). Ingested and injected AgNPs are eliminated from most organs fairly quickly, though these materials are retained for months within the brain (Bergin et al. 2016; Dziendzikowska et al. 2012; Zande et al. 2012). This is particularly concerning, as AgNPs may induce oxidative stress in various tissues (Martins et al 2017) and alter gene expression in multiple regions of the brain, resulting in apoptosis and neurotoxicity (Rahman et al. 2009). AgNPs have also been demonstrated to stimulate an inflammatory response in both in vitro and in vivo

models. Various cell types have been shown to exhibit increased expression of pro-inflammatory markers following exposure to AgNPs, including macrophages, fibroblasts, and endothelial cells (Park et al. 2011; Trickler et al. 2010). In animal models, AgNP exposure was found to exert a similar effect, eliciting enhanced expression of pro-inflammatory cytokines primarily in liver, a major site of AgNP deposition (Chen et al. 2016; Ramadi et al. 2016). However, while the toxicity of AgNPs has been the subject of much scrutiny, there remain gaps in the scientific knowledge regarding susceptible subpopulations that may be at risk for unexpected and exacerbated responses following exposure. The majority of studies conducted investigating AgNP toxicity have been performed in healthy models. This is a major oversight, as medical treatments, including those containing AgNPs, are utilized primarily in individuals who are in some way unhealthy. Examples include the use of AgNPs in the treatment of injuries, such as in burn creams or in surgeries as an antibacterial/antifungal coating on tools and implants (Chaloupka, Malam, and Seifalian 2010; Ge et al. 2014; Song and Kim 2009). Further, many individuals in the United States and worldwide exist with some form of underlying disease state (Buttorff, Ruder, and Bauman 2017; Halpin, Morales-suárez-varela, and Martin-moreno 2010). Metabolic syndrome (MetS), a disease characterized by dyslipidemia, elevated blood pressure, insulin resistance, and increased body weight, affects over one-fifth of the United States population (Aguilar et al. 2015; Beltrán-Sánchez et al. 2013). In addition, the prevalence of MetS in the United States and worldwide is increasing (Desroches and Lamarche 2007; Ford, Giles, and Mokdad 2004). MetS is an established risk factor for the development of many serious chronic diseases, including renal disease, diabetes, and cardiovascular disease (Cirillo et al. 2006; Galassi, Reynolds, and He 2006; Grundy 2006). Individuals with MetS have been noted to be more vulnerable to adverse health outcomes such as cardiovascular depression, heartbeat variability, and altered cardiac repolarization as a result of exposure to nano-sized particulate matter (Chen and Schwartz 2008; Devlin et al. 2014; Wagner et al. 2014). Evaluations of the NHANES database in conjunction with the US EPA's Aerometric Information Retrieval system demonstrated an association between PM₁₀ and PM_{2.5} exposures and circulating white blood cells and elevated levels of C-reactive protein, a cardiovascular disease inflammatory marker, which worsened as severity of MetS rose. This further demonstrates the increased susceptibility of diseased individuals to enhanced inflammation following exposures (Chen and Schwartz 2008; Dabass et al. 2018). Although the mechanisms underlying this increased susceptibility are not fully understood, it is thought that individuals with MetS experience higher

levels of baseline inflammation, predisposing them to both acute adverse health outcomes and development of chronic diseases (Esser et al. 2014; Haffner 2006; Isomaa et al. 2001; Paoletti et al. 2006). It is likely that individuals with MetS may be susceptible not only to particulate matter (PM) inhalation, but also to intravenous exposure to biomedically utilized engineered particles such as AgNPs. The aim of this study was to examine variations in inflammatory responses and biodistribution following intravenous exposure to AgNPs through the utilization of mouse models representing either healthy or MetS conditions. An understanding of differences in inflammation and biodistribution between healthy and diseased conditions might enable a better understanding of the differential exposure responses, and thus susceptibility of vulnerable subpopulations. Ultimately, these results might assist in the utilization of in vitro and in vivo studies to service the development of medical devices containing AgNPs and their use in clinical settings.

4.3 Materials and Methods

4.3.1 AgNP Characterization.

AgNPs with a diameter of 20 nm suspended in citrate were purchased (Nanocomposix, San Diego, CA). AgNPs were characterized to verify the specifications provided by the manufacturer. Polydispersion index, ζ -potential, and hydrodynamic size were assessed in DI water with AgNPs at a concentration of 25 $\mu\text{g/ml}$ ($n = 4/\text{AgNP}$). The number of AgNPs/ml was determined by NP tracking software (Nanosight, Malvern, Westborough, MA) ($n = 4/\text{AgNP}$). While many varieties of AgNPs are commercially available, AgNPs utilized in this study display similar properties to certain formulations used in biomedicine (Dunn and Edwards-Jones 2004; Park and Lee 2013).

4.3.2 Induction of MetS and AgNP Exposure.

Healthy male 6-week-old C57BL6 mice (Charles River Laboratories, Wilmington, MA) were provided with water ad libitum and fed either a normal diet (10% kcal from fat) or a high-fat Western diet (60% kcal from fat) (Research Diets, New Brunswick, NJ) to induce the development of MetS. Mice were assessed for key components of MetS, obesity, dyslipidemia, and insulin resistance to verify the development of the disease. While markers of hyperglycemia were not directly measured, it may be extrapolated that animals were likely hyperglycemic based upon previous studies utilizing the same high-fat diet-induced model of MetS (Kennedy et al. 2010).

Following 14 weeks on the diets, mice were injected via the tail vein with 2 mg/kg of AgNPs or saline as a control. While many previous studies have utilized injection doses in excess of 50 mg/kg, toxicological effects have been observed at doses of approximately 2 mg/kg (Xue et al. 2012; Tang et al. 2008, 2009; Mahdy et al. 2014). The selected dose of 2 mg/kg, in addition to being known to induce adverse effects from other studies, is also relevant to real-world exposures. Medical textiles were found to leach significant amounts of AgNPs (Benn and Cavanagh 2010). The use of these textiles in combination with medical tools or implants which also contain an AgNP coating has the capacity to increase human exposure to and beyond the dose utilized in this study. Further, AgNPs are proposed as a cancer treatment and vaccine adjuvant, both applications which would result in the direct introduction of a significant amount of AgNPs into the circulatory system (Chugh et al. 2018; Sanchez Guzman et al. 2019). Mice were separated into two groups, one of which was utilized for an assessment of inflammation and the other to examine differential biodistribution. Animals were housed in a temperature-controlled, 12 hr light/dark cycle room for the duration of the study, which was conducted in compliance with the regulation and approved by the Animal Care and Use Committee of Purdue University.

4.3.3 Organ Collection and Blood Characterization.

Twenty-four hr following AgNP injection, mice were sacrificed, and the liver, spleen, kidneys, intestines, lungs, brain, heart, and aorta extracted. Organs were immediately frozen in liquid nitrogen following removal. Blood was collected via cardiac puncture, and the aorta severed to remove additional blood from the circulation. In accordance with previous investigations of injected NPs, perfusion of the body was not performed (Javidi et al. 2019; Lee et al. 2016; Meng et al. 2014; Snyder et al. 2016; Sumner et al. 2016; Yang et al. 2017). Immediately following collection, an aliquot of blood was set aside for assessment of glycated hemoglobin (HBA1c) using a commercially available assay kit (Crystal Chem, Elk Grove Village, IL). The remaining blood was centrifuged for 10 min at 3,500 g and 4°C to isolate serum. Serum was characterized for traditional lipid endpoints via commercially available kits to measure total bound and unbound cholesterol, HDL, and LDL/VLDL (Bioassay Systems, San Francisco, CA). Serum insulin was also measured in serum using a commercially available assay kit (Crystal Chem, Elk Grove Village, IL).

4.3.4 Gene Expression Assessment.

Total RNA was isolated from each organ of the gene expression cohort and converted to cDNA. AgNP-induced variations in the inflammatory response were measured through assessment of alterations in gene expression for tumor necrosis factor- α (TNF α), chemokine (C-C motif) ligand 2 (CCL2), chemokine (C-X-C motif) ligand 1 (CXCL1), chemokine (C-X-C motif) ligand 2 (CXCL2), interleukin 4 (IL4), and interleukin 13 (IL-13). In addition, fibrotic marker transforming growth factor- β (TGF- β) and oxidative stress marker heme oxygenase 1 (HO-1) were assessed. Glyceraldehyde 3-phosphate dehydrogenase (GAPDH) was used as the internal control. All genes were analyzed via real-time RT-qPCR (n = 7–8 per group).

4.3.5 Metal Quantification.

All organs from the biodistribution cohort were digested with concentrated nitric acid in a MARSXpress microwave-accelerated reaction system. Digested samples were diluted up to 1000-fold in 0.1% nitric acid prior to quantification using an atomic absorption spectrophotometer with a graphite tube atomizer (Agilent, Santa Clara, CA). Sample concentration was normalized to tissue weight of the digested organ for each measurement.

4.3.6 Statistical Analysis.

Significant differences in blood parameters, organ metal content, and gene expression were determined using a two-way ANOVA with disease (healthy or MetS) and exposure (control or AgNP exposure) as the two factors. A Tukey's post-hoc test was utilized for multi-comparison analysis ($p < .05$). GraphPad Prism 8 software (GraphPad, San Diego, CA) was used to generate graphs and for all statistical assessment. Graphed data are presented as mean \pm standard error of the mean (SEM.)

4.4 Results

4.4.1 Characterization of Mouse Model and AgNPs.

AgNPs were characterized based upon the parameters of hydrodynamic size, polydispersion index, and ζ -potential and found to match the manufacturer's specifications (Table 4.1). MetS mice

exhibited elevated body weight, HDL, LDL/VLDL, and total cholesterol compared to healthy animals (Table 4.2). These results were expected and consistent with previous models of diet-induced MetS (Cao et al. 2014; Pettersson et al. 2012). Further, serum insulin was increased in MetS mice, suggesting the presence of insulin resistance, a component of MetS (Beltrán-Sánchez et al. 2013). HBA1c, a marker of diabetes, was unchanged between healthy and MetS models. AgNP exposure did not markedly alter weight or any of the assessed blood parameters.

Table 4.1. AgNP Characterization. Data represent mean \pm SEM, n=4/group. AgNPs were characterized via assessment of ζ -potential, hydrodynamic size, and polydispersion index.

	Particle Concentration (NPs/ μ g \times 10^9)	Hydrodynamic Size (nm)	Polydispersion Index	ζ Potential (mV)
AgNPs	5.5 \pm 0.6	27.0 \pm 0.2	0.09 \pm 0.006	-54.8 \pm 0.3

Table 4.2. Characterization of Healthy and MetS Mice. Serum from healthy and MetS mice was characterized for traditional lipid endpoints via commercially available kits to measure total bound and unbound cholesterol, HDL, LDL/VLDL, insulin, and glycated hemoglobin (HBA1c). # denotes statistical significance as compared to the corresponding healthy group. Comparisons were performed by two-way ANOVA with Tukey post hoc analysis; p<0.05). All analyses are reported as mean \pm SEM, n= 7-8/group.

	Healthy Control	Healthy AgNPs	MetS Control	MetS AgNPs
Body Weight (g)	34.3 \pm 0.9	32.6 \pm 1.7	50.4 \pm 1.1 [#]	48.75 \pm 1.2 [#]
HDL (mg/dL)	132.7 \pm 10.1	128.7 \pm 13.4	220.9 \pm 10.7 [#]	244.3 \pm 19.18 [#]
LDL/VLDL (mg/dL)	43.1 \pm 1.3	46.3 \pm 2.7	56.1 \pm 2.7 [#]	61.3 \pm 4.1 [#]
Total Cholesterol mg/dL)	159.8 \pm 12.9	157.8 \pm 10.3	273.5 \pm 18.6 [#]	298.4 \pm 16.1 [#]
Insulin (ng/mL)	0.53 \pm 0.1	0.59 \pm 0.1	8.26 \pm 2.4 [#]	7.52 \pm 2.1 [#]
% HBA1c	4.21 \pm 0.1	4.45 \pm 0.2	4.55 \pm 0.6	4.78 \pm 0.2

4.4.2 AgNP Biodistribution.

AgNPs were determined to primarily biodistribute to the liver, intestines, and spleen, with minor amounts in lungs, blood, kidneys, brain, heart, and aorta (Figure 4.1). A larger proportion of AgNPs was detected in the liver of MetS mice than healthy mice, while a smaller portion was identified in the intestines, spleen, and lungs. In each specific organ tested, silver levels were at or below the limit of detection for unexposed control animals (Figure 4.2). The concentration of Ag

present in the spleen 24 hr following injection was the same between healthy and MetS mice. MetS mice possessed a higher Ag concentration in the liver, kidneys, and heart. The concentration of Ag in the lungs was higher in healthy mice than MetS mice. Both MetS mice and healthy mice had the same concentration of Ag in the brain.

	Liver		Spleen		Kidney		Heart		Lung		Brain	
	Healthy	MetS										
Chemokine (C-C motif) ligand 2 (CCL2)	↑	↑	-	-	-	↓	-	↑	↓	↓	↑	-
Chemokine (C-X-C motif) ligand 1 (CXCL1)	-	↑	↑	-	↑	↓	-	↑	↓	↓	↓	↓
Chemokine (C-X-C motif) ligand 2 (CXCL2)	↑	↑	-	-	↑	-	-	↑	-	↓	-	-
Tumor necrosis factor α (TNF- α)	↑	↑	↑	-	↓	-	-	↑	↓	-	↓	-
Transforming growth factor β (TGF- β)	↑	↑	↑	-	↓	↑	-	-	↓	↓	↓	-
Heme oxygenase 1 (HO-1)	↑	↑	↑	-	-	↑	-	-	↓	-	↓	↓
Interleukin 4 (IL-4)	-	-	↑	↓								
Interleukin 13 (IL-13)	-	-	-	↓								

Table 4.3. Summary of Changes in Gene Expression Following Exposure to AgNPs. Statistically significant increases and decreases in expression as compared to unexposed groups are denoted by “up” and “down” arrows, respectively. Lack of any statistically significant change is indicated by a dash.

4.4.3 Gene Expression.

The expression of genes related to inflammation, fibrosis, and oxidative stress was assessed in a variety of tissues in order to determine differential responses to MetS and AgNP exposure. A full summary of genes assessed and organ-specific responses to AgNP exposure may be found in Table 4.3. MetS was found to decrease IL-13 and CXCL1 expression in the liver compared to healthy control mice (Figure 4.3). AgNP exposure enhanced expression of Th1 inflammatory response genes (CCL2, TNF- α , CXCL1, CXCL2), TGF- β (a marker of fibrosis), and HO-1 (indicative of oxidative stress) in healthy and MetS mice, with all increases reaching the level of statistical significance with the exception of CXCL1 in healthy mice. Liver expression of Th2 inflammatory response genes (IL-4 and IL-13) were unaffected by AgNP exposure, remaining at approximately the same levels as observed in saline-treated control mice.

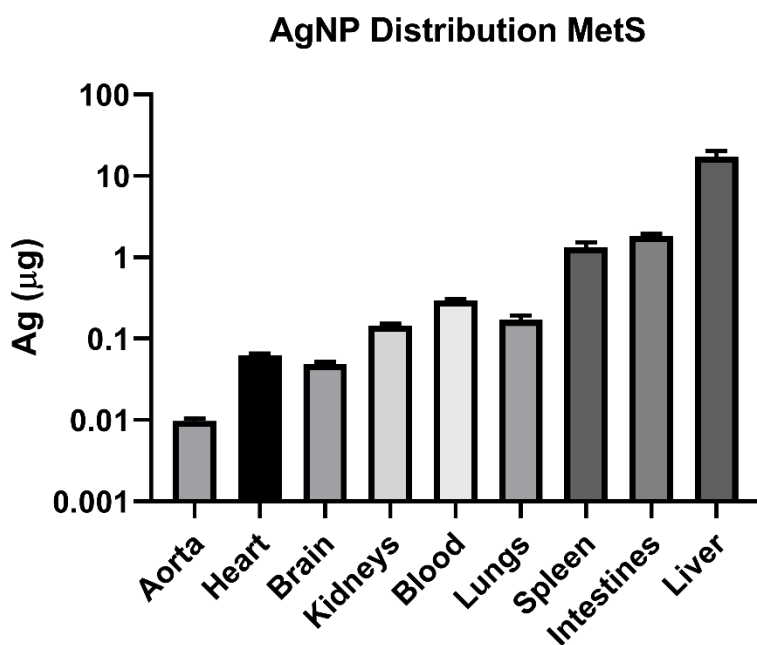
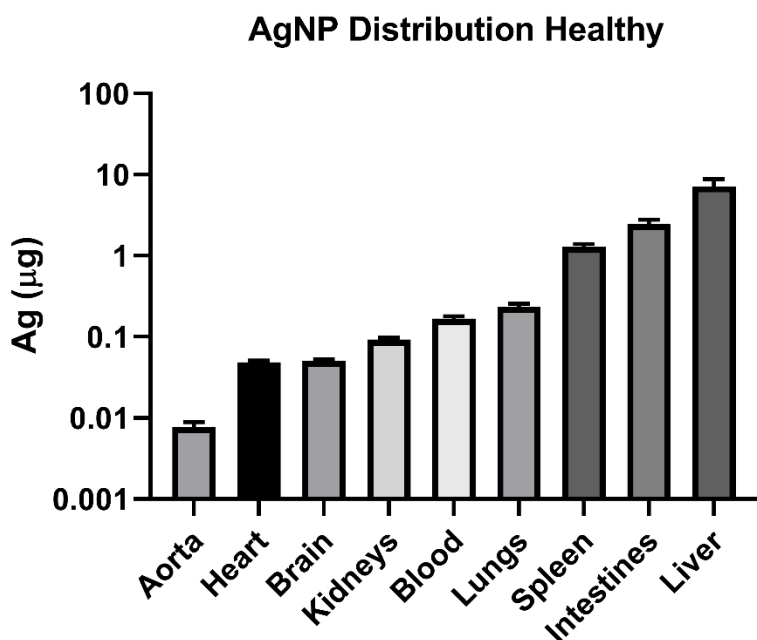


Figure 4.1. Average Abundance of AgNPs in Each Organ of Healthy and MetS Mice Treated with AgNPs. The Ag content of each organ of mice treated with AgNPs was assessed via atomic absorption spectroscopy.

At baseline, MetS mice displayed a higher expression of CCL2, TNF- α , CXCL2, HO-1, TGF- β , and IL13 in the spleen compared to healthy mice (Figure 4.4). In healthy mice, AgNP exposure resulted in an elevated expression of TNF- α , CXCL1, HO-1, TGF- β , and IL4 in the spleen. The influence of AgNP exposure on gene expression was less consistent in MetS mice. Both IL-4 and IL-13 expression were significantly decreased compared to control MetS. CXCL2 within the spleen was unaffected by MetS or exposure to AgNPs.

The reaction of kidney to MetS was variable based upon the gene examined. CCL2, CXCL1, and CXCL2 were all significantly higher at baseline in MetS than healthy mice, while TNF- α and TGF- β were significantly lower (Figure 4.5). HO-1 was unaffected at baseline by MetS. Alterations in kidney gene expression of mice following AgNP exposure were similarly variable; in healthy mice, CXCL1 and CXCL2 expression were up-regulated by AgNP exposure, TNF- α and TGF- β expression were down-regulated, and CCL2 and HO-1 were unaltered. MetS exhibited differential responses to AgNPs, with CCL2 and CXCL1 down regulated, HO-1 and TGF- β up-regulated, and CXCL2 unaltered.

Within the heart, most cytokines tested were the same between healthy and MetS at baseline, with the exceptions of TNF- α and TGF- β , which were lower in MetS compared to healthy animals (Figure 4.6). AgNP exposure did not induce any significant alterations in the expression of genes evaluated in healthy mice. In contrast, MetS mice exhibited significant elevations in the expression of CCL2, TNF- α , CXCL1, and CXCL2 following AgNP exposure. HO-1 and TGF- β expression in the MetS heart were unaffected by AgNP exposure.

The lung was among the most consistent of the organs tested regarding alterations in gene expression. CCL2, TNF- α , HO-1, and TGF- β gene expression was noted to be down-regulated in unexposed MetS animals compared to unexposed healthy, while unexposed MetS mice displayed higher expression of CXCL1 and CXCL2 than healthy (Figure 4.7). Upon exposure to AgNPs, gene expression was reduced in both healthy and MetS mice. In healthy mice, this decrease was significant for all genes with the exception of CXCL2, and in MetS mice, the fall was significant in CCL2, CXCL1, CXCL2, and TGF- β .

Gene expression within the brain was also found to be altered in MetS; specifically, TNF- α was determined to be significantly lower in MetS mice compared to healthy at baseline (Figure 4.8). AgNP exposure increased gene expression of CCL2 in the brain of healthy mice while lowering the expression of TNF- α , CXCL1, HO-1, and TGF- β . Following AgNP exposure, MetS mice demonstrated reduced gene expression of CXCL1 and HO-1.

4.5 Discussion

MetS is a common condition, and individuals with MetS have demonstrated enhanced susceptibility to exposures. Although AgNPs are increasingly incorporated into biomedical applications due to their antibacterial and antifungal properties, more research is needed to fully understand potential toxicological effects. Most studies of NP safety have focused on healthy models; however, NP toxicity and biological interactions may be altered by diseases such as MetS. This study utilized healthy and diseased mouse models to examine differential organ-specific inflammatory responses to AgNPs in MetS. Our data determined that MetS mice exhibit organ-specific inflammatory responses that are, in some cases, distinct from those of healthy animals, and that these effects are not explained solely by differential biodistribution patterns.

At baseline, prior to the introduction of any AgNPs, MetS mouse livers contained the same or lower levels of inflammatory gene expression than healthy mice. This is seemingly contradictory with many previous studies of the effect of MetS, which have shown increased expression of inflammatory markers in the liver, including TNF- α , CCL2, and others (Bieghs and Trautwein 2013; Rector et al. 2008). However, recent investigations have demonstrated that chronic inflammatory stimulation, such as that produced by obesity, results in a phenomenon known as T cell exhaustion (Aguilar and Murphy 2018; Green and Beck 2017; Wang et al. 2019). T cell exhaustion is characterized by progressive loss of function, decreased proliferation, and overall inactivity (Wherry 2011; Wherry and Kurachi 2015). It is conceivable that our MetS mice, having been fed a high-fat Western diet, generated the necessary conditions to induce hepatic T cell exhaustion. These conditions include dysregulation of immune-active metabolites such as leptin, adiponectin, and glucose, all of which are known to be altered due to increased body weight (Aguilar and Murphy 2018; Beyer et al. ; Sun and Karin 2012). Further, there is evidence to support that insulin resistance, which is a component of MetS, may lead to decreased activation of T cells and reductions in inflammatory cytokines (Andersen, Murphy, and Fernandez 2016; Lteif, Han,

and Mather 2005; Roberts, Hevener, and Barnard 2013). Unlike the liver, T cells within the spleen do not appear to have experienced exhaustion, likely because the spleen is not a major site of ectopic fat deposition (Pou et al. 2009). Baseline expression of the majority of cytokines tested in the spleen was higher in MetS than healthy, possibly due to an elevated number of macrophages and activated T cells producing Th1 and Th2 cytokines. Taken together, our findings demonstrate that MetS in mice, when induced by a high-fat Western diet, results in organ-dependent inflammatory dysregulation.

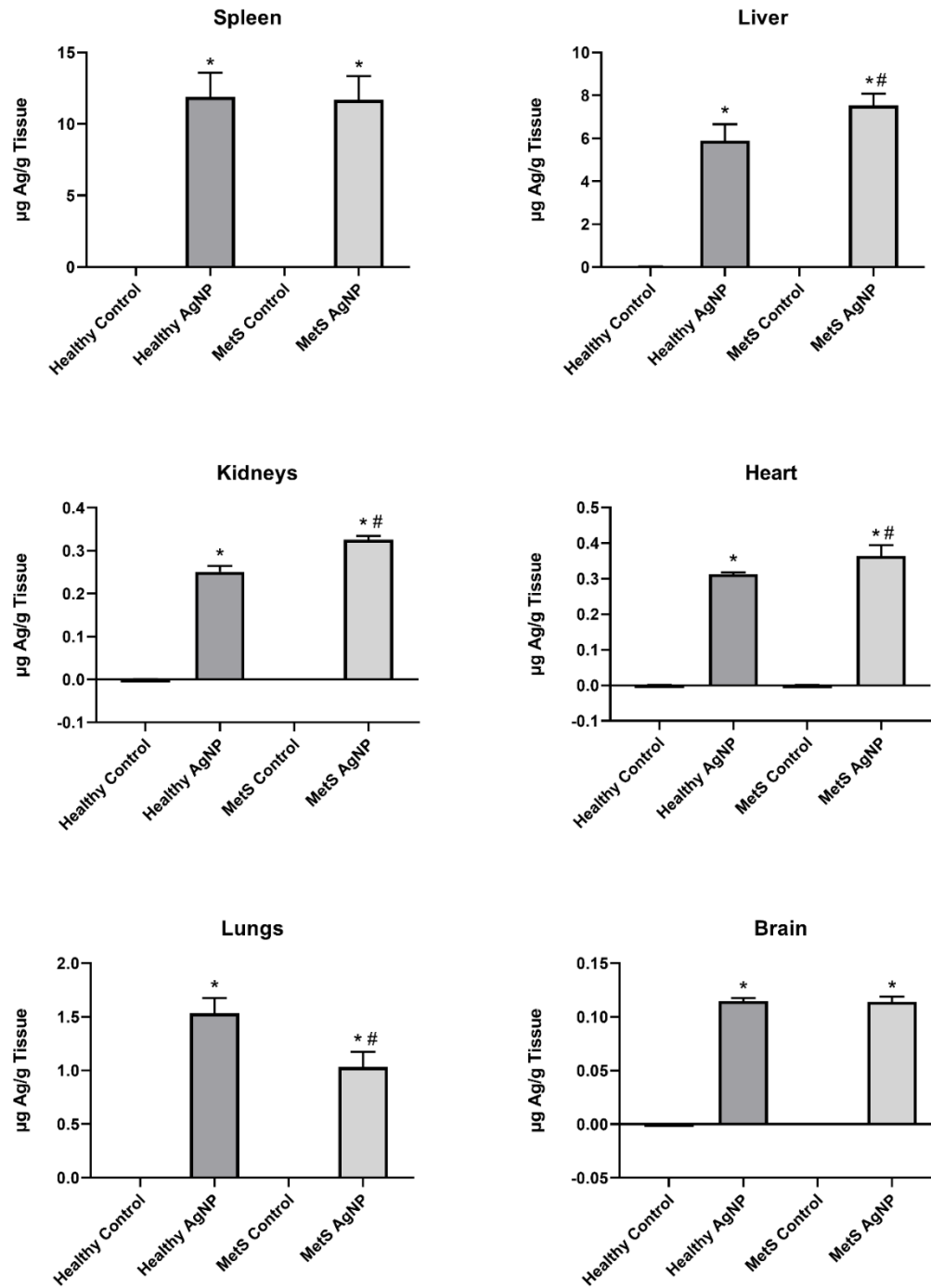


Figure 4.2. Average Concentration of AgNPs in Selected Organs of Treated and Control Healthy and MetS Mice. The Ag content of each organ was assessed via atomic absorption spectroscopy. The metal content in μg was divided by the weight of the organ in g in order to assess data in terms of Ag concentration. All analyses are reported as mean \pm SEM ($n = 6-8$ per group). * denotes statistical significance as compared to the corresponding untreated control group, and # denotes statistical significance as compared to the corresponding healthy group. Comparisons were performed by two-way ANOVA with Tukey post hoc analysis; $p < 0.05$.

Following 14 weeks on a healthy or high-fat Western diet, animals were injected with 2 mg/kg of AgNPs. While previous investigators have utilized doses at and above 50 mg/kg to elicit an inflammatory response, such a dose is not relevant to real-world exposures (Xue et al. 2012; Tang et al. 2008, 2009; Mahdy et al. 2014). The dose of 2 mg/kg was selected for (1) therapeutic relevance given AgNP leaching from currently utilized medical textiles and devices, (2) proposed uses in vaccines and cancer treatment, and (3) capacity to induce a toxicological response. Differences in biodistribution were observed between the healthy and MetS groups that did not appear to be a result of the overall larger dose administered to MetS mice. Specifically, only the livers, kidneys, and hearts of MetS mice were observed to exhibit a higher concentration of Ag than healthy mice, while other organs such as the spleen and brain had equivalent Ag levels. Despite receiving a lesser total amount of AgNPs at dosing, lungs from healthy mice contained a higher concentration of Ag compared to MetS mice. Within the liver, a higher % Ag accumulated in MetS mice compared to healthy, suggesting differential hepatic deposition. The healthy mice possessed a far larger proportion of total Ag in intestines, likely as a result of elimination in fecal matter, which is the primary route for elimination of NPs which enter the body (Zhang et al. 2016b). Taken together, these data indicate that MetS mice eliminate AgNPs more slowly than healthy animals. While information is lacking regarding the influence of MetS on NP clearance, it is known that liver function is impaired in obesity, and hepatobiliary clearance is the primary method of eliminating NPs from the body (Kim and Younossi 2008; Watanabe et al. 2008; Zhang et al. 2016b). Thus, it is probable that MetS-induced reduction in liver function impaired the ability of the liver to remove AgNPs from the bloodstream, resulting in less efficient clearance and a higher proportion of AgNPs retained within the liver.

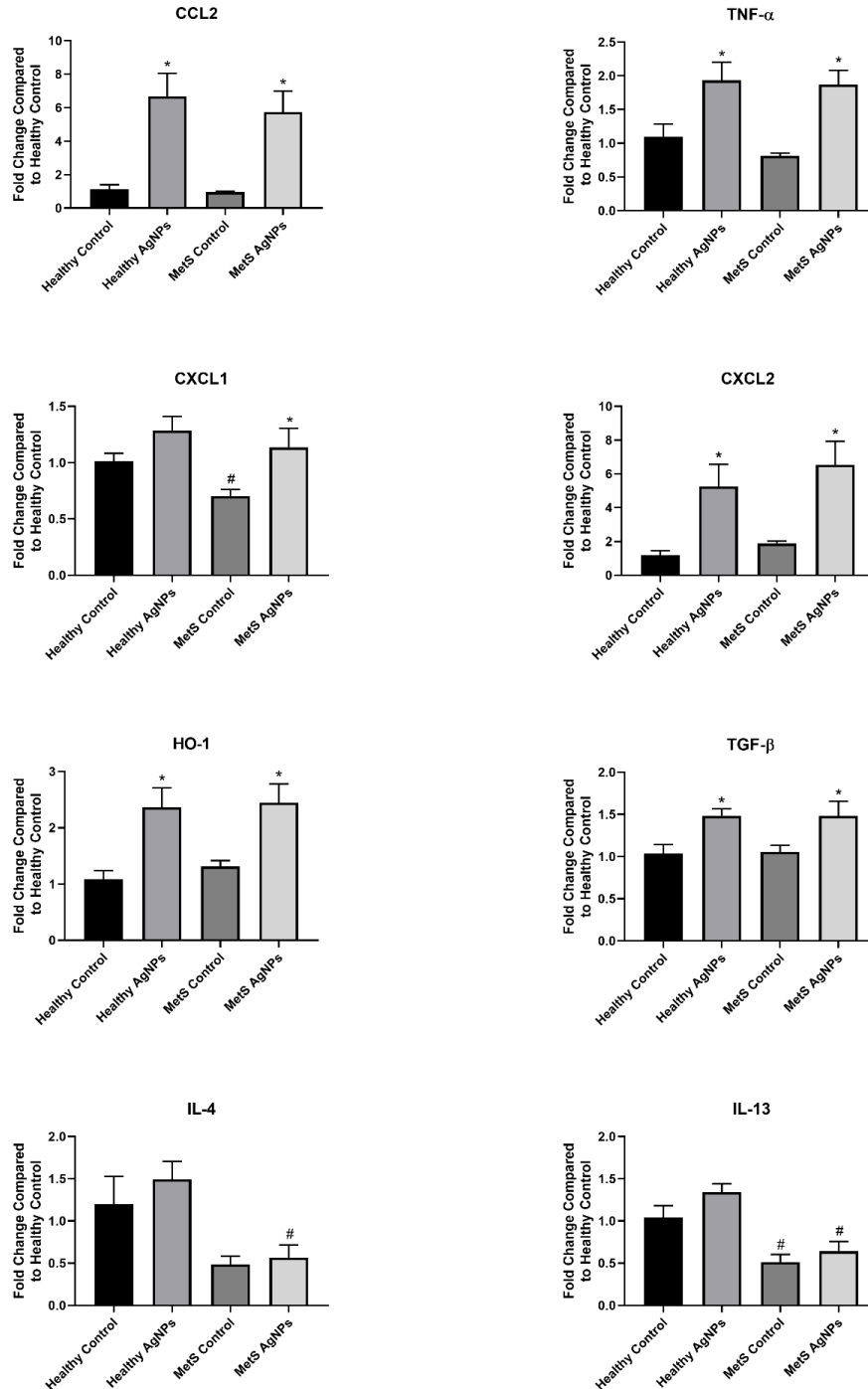


Figure 4.3. Changes in Gene Expression in the Liver Following Exposure to AgNPs in Healthy or MetS Mice. Gene expression of TNF- α , CCL2, CXCL1, CXCL2, HO-1, and TGF- β and GAPDH (control) was assessed through PCR to evaluate the inflammatory, pro-fibrotic, and oxidative stress responses induced by AgNP exposure. All analyses are reported as mean \pm SEM (n = 6-8 per group). * denotes statistical significance as compared to the corresponding untreated control group, and # denotes statistical significance as compared to the corresponding healthy group. Comparisons were performed by two-way ANOVA with Tukey post hoc analysis; p < 0.05.

Although a greater concentration of AgNPs was present in the liver of MetS compared to healthy mice, both models demonstrated a similar magnitude of inflammatory gene expression changes. This may be attributed to immune cells in MetS liver being less able to respond to an immune challenge than those of healthy mice, an assertion supported by (Wang et al. 2018), who showed that exhausted T cells maintain their phenotype even after repeated exposure to antigens. The apparent lack of altered expression of Th2 cytokines IL-4 and IL-13 in response to AgNP exposure may be easily understood in MetS mice, as those cytokines are produced primarily by T cells, which may be impaired due to disease (Rael and Lockey 2011; Rincón et al. 1997). However, the lack of expression of Th2 cytokines in healthy mice seems counter to previous findings, which have found slight elevation of IL-4 and IL-13 as a result of AgNP exposure (Chang et al. 2013; Park et al. 2010). These seemingly contradictory results may be attributed to the kinetics of AgNP elimination; specifically, the half-life of AgNPs in male mice has been reported to be approximately 15 hr, indicating that the mice in our study were able to go through almost two full half-lives between the time of exposure and necropsy (Xue et al. 2012). Further, previous investigations which have demonstrated increased expression of Th2 cytokines have been conducted in lungs and serum, but not liver. This, in combination with our data, indicates that the modest Th2 response which likely occurred in the healthy liver following exposure to AgNPs had already resolved by the time of necropsy and organ collection, yielding to a more Th1-dominant inflammatory response in the healthy mouse model.

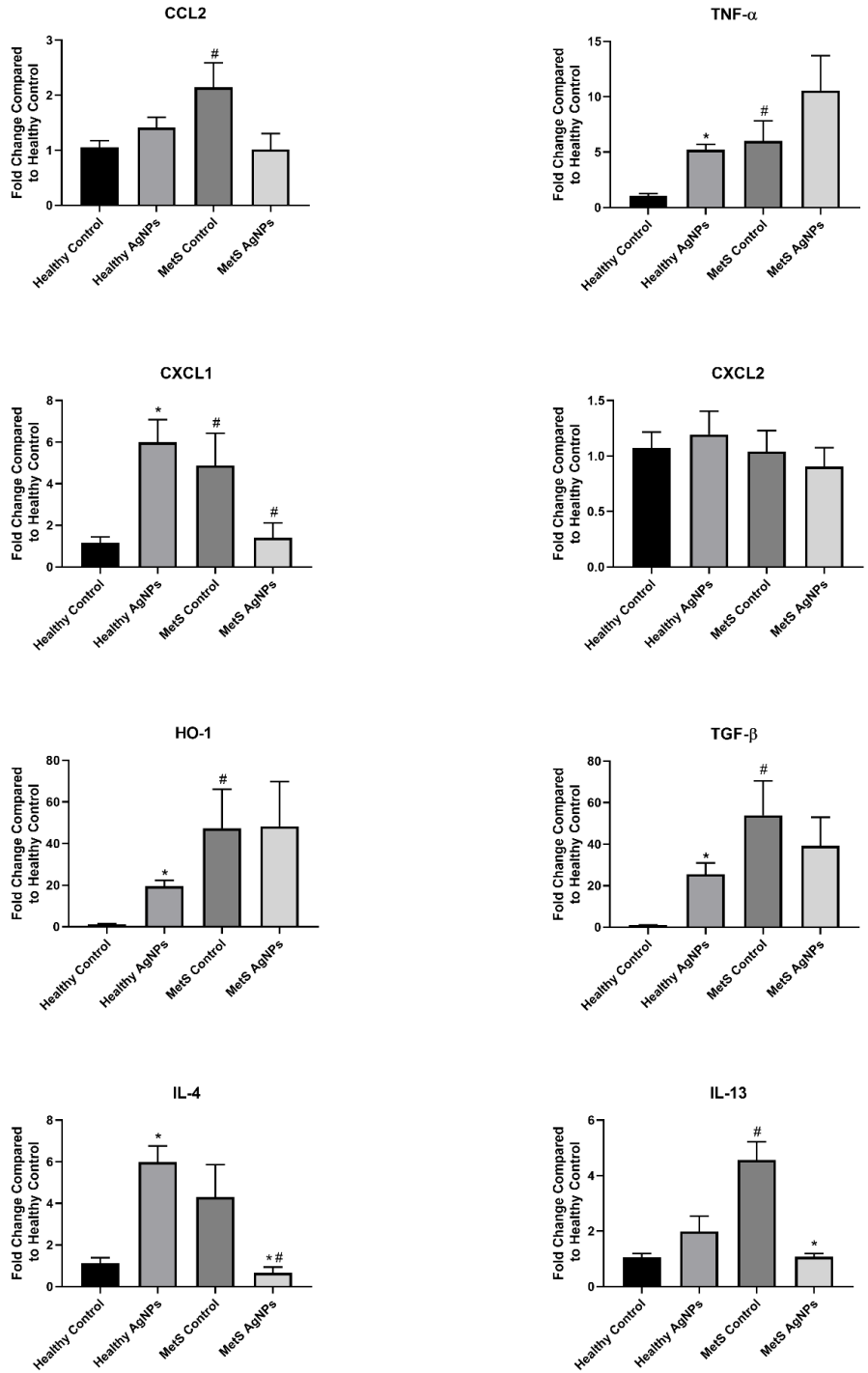


Figure 4.4. Changes in Gene Expression in the Spleen Following Exposure to AgNPs in Healthy or MetS Mice. Gene expression of TNF- α , CCL2, CXCL1, CXCL2, HO-1, and TGF- β and GAPDH (control) was assessed through PCR to evaluate the inflammatory, pro-fibrotic, and oxidative stress responses induced by AgNP exposure. All analyses are reported as mean \pm SEM (n = 6-8 per group). * denotes statistical significance as compared to the corresponding untreated control group, and # denotes statistical significance as compared to the corresponding healthy group. Comparisons were performed by two-way ANOVA with Tukey post hoc analysis; $p < 0.05$.

Following exposure to AgNPs, expression of all cytokines assessed in the spleen of the healthy mice was increased, with the exception of CXCL2. Previous investigations have demonstrated that AgNPs, upon entering the spleen, cause tissue damage and a loss of cellularity to the red pulp (Genter et al. 2012; Sardari et al. 2012). Further, intravenously and intranasally administered AgNPs have been found to elevate the level of T cells and macrophages within the spleen following exposure (Genter et al. 2012; Jong et al. 2013). Thus, it is probable that AgNPs entered the spleen through the circulation and caused damage to the red pulp, resulting in enhanced expression of TNF- α , CXCL1, HO-1, TGF- β , and IL-4. In the MetS group, the reaction of the spleen varied from that of healthy mice. In comparison to the unexposed group, CXCL2 and HO-1 remained unchanged, while IL-4 and IL-13 were reduced. Given the high degree of cytotoxicity of AgNPs to macrophages and T cells observed in in vitro studies, this drop in expression may be primarily attributed to the death of the cells which were previously producing cytokines (Eom and Choi 2010; Pratsinis et al. 2013). In addition, a portion of the immune cells within the spleen likely migrated to other areas of the body following AgNP exposure in an attempt to resolve the insult, further contributing to diminished cytokine expression (Haan and Kraal 2012). Taken together, this data indicates that differential immune responses in the spleen resulting from AgNP exposure may be attributed to MetS. The presence of MetS reduces immune responses from the spleen and impairs its ability to manage subsequent immune challenges.

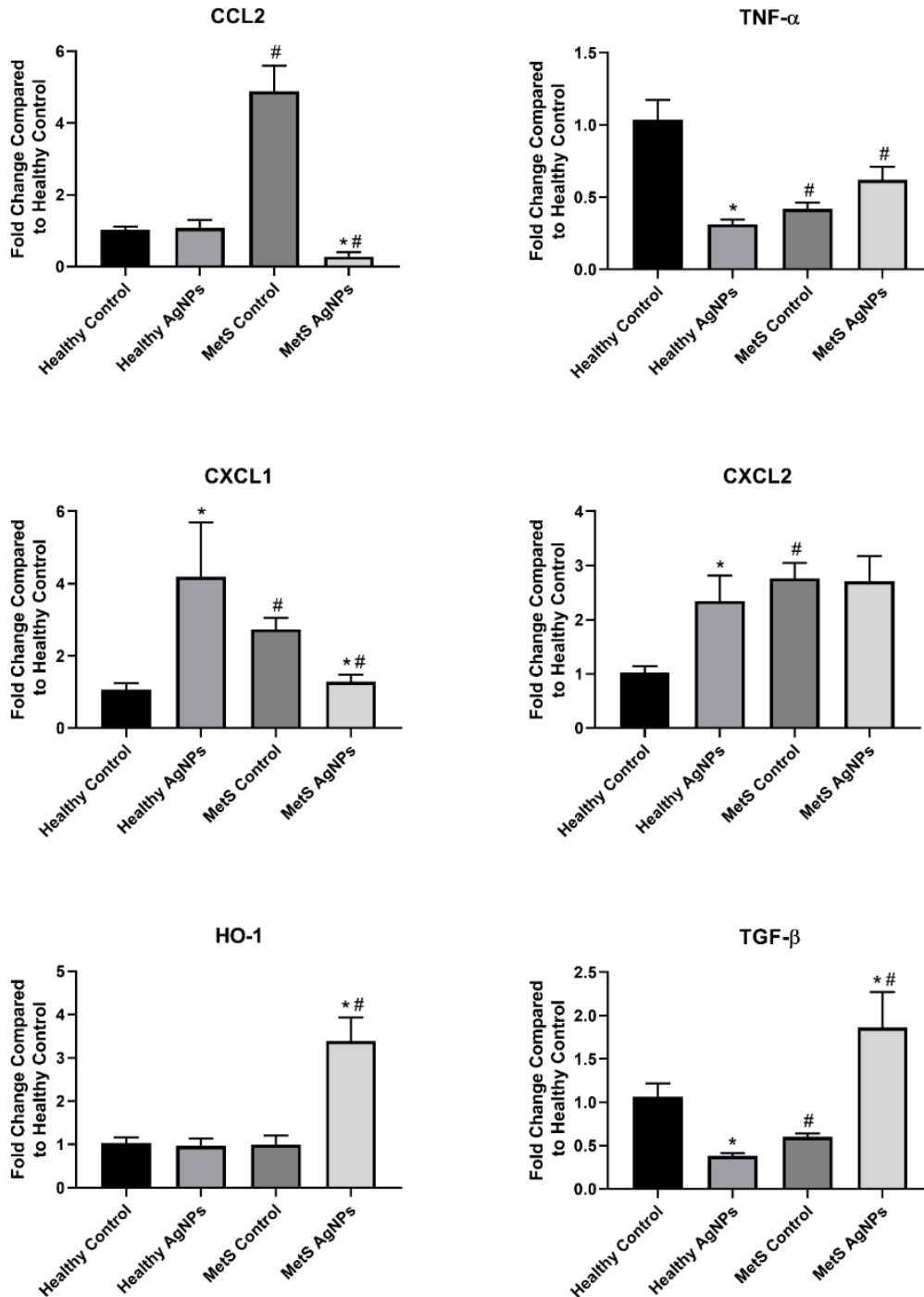


Figure 4.5. Changes in Gene Expression in the Kidney Following Exposure to AgNPs in Healthy or MetS Mice. Gene expression of TNF- α , CCL2, CXCL1, CXCL2, HO-1, and TGF- β and GAPDH (control) was assessed through PCR to evaluate the inflammatory, pro-fibrotic, and oxidative stress responses induced by AgNP exposure. All analyses are reported as mean \pm SEM (n = 6-8 per group). * denotes statistical significance as compared to the corresponding untreated control group, and # denotes statistical significance as compared to the corresponding healthy group. Comparisons were performed by two-way ANOVA with Tukey post hoc analysis; p<0.05.

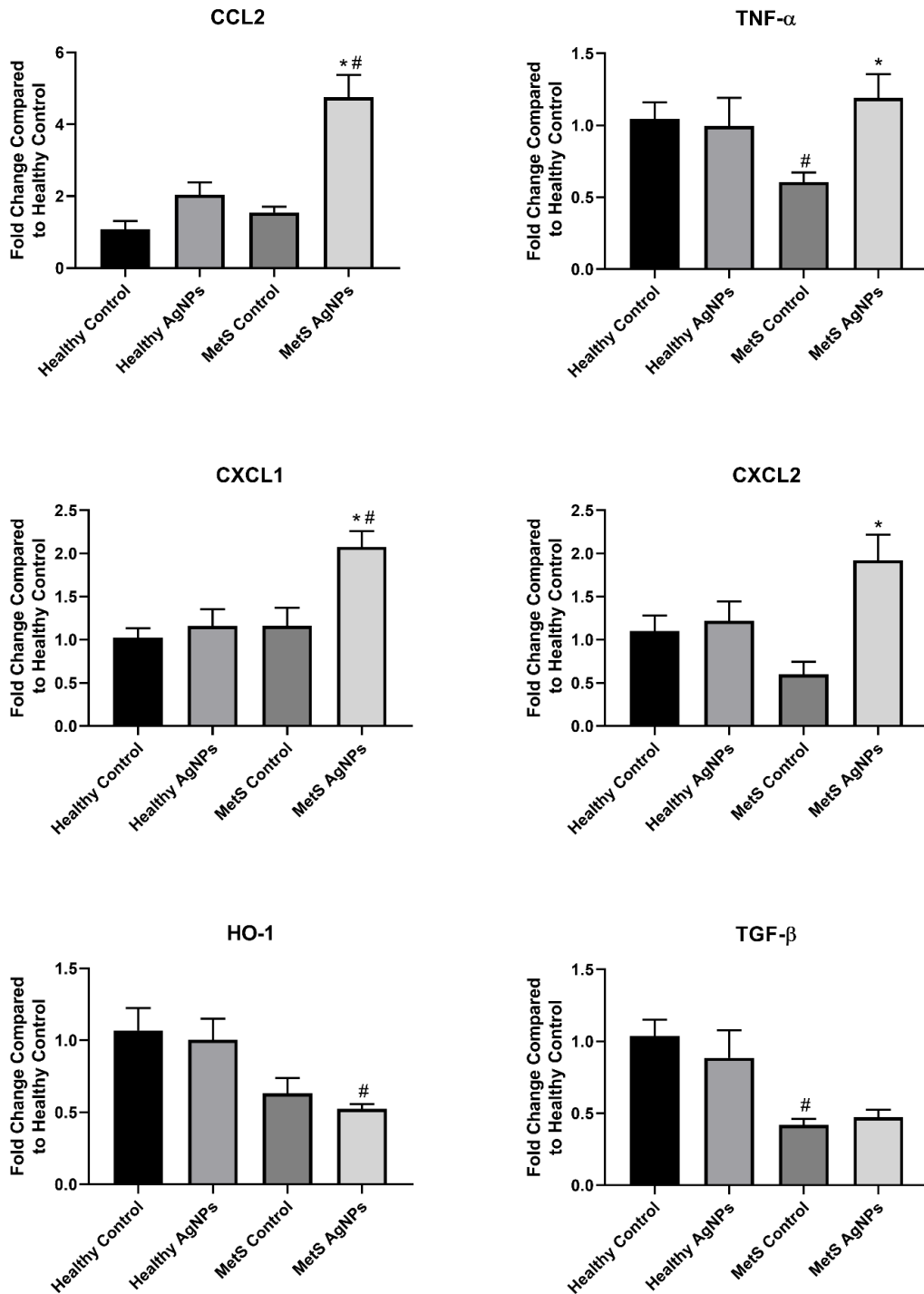


Figure 4.6. Changes in Gene Expression in the Heart Following Exposure to AgNPs in Healthy or MetS Mice. Gene expression of TNF- α , CCL2, CXCL1, CXCL2, HO-1, and TGF- β and GAPDH (control) was assessed through PCR to evaluate the inflammatory, pro-fibrotic, and oxidative stress responses induced by AgNP exposure. All analyses are reported as mean \pm SEM (n = 6-8 per group). * denotes statistical significance as compared to the corresponding untreated control group, and # denotes statistical significance as compared to the corresponding healthy group. Comparisons were performed by two-way ANOVA with Tukey post hoc analysis; $p < 0.05$.

Although the majority of Ag was identified in the spleen and liver of mice 24 hr following exposure, alterations in gene expression were observed in other organs with relatively minor accumulation such as the lungs, kidney, heart, and brain. Interestingly, the introduction of AgNPs into the healthy kidney altered cytokine expression such that its gene expression resembled that of a MetS kidney. This may be due to AgNPs inducing general inflammatory mechanisms similar to those enhanced due to MetS. This has been observed in other exposures; specifically, Gottipolu et al. (2009) noted that diesel exhaust inhalation has been shown to result in transcriptomic profiles in healthy rats similar to models of cardiovascular disease. Further, studies have demonstrated that exposures may contribute to the development and progression of chronic diseases (Anto et al. 2001; Chen, Goldberg, and Villeneuve 2008). Several investigations have also reported that individuals with preexisting diseases may be increasingly sensitive to exposures (Chen and Schwartz 2008; Devlin et al. 2014; Wagner et al. 2014). In our current study, MetS resulted in exacerbated induction of inflammatory genes in the heart that were not observed in healthy animals. This suggests that the cardiovascular system of individuals with MetS may be increasingly susceptible to the adverse responses associated with AgNP exposure. MetS is a risk factor for cardiovascular disease development. This enhanced inflammatory signaling may accelerate the progression of cardiovascular disease.

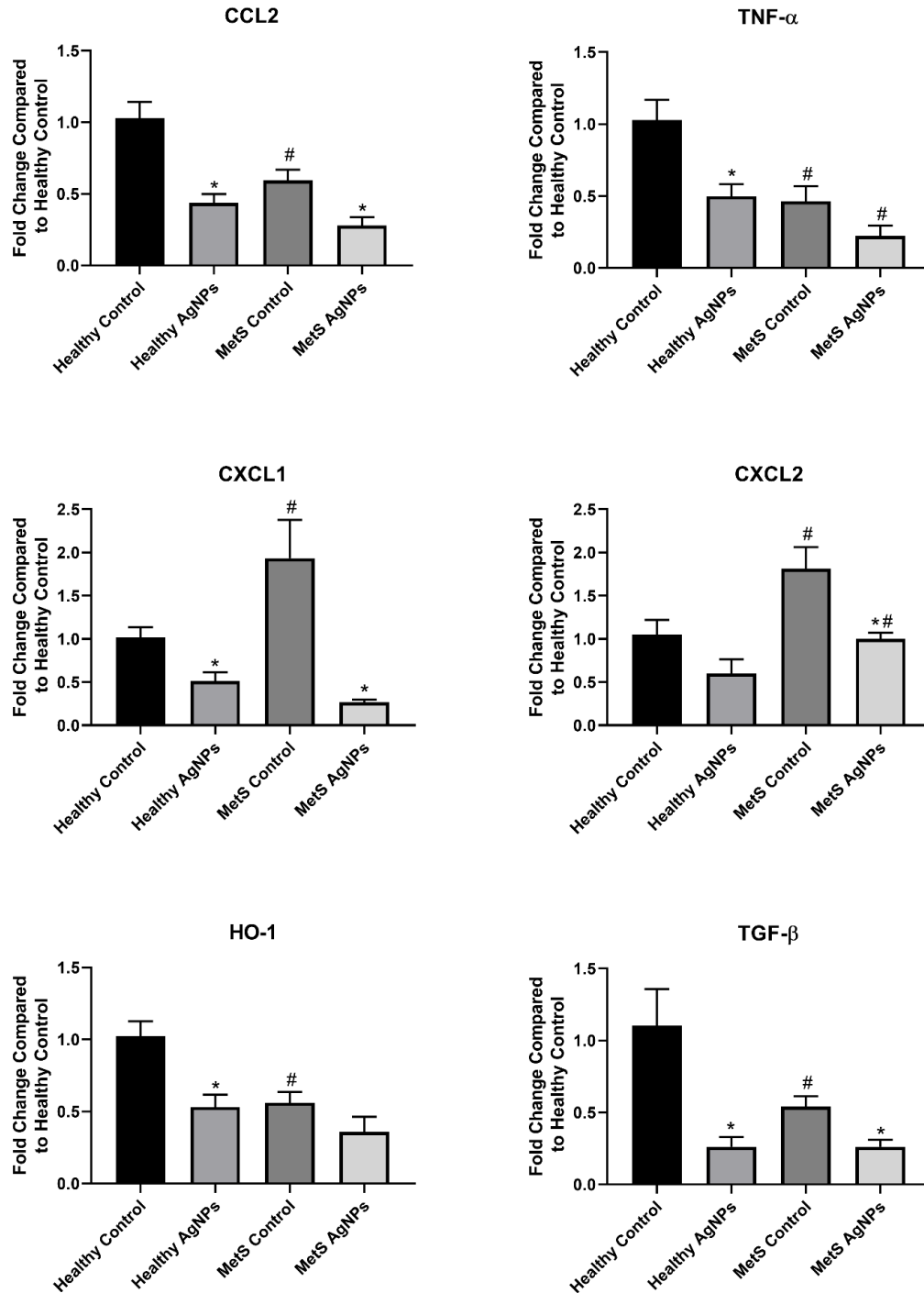


Figure 4.7. Changes in Gene Expression in the Lung Following Exposure to AgNPs in Healthy or MetS Mice. Gene expression of TNF- α , CCL2, CXCL1, CXCL2, HO-1, and TGF- β and GAPDH (control) was assessed through PCR to evaluate the inflammatory, pro-fibrotic, and oxidative stress responses induced by AgNP exposure. All analyses are reported as mean \pm SEM (n = 6-8 per group). * denotes statistical significance as compared to the corresponding untreated control group, and # denotes statistical significance as compared to the corresponding healthy group. Comparisons were performed by two-way ANOVA with Tukey post hoc analysis; $p < 0.05$.

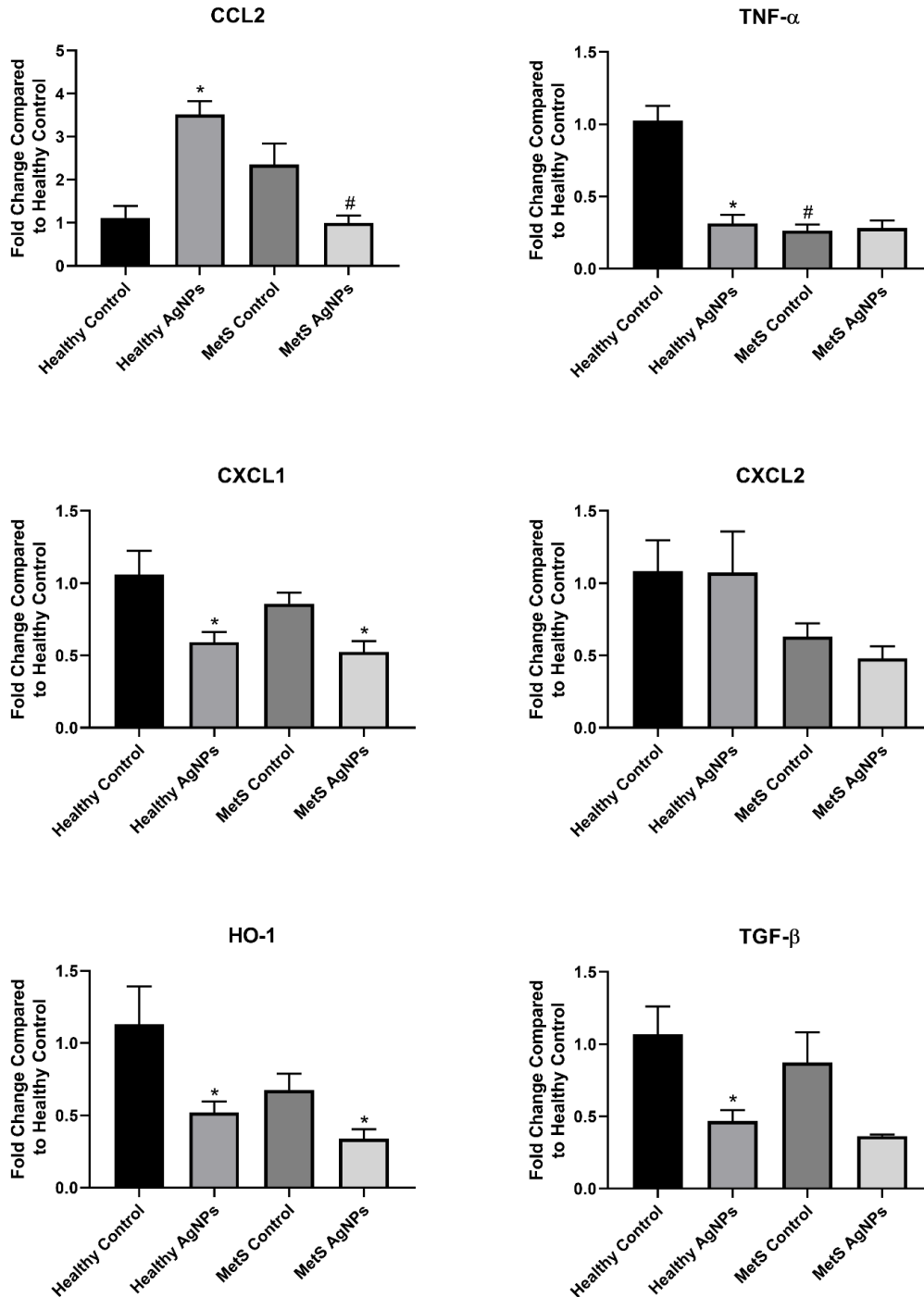


Figure 4.8. Changes in Gene Expression in the Brain Following Exposure to AgNPs in Healthy or MetS Mice. Gene expression of TNF- α , CCL2, CXCL1, CXCL2, HO-1, and TGF- β and GAPDH (control) was assessed through PCR to evaluate the inflammatory, pro-fibrotic, and oxidative stress responses induced by AgNP exposure. All analyses are reported as mean \pm SEM (n = 6-8 per group). * denotes statistical significance as compared to the corresponding untreated control group, and # denotes statistical significance as compared to the corresponding healthy group. Comparisons were performed by two-way ANOVA with Tukey post hoc analysis; $p < 0.05$.

As expected, the brain demonstrated the least accumulation of Ag 24 hr following injection in both models. However, AgNPs were determined to be present within the brain tissue as well as within the brain circulatory system. The presence of AgNPs within brain tissue is based upon a volume of 35–40 μl blood/g brain tissue and the mean measured concentration of Ag within blood (0.25 $\mu\text{g/g}$ for healthy and 0.39 $\mu\text{g/g}$ for the MetS mice), indicating crossing of the blood-brain barrier (Chugh et al. 2009). Expression of CCL2, a macrophage chemotactic gene, was elevated only in the healthy model. This indicates that MetS may decrease the ability of the brain to respond to challenges and exposures that require an immune response via the up-regulation of CCL2 and recruitment of macrophages. Other markers of inflammation and oxidative stress were reduced in the brain in response to AgNP exposure. Gonzalez-Carter et al. (2017) demonstrated that AgNPs reduce inflammation in microglia which have experienced an immune challenge. While the amount of AgNPs that accumulate in the brain is small, Lee et al. (2013) showed that AgNPs remain in the tissue for extended periods of time. This may indicate that exposures that result in AgNP deposition in the brain may initiate greater long-term effects than those observed in other organs.

The reductions in inflammatory gene expression observed in our study may inhibit brain immune responses to subsequent challenges. Interestingly, although less Ag was found to accumulate within the lung in MetS compared to healthy, similar decreases in inflammatory genes were noted following exposure. Inhalation of AgNPs has been demonstrated to induce an inflammatory response in healthy mouse models, suggesting variations in immune response within organs based upon the route of administration. Taken together, this data suggests that intravenously delivered AgNPs reduce the expression of a number of pro-inflammatory genes within the brain and lung of both healthy and MetS mice. In this study, differential alterations were observed between healthy and MetS mice in the expression of genes involved in inflammation, oxidative stress, and fibrosis, suggesting distinct susceptibility due to underlying disease. Further, biodistribution of AgNPs varies due to the presence of MetS.

While this study furthered our understanding of the toxicological impact of MetS on AgNP exposures, there is still much that remains unknown. Our study was not without limitations, as the results are specific to AgNPs within the circulation and may have limited applications to other

routes of administration, such as oral or inhalation exposure to AgNPs. In addition, our study examined only a single dose and time point, eliminating the possibility of identifying disease-induced differences in dose-response or biokinetics of AgNPs. Future studies are needed to assess alternate exposure routes, multiple time points, and a variety of doses following exposure to identify the disease-dependent variations in elimination rates of AgNPs and responses. Further, the effects of AgNPs on immunological cells in each organ require additional evaluation, particularly T cells and macrophages. Research into the toxicological impact of exposures such as AgNPs in diseased individuals is vital, as they represent a susceptible subpopulation.

4.6 References

- Aguilar, E. G., and W. J. Murphy. (2018). Obesity induced T cell dysfunction and implications for cancer immunotherapy. *Curr. Opin. Immunol.* 51:181–86. doi:10.1016/j.coi.2018.03.012.Obesity.
- Aguilar, M., T. Bhuket, S. Torres, B. Liu, and R. J. Wong. (2015). Prevalence of the metabolic syndrome in the United States, 2003-2012. *JAMA* 313 (19):1973–74. doi:10.1001/jama.2015.4260.
- Alaraby, M., B. Annangi, R. Marcos, and A. Hernández. (2016). *Drosophila melanogaster* as a suitable in vivo model to determine potential side effects of nanomaterials: A review. *J. Toxicol. Environ. Health B* 19:65–104. doi:10.1080/10937404.2016.1166466.
- Andersen, C. J., K. E. Murphy, and M. L. Fernandez. (2016). Impact of obesity and metabolic syndrome on immunity. *Adv. Nutr.* 7:66–75. doi:10.3945/an.115.010207.66.
- Anto, J. M., P. Vermeire, J. Vestbo, and J. Sunyer. (2001). Epidemiology of chronic obstructive pulmonary disease. *Eur. Respir. J.* 17:982–94. doi:10.1183/09031936.01.17509820.
- Beltrán-Sánchez, H., M. O. Harhay, M. M. Harhay, and S. McElligott. (2013). Prevalence and trends of metabolic syndrome in the adult US population, 1999–2010. *J. Am. Coll. Cardiol.* 62:697–703. doi:10.1016/j.jacc.2013.05.064.Prevalence.

- Benn, T., and B. Cavanagh. (2010). The release of nanosilver from consumer products used in the home. *J. Environ. Qual.* 39:1875–82. doi:10.2134/jeq2009.0363.
- Bergin, I. L., L. A. Wilding, M. Morishita, K. Walacavage, A. P. Ault, J. L. Axson, D. I. Stark, S. A. Hashway, S. S. Capracotta, P. R. Leroueil, et al. (2016). Effects of particle size and coating on toxicologic parameters, fecal elimination kinetics and tissue distribution of acutely ingested silver nanoparticles in a mouse model. *Nanotoxicology* 10:352–60. doi:10.3109/17435390.2015.1072588.
- Beyer, M., Z. Abdullah, J. M. Chemnitz, D. Maisel, J. Sander, C. Lehmann, Y. Thabet, P. V. Shinde, L. Schmidleithner, M. Köhne, et al. (2016). Tumor-necrosis factor impairs CD4 + T cell – Mediated immunological control in chronic viral infection. *Nat. Immunol.* 17:593–603. doi:10.1038/ni.3399.
- Bieghs, V., and C. Trautwein. (2013). The innate immune response during liver inflammation and metabolic disease. *Trends Immunol.* 34:446–52. doi:10.1016/j.it.2013.04.005.
- Buttorff, C., T. Ruder, and M. Bauman. (2017). Multiple chronic conditions in the United States. *Rand.* Online only. doi:10.7249/TL221
- Cao, K., J. Xu, X. Zou, Y. Li, C. Chen, A. Zheng, H. Li, H. Li, I. M.-Y. Szeto, Y. Shi, et al. (2014). Free radical biology and medicine hydroxytyrosol prevents diet-induced metabolic syndrome and attenuates mitochondrial abnormalities in obese mice. *Free Radical Biol. Med.* 67:396–407. doi:10.1016/j.freeradbiomed.2013.11.029.
- Chaloupka, K., Y. Malam, and A. M. Seifalian. (2010). Nanosilver as a new generation of nanoparticle in biomedical applications. *Trends Biotechnol.* 28:580–88. doi:10.1016/j.tibtech.2010.07.006.

- Chang, H., T. Hsiao, C. Wu, H. Chang, C. Lee, C. Chang, and T. Cheng. (2013). Allergenicity and toxicology of inhaled silver nanoparticles in allergen-provocation mice models. *Int. J. Nanomedicine* 8:4495–506. doi:10.2147/IJN.S52239.
- Chen, H., M. S. Goldberg, and P. J. Villeneuve. (2008). A systematic review of the relation between long-term exposure to ambient air pollution and chronic diseases. *Rev. Environ. Health*. 23:243–91. doi:10.1515/reveh.2008.23.4.243.
- Chen, J., and J. Schwartz. (2008). Metabolic syndrome and inflammatory responses to long-term particulate air pollutants. *Environ. Health Perspect.* 116:612–17. doi:10.1289/ehp.10565.
- Chen, R., L. Zhao, R. Bai, Y. Liu, L. Han, Z. Xu, F. Chen, H. Autrup, D. Long, and C. Chen. (2016). Silver nanoparticles induced oxidative and endoplasmic reticulum stresses in mouse tissues: Implications for the development of acute toxicity after intravenous administration. *Toxicol. Res. (Camb)* 1:602–08. doi:10.1039/c5tx00464k.
- Chugh, B. P., J. P. Lerch, L. X. Yu, M. Pienkowski, R. V. Harrison, R. M. Henkelman, and J. G. Sled. (2009). NeuroImage measurement of cerebral blood volume in mouse brain regions using micro-computed tomography. *NeuroImage* 47:1312–18. doi:10.1016/j.neuroimage.2009.03.083.
- Chugh, H., D. Sood, I. Chandra, V. Tomar, G. Dhawan, and R. Chandra. (2018). Role of gold and silver nanoparticles in cancer nano-medicine. *Artif. Cells Nanomed. Biotechnol.* 46:1210–20. doi:10.1080/21691401.2018.1449118.
- Cirillo, P., W. Sato, S. Reungjui, M. Heinig, M. Gersch, Y. Sautin, T. Nakagawa, and R. J. Johnson. (2006). Uric acid, the metabolic syndrome, and renal disease. *J. Am. Soc. Nephrol.* 17:165–68. doi:10.1681/ASN.2006080909.

Dabass, A., E. O. Talbott, J. R. Rager, G. M. Marsh, A. Venkat, F. Holguin, and R. K. Sharma. (2018). Systemic inflammatory markers associated with cardiovascular disease and acute and chronic exposure to fine particulate matter air pollution (PM_{2.5}) among US NHANES adults with metabolic syndrome. *Environ. Res.* 161:485–91.

doi:10.1016/j.envres.2017.11.042.

Desroches, S., and B. Lamarche. (2007). The evolving definitions and increasing prevalence of the metabolic syndrome. *Appl. Physiol. Nutr. Metab.* 32:23–32. doi:10.1139/H06-095.

Devlin, R. B., C. B. Smith, M. T. Schmitt, A. G. Rappold, A. Hinderliter, and D. Graff. (2014). Controlled exposure of humans with metabolic syndrome to concentrated ultrafine ambient particulate matter causes cardiovascular effects. *Toxicol. Sci.* 140:61–72.

doi:10.1093/toxsci/kfu063.

Dunn, K., and V. Edwards-Jones. (2004). The role of acticoat™ with nanocrystalline silver in the management of burns. *Burns* 30:S1–S9. doi:10.1016/j.burns.2004.06.000.

Dziendzikowska, K., J. Gromadzka-ostrowska, A. Lankoff, M. Oczkowski, A. Krawczy, J. Chwastowska, M. Sadowskabratek, E. Chajduk, M. Wojewódzka, and M. Du. (2012). Time-dependent biodistribution and excretion of silver nanoparticles in male wistar rats. *J App Toxicol.* 32:920–28. doi:10.1002/jat.2758.

Echegoyen, Y., and C. Nerín. (2013). Nanoparticle release from nano-silver antimicrobial food containers. *Food Chem. Toxicol.* 62:16–22. doi:10.1016/j.fct.2013.08.014.

Eom, H., and J. Choi. (2010). P38 MAPK activation, DNA damage, cell cycle arrest and apoptosis as mechanisms of toxicity of silver nanoparticles in jurkat T cells. *Environ. Sci. Technol.* 44:8337–42. doi:10.1021/es1020668.

- Esser, N., S. Legrand-poels, J. Piette, J. Scheen, and N. Paquot. (2014). Inflammation as a link between obesity, metabolic syndrome and type 2 diabetes. *Diabetes Res. Clin. Pract.* 105:141–50. doi:10.1016/j.diabres.2014.04.006.
- Ford, E. S., W. H. Giles, and A. H. Mokdad. (2004). Increasing prevalence of the metabolic syndrome among U.S adults. *Diabetes Care* 27:2444–49. doi:10.2337/diacare.27.10.2444.
- Galassi, A., K. Reynolds, and J. He. (2006). Metabolic syndrome and risk of cardiovascular disease: A meta-analysis. *Am. J. Med.* 119:812–19. doi:10.1016/j.amjmed.2006.02.031.
- Ge, L., Q. Li, M. Wang, J. Ouyang, X. Li, and M. Q. M. Xing. (2014). Nanosilver particles in medical applications: Synthesis, performance, and toxicity. *Int. J. Nanomedicine* 9:2399–407. doi:10.2147/IJN.S55015.
- Genter, M. B., N. C. Newman, S. G. Howard, S. F. Ali, and B. Bolton. (2012). Distribution and systemic effects of intranasally administered 25 nm silver nanoparticles in adult mice. *Toxicol. Pathol.* 40:1004–13. doi:10.1177/0192623312444470.
- Gonzalez-Carter, D. A., B. F. Leo, P. Ruenraroengsak, S. Chen, A. E. Goode, I. G. Theodorou, K. F. Chung, R. Carzaniga, M. S. P. Shaffer, D. T. Dexter, et al. (2017). Silver nanoparticles reduce brain inflammation and related neurotoxicity through induction of H₂S-synthesizing enzymes. *Sci. Rep.* 7:1–14. doi:10.1038/srep42871.
- Gottipolu, R. R., J. G. Wallenborn, E. D. Karoly, M. C. Schladweiler, A. D. Ledbetter, T. Krantz, W. P. Linak, A. Nyska, J. A. Johnson, R. Thomas, et al. (2009). One-month diesel exhaust inhalation produces hypertensive gene expression pattern in healthy rats. *Environ. Health Perspect.* 117:38–46. doi:10.1289/ehp.11647.
- Green, W. D., and M. A. Beck. (2017). Obesity altered T cell metabolism and the response to infection. *Curr. Opin. Immunol.* 46:1–7. doi:10.1016/j.coi.2017.03.008.

- Grundy, S. M. (2006). Metabolic syndrome: Connecting and reconciling cardiovascular and diabetes worlds. *J. Am. Coll. Cardiol.* 47:1093–100. doi:10.1016/j.jacc.2005.11.046.
- Haan, J. M. M. D., and G. Kraal. (2012). Innate immune functions of macrophage subpopulations in the spleen. *J. Innate Immun.* 4:437–45. doi:10.1159/000335216.
- Haase, A., J. Tentschert, H. Jungnickel, P. Graf, A. Manton, F. Draude, J. Plandl, M.E. Goetz, S. Galla, A. Mašić. (2011). Toxicity of silver nanoparticles in human macrophages: Uptake, intracellular distribution and cellular responses. *J. Phys. Conf. Ser.* 304:1–14. doi:10.1088/1742-6596/304/1/012030.
- Hackenberg, S., A. Scherzed, M. Kessler, S. Hummel, A. Technau, K. Froelich, C. Ginzkey, C. Koehler, R. Hagen, and N. Kleinsasser. (2011). Silver nanoparticles: Evaluation of DNA damage, toxicity and functional impairment in human mesenchymal stem cells. *Toxicol. Lett.* 201:27–33. doi:10.1016/j.toxlet.2010.12.001.
- Haffner, S. M. (2006). The metabolic syndrome: Inflammation, diabetes mellitus, and cardiovascular disease. *Am. J. Cardiol.* 97:2–11. doi:10.1016/j.amjcard.2005.11.010.
- Halpin, H. A., M. M. Morales-suárez-varela, and J. M. Martin-moreno. (2010). Chronic disease prevention and the new public health. *Public Health Rev.* 32:120–54. doi:10.1007/BF03391595.
- Isomaa, B., P. Almgren, T. Tuomi, B. Forsen, K. Lahti, M. Nissen, M. Taskinen, and L. Groop. (2001). Cardiovascular morbidity and mortality associated with the metabolic syndrome. *Diabetes Care* 24:683–89. doi:10.2337/diacare.24.4.683.
- Javidi, J., A. Haeri, F. Nowroozi, and S. Dadashzadeh. (2019). Pharmacokinetics, tissue distribution and excretion of Ag₂S quantum dots in mice and rats: The effects of injection dose, particle size and surface charge. *Pharm. Res.* 36:1–16. doi:10.1007/s11095-019-2571-1.

- Johanson, G., and U. Carlander. (2016). Uptake and biodistribution of nanoparticles—a review. *Kemi Swedish Chemicals Agency*.
- Jong, W. H. D., L. T. M. Van Der Ven, A. Sleijffers, M. V. D. Z. Park, E. H. J. M. Jansen, H. Van Loveren, and R. J. Vandebriel. (2013). Biomaterials systemic and immunotoxicity of silver nanoparticles in an intravenous 28 days repeated dose toxicity study in rats. *Biomaterials* 34:8333–43. doi:10.1016/j.biomaterials.2013.06.048.
- Kaweeterawat, C., P. N. Ubol, S. Sangmuang, S. Aueviriyavit, and R. Maniratanachote. (2017). Mechanisms of antibiotic resistance in bacteria mediated by silver nanoparticles. *J. Toxicol. Environ. Health A* 80:1276–89. doi:10.1080/15287394.2017.1376727.
- Kennedy, A. J., K. L. J. Ellacott, V. L. King, and A. H. Hasty. (2010). Mouse models of the metabolic syndrome. *Dis. Model. Mech.* 3:156–66. doi:10.1242/dmm.003467.
- Kermanizadeh, A., I. Gosens, L. MacCalman, H. Johnston, P. H. Danielsen, N. R. Jacobsen, A.-G. Lenz, T. Frenandes, R. Scins, F. R. Cassee, et al. (2016.) A multilaboratory toxicological assessment of a panel of 10 engineered nanomaterials to human health- the highlights, limitations, and current and future challenges. *J. Toxicol. Environ. Health B* 19:1–28. doi:10.1080/10937404.2015.1126210.
- Kim, C. H., and Z. M. Younossi. (2008). Nonalcoholic fatty liver disease: A manifestation of the metabolic syndrome. *Cleve Clin. J. Med.* 74:721–28. doi:10.3949/ccjm.75.10.721.
- Lam, P. K., E. S. Y. Chan, W. S. Ho, and C. T. Liew. (2004). In vitro cytotoxicity testing of a nanocrystalline silver dressing (acticoat) on cultured keratinocytes. *Br. J. Biomed. Sci.* 61:125–27. doi:10.1080/09674845.2004.11732656.
- Lee, C. L. D., S. B. Fashir, M. L. Castilho, M. A. Hupman, L. J. Raniero, I. Alwayn, and K. C. Hewitt. (2016). Epidermal growth factor receptor-specific nanoprobe biodistribution in mouse models. *J. Pharm. Sci.* 105:25–30. doi:10.1016/j.xphs.2015.10.005.

- Lee, J. H., Y. S. Kim, K. S. Song, H. R. Ryu, J. H. Sung, J. D. Park, H. M. Park, N. Song, B. Shin, D. Marshak, et al. (2013). Biopersistence of silver nanoparticles in tissues from sprague–dawley rats. *Part Fibre Toxicol.* 10:1–14. doi:10.1186/1743-8977-10-36.
- Lteif, A. A., K. Han, and K. J. Mather. (2005). Obesity, insulin resistance, and the metabolic syndrome determinants of endothelial dysfunction in whites and blacks. *Circulation* 112:32–38. doi:10.1161/CIRCULATIONAHA.104.520130.
- Mahdy, M. M. E., T. A. S. Ahmed, H. S. Aly, F. F. Mohammed, and M. I. Shaalan. (2014). Evaluation of hepatotoxic and genotoxic potential of silver nanoparticles in albino rats. *Exp. Toxicol. Pathol.* 67:21–29. doi:10.1016/j.etp.2014.09.005.
- Martins, A. C., Jr, L. F. Azevedo, C. C. S. Rocha, M. F. H. Carneiro, V. P. Venancio, M. R. Almeida, L. M. G. Antunes, R. C. Hott, J. L. Rodrigues, A. T. Ogunjimi, et al. (2017). Evaluation of distribution, redox parameters, and genotoxicity in wistar rats co-exposed to silver and titanium dioxide nanoparticles. *J. Toxicol. Environ. Health A* 80:1156–65. doi:10.1080/15287394.2017.1357376.
- Meng, J., Y. Ji, J. Liu, X. Cheng, H. Guo, W. Zhang, X. Wu, and H. Xu. (2014). Using gold nanorods core/silver shell nanostructures as model material to probe biodistribution and toxic effects of silver nanoparticles in mice. *Nanotoxicology* 8:686–96. doi:10.3109/17435390.2013.822593.
- Paddle-Ledinek, J. E., Z. Nasa, and H. J. Cleland. (2006). Effect of different wound dressings on cell viability and proliferation. *Plast. Reconstr. Surg.* 117:110S–118S. doi:10.1097/01.prs.0000225439.39352.ce.
- Paoletti, R., C. Bolego, A. Poli, and A. Cignarella. (2006). Metabolic syndrome, inflammation and atherosclerosis. *Vasc. Health Risk Manag.* 2:145–52. doi:10.2147/vhrm.2006.2.2.145.

- Park, E., E. Bae, J. Yi, Y. Kim, K. Choi, S. Hee, J. Yoon, B. Chun, and K. Park. (2010). Repeated-dose toxicity and inflammatory responses in mice by oral administration of silver nanoparticles. *Environ. Toxicol. Pharmacol.* 30:162–68. doi:10.1016/j.etap.2010.05.004.
- Park, K., and Y. Lee. (2013). The stability of citrate-capped silver nanoparticles in isotonic glucose solution for intravenous injection. *J. Toxicol. Environ. Health A* 76:1236–45. doi:10.1080/15287394.2013.849215.
- Park, M. V. D. Z., A. M. Neigh, J. P. Vermeulen, L. J. J. De, H. W. Verharen, J. J. Briedé, H. Van Loveren, and W. H. De Jong. (2011). The effect of particle size on the cytotoxicity, inflammation, developmental toxicity and genotoxicity of silver nanoparticles. *Biomaterials* 32:9810–17. doi:10.1016/j.biomaterials.2011.08.085.
- Pettersson, U. S., T. B. Walde, P. Carlsson, L. Jansson, and M. Phillipson. (2012). Female mice are protected against high-fat diet induced metabolic syndrome and increase the regulatory T cell population in adipose tissue. *PLoS ONE* 7:1–10. doi:10.1371/journal.pone.0046057.
- Poon, V. K. M., and A. Burd. (2004). In vitro cytotoxicity of silver: Implication for clinical wound care. *Burns* 30:140–47. doi:10.1016/j.burns.2003.09.030.
- Pou, K. M., J. M. Massaro, U. Hoffman, K. Lieb, R. S. Vasan, C. J. O'Donnell, and C. S. Fox. (2009). Patterns of abdominal fat distribution. *Diabetes Care* 32:481–85. doi:10.2337/dc08-1359.
- Pratsinis, A., P. Hervella, J. Leroux, and S. E. Pratsinis. (2013). Toxicity of silver nanoparticles in macrophages. *Small* 9:2576–84. doi:10.1002/smll.201202120.
- Rael, E. L., and R. F. Lockey. (2011). Interleukin-13 signaling and its role in asthma. *World Allergy Organ. J.* 4:54–64. doi:10.1097/WOX.0b013e31821188e0.

- Rahman, M. F., J. Wang, T. A. Patterson, U. T. Saini, B. L. Robinson, G. D. Newport, R. C. Murdock, J. J. Schlager, S. M. Hussain, and S. F. Ali. (2009). Expression of genes related to oxidative stress in the mouse brain after exposure to silver-25 nanoparticles. *Toxicol. Lett.* 187:15–21. doi:10.1016/j.toxlet.2009.01.020.
- Ramadi, K. B., Y. A. Mohamed, A. Al-sbiei, S. Almarzooqi, G. Bashir, A. Al-Dhanhani, D. Sarawathiamma, S. Qadri, J. Yasin, A. Nemmar, et al. (2016). Acute systemic exposure to silver-based nanoparticles induces hepatotoxicity and NLRP3-dependent inflammation. *Nanotoxicology* 10:1061–74. doi:10.3109/17435390.2016.1163743.
- Rector, R. S., J. P. Thyfault, Y. Wei, and J. A. Ibdah. (2008). Non-alcoholic fatty liver disease and the metabolic syndrome: An update. *World J. Gastroenterol.* 14:185–92. doi:10.3748/wjg.14.185.
- Rincón, B. M., J. Anguita, T. Nakamura, E. Fikrig, and R. A. Flavell. (1997). Interleukin (IL)-6 directs the differentiation of IL-4–producing CD4+ T cells. *J. Exp. Med.* 185:461–70. doi:10.1084/jem.185.3.461.
- Roberts, C. K., A. L. Hevener, and R. J. Barnard. (2013). Metabolic syndrome and insulin resistance: Underlying causes and modification by exercise training. *Compr. Physiol.* 3:1–58. doi:10.1002/cphy.c110062.Metabolic.
- Rosario, F., P. Hoet, A. J. A. Nogueira, C. Santos, and H. Oliveira. (2018). Differential pulmonary in vitro toxicity of two small-sized polyvinylpyrrolidone-coated silver nanoparticles. *J. Toxicol. Environ. Health A* 81:675–90. doi:10.1080/15287394.2018.1468837.

- Sanchez-Guzman, D., P. Le, B. Villeret, N. Sola, R. Le, A. Guyard, A. Kemmel, B. Crestani, J. Sallenave, and I. Garcia-verdugo. (2019). Biomaterials silver nanoparticle-adjuvanted vaccine protects against lethal influenza infection through inducing BALT and IgA-mediated mucosal immunity. *Biomaterials* 217:1–14.
doi:10.1016/j.biomaterials.2019.119308.
- Sardari, R. R. R., S. R. Zarchi, A. Talebi, S. Nasri, S. Imani, A. Khoradmehr, and S. A. R. Sheshde. (2012). Toxicological effects of silver nanoparticles in rats. *Afr. J. Microbiol. Res.* 6:5587–93. doi:10.5897/AJMR11.1070.
- Snyder, R. W., T. R. Fennell, C. J. Wingard, N. P. Mortensen, N. A. Holland, J. H. Shannahan, W. Pathmasiri, A. H. Lewin, and S. C. J. Sumner. (2016). Distribution and biomarker of carbon-14 labeled fullerene C60 ([¹⁴C(U)]C60) in pregnant and lactating rats and their offspring after maternal intravenous exposure. *J App Toxicol.* 35:1438–51.
doi:10.1002/jat.3177.Distribution.
- Song, J. Y., and B. S. Kim. (2009). Rapid biological synthesis of silver nanoparticles using plant leaf extracts. *Bioprocess Biosyst. Eng.* 32:79–84. doi:10.1007/s00449-008-0224-6.
- Sumner, S. C. J., R. W. Snyder, C. Wingard, N. P. Mortensen, N. A. Holland, J. H. Shannahan, S. Dhungana, W. Pathmasiri, A. H. Lewin, and T. R. Fennell. (2016). Distribution and biomarkers of carbon-14 labeled fullerene C60 ([¹⁴C(U)]C60) in female rats and mice for up to 30 days after intravenous exposure. *J App Toxicol.* 35:1452–64.
doi:10.1002/jat.3110.Distribution.
- Sun, B., and M. Karin. (2012). Obesity, inflammation, and liver cancer. *J. Hepatol.* 56:704–13.
doi:10.1016/j.jhep.2011.09.020.
- Taha, E., F. Djouider, and E. Banoqitah. (2019). Monte Carlo simulation of dose enhancement due to silver nanoparticles implantation in brain tumor brachytherapy using a digital phantom. *Radiat. Phys. Chem.* 156:15–21. doi:10.1016/j.radphyschem.2018.10.027.

- Takenaka, S., E. Karg, C. Roth, H. Schulz, A. Ziesenis, U. Heinzmann, P. Schramel, and J. Heyder. (2001). Pulmonary and systemic distribution of inhaled ultrafine silver particles in rats. *Environ. Health Perspect.* 109:547–51. doi:10.1289/ehp.01109s4547.
- Tang, J., L. Xiong, S. Wang, J. Wang, L. Liu, J. Li, Z. Wan, and T. Xi. (2008). Influence of silver nanoparticles on neurons and blood-brain barrier via subcutaneous injection in rats. *Appl. Surf. Sci.* 255:502–04. doi:10.1016/j.apsusc.2008.06.058.
- Tang, J., L. Xiong, S. Wang, J. Wang, L. Liu, L. Jiage, F. Yuan, and X. Tingfei. (2009). Distribution, translocation and accumulation of silver nanoparticles in rats. *J. Nanosci. Nanotechnol.* 9:4924–32. doi:10.1166/jnn.2009.1269.
- Tran, Q. H., V. Q. Nguyen, and A. Le. (2013). Silver nanoparticles: Synthesis, properties, toxicology, applications and perspectives. *Adv. Nat. Sci.: Nanosci. Nanotechnol.* 4:1–20.
- Trickler, W. J., S. M. Lantz, R. C. Murdock, A. M. Schrand, B. L. Robinson, G. D. Newport, J. J. Schlager, S. J. Oldenburg, M. G. Paule, W. Slikker, et al. (2010). Silver nanoparticle induced blood-brain barrier inflammation and increased permeability in primary rat brain microvessel endothelial cells. *Toxicol. Sci.* 118:160–70. doi:10.1093/toxsci/kfq244.
- Wagner, J. G., K. Allen, H. Yang, B. Nan, M. Morishita, and B. Mukherjee. (2014). Cardiovascular depression in rats exposed to inhaled particulate matter and ozone: Effects of diet-induced metabolic syndrome. *Environ. Health Perspect.* 122:27–33. doi:10.1289/ehp.1307085.
- Wang, Q., W. Pan, Y. Liu, J. Luo, D. Zhu, Y. Lu, X. Feng, J. P. Gigley, and M. A. Franco. (2018). Hepatitis B virus-specific CD8+ T cells maintain functional exhaustion after antigen reexposure in an acute activation immune environment. *Front. Immunol.* 9:1–14. doi:10.3389/fimmu.2018.00219.

- Wang, Z., E. G. Aguilar, J. I. Luna, C. Dunai, L. T. Khuat, C. T. Le, A. Mirsoian, C. M. Minnar, K. M. Stoffel, I. R. Sturgill, et al. (2019). Function during tumor progression and PD-1 checkpoint blockade. *Nat. Med.* 25:141–51. doi:10.1038/s41591-018-0221-5.
- Watanabe, S., R. Yaginuma, K. Ikejima, and A. Miyazaki. (2008). Liver diseases and metabolic syndrome. *J. Gastroenterol.* 43:509–18. doi:10.1007/s00535-008-2193-6.
- Wherry, E. J. (2011). T cell exhaustion. *Nat. Immunol.* 12:6–13. doi:10.1038/ni.2035.
- Wherry, E. J., and M. Kurachi. (2015). Molecular and cellular insights into T cell exhaustion. *Nat. Rev. Immunol.* 15:486–99. doi:10.1038/nri3862.
- Xue, Y., S. Zhang, Y. Huang, T. Zhang, X. Liu, Y. Hu, Z. Zhang, and M. Tang. (2012). Acute toxic effects and gender-related biokinetics of silver nanoparticles following an intravenous injection in mice. *J App Toxicol.* 32:890–99. doi:10.1002/jat.2742.
- Yang, L., H. Kuang, W. Zhang, Z. P. Aguilar, H. Wei, and H. Xu. (2017). Comparisons of the biodistribution and toxicological examinations after repeated intravenous administration of silver and gold nanoparticles in mice. *Sci. Rep.* 7:1–12. doi:10.1038/s41598-017-03015-1.
- Zande, M. V. D., R. J. Vandebriel, E. V. Doren, E. Kramer, Z. H. Rivera, C. S. Serrano-rojero, E. R. Gremmer, J. Mast, R. J. Peters, P. C. Hollman. (2012). Distribution, elimination, and toxicity of silver nanoparticles and silver ions in rats after 28-day oral exposure. *ACS Nano* 6:7427–42. doi:10.1021/nn302649p.
- Zhang, X., Z. Liu, W. Shen, and S. Gurunathan. (2016a). Silver nanoparticles: Synthesis, characterization, properties, applications, and therapeutic approaches. *Int. J. Mol. Sci.* 17:1534. doi:10.3390/ijms17091534.

Zhang, Y., W. Poon, A. J. Tavares, I. D. Mcgilvray, and W. C. W. Chan. (2016b). Nanoparticle–liver interactions: Cellular uptake and hepatobiliary elimination. *J. Cont. Rel.* 240:332–48. doi:10.1016/j.jconrel.2016.01.02.

CHAPTER 5. CONCLUSION

The research described here was performed with the intent of identifying and describing differential toxicity in diseased conditions as a result of exposure to biomedically relevant nanoparticles (NPs). Specifically, we hypothesized that obesity, high cholesterol, and metabolic syndrome (MetS) would cause differences in the quantities and varieties of biomolecules adsorbed to the NP surface, which would result in exacerbated adverse reactions to medically relevant NPs. Prior to the completion of the research, it was unknown if the composition of the biocorona (BC) varied between healthy and diseased conditions, or between individual human subjects. Further, it was unknown how this variation in the BC impacted the cellular and organismal reactions to NP exposure. This lack of knowledge hindered the development, translation, and safe clinical use of NPs in biomedical applications. To address these gaps in the existing scientific knowledge and further the progression of science and medicine, a study was performed which was divided into several aims.

5.1 Overall Conclusions and the Future of NP Therapeutics in Medicine

Taken together, these studies demonstrate that both individual variability and disease alter the BC, and that these alterations have toxicological consequences which may ultimately impact NP utilization in biomedical applications. Specifically, common diseases including obesity, high cholesterol, and MetS cause changes to the composition of the physiological environment, which subsequently translate to changes to the identities and quantities of biomolecules in the NP BC. NPs in diseased conditions appear to accumulate BC proteins in a largely abundance-driven manner, i.e., NPs in a high cholesterol environment will accumulate more cholesterol and cholesterol-associated biomolecules. The differences observed between the healthy and diseased BCs are highly consequential, as they cause distinct cellular and organismal immune and inflammatory responses. This indicates that the current toxicity testing of NPs and NP therapeutics is wholly inadequate at representing the risk faced by a significant and growing proportion of the population which suffers from some form of chronic disease. By testing NPs only in conditions in which a healthy BC is formed, or worse still, no BC at all, the information gained is incomplete and difficult to translate. It is necessary to utilize both healthy and unhealthy models to accurately

reflect the conditions in which NP therapeutics will be used, such that the safety and efficacy of proposed treatments may be properly assessed. By identifying differences which exist between subpopulations in BC composition and immune responses, medical professionals and engineers may take these variations into consideration when applying or designing NP therapeutics for use by the general public, leading to increased potential for utilization in individuals or groups with unique biomolecular profiles such that a larger number of patients may experience the benefits of medical nanotechnology.

However, further development of the technology is needed before NP therapeutics may be utilized to their full potential. While the unique properties of NPs mean that they have the capacity to vastly improve the quality of care in biomedicine, more information is needed to maximize their safety and efficacy. Specifically, the described research may be continued and expanded, because while the above research and the conclusions of such are robust, there remains much which is unknown, such as the details and mechanisms of preferential biomolecular adsorption. While our research has definitively shown that certain biomolecules preferentially associate with NPs due to certain properties, the precise process by which this occurs is not fully understood. NP properties such as charge and surface curvature are known to influence biomolecular association, but it is yet to be examined in detail how precise modifications may cause preferential adsorption of certain molecules or classes of molecules to the NP surface (Neagu, Piperigkou, Karamanou, & Engin, 2017; Walkey, Olsen, Guo, Emili, & Chan, 2012). However, a number of studies have examined NP properties in relation to biomolecular association and determined specific factors which influence interactions. For example, the aromatic groups on the surface of carbon nanomaterials have been shown to alter protein binding by interacting with the amine groups in proteins (Bradley, Briman, Star, & Gru, 2004). NP size has been found to influence the nature of biomolecular interactions, in that smaller NPs (2-4 nm) interacted with surrounding biomolecules primarily through hydrophobic interactions, while the main binding force for larger NPs (16 nm) was electrostatic interactions (Jiang, Jiang, Jin, Wang, & Dong, 2005). AuNPs form strong bonds with thiol groups, potentially indicating preferential binding of proteins containing higher numbers of cysteine residues (Bhattacharya et al., 2004; Brewer, Glomm, Johnson, Knag, & Franzen, 2005). It has been proposed that this property may be utilized to preferentially adsorb heparin binding growth factors over non-heparin binding growth factors and inhibit tumor angiogenesis

(Bhattacharya et al., 2004; Mukherjee et al., 2005). By furthering our understanding of how NP properties influence biomolecular interactions, NPs may be created which adhere engineered BCs that contain the desired proteins in the correct proportions. If perfected, this technology may be utilized to create NP therapeutics which collect and remove certain biomolecules from the circulation and improve patient health, or adhere certain biomolecules which influence the cellular reaction to NP exposure in a positive way. For instance, a fibrinogen-rich BC has been shown to reduce the inflammatory response following NP exposure (Ge et al., 2011; Lu, Sui, Tian, & Peng, 2018). Thus, when designing a NP therapeutic for medical use, it may be desirable to modify the NP properties such that it preferentially associates high quantities of fibrinogen, thus reducing any adverse effects of NP exposure. Further, additional research is needed to further our understanding of how the physiological environment influences the composition of the BC. Expanding on our study of the effects of LDL-supplemented serum on BC formation and the cellular response, experiments may be performed to further elucidate the role of LDL and HDL cholesterol. Specifically, serum may be supplemented with varying levels of HDL and LDL cholesterol representing both healthy and unhealthy physiological conditions. This would assist in clarifying the role of cholesterol in BC formation and how cholesterol influences NP toxicity. Further, the incorporation of multiple factors that are modified within our population may provide a more real-world assessment of the BC and its biological effects.

Alternatively, future research may focus less on the intricacies of the BC and more on the ultimate health outcomes for exposed individuals. In previous research, AuNPs have been shown to exhibit anti-inflammatory properties, reducing the expression of pro-inflammatory cytokines by macrophages following an immune challenge (Kingston, Pfau, Gilmer, & Brey, 2016). However, previous unpublished research by our lab as demonstrated that by reversing the order of exposures, the cellular response is also reversed. Macrophages which first experienced an immune challenge and were then exposed to AuNPs had a higher expression of inflammatory and oxidative stress mRNA markers (TNF- α , IL-6, and HO-1) than macrophages which were treated with lipopolysaccharide (LPS) alone. This indicates that the ability of AuNPs to provide anti-inflammatory benefits may be situationally and temporally dependent, in that the timing of exposures appears to reverse the effect of AuNP exposure. To investigate this further, experiments may be performed which consolidate and clarify these findings. Macrophages may be treated with

LPS and exposed to AuNPs, as well as the reverse, before examining the cellular inflammatory response. These responses may also be impacted via association of BCs, as we have demonstrated that they can modulate inflammatory signaling. Overall, these examinations may inform the use of AuNPs in medicine and allow physicians to determine the best time to administer AuNP therapeutics to deliver them maximum benefit and minimize any potential harm. Additionally, few studies have been performed regarding the *in vivo* toxicity of NPs in disease. Our study represents one of the few to examine the toxicological effects of medically relevant NPs in an unhealthy environment; which is, by definition, the model in which NP therapeutics will be used. More research is needed to elucidate the mechanisms of differential biodistribution and toxicity between healthy and diseased individuals, as well as potential differences in kinetics and NP elimination. Specifically, a time course may be performed to determine if individuals with MetS retain greater amounts of NP therapeutics such as silver than healthy individuals. If individuals with MetS are found to retain AgNPs for a longer time, it may indicate that any therapeutic intervention which utilizes NP therapeutics must be used more sparingly in diseased individuals, such that they are able to process the material.

By altering the BC, disease fundamentally changes how the surrounding cells interact with the NP, frequently enhancing cellular uptake and the inflammatory response. This indicates that those with diseases may be more susceptible to negative effects as a result of NP-induced inflammation caused by exposure in a medical environment. Organs which are already under stress as a result of the existing disease condition, such as the cardiovascular system, may be particularly vulnerable. Exposure to a NP therapeutic which induces inflammation may contribute to disease progression, worsening the health of those exposed. However, in some cases, NP exposure may not cause immune activation and inflammation, but rather the opposite problem: immune suppression. In situations where there is already a population of activated immune cells within the body, such as in MetS, the introduction of NPs may result in a significant loss in the number of immune cells which are alive and able to respond to an immune challenge. This would result in exposed individuals being immunocompromised and more susceptible to bacterial and viral infections that require an immune response. Disease may also impact the use of NP therapeutics in another way, by modifying the composition of the biological milieu over time such that the biomolecules within the BC are altered to the point of impacting the effectiveness of the NP therapeutic. One such

condition in which this may occur is kidney disease, which is known to alter the levels of many different proteins and lipids within the circulation (Aveles et al., 2010; Lopez-giacoman & Madero, 2015; Zhao, Vaziri, & Lin, 2015). These differences in serum composition over time would likely translate to the BC composition of any NP therapeutic which is introduced to a physiological environment currently under the effect of kidney disease. These differences in BC composition may cause the NP therapeutic to be less effective, possibly indicating a small temporal window for maximum effectiveness. Any condition which alters levels of circulating biomolecules over time has the capacity to greatly decrease the reliability of NP therapeutics, presenting another obstacle to clinical use. This indicates that NP therapeutics may be appropriate for use only in a specific and shrinking proportion of the population, healthy individuals. However, even this use likely comes with caveats; as the above research has demonstrated that individual variability, similarly to disease, alters the BC composition and subsequent cellular reaction to NP exposure. The results of this study provide evidence that in their current form, NP therapeutics may not be appropriate for use by the general patient population, but instead are more suitable personalized medicine in which patients may be individually screened prior to utilization.

Though the described research seemingly delivers mixed results for the future use of NPs as tools in biomedicine, it may in fact demonstrate a potential method for the testing and development of NP therapeutics. The utilization of human serum to form a BC *ex vivo* and subsequent exposure of the NP in question to human cell lines may serve as a future method to examine the safety and biocompatibility of NP therapeutics without the use of animal models. This method could potentially allow for the high-throughput, low-cost testing of NP therapeutics in potentially susceptible subpopulations while simultaneously maintaining a high degree of relevance to real-world clinical scenarios. However, further verification of the veracity of this method is needed before it may be considered as a viable alternative to *in vivo* testing. Additionally, this research may serve as a tool and guide for the further development of biomimetic BCs as an instrument of increasing the safety and efficacy NP therapeutics. Biomimetic BCs have great potential to increase the effectiveness of NP therapeutics by enhancing targeting abilities and extending circulation time. This is done by disguising the NP from the immune system by pre-forming a BC which the immune system is not able to identify as foreign, and thus is not targeted for elimination. Multiple approaches have been utilized towards this end, using both simple and complex BCs.

Some researchers have elected to use or emulate the membranes of other cells within the body. Functionalization of silica NPs with leukocyte membranes allowed them to avoid phagocytic clearance and to more efficiently cross an inflamed endothelial cell barrier to deliver a therapeutic payload (Parodi et al., 2013). Similarly, the addition of a lipid bilayer to silica NPs allowed researchers to create a therapeutic that was classified as a cell by body's immune systems, leading to their being deemed "protocells." These "protocells" were not only able to avoid immune detection, but had a 10,000 fold higher affinity for hepatocellular carcinoma cells than for immune cells, leading to enhanced chemotherapeutic drug delivery (Ashley et al., 2011). Others have done the opposite, using a single synthesized protein based on the self-identifying protein CD-47, to achieve similar goals. Polystyrene nanobeads with a coating of synthetic CD-47 were better able to avoid macrophage uptake and had a prolonged circulation time compared to uncoated nanobeads (Rodriguez et al., 2014). Research into the use of biomimetic coatings has been promising, and further scientific progress will allow for the refinement of the design of biomimetic BCs to expand and hone their abilities, allowing them to be utilized in a greater number of scenarios and applications and target smaller, more specialized cell populations.

While biomimetic coatings have great potential for the disguise and targeting of NP therapeutics, there are also benefits to a NP therapeutic that is quickly identified as foreign. Specifically, NP therapeutics which are readily phagocytized by macrophages may be used to target the immune system in autoimmune disorders such as systemic Lupus erythematosus, rheumatoid arthritis, inflammatory bowel disease, and others. Following opsonization and phagocytosis, NPs will be in place to dose therapeutics directly within the immune cells, allowing for highly targeted drug delivery which alters the behavior of the immune system on a cellular level. An attempt was made to enhance macrophage-NP interaction by pre-coating a silica NP with gamma globulins, though it was unsuccessful due to the association of additional proteins to the initial layer of opsonins (Mirshafiee, Kim, Park, Mahmoudi, & Kraft, 2016). Despite this, use of a pre-formed BC to enhance immune cell engagement still has the potential to enhance the treatment of immune disorders, as other methods have been identified, such the use of PEG, to prevent non-specific protein adsorption (Besnard, Noel, Appel, Angelo, & Couvreur, 1999; Papi et al., 2017; Runa et al., 2014). Combination of these techniques has the potential to result in the design of a NP therapeutic which is recognized and taken up by macrophages and is able to more effectively treat

immune disorders. Designer BCs also have the capacity to potentially aid in disease therapies; by tuning the properties of a NP such that it adsorbs certain specific biomolecules, proteins and lipids which are in excess may be collected and removed. This could potentially aid in the treatment of diseases such as amyloidosis, in which excess misfolded protein accumulates, causing health problems such as neuropathy, carpal-tunnel syndrome, and organ failure, depending on the part(s) of the body which are affected (Kyle & Bayrd, 1975; Merlini & Bellotti, 2003). Through the selected removal of misfolded proteins, disease symptoms of amyloidosis may be lessened or even eliminated. Tuning of the NP to specify biomolecular adsorption also has the potential to treat cancer through the targeting of specific biomolecules within the tumor microenvironment. By adsorbing to specific proteins or lipids and preventing them from functioning normally, the NP may inhibit the ability of the tumor to grow and metastasize in other areas of the body. For instance, NPs have been developed which preferentially adsorb heparin binding growth factor over non-heparin binding growth factors, which could potentially be used to inhibit tumor angiogenesis (Bhattacharya et al., 2004). Additionally, adsorption of specific biomolecules may be used to reach areas which are difficult to access using standard treatments, such as the brain. NPs which are functionalized with apolipoproteins have been demonstrated to more easily cross the blood-brain barrier, potentially indicating an alternative delivery mechanism for central nervous system treatments (Neves, Queiroz, & Reis, 2016; Neves et al., 2015). NPs may also be used as a diagnostic tool in this way; by preferentially associating biomolecular targets which are expressed in disease, the composition of the BC may be used as a method of detection which is potentially more sensitive than traditional blood tests. This may be used to determine with greater accuracy the state of a patient's disease progression, or for early detection of disease. By looking beyond the BC as a hindrance to biomedical usage, multiple avenues of future research and development may be identified; the BC as a method of disguising NP therapeutics, the BC as an identification flag for the immune system, the BC as a vehicle for biomolecular removal. By gaining a more complete understanding of how the physiological environment impacts BC composition and how the resultant BC affects cellular interactions, the use of NPs in biomedicine may continue to progress such that they may be utilized to their fullest potential.

The utilization of NPs in biomedicine is currently limited, though the frequency of their use is rapidly expanding. Dozens of NP therapeutics have been clinically approved for intravenous use,

and many more are currently in clinical trials. As the use of NPs in medicine continues to increase, so too does patient exposure, and thus the potential hazard. While NPs possess unique properties which make seemingly ideal for use in medicine, these same properties may cause them to be harmful in certain scenarios or certain patient subpopulations. The ability of NPs to travel throughout the body and adhere specific biomolecules based on NP composition, size, and charge may be utilized to the advantage of doctors and patients if it is acknowledged and accounted for; however, these same properties may result in unintended consequences such as biopersistence, inflammation, and detrimental alterations in circulating biomolecules if ignored. By performing the above described experiments, vulnerable subpopulations which may be more susceptible to adverse health outcomes as a result of NP exposure may be identified, allowing for more effective patient care and the protection of public health.

5.2 References

- Adamson, S. X. F., Lin, Z., Chen, R., Kobos, L., & Shannahan, J. (2018). Experimental challenges regarding the in vitro investigation of the nanoparticle-biocorona in disease states. *Toxicology in Vitro*, *51*(January), 40–49. <https://doi.org/10.1016/j.tiv.2018.05.003>
- Alnasser, F., Castagnola, V., Boselli, L., Esquivel-gaon, M., Efeoglu, E., McIntyre, J., ... Dawson, K. A. (2019). Graphene Nanoflake Uptake Mediated by Scavenger Receptors. *Nano Letters*, *19*, 1260–1268. rapid-communication. <https://doi.org/10.1021/acs.nanolett.8b04820>
- Ashley, C. E., Carnes, E. C., Phillips, G. K., Padilla, D., Durfee, P. N., Brown, P. A., ... Brinker, C. J. (2011). The targeted delivery of multicomponent cargos to cancer cells by nanoporous particle-supported lipid bilayers, *10*(April). <https://doi.org/10.1038/NMAT2992>
- Aveles, P. R., Criminácio, C. R., Gonçalves, S., Bignelli, A. T., Maria, L., Sérgio, C., ... Roberto, S. N. (2010). Association between Biomarkers of Carbonyl Stress with Increased Systemic Inflammatory Response in Different Stages of Chronic Kidney Disease and after Renal Transplantation. *Nephron Clinical Practice*, *116*(4), 294–299. <https://doi.org/10.1159/000318792>

- Babes, L., Jacques, J., Jeune, L., & Jallet, P. (1999). Synthesis of Iron Oxide Nanoparticles Used as MRI Contrast Agents : A Parametric Study. *Journal of Colloid and Interface Science*, 212, 474–482.
- Besnard, M., Noel, J. P., Appel, M., Angelo, J., & Couvreur, P. (1999). Stealth ® PEGylated polycyanoacrylate nanoparticles for intravenous administration and splenic targeting, 60, 121–128.
- Bhattacharya, R., Mukherjee, P., Xiong, Z., Atala, A., Soker, S., & Mukhopadhyay, D. (2004). Gold Nanoparticles Inhibit VEGF165-Induced Proliferation of HUVEC Cells. *Nano Letters*, 4(12), 2479–2481. <https://doi.org/10.1021/nl0483789>
- Bradley, K., Briman, M., Star, A., & Gru, G. (2004). Charge Transfer from Adsorbed Proteins. *Nano Letters*, 4(2), 256–256. <https://doi.org/10.1021/nl0349855>
- Brewer, S. H., Glomm, W. R., Johnson, M. C., Knag, M. K., & Franzen, S. (2005). Probing BSA Binding to Citrate-Coated Gold Nanoparticles and Surfaces. *Langmuir*, 62(17), 9303–9307. <https://doi.org/10.1021/la050588t>
- Ge, C., Du, J., Zhao, L., Wang, L., Liu, Y., Li, D., ... Zhou, R. (2011). Binding of blood proteins to carbon nanotubes reduces cytotoxicity. <https://doi.org/10.1073/pnas.1105270108>
- Ghazanfari, M. R., Kashefi, M., Shams, S. F., & Jaafari, M. R. (2016). Perspective of Fe₃O₄ Nanoparticles Role in Biomedical Applications. *Biochemistry Research International*, 1.
- Jiang, X., Jiang, J., Jin, Y., Wang, E., & Dong, S. (2005). Effect of Colloidal Gold Size on the Conformational Changes of Adsorbed Cytochrome c : Probing by Circular Dichroism , UV - Visible , and Infrared Spectroscopy. *Biomacromolecules*, 6, 46–53. <https://doi.org/10.1021/bm049744l>

- Jovicic, S., Ignjatovic, S., Dajak, M., Kangrga, R., & Majkic-Singh, N. (2009). Association of Lipid and Inflammatory Markers with C-Reactive Protein in Cardiovascular Risk Assessment for Primary Prevention Association of Lipid and Inflammatory Markers with C-Reactive Protein in Cardiovascular Risk Assessment for Primary Prevention. *Clinical Laboratory*, 55(11).
- Kaempf-rotzoll, D. E., Traber, M. G., & Arai, H. (2003). Vitamin E and transfer proteins. *Current Opinion in Lipidology*, 14, 249–254.
<https://doi.org/10.1097/01.mol.0000073505.41685.09>
- Kingston, M., Pfau, J. C., Gilmer, J., & Brey, R. (2016). Selective Inhibitory Effects of 50-nm Gold Nanoparticles on Mouse Macrophage and Spleen Cells. *Journal of Immunotoxicology*, 13(2), 198–208. <https://doi.org/10.3109/1547691X.2015.1035819>. Selective
- Kuklina, E. V., Carroll, M. D., Shaw, K. M., & Hirsch, R. (2013). Trends in High LDL Cholesterol, Cholesterol-lowering Medication Use, and Dietary Saturated-fat Intake: United States, 1976–2010. *NCHS Data Brief*, (117), 1–8.
- Kyle, R. A., & Bayrd, E. D. (1975). Amyloidosis: Review of 236 Cases. *Medicine*, 51(4), 271–299.
- Lopez-giacoman, S., & Madero, M. (2015). Biomarkers in chronic kidney disease, from kidney function to kidney damage. *World Journal of Nephrology*, 4(1), 57–73.
<https://doi.org/10.5527/wjn.v4.i1.57>
- Lu, N., Sui, Y., Tian, R., & Peng, Y. Y. (2018). Adsorption of Plasma Proteins on Single-Walled Carbon Nanotubes Reduced Cytotoxicity and Modulated Neutrophil Activation. *Chemical Research in Toxicology*, 31(10), 1061–1068. research-article.
<https://doi.org/10.1021/acs.chemrestox.8b00141>

- Merlini, G., & Bellotti, V. (2003). Molecular Mechanisms of Amyloidosis. *The New England Journal of Medicine*, 349(6), 583–596.
- Mirshafiee, V., Kim, R., Park, S., Mahmoudi, M., & Kraft, M. L. (2016). Impact of protein pre-coating on the protein corona composition and nanoparticle cellular uptake. *Biomaterials*, 75, 295–304. <https://doi.org/10.1016/j.biomaterials.2015.10.019>
- Mukherjee, P., Bhattacharya, R., Wang, P., Wang, L., Basu, S., Nagy, J. A., ... Soker, S. (2005). Cancer Therapy : Preclinical Antiangiogenic Properties of Gold Nanoparticles. *Clinical Cancer Research*, 11(9), 3530–3535.
- Neagu, M., Piperigkou, Z., Karamanou, K., & Engin, A. B. (2017). Protein bio - corona : critical issue in immune nanotoxicology. *Archives of Toxicology*, 91(3), 1031–1048. <https://doi.org/10.1007/s00204-016-1797-5>
- Neuberger, T., Scho, B., Hofmann, M., & Rechenberg, B. Von. (2005). Superparamagnetic nanoparticles for biomedical applications : Possibilities and limitations of a new drug delivery system. *Journal of Magnetism and Magnetic Materials*, 293, 483–496. <https://doi.org/10.1016/j.jmmm.2005.01.064>
- Neves, A. R., Queiroz, J. F., & Reis, S. (2016). Brain - targeted delivery of resveratrol using solid lipid nanoparticles functionalized with apolipoprotein E. *Journal of Nanobiotechnology*, 14(27), 1–11. <https://doi.org/10.1186/s12951-016-0177-x>
- Neves, A. R., Queiroz, J. F., Weksler, B., Romero, I. A., Couraud, P., & Reis, S. (2015). Solid lipid nanoparticles as a vehicle for brain-targeted drug delivery : two new strategies of functionalization with apolipoprotein E. *Nanotechnology*, 26(11).
- Papi, M., Caputo, D., Palmieri, V., Coppola, R., Palchetti, S., Bugli, F., ... Caracciolo, G. (2017). Clinically approved PEGylated nanoparticles the uptake by cancer cells, 9, 10327–10334. <https://doi.org/10.1039/c7nr03042h>

- Parodi, A., Quattrocchi, N., Ven, A. L. van de, Chiappini, C., Evangelopoulos, M., Martinez, J. O., ... Tasciotti, E. (2013). Biomimetic functionalization with leukocyte membranes imparts cell like functions to synthetic particles, 8(1), 61–68.
<https://doi.org/10.1038/nnano.2012.212.Biomimetic>
- Rhains, D., & Brissette, L. (2004). The role of scavenger receptor class B type I (SR-BI) in lipid trafficking Defining the rules for lipid traders. *The International Journal of Biochemistry & Cell Biology*, 36, 39–77. [https://doi.org/10.1016/S1357-2725\(03\)00173-0](https://doi.org/10.1016/S1357-2725(03)00173-0)
- Rodriguez, P. L., Harada, T., Christian, D. A., Pantano, D. A., Richard, K., & Discher, D. E. (2014). Minimal “Self” Peptides That Inhibit Phagocytic Clearance and Enhance Delivery of Nanoparticles, 339(August 2010), 971–975.
<https://doi.org/10.1126/science.1229568.Minimal>
- Runa, S., Hill, A., Cochran, V. L., Payne, C. K., Runa, S., Hill, A., ... Payne, C. K. (2014). PEGylated nanoparticles: protein corona and secondary structure, (September 2014).
<https://doi.org/10.1117/12.2062767>
- Stehle, J. R., Leng, X., Kitzman, D. W., Nicklas, B. J., Kritchevsky, S. B., & High, K. P. (2012). Lipopolysaccharide-Binding Protein , a Surrogate Marker of Microbial Translocation , Is Associated With Physical Function in Healthy Older Adults. *Journal of Gerontology*, 67(11), 1212–1218. <https://doi.org/10.1093/gerona/gls178>
- Suikkari, A., Sane, T., Seppala, M., Yki-Jarvinen, H., Karonen, S.-L., & Koivisto, V. A. (1989). Prolonged Exercise Increases Serum Insulin-Like Growth Factor-Binding Protein Concentrations. *Journal of Clinical Endocrinology and Metabolism*, 68(1), 141–144.
- Walkey, C. D., Olsen, J. B., Guo, H., Emili, A., & Chan, W. C. W. (2012). Nanoparticle Size and Surface Chemistry Determine Serum Protein Adsorption and Macrophage Uptake. *Journal of the American Chemical Society*. <https://doi.org/10.1021/ja2084338>

Zhao, Y., Vaziri, N. D., & Lin, R. (2015). Lipidomics : New Insight Into Kidney Disease. In *Advances in Clinical Chemistry* (1st ed., Vol. 68, pp. 153–175). Elsevier Inc.
<https://doi.org/10.1016/bs.acc.2014.11.002>

VITA

Education

Purdue University, West Lafayette, Indiana (2016 - 2020)

Doctor of Philosophy: Toxicology

Dissertation: An Assessment of the Toxicological Impact of Medically Relevant Nanomaterials in Diseased Conditions

Purdue University, West Lafayette, Indiana (2012 - 2015)

Bachelor of Science in Biology: Neurobiology and Physiology

Minor: Psychology

Minor: Forensic Science

Research Experience

Purdue University, College of Health and Human Sciences, School of Health Sciences

Principal Investigator - Dr. Jonathan Shannahan

- Analysis of mechanisms of toxicity in disease environments
- Evaluation of emerging environmental and occupational exposures such as cured-in-place-pipe emissions and nanotechnology
- Investigation of modulated immune responses following environmental and biomedical nanoparticle exposures
- Examination of nanoparticle-biocorona composition and toxicity via integrative mass spectrometry -omics approaches
- Use of *in vitro* and *in vivo* models for toxicity assessment
- Development of mass spectrometry -omics procedures for the investigation of toxicology
- Utilization of a variety of molecular biology techniques, including PCR, and RNA isolation

Work/Leadership Experience

Ohio Valley Society of Toxicology (OVSOT) Graduate Student Representative

November 2018-April 2020

- Active Executive Committee member
- Organize and coordinate OVSOT Summer Student Scientific Meeting

- Contribute to organization of OVSOT annual meeting and national meeting events
- Act as point of contact for those interested in joining OVSOT

National Society of Toxicology (SOT) Continuing Education (CE) Committee Student Representative
May 2019-May 2020

- Contribute to selection and organization of Continuing Education courses at SOT national meeting
- Solicit and organize volunteers for SOT national meeting
- Coordinate Continuing Education volunteer activities

National Society of Toxicology (SOT) Graduate Student Leadership Committee Member
May 2019-May 2020

- Assist in organization of events to benefit graduate attendees to the National SOT meeting
- Communicate with distinguished toxicologists to facilitate their participation in “Chat with an Expert” events
- Communicate with SOT staff to plan logistics of Graduate/Postdoctoral Student Mixer at SOT national meeting

Purdue Health Sciences Graduate Student Organization Treasurer June 2019-June 2020

- Oversee creation of yearly and event-specific budgets
- Ensure timely resolution of outstanding financial obligations
- Organize and plan departmental events (Departmental Picnic, 40th Anniversary Research Retreat)

Teaching Assistant, Purdue University

August 2016-May 2018 (HSCI 560 – Toxicology, HSCI 202 – Essentials of Environmental, Occupational, and Radiological Health Sciences, HSCI 131 – Medical Terminology)

- Proctor student examinations
- Write and edit student examinations prior to administration
- Hosted office hours to meet with students to assist in understanding of the class material
- Organize and host review sessions prior to exams
- Grade students’ examinations and homework

Awards/Honors

- Purdue Health Sciences Graduate Service Award – March 2020
- Society of Toxicology Graduate Student Travel Support Funding Recipient – November 2019
- Ohio Valley Society of Toxicology Regional Chapter: Annual Meeting – 2nd Place Tox on the Clock Presentation – October 2019
- Society of Toxicology Supplemental Training for Education (STEP) Funding Recipient – July 2019
- Ohio Valley Society of Toxicology Regional Chapter: Annual Meeting – 1st Place PhD. Platform Presentation – November 2018
- Nanotoxicology Specialty Section: National Society of Toxicology – Outstanding Graduate Student Award, 2nd Place – March 2018

Memberships

- Society of Toxicology – 2015-Current
- Ohio Valley Regional Chapter: Society of Toxicology – 2016-Current
- Nanoscience and Advanced Materials Specialty Section: Society of Toxicology – 2016-Current

Publications

- Primary Author: **Lisa Kobos**, Saeed Alqahtani, Li Xia, Vincent Coltellino, Riley Kishman, Carlos Perez-Torres, Daniel McIlrath, Jonathan Shannahan. (2020). Comparison of Silver Nanoparticle-Induced Inflammatory Responses and Biodistribution and Between Healthy and Metabolic Syndrome Mouse Models. *Journal of Toxicology and Environmental Health, Part A: Current Issues*, (Accepted)
- Co-Author: Saeed Alqahtani, **Lisa Kobos**, Li Xia, Christina Ferreira, Jackeline Marmolejo, Xuqin Du, Jonathan Shannahan. (2020). Exacerbation of nanoparticle-induced acute pulmonary inflammation in a mouse model of metabolic syndrome. *Frontiers in Immunology*, (Accepted)
- Primary Author: **Lisa Kobos**, Saeed Alqahtani, Christina R. Ferreira, Uma K. Aryal, Tiago J. P. Sobreira, Jonathan Shannahan. (2019). An Integrative Proteomic/Lipidomic Analysis of the Gold Nanoparticle Biocorona in Healthy and Obese Conditions. *Applied In Vitro Toxicology*, 5(3), 150-166.

- Primary Author: **Lisa Kobos**, Jonathan Shannahan. (2019). Biocorona-Induced Modifications in Engineered Nanomaterial-Cellular Interactions Impacting Biomedical Applications. *Wiley Interdisciplinary Reviews: Nanomedicine and Nanobiotechnology*, e1608.
- Primary Author: **Lisa Kobos**, Seyedeh Mahboobeh Teimouri Sendesi, Andrew Whelton, John Howarter, Brandon Boor, Jonathan Shannahan. (2019). In Vitro Toxicity Assessment of Emitted Materials Collected during the Manufacture of Water Pipe Plastic Linings. *Inhalation toxicology*, 1-16.
- Primary Author: **Lisa M. Kobos**, Sherleen Xue-Fu Adamson, Sheelagh Evans, Timothy Gavin, Jonathan Shannahan. Altered Formation of the Iron Oxide Nanoparticle-Biocorona due to Individual Variability and Exercise. (2018) *Environmental Toxicology and Pharmacology*, 62, 215-226. (Accepted as-is)
- Co-Author: Sherleen Xue-Fu Adamson, Zhoumeng Lin, Ran Chen, **Lisa Kobos**, Jonathan Shannahan. (2018). Experimental Challenges Regarding the *in vitro* Investigation of the Nanoparticle- Biocorona in Disease States. *Toxicology In Vitro*, 51, 40-49.
- Co-Author: Teimouri Sendesi, S. M., Ra, K., Conkling, E. N., Boor, B. E., Nuruddin, M., Howarter, J. A., Youngblood J.P., **Kobos L.M.**, Shannahan J.H., Jafvert C.T., & Whelton, A. J. (2017). Worksite Chemical Air Emissions and Worker Exposure during Sanitary Sewer and Stormwater Pipe Rehabilitation Using Cured-in-Place-Pipe (CIPP). *Environmental Science & Technology Letters*, 4(8), 325-333.

Accepted Abstracts/Presentations

- Society of Toxicology Annual Meeting, Anaheim, CA – Spring 2020 (poster)
- Health and Disease: Science, Technology, Culture, and Policy Research Poster Session, West Lafayette, IN – Spring 2020 (poster)
- Purdue University Health and Human Sciences Fall Research Day, West Lafayette, IN – Fall 2019 (poster)
- Ohio Valley Regional Chapter: Society of Toxicology Annual Meeting, Mason, OH – Fall 2019 (oral and poster)
- Purdue Health Sciences Departmental Seminar, West Lafayette, IN – Fall 2019 (oral)

- Bindley-Waters -Omics Symposium, West Lafayette, IN – Fall 2019 (Invited Speech)
- 2nd Annual North American Mass Spectrometry Summer School, University of Madison-Wisconsin, WI – Spring 2019 (poster)
- Purdue Office of Interdisciplinary Graduate Programs Spring Reception, West Lafayette, IN – Spring 2019 (poster)
- Purdue School of Health Sciences Graduate Student Retreat, Indianapolis, IN – Spring 2019 (oral)
- Society of Toxicology Annual Meeting, Baltimore, MD – Spring 2019 (oral)
- Ohio Valley Regional Chapter: Society of Toxicology Annual Meeting, Louisville, KY – Fall 2018 (oral)
- Purdue University Life Science Annual Retreat, West Lafayette, IN – Fall 2018 (poster)
- Purdue Office of Interdisciplinary Graduate Programs Spring Reception, West Lafayette, IN – Spring 2018 (poster)
- Health and Disease: Science, Technology, Culture, and Policy Research Poster Session, West Lafayette, IN – Spring 2018 (poster)
- Society of Toxicology Annual Meeting, San Antonio, TX – Spring 2018 (poster)
- Ohio Valley Regional Chapter: Society of Toxicology Annual Meeting, West Lafayette, IN - Fall 2017 (poster)
- Purdue University Health and Human Sciences Fall Research Day, West Lafayette, IN – Fall 2017 (poster)

Continuing Education

Second Annual North American Mass Spectrometry Summer School, Madison, WI – July 2019

- Attended Lectures on mass analyzers, ionization, shotgun proteomics, and other topics
- Participated in hands-on demonstrations of mass spectrometry equipment and principles
- Learned how to manually interpret mass spectrometry data

Introduction to Industrial Hygiene, OSHAcademy, online – April 2020

- Studied material detailing worksite analysis, air quality, exposure limits, and other topics
- Learned about potential hazards (chemical, physical, biological) industrial hygienists may potentially encounter
- Reviewed methods to assess and mitigate the risk presented by exposure to various hazards

PUBLICATIONS

Primary Author: **Lisa Kobos**, Saeed Alqahtani, Li Xia, Vincent Coltellino, Riley Kishman, Carlos Perez-Torres, Daniel McIlrath, Jonathan Shannahan. (2020). Comparison of Silver Nanoparticle Biodistribution and Responses Between Healthy and Metabolic Syndrome Mouse Models. *Journal of Toxicology and Environmental Health, Part A: Current Issues*, (Accepted)

Co-Author: Saeed Alqahtani, **Lisa Kobos**, Li Xia, Christina Ferreira, Jackeline Marmolejo, Xuqin Du, Jonathan Shannahan. (2020). Exacerbation of nanoparticle-induced acute pulmonary inflammation in a mouse model of metabolic syndrome *Frontiers in Immunology*, (Accepted)

Primary Author: **Lisa Kobos**, Saeed Alqahtani, Christina R. Ferreira, Uma K. Aryal, Tiago J. P. Sobreira, Jonathan Shannahan. (2019). An Integrative Proteomic/Lipidomic Analysis of the Gold Nanoparticle Biocorona in Healthy and Obese Conditions. *Applied In Vitro Toxicology*, 5(3), 150-166.

Primary Author: **Lisa Kobos**, Jonathan Shannahan. (2019). Biocorona-Induced Modifications in Engineered Nanomaterial-Cellular Interactions Impacting Biomedical Applications. *Wiley Interdisciplinary Reviews: Nanomedicine and Nanobiotechnology*, e1608.

Primary Author: **Lisa Kobos**, Seyedeh Mahboobeh Teimouri Sendesi, Andrew Whelton, John Howarter, Brandon Boor, Jonathan Shannahan. (2019). In Vitro Toxicity Assessment of Emitted Materials Collected during the Manufacture of Water Pipe Plastic Linings. *Inhalation toxicology*, 1-16.

Primary Author: **Lisa M. Kobos**, Sherleen Xue-Fu Adamson, Sheelagh Evans, Timothy Gavin, Jonathan Shannahan. Altered Formation of the Iron Oxide Nanoparticle-Biocorona due to Individual Variability and Exercise. (2018) *Environmental Toxicology and Pharmacology*, 62, 215-226. (Accepted as-is)

Co-Author: Sherleen Xue-Fu Adamson, Zhoumeng Lin, Ran Chen, **Lisa Kobos**, Jonathan Shannahan. (2018). Experimental Challenges Regarding the in vitro Investigation of the Nanoparticle- Biocorona in Disease States. *Toxicology In Vitro*, 51, 40-49.

Co-Author: Teimouri Sendesi, S. M., Ra, K., Conkling, E. N., Boor, B. E., Nuruddin, M., Howarter, J. A., Youngblood J.P., **Kobos L.M.**, Shannahan J.H., Jafvert C.T., & Whelton, A. J. (2017). Worksite Chemical Air Emissions and Worker Exposure during Sanitary Sewer and Stormwater Pipe Rehabilitation Using Cured-in-Place-Pipe (CIPP). *Environmental Science & Technology Letters*, 4(8), 325-333.